

EFFECT OF CENOSPHERE ON THE MECHANICAL AND TRIBOLOGICAL PROPERTIES OF NATURAL FIBER REINFORCED HYBRID COMPOSITE

Dissertation submitted in partial fulfillment

of the requirements of the degree of

Doctor of Philosophy

in

Industrial Design

by

Soma Dalbehera

(Roll Number: 512ID1005)

based on research carried out

Under the supervision of

Prof. Samir Kumar Acharya



August, 2016

Department of Industrial Design

National Institute of Technology Rourkela



Department of Industrial Design

National Institute of Technology Rourkela

Certificate of Examination

Roll Number: 512ID1005

Name: Soma Dalbehera

Title of Dissertation: Effect of cenosphere on the mechanical and tribological
Properties of natural fiber reinforced hybrid composite

We the below signed, after checking the dissertation mentioned above and the official record book (s) of the student, hereby state our approval of the dissertation submitted in partial fulfillment of the requirements of the degree of *Doctor of Philosophy in Industrial Design* at *National Institute of Technology Rourkela*. We are satisfied with the volume, quality, correctness, and originality of the work.

Prof. D. Sarkar
Member, DSC

Prof. S.K. Acharya
Principal Supervisor

Prof. H.B. Sahu
Member, DSC

Prof. B B V L Deepak
Member, DSC

Prof. B. B. Biswal
Chairperson, DSC

External Examiner

Prof. Md. Rajik Khan
Head of the Department



Department of Industrial Design
National Institute of Technology Rourkela

Prof. Samir Kumar Acharya
Professor

22nd August 2016

Supervisors' Certificate

This is to certify that the work presented in this dissertation entitled “*Effect of cenosphere on the mechanical and tribological Properties of natural fiber reinforced hybrid composite*” by *Soma Dalbehera*, Roll Number *512ID1005*, is a record of original research carried out by her under my supervision and guidance in partial fulfillment of the requirements of the degree of *Doctor of Philosophy in Industrial Design*. Neither this dissertation nor any part of it has been submitted for any degree or diploma to any institute or university in India or abroad.

Samir Kumar Acharya
Professor

*Dedicated to my parents
and family members*

Declaration of Originality

I, *Soma Dalbehera*, Roll Number *512ID1005* hereby declare that this dissertation entitled “*Effect of cenosphere on the mechanical and tribological Properties of natural fiber reinforced hybrid composite*” represents my original work carried out as a doctoral student of NIT Rourkela and, to the best of my knowledge, it contains no material previously published or written by another person, nor any material presented for the award of any degree or diploma of NIT Rourkela or any other institution. Any contribution made to this research by others, with whom I have worked at NIT Rourkela or elsewhere, is explicitly acknowledged in the dissertation. Works of other authors cited in this dissertation have been duly acknowledged under the section “Reference”. I have also submitted my original research records to the scrutiny committee for evaluation of my dissertation.

I am fully aware that in case of any non-compliance detected in future, the Senate of NIT Rourkela may withdraw the degree awarded to me on the basis of the present dissertation.

22nd August 2016
NIT Rourkela

Soma Dalbehera

Acknowledgement

I would like to express my special appreciation and thanks to my supervisor **Prof. S.K. Acharya**, Department of Mechanical Engineering, NIT Rourkela for suggesting the topic of my thesis and his ready and able supervision throughout the course of my work. I am highly indebted to my mentor for his invaluable guidance, continuous encouragement and thoughtfulness towards the accomplishment of my research work.

I express my sincere thanks to Director NIT Rourkela **Prof. R.K. Sahoo** and **Prof. Md. Rajik Khan**, Head of the Department of Industrial Design and **Prof. B.B. Biswal** for providing all academic and administrative help during the course of research work.

The guidance, review and critical suggestion of the Doctoral scrutiny Committee (DSC) during various presentations and review meeting comprising of **Prof. D. Sarkar**, **Prof. H.B. Sahu** and **Prof. B B V L Deepak** are acknowledged. I also express my thanks to **Prof. S. K. Pratihara** of Ceramic Engineering Department for his help and guidance during my experimental work in the laboratory.

I am also thankful to all the staff members of the Department of Mechanical Engineering, Metallurgical Engineering, Ceramic Engineering and Industrial Design for their timely help in completing my thesis work. I am thankful to all **PhD and M-tech** Scholars of Tribology Laboratory of Mechanical Engineering department for providing necessary information regarding the research work.

Last but not least, I would like to pay high regards to my father **Mr. Prafulla Kumar Dalbehera** and my mother **Mrs. Premalata Dalbehera** & my brother-in-law for their blessing, guidance and supports. This work could have been impossible if I could not get the moral encouragement from my father **Er. P.K. Dalbehera** throughout my research work in every step at this stage and also supports from my near friends. This thesis is the outcome of the sincere prayers and dedicated support of my family members without which the research could not have reached the present form. Above all I would like to thank almighty for his continued blessings that have helped me complete this work successfully.

22nd August 2016
NIT Rourkela

Soma Dalbehera
Roll Number: 512ID1005

Abstract

There is a growing interest in use of agro-fibers as reinforcing components for plastics because they are renewable, biodegradable and environmentally friendly. Again, the growing environmental concern has made plastics a target of criticism due to lack of degradability. So there has been a lot of interest in research committed to the design of biodegradable plastic composites. These composites can be very cost-effective material especially for building and construction industry, packing, automobile and railway coach interiors and storage devices. The term filler is very broad and encompasses a very wide range of materials which plays an important role for the improvement in performance of polymers and their composites. Filler materials are used to reduce the material cost and to improve the mechanical properties to some extent and in some cases to improve processability. Besides it also increases properties like abrasion resistance, hardness and reduces shrinkages.

Cenosphere is a ceramic rich industrial waste produced during burning of coal in thermal power plants. The present study deals with the effect of cenosphere as particulate filler on mechanical and tribological behavior of natural fiber reinforced polymer composite.

The priority of this work is to prepare polymer matrix composites using jute and glass fiber as reinforcement material to improve the interfacial strength between the fiber and the matrix. The fiber characterization has been carried out by Fourier Transform Infrared spectroscopy (FTIR) and X-Ray diffraction (XRD) method.

Different doses of cenosphere are added as particulate filler material to the composite and the mechanical properties of the composite like tensile, flexural, impact test has been evaluated. The study also includes investigation of different tribological tests like solid particle erosion test and three-body abrasion test as per ASTM standards. The work presented in this dissertation has been carried out with the following scheme.

1. Preparation of hybrid composites of different stacking sequence (JJJJ, GJGJ, JGGJ and GJJG) by hand lay-up technique.
2. Determination of density, void fraction and hardness of above all composite samples.
3. Characterization of reinforced composite with XRD, FTIR, TGA analysis.
4. EDS analysis of jute fiber and cenosphere powder.

5. Study of mechanical properties (Tensile strength, Flexural strength, ILSS, Impact strength) of hybrid jute-glass epoxy composite with specific orientation of fiber for different stacking sequences (JJJJ, GJGJ, JGGJ, GJJG).
6. Study on erosive wear behaviour of above all composites developed under different parameters like impingement angle, impact velocity and stand of distance.
7. SEM study (both mechanical and erosion) of above all composite samples.
8. Study of mechanical properties (Tensile strength, Flexural strength, ILSS and modulus) of different weight percentage(5,10,15 and 20%) of cenosphere filled hybrid jute-glass epoxy composite for optimum mechanical performance of stacking sequence (GJJG) developed composite.
9. Erosion test of different weight percentage of particulate filled hybrid jute-glass epoxy composite for the sequence GJJG.
10. SEM studies on mechanical properties and erosion wear response of cenosphere filled hybrid jute-glass epoxy composite.
11. Study on moisture absorption performance of hybrid composites.
12. Study for Three-body dry sand abrasion wear test of cenosphere filled developed composites.

From the experimental work and result analysis of hybrid jute-glass reinforced epoxy composites it was found that the presence of glass fiber at the outer layer of composites provides better mechanical strength for the sequence GJJG. Further addition of different doses of cenosphere filler to the developed glass-jute(GJJG) composite shows improved mechanical strength. The highest strength was observed for 15wt. percentage of cenosphere filled hybrid composite as compared to others.

Moisture absorption behavior of particulate filled hybrid glass-jute composite was also carried out. The moisture absorption kinetics of the composites has also been studied. The study confirmed that the Fickian's diffusion mechanism can be used to adequately describe the moisture absorption performance of the developed composites.

The erosion wear response of the hybrid composite with different stacking sequences is evaluated using a solid particle erosion test rig. The experimental results illustrate that under all impact velocities the erosive wear performance of all composites exhibit semi ductile behavior. It is observed that layering sequence and velocity of impact has significant influence on the erosion rate of the composite and the erosive strength of

jute fiber increases by hybridization with synthetic fiber glass. Again with addition of cenosphere filler to the hybrid glass-jute composite shows similar material response indicating that inclusion of high weight percentage of filler (20%) provides better erosion resistance of developed composites. Similarly three-body abrasion wear test of filled composites show improved abrasion resistance as compared to only hybrid glass-jute composites in subsequent section.

This work can be further extended to utilization of other composite fabrication techniques with surface modification of fibers. However the results reported here can act as a starting point for both industrial designer and researchers to design and develop hybrid polymer matrix composite (PMC) components. Against this back ground the present research work has been focused with an objective to explore the use of natural fiber jute and synthetic fiber glass, as reinforcement material in epoxy base along with addition of plant waste material cenosphere as particulate filler for preparation of hybrid composites.

Keywords: Jute and Glass fiber; Cenosphere; Hybrid jute-glass composites; Mechanical properties; Moisture absorption; Erosive wear; Abrasion wear; SEM

Contents

Certificate of Examination	i
Supervisor's Certificate	ii
Dedication	iii
Declaration of Originality	iv
Acknowledgment	v
Abstract	vi
List of Tables	xv
List of Figures	xvii
List of Symbol	xviii

Chapter-1 Introduction

1.1	Back ground	1
1.2	Composites	3
1.3	Classification of Composites	3
	1.3.1 Particulate reinforced composites	4
	1.3.2 Fiber reinforced composites	4
	1.3.3 Hybrid composites	5
	1.3.4 Laminates	6
1.4	Components of a composite material	7
	1.4.1 Role of matrix in a composite	7
	1.4.2 Materials used as matrices in composites	7
	1.4.2.1 Bulk Phases	7
	1.4.2.2 Reinforcement	9
	1.4.2.3 Interface	9
1.5	Natural fiber composites	
	1.5.1 Jute fiber	11
	1.5.2 Glass fiber	14
	1.5.3 Limitation of glass fiber	15
1.6	FILLERS	

1.6.1	Conventional Fillers	15
1.6.2	Micro Fillers	16
1.6.3	Nano Fillers	16
1.7	Particulate Filler	17
1.7.1	Cenosphere	18
1.7.2	Need for cenosphere as reinforcing filler material	18
 Chapter-2 Literature Survey		
2.1	Introduction	22
2.2	Material selection	23
2.2.1	Thermosets	23
2.2.2	Bio-derived Thermoplastic Matrices	25
2.2.3	Reinforcement	27
2.2.4	Reinforcement Materials	28
2.3	Fabrication methods of polymer matrix composites	28
2.3.1	Open Molding Method	29
2.3.2	Closed Molding Method	31
2.4	Natural fiber reinforced polymer composites	35
 Chapter-3 Mechanical properties of hybrid Jute-Glass fiber epoxy composites with and without cenosphere filler		
3.1	Introduction	47
3.2	Materials and methods	51
3.2.1	Raw materials used	51
3.2.1.1	Jute fiber	51
3.2.1.2	E-glass fiber	52
3.2.1.3	Epoxy resin and Hardener	52
3.2.2	Preparation of Hybrid composites	53
3.2.3	Density and void fraction measurement	55
3.2.4	Tensile Strength	56
3.2.5	Flexural Strength	57
3.2.6	Interlaminar shear Strength	58
3.2.7	Impact test	59
3.3	Results and discussion	60

3.3.1	Hybrid Composites	
3.3.1.1	Effect of tensile strength on hybrid jute-glass epoxy composites	60
3.3.1.2	Effect of flexural strength on hybrid jute-glass epoxy composites	61
3.3.1.3	Effect of Interlaminar shear strength on hybrid jute-glass epoxy composites	63
3.3.1.4	Effect of Impact strength on hybrid jute-glass epoxy composites	63
3.3.2	Morphological studies of hybrid jute-glass epoxy composite	64
3.4	Micro Filler Hybrid Composites	66
3.4.1	Density and void fraction measurement	66
3.5	Materials and methods	66
3.5.1	Raw materials used	66
3.5.2	Preparation of Composites	67
3.5.3	Tensile Strength	67
3.5.4	Flexural Strength	69
3.5.5	Interlaminar shear Strength	70
3.6	Results and discussion	71
3.6.1	Density and void fraction of composites	71
3.6.2	Effect of cenosphere on mechanical properties of hybrid glass-jute epoxy composite for stacking sequence (GJJG)	72-75
3.6.3	Morphological studies of hybrid glass-jute epoxy Composites with and without Filler	75-77
3.7	Conclusions	78
 Chapter-4 Moisture absorption behaviour of cenosphere filled hybrid jute-glass epoxy composites		
4.1	Introduction	79
4.2	Characterization studies	82
4.2.1	EDX analysis of cenosphere filler and raw jute fiber	83

4.2.2	FTIR Spectroscopy	85
4.2.3	X-ray Diffraction studies	86
4.2.4	Thermogravimetric analysis (TGA) of cenosphere filled hybrid Glass-jute epoxy composite	88
4.3	Composite fabrication	90
4.3.1	Jute and Glass fiber	90
4.3.2	Cenosphere	90
4.3.3	Epoxy Resin and Hardener	90
4.3.4	Composite preparation	90
4.4	Study of environmental effect	91
4.4.1	Moisture absorption test	92
4.4.2	Mechanical Tests	92
4.4.3	Fractography Studies	93
4.5	Results and discussions	93
4.5.1	Effect of filler loading on moisture absorption behaviour	93
4.5.2	Thickness swelling behaviour	94
4.5.3	Measurement of Diffusivity	95
4.5.4	Effect of moisture absorption on Mechanical properties	97
4.6	SEM studies of fractured surface	98
4.7	Conclusions	100

Chapter-5 Solid particle erosion performance of hybrid jute glass fiber reinforced epoxy composites

5.1	Introduction	117
5.2	Types of wear	118
5.2.1	Abrasive wear	119
5.2.2	Erosive wear	120
5.2.3	Adhesive Wear	121
5.2.4	Surface Fatigue	122
5.2.5	Corrosive Wear	123
5.3	Symptoms of wear	124
5.4	Solid particle erosion of hybrid polymer matrix composites	126
5.5	Experiment	130
5.5.1	Preparation of the test specimens	130

5.5.2	Micro-Hardness	130
5.5.3	Measurement of impact velocity of erodent particles: Double disc Method	131
5.6	Test apparatus and experiment	133
5.7	Results and discussion	136
5.8	Surface Morphology of Eroded Surfaces	138
5.9	Conclusion	139
 Chapter-6 Solid particle erosion studies of cenosphere filled hybrid jute-glass epoxy composites		
6.1	Introduction	150
6.2	Materials and method	152
6.2.1	Raw Materials used	152
6.2.2	Jute fiber	152
6.2.3	E glass fiber	152
6.2.4	Epoxy resin and Hardener	152
6.2.5	Cenosphere filler	152
6.3	Methods	
6.3.1	Preparation of Composites	152
6.3.2	Test apparatus and Experiment	153
6.4	Results and discussions	153
6.4.1	Surface Morphology of Eroded surfaces	155
6.5	Conclusions	156
 Chapter-7 Three-body abrasive wear studies of cenosphere filled hybrid glass-jute epoxy composites		
7.1	Introduction	170
7.2	Materials and Method	172
7.2.1	Raw Materials Used	172
7.2.1.1	Jute fiber	172
7.2.1.2	E-glass fiber	172
7.2.1.3	Epoxy resin and Hardener	172
7.2.1.4	Cenosphere filler	172

7.3	Methods	
7.3.1	Fabrication of the test specimens	173
7.3.2	Three-Body Abrasion Test and Experimental Set up	173
7.3.3	Calculation for Abrasive Wear	175
7.4	Results and discussions	
7.4.1	Effect of cenosphere on abrasive wear behaviour of glass-jute epoxy composites	175
7.4.2	Worn surface morphology of abraded surfaces	177
7.5	Conclusions	177-178

Chapter-8 Conclusions and Scope for Future Work

8.1	Conclusions	187
8.2	Recommendation for further research	188
References		189-209
Dissemination		210-211
Vitae		212

List of Figures

Figure No.	Title	Page no.
1.1	Classification of composites	3
1.2	Schematic diagram of jute fiber structure	12
1.3	Structure of cellulose as it occurs in a plant cell wall	13
2.1	Chemical structure of DGEBA	24
2.2	Hand Lay-Up Technique	43
2.3	Spray up Technique	43
2.4	Filament Winding Process	44
2.5	Compression Molding Technique	44
2.6	Pultrusion Process	45
2.7	Vacuum Bag Molding	45
2.8	Vacuum Infusion Process	46
2.9	Resin Transfer Molding	46
3.1	Cell wall structure of natural fiber	47
3.2	Woven Jute fiber mat	51
3.3	E-Glass fiber mat	51
3.4	Photograph of (a) Mold used for composite preparation(b) composite slab(c) Specimen for Tensile test and(d) Flexural test	54
3.5	Tensile specimen	56
3.6	Photograph of (a) INSTRON H10KS testing machine(b) Sample in loading condition (c) Tested samples	57
3.7	Photograph of (a) Flexural specimen (b) Sample in loading position (c) Testing samples	58

3.8	(a-b): Impact test machine and Configuration of impact test specimen	59
3.9	Tensile strength of hybrid jute-glass fiber reinforced epoxy composite	61
3.10	Tensile modulus of hybrid jute-glass fiber reinforced epoxy composites	61
3.11	Flexural strength of jute-glass fiber reinforced epoxy composites	62
3.12	Flexural modulus of jute-glass fiber reinforced epoxy composites	62
3.13	Interlaminar shear strength of hybrid jute-glass laminate epoxy composites	63
3.14	Impact strength of hybrid jute-glass epoxy composites	64
3.15	SEM image of (a) Tensile fractured surface of hybrid GJJG epoxy composite(b) Flexural fractured surface of GJJG epoxy composite	65
3.16	Photograph of (a) Specimen for testing (b) Tensile fractured samples	68
3.17	Photograph of (a) Flexural testing samples (b) Fractured samples	69
3.18	Tensile strength of cenosphere filled hybrid jute-glass epoxy composites	71
3.19	Tensile modulus of cenosphere filled hybrid jute-glass epoxy composites	72
3.20	Flexural strength of cenosphere filled hybrid jute-glass epoxy composites	72
3.21	Flexural modulus of cenosphere filled hybrid jute-glass epoxy composites	73
3.22	Interlaminar shear strength of cenosphere filled hybrid jute-glass epoxy composites	73
3.23	SEM images of flexural fractured surface of (a) Glass fiber composite (b) Jute fiber composite(c) Jute-glass hybrid composite (d) Cenosphere filled GJJG hybrid composite	75
3.24	SEM images of tensile fractured surface of (a) Jute fiber composite (b) Glass Fiber composite (c) Jute-glass hybrid composite (d) Cenosphere filled GJJG Hybrid composite	76
4.1	(a) SEM micrograph Cenosphere (b) EDX analysis of cenosphere	81-82

4.2	(a) SEM micrograph of jute fiber (b) EDX analysis of jute fiber	83
4.3	Percentage Transmittance of cenosphere powder and jute fiber	84
4.4	a) X-Ray diffractograms of cenosphere powder b) X-Ray diffractograms of jute fiber	86
4.5	TGA Thermograms of cenosphere filled glass-jute reinforced composites	88
4.6	Specimen for (a) Tensile and (b) Flexural test subjecting to different environmental condition	90
4.7	Variation of moisture absorption of cenosphere filled jute-glass(GJJG) composites with immersion time in distilled water for tensile specimens	100
4.8	Variation of moisture absorption of cenosphere filled jute-glass(GJJG) composites with immersion time in saline water for tensile specimens	100
4.9	Variation of moisture absorption of cenosphere filled jute-glass(GJJG) composites with immersion time in saline water for flexural specimens	101
4.10	Variation of moisture absorption of cenosphere filled jute-glass(GJJG) composites with immersion time in distilled water for flexural specimens	101
4.11	Variation of thickness swelling of cenosphere filled jute-glass (GJJG) composites with immersion time at distilled water for tensile specimen	102
4.12	Variation of thickness swelling of cenosphere filled jute-glass (GJJG) composites with immersion time at saline water for tensile specimen	102
4.13	Variation of thickness swelling of cenosphere filled jute-glass (GJJG)composites with immersion time at distilled water for flexural specimen	103
4.14	Variation of thickness swelling of cenosphere filled jute-glass composites with immersion time at saline water for flexural specimen	103
4.15	Diffusion curve fitting for cenosphere filled hybrid jute-glass epoxy composites under saline water environment for tensile specimen	104
4.16	Diffusion curve fitting for cenosphere filled hybrid jute-glass epoxy composites under distilled environment for tensile specimen	104
4.17	Diffusion curve fitting for cenosphere filled hybrid jute-glass epoxy	105

	composites under distilled environment for flexural specimen	
4.18	Diffusion curve fitting for cenosphere filled hybrid jute-glass epoxy composites under saline environment for flexural specimen	105
4.19	Example Plot of percentage of moisture absorption versus square root of time for calculation of Diffusivity	106
4.20	Variation of moisture absorption of cenosphere filled glass-jute(GJJG) composites with square root of immersion time at distilled water for tensile specimen	106
4.21	Variation of moisture absorption of cenosphere filled glass-jute (GJJG) composites with square root of immersion time at saline water for tensile specimen	107
4.22	Variation of moisture absorption of cenosphere filled glass-jute (GJJG) composites with square root of immersion time at distilled water for flexural specimen	107
4.23	Variation of moisture absorption of cenosphere filled glass-jute (GJJG) composites with square root of immersion time at saline water for flexural specimen	108
4.24	Flexural strength of cenosphere filled hybrid glass-jute (GJJG) epoxy composite after exposure to environmental conditions	108
4.25	Tensile strength of cenosphere filled hybrid glass-jute (GJJG) epoxy composites after exposure to environmental conditions	109
4.26	(a-d): SEM images of tensile fractured surfaces of 20wt.% cenosphere filled hybrid glass-jute (GJJG) epoxy composites in distilled and saline water environment at lower and higher magnification	110
4.27	(a-d): SEM images of flexural fractured surfaces of 20wt.% cenosphere filled hybrid glass-jute (GJJG) epoxy composites in distilled and saline water environment at lower and higher magnification	111
5.1	Flow chart of various wear mechanisms	119
5.2	(a) and (b) Schematic representations of the abrasion wear phenomena	120
	(c) Abrasion in the microscale	121

5.3	Schematic representations of the erosive wear mechanism	122
5.4	Schematic of generation of a wear particle as a result of adhesive wear process	123
5.5	Schematic representations of the surface fatigue wear mechanism	124
5.6	Schematic representations of the corrosive wear mechanism	124
5.7	Schematic diagram of brittle, semi-brittle, semi-ductile and ductile type erosive wear	128
5.8	Effect of hardness on stacking sequences of hybrid jute-glass epoxy composites	132
5.9	Schematic diagram of methodology used for velocity calibration	133
5.10	(a) Schematic diagram of erosion test rig (b) Parts of solid particle erosion test set up	134-135
5.11	Variation of erosion rate of hybrid jute-glass composite with different impingement angle at velocity 48m/s	146
5.12	Variation of erosion rate of hybrid jute-glass composite with different impingement angle at velocity 70m/s	146
5.13	Variation of erosion rate of hybrid jute-glass composite with different impingement angle at velocity 82m/s	146
5.14	Histogram showing the steady state erosive wear rates of hybrid composites at different impact velocities (48, 70 and 82 m/s) for 30° impact angle	147
5.15	Histogram showing the steady state erosive wear rates of hybrid composites at different impact velocities (48, 70 and 82 m/s) for 45° impact angle	147
5.16	Histogram showing the steady state erosive wear rates of hybrid composites at different impact velocities (48, 70 and 82 m/s) for 60° impact angle	148

5.17	Histogram showing the steady state erosive wear rates of hybrid composites at different impact velocities (48, 70 and 82 m/s) for 90° impact angle	148
5.18	Variation of erosion efficiency of hybrid composites with particle velocity at impingement angle 45°	149
5.19	Variation of erosion efficiency of hybrid composites with particle velocity at impingement angle 60°	149
5.20	(a-c):Micrographs of eroded samples of hybrid jute-glass epoxy composites	150
6.1	Variation of erosion rate of cenosphere filled jute-glass (GJJG) composites with different impingement angles at velocity 48m/s	165
6.2	Variation of erosion rate of cenosphere filled jute-glass (GJJG) composites with different impingement angles at velocity 70 m/s	165
6.3	Variation of erosion rate of cenosphere filled jute-glass (GJJG) composites with different impingement angles at velocity 82 m/s	165
6.4	Histogram showing the steady state erosion wear rates of filled hybrid composites at three impact velocities (48, 70,82m/s) for 30° impact angle	166
6.5	Histogram showing the steady state erosion wear rates of filled hybrid composites at three impact velocities (48,70,82m/s) for 45°impact angle	166
6.6	Histogram showing the steady state erosion wear rates of filled hybrid composites at three impact velocities (48,70,82m/s) for 60°impact angle	167
6.7	Histogram showing the steady state erosion wear rates of filled hybrid composites at three impact velocities (48, 70,82m/s) for 90°impact angle	167
6.8	Erosion efficiency as a function of impact velocity for cenosphere filled glass-jute(GJJG) hybrid epoxy composites at angle 45°	168
6.9	Erosion efficiency as a function of impact velocity for cenosphere filled glass-jute (GJJG) hybrid epoxy composites at angle 60°	168
6.10	(a) and (b) Micrographs of eroded surface of 5 wt.% of cenosphere filled glass-jute (GJJG) composite at lower and higher magnification at angle 45°	169

6.11	(a) and (b) Micrographs of eroded surface of 20 wt.% of cenosphere filled glass-jute (GJJG) composite at lower and higher magnification at angle 60°	169
7.1	(a) Schematic diagram of abrasive wear test rig (b) Dry sand rubber/wheel abrasion test setup	181
7.2	Schematic representation of different zones on the wear scar	182
7.3	(a) Photographic image of the abraded hybrid glass-jute epoxy composite (b) Photographic image of the abraded cenosphere filled GJJG epoxy composite	182
7.4	Variation of wear volume with respect to loads (N) for different cenosphere weight percentage of abraded hybrid glass-jute(GJJG) epoxy composites	183
7.5	Variation of wear rate with respect to loads (N) for different cenosphere wt. percentage of abraded hybrid glass-jute (GJJG) epoxy composites	183
7.6	Variation of specific wear rate with respect to loads (N) for different cenosphere wt. percentage of abraded hybrid glass-jute (GJJG) epoxy composites	184
7.7	Variation of wear volume with respect to sliding distances(m) for different cenosphere wt. percentage of abraded hybrid glass-jute (GJJG) epoxy composites	184
7.8	Variation of wear rate with respect to sliding distances(m) for different cenosphere wt. percentage of abraded hybrid glass-jute (GJJG) epoxy composites	185
7.9	Variation of specific wear rate with respect to sliding distances(m) for different cenosphere wt. percentage of abraded hybrid glass-jute(GJJG) epoxy composites	185
7.10	Microscopic pictures of abraded hybrid glass-jute(GJJG) epoxy composites at various loads	186
7.11	Microscopic pictures of cenosphere filled abraded hybrid glass-jute(GJJG) epoxy composites	186

List of Tables

Table No.	Title	Page no.
1.1	Advantages and limitations of polymeric matrix materials	8
1.2	A typical composition of jute fiber	13
1.3	Approximate chemical composition of some glass fibers (wt. %)	14
2.1	List of researchers worked on cenosphere filler composites	40-41
3.1	Laminate stacking sequence of hybrid jute-glass epoxy composites	53
3.2	Density and void content of hybrid jute-glass epoxy composites	56
3.3	Mechanical properties of hybrid jute-glass epoxy Composites	60
3.4	Laminate stacking sequence of cenosphere filled hybrid glass-jute epoxy composites	67
3.5	Density and void content of cenosphere filled hybrid jute-glass epoxy composites	70
3.6	Mechanical properties of cenosphere filled hybrid jute-glass epoxy composites	71
4.1	Crystallinity Index of jute fiber and cenosphere powder	86
4.2	Thermal characterization of cenosphere filled hybrid glass-jute epoxy composites	87
4.3	Laminate stacking sequence of cenosphere filled glass-jute(GJJG) epoxy composite	90
4.4	Variation of weight gain and thickness swelling of cenosphere filled hybrid jute-glass(GJJG) epoxy composite with immersion time exposure at distilled water environment for flexural specimens	112
4.5	Variation of weight gain and thickness swelling of cenosphere filled hybrid jute-glass(GJJG) epoxy composite with immersion time exposure at saline water environment for flexural specimens	113
4.6	Variation of weight gain and thickness swelling of cenosphere filled	114

	hybrid jute-glass(GJJG) epoxy composite with immersion time exposure at distilled water environment for tensile specimens	
4.7	Variation of weight gain and thickness swelling of cenosphere filled hybrid jute-glass(GJJG) epoxy composite with immersion time exposure at saline water environment for tensile specimens	115
4.8	Swelling rate parameter of cenosphere filled hybrid jute-glass(GJJG) epoxy composite at different environmental conditions	116
4.9	Diffusion case selection parameter for cenosphere filled hybrid jute-glass(GJJG) epoxy composite	116
4.10	Diffusivity of cenosphere filled hybrid jute-glass(GJJG) epoxy composite	117
5.1	Symptoms and appearance of different types of wear	126
5.2	Impact velocity calibration at various pressures	133
5.3	Test parameters of erosion test	141
5.4	Weight loss and Erosion rate of JJJJ (S1) epoxy composites with respect to impingement angle due to erosion for a period of 15min	141
5.5	Weight loss and Erosion rate of hybrid epoxy composite JGGJ (S2) with respect to impingement angle due to erosion for a period of 15min	142
5.6	Weight loss and Erosion rate of hybrid epoxy composite GJGJ(S3) with respect to impingement angle due to erosion for a period of 15min	142
5.7	Weight loss and Erosion rate of hybrid epoxy composite GJJG(S4) with respect to impingement angle due to erosion for a period of 15min	143
5.8	Parameters characterizing the velocity dependence of erosion rate of hybrid jute-glass epoxy composites	144
5.9	Erosion Efficiency of hybrid jute-glass epoxy composites	145
6.1	Weight loss and Erosion rate of 5% Cenosphere filled GJJG hybrid epoxy composites with respect to impingement angle due to erosion	159

	for a period of 15min	
6.2	Weight loss and Erosion rate of 10% Cenosphere filled GJJG hybrid epoxy composites with respect to impingement angle due to erosion for a period of 15min	160
6.3	Weight loss and Erosion rate of 15% Cenosphere filled GJJG hybrid epoxy composites with respect to impingement angle due to erosion for a period of 15min	161
6.4	Weight loss and Erosion rate of 20% Cenosphere filled GJJG hybrid epoxy composites with respect to impingement angle due to erosion for a period of 15min	162
6.5	Parameters characterizing the velocity dependence of erosion rate of cenosphere filled hybrid glass-jute (GJJG) epoxy composites	163
6.6	Erosion efficiency (η) of cenosphere filled hybrid glass-jute(GJJG) epoxy composites	164
7.1	Test conditions of three-body abrasive wear test	178
7.2	Abrasive wear rate, wear volume and specific wear rate of cenosphere filled hybrid glass-jute(GJJG) epoxy composites at different loads	179
7.3	Abrasive wear rate, wear volume and specific wear rate of cenosphere filled hybrid glass-jute (GJJG) epoxy composites at different sliding distances	180

List of Symbols

D_x	Diffusion coefficient
E_r	Erosion rate
EDX	Energy dispersive X-ray spectroscopy
$FTIR$	Fourier Transform Infrared Spectroscopy
H_0	Sample thickness at any time 't'
H_∞	Sample thickness at equilibrium condition
I_c	Crystallinity index
K_{SR}	Thickness swelling parameter
F	Applied Normal Load in Newton (N)
M_m	Maximum percentage of moisture content
M_t	Moisture absorption at time 't'
SEM	Scanning electron microscope
t	Time
$T(s)$	Thickness swelling
TGA	Thermo gravimetric Analysis
V	Impact velocity in m/s
V_v	Voids content
W	Weight of sample
W_0	Oven-dry weight of sample
W_t	Weight after time 't'
XRD	X-ray Diffraction
Δw	Wear loss/ Weight loss
α	Impingement / Impact angle
η	Erosion efficiency
ρ	Density of composite sample

Chapter 1

Introduction

1.1 Back ground

Composite materials are new generation materials developed to meet the demands of rapid growth of technological changes of the industry. There is always an urge from the engineer for finding an alternative to conventional materials keeping in view a combination of properties expected from new ones. Composites are formed by combining materials together to form an overall structure that is better than the sum of the individual components. The individual components remain separate and distinct within the finished structure. In contrast to metallic alloys, each material retains its separate chemical, physical, and mechanical properties. The earliest man-made composite materials were straw and mud combined to form bricks for building construction. Then the next composite material can be seen from Egypt around 4000 BC where fibrous composite materials were used for preparing the writing material. These were the laminated writing materials fabricated from the papyrus plant. Further, Egyptians made containers from coarse fibers that were drawn from heat softened glass. The most visible applications pave our roadways are in the form of either steel and aggregate reinforced portland cement or asphalt concrete. Those composites closest to our personal hygiene form our shower stalls and bath tubs made of fiber glass, solid surface, imitation granite and cultured marble sinks and counter tops are widely used to enhance our living experiences. These are also used for making bridges, structures such as boat hulls, swimming pool panels, race car bodies and storage tanks. The most advanced examples perform routinely on spacecraft and aircraft in demanding environments. The two main constituents of composite materials are reinforcement and matrix. By choosing an appropriate combination of reinforcement and matrix material, manufacturers can produce properties that exactly fit the requirements for a particular structure for a specific purpose. Composites had a direct impact on materials technology and indirectly reoriented materials science and engineering. Over the last thirty years composite materials, plastics and ceramics have been

the dominant emerging materials. The volume and number of applications of composite materials have grown steadily, penetrating and conquering new markets relentlessly.

Modern composite materials constitute a significant proportion of the engineered materials market ranging from everyday products to sophisticated applications. Composites had a direct impact on materials technology and indirectly reoriented materials science and engineering. Over the last thirty years composite materials, plastics and ceramics have been the dominant emerging materials. The volume and number of applications of composite materials have grown steadily, penetrating and conquering new markets relentlessly. Modern composite materials constitute a significant proportion of the engineered materials market ranging from everyday products to sophisticated applications. While composites have already proven their worth as weight-saving materials, the current challenge is to make them cost effective. The efforts to produce economically attractive composite components have resulted in several innovative manufacturing techniques currently being used in the composites industry. It is obvious, especially for composites, that the improvement in manufacturing technology alone is not enough to overcome the cost hurdle. It is essential that there be an integrated effort in design, material, process, tooling, quality assurance, manufacturing, and even program management for composites to become competitive with metals. Demands on high performance engineering materials have led to the extensive research and development in the field of composite material. This worldwide interest during the last four decades has led to the prolific advancement in the field of composite materials and structures. Substantial progress has been made in the development of stronger and stiffer fibres, metal, ceramic, polymer matrix and nano composite, manufacturing and machining processes, quality control, non-destructive evaluation techniques, test methods as well as design and analysis methodology.

Composites are one of the fastest growing industries and continue demonstrate a significant impact on the material world. Hence there has been an extraordinary explosion in composite usages, research and application. Now advanced composites find unusual and exotic applications in industrial, automotive, aircraft, structural and superconductive sectors. Thus the modern man made composites have now firmly established as the future material and are destined to dominate the material scenario right through the twenty first century.

1.2 Composites

Composites are one of the most advanced and adaptable engineering materials known to human beings. Progresses in the field of materials science and technology have given birth to these fascinating and wonderful materials. Composites are heterogeneous in nature, created by the assembly of two or more components with fillers or reinforcing fibers and a compactable matrix [1]. The matrix may be metallic, ceramic or polymeric in origin. It gives the composites their shape, surface appearance, environmental tolerance and overall durability while the fibrous reinforcement carries most of the structural loads thus giving macroscopic stiffness and strength [2]. A composite material can provide superior and unique mechanical and physical properties because it combines the most desirable properties of its constituents while suppressing their least desirable properties. At present composite materials play a key role in aerospace industry, automobile industry and other engineering applications as they exhibit outstanding strength to weight and modulus to weight ratio. High performance rigid composites made from glass, graphite, kevlar, boron or silicon carbide fibers in polymeric matrices have been studied extensively because of their application in aerospace and space vehicle technology.

1.3 Classification of Composites

Composite materials can be classified in different ways [3]. Classification based on the geometry of a representative unit of reinforcement is convenient since it is the geometry of the reinforcement which is responsible for the mechanical properties and high performance of the composites. Based on the types of reinforcement used, the composites are classified as follows is shown in figure1.1.

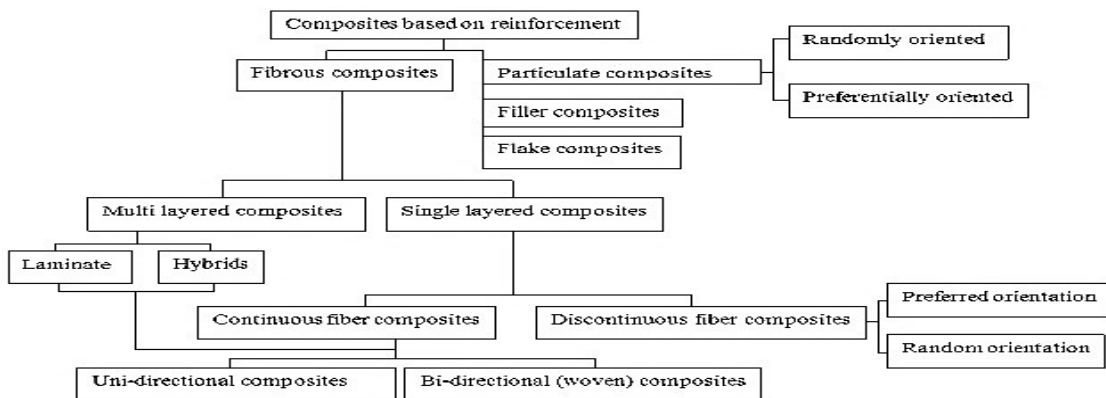


Figure 1.1: Classification of composites

1.3.1 Particulate reinforced composites

A composite whose reinforcement is a particle with all the dimensions roughly equal are called particulate reinforced composites. Particulate fillers are employed to improve high temperature performance, reduce friction, increase wear and abrasion resistance and to reduce shrinkage. [4] The particles will also share the load with the matrix, but to a lesser extent than a fiber. A particulate reinforcement therefore improves stiffness but will not generally strengthen. The name itself indicates that the reinforcement is of particle nature. It may be spherical, cubic, tetragonal, a platelet, or of other regular or irregular shape, but it is approximately equiaxed. In general, particles are not very effective in improving fracture resistance but they enhance the stiffness of the composite to a limited extent. Hence particulate fillers are widely used to improve the properties of matrix materials such as to modify the thermal and electrical conductivities, improve machinability and increase surface hardness.

1.3.2 Fiber reinforced composites

Fiber reinforced composites contain reinforcements having lengths higher than cross sectional dimension. Fibrous reinforcement represents physical rather than a chemical means of changing a material to suit various engineering applications. Reinforcing fiber in a single layer composite may be short or long based on its overall dimensions. Composites with long fibers are called continuous fiber reinforcement and composite in which short or staple fibers are embedded in the matrix are termed as discontinuous fiber reinforcement (short fiber composites). In continuous fiber composites fibers are oriented in one direction to produce enhanced strength properties. In short fiber composites, the length of short fiber is neither too high to allow individual fibers to entangle with each other nor too small for the fibers to lose their fibrous nature. The reinforcement is uniform in the case of composites containing well dispersed short fibers. There is a clear distinction between the behavior of short and long fiber composites. Fibers, because of their small cross-sectional dimensions, are not directly usable in engineering applications. They are, therefore, embedded in matrix materials to form fibrous composites. The matrix serves to bind the fibers together and protect them against environmental attack and damage due to handling. In discontinuous fibre reinforced composites, the load transfer function of the matrix is more critical than in continuous fibre composites.

1.3.3 Hybrid composites

Composite materials incorporated with two or more different types of fillers especially fibers in a single matrix are commonly known as hybrid composites. Hybridisation is commonly used for improving the properties and for lowering the cost of conventional composites. There are different types of hybrid composites classified according to the way in which the component materials are incorporated. Hybrids are designated as i) sandwich type ii) interply iii) intraply and iv) intimately mixed [5-6]. In sandwich hybrids, one material is sandwiched between layers of another, whereas in interply, alternate layers of two or more materials are stacked in regular manner. Rows of two or more constituents are arranged in a regular or random manner in intraply hybrids while in intimately mixed type, these constituents are mixed as much as possible so that no concentration of either type is present in the composite material. Hybrid materials obtained through interaction of chemically different constituents, usually organic and inorganic, which form a specific (crystal, spatial) structure that is different from the structures of initial reagents, but often inherits certain motifs and functions of the original structures. Hybrid composites are manufactured by combining two or more fibers in a single matrix. Hybrid materials are also composites consisting of two constituents at the nanometer or molecular level. Thus, they differ from traditional composites where the constituents are at the macroscopic (micrometer to millimeter level). Mixing at the microscopic scale leads to a more homogeneous material that either shows characteristics in between the two original phases or even new properties. The purpose of hybridization is to increase a resistance against the interlaminar toughness that cannot be obtained with only conventional composite material. The use of hybrid materials in composite structural is become more in a day. The fibres can be arranged in various orientations during preparation of composite. However, there are other factors such as cost, weight, post-failure behaviour lead the designer to use of hybridization in order to tailor the material to exact needs under design.

Hybrid polymer composites were developed mostly using thermosetting resins, ranging from epoxy to polyester and poly vinyl ester, etc. Epoxy resins and derived blends were preferred due to their versatility in use with all manufacturing technologies, good compatibility with almost all types of fibers, both synthetic and natural. The consumption of composites, either thermoplastics or thermosetting, is controlled by user market demand. The

ability to adapt these materials to economic and technical market requirements relies on the innovation in terms of both materials and processes, supplemented by adaptability to the environmental constraints (i.e. circular 3R concept-Recycling, reusing and remanufacturing). Specially epoxy resin is used in these hybrid composites because it provides a unique balance of chemical and mechanical properties combined with extreme processing versatility. In all cases, thermoset resins may be tailored to some degree to satisfy particular requirements.

Hybrid laminated composite are prepared by stacking sheets of Glass/Carbon fibres to required orientation to form angle ply laminates. An individual structural glass fibre is both stiff in tensile and compression. The development of composite materials based on two or more different types of fillers in a single matrix leads to multicomponent system composites with a great diversity of material properties. The multicomponent system also known as hybrid composites. The reinforcement may be fibers, particulate fillers or both. Research has revealed that the behavior of hybrid composites appears to be the weighted sum of the individual components in which there is a more favorable balance between the advantages and disadvantages inherent in any composite material. It is generally accepted that properties of hybrid composites are controlled by factors such as nature of matrix, length and relative composition of the reinforcements, fiber matrix interface and hybrid design [7-8].

1.3.4 Laminates

When there is a single ply or a lay-up in which all of the layers or plies are stacked in the same orientation, the lay-up is called a lamina. When the plies are stacked at various angles, the lay-up is called a laminate. Continuous-fiber composites are normally laminated materials in which the individual layers, plies, or laminae are oriented in directions that will enhance the strength in the primary load direction. A laminate is fabricated by stacking a number of laminae in the thickness direction. Generally three layers are arranged alternatively for better bonding between reinforcement and the polymer matrix, for example plywood and paper. These laminates can have unidirectional or bi-directional orientation of the fiber reinforcement according to the end use of the composite. A hybrid laminate can also be fabricated by the use of different constituent materials or of the same material with

different reinforcing pattern. In most of the applications of laminated composite, man-made fibers are used due to their good combination of physical, mechanical and thermal behaviour.

1.4 Components of a composite material

In its most basic form, a composite material is one, which is composed of at least two elements working together to produce material properties that are different to the properties of those elements on their own. In practice, most composites consist of a bulk material (the 'matrix'), and a reinforcement of some kind, added primarily to increase the strength and stiffness of the matrix.

1.4.1 Role of matrix in a composite

Many materials when they are in a fibrous form exhibit very good strength property but to achieve these properties the fibers should be bonded by a suitable matrix. The matrix distributes the loads evenly between fibers so that all fibers are subjected to the same amount of strain. It helps to avoid propagation of crack growth through the fibers by providing alternate failure path along the interface between the fibers and the matrix. It has also good flow characteristics so that it penetrates the fibre bundles completely and eliminates voids during the compacting/curing process. A good matrix improves impact and fracture resistance of a composite and also carries interlaminar shear. It reduces moisture absorption and possesses low shrinkage and coefficient of thermal expansion. The matrix also protects the fibers from hazardous environment attack.

1.4.2 Materials used as matrices in composites

Based on the matrix material which forms the continuous phase, the composites are broadly classified into metal matrix (MMC), ceramic matrix (CMC) and polymer matrix (PMC) composites.

1.4.2.1 Bulk Phases

(1) Metal Matrices

Metal matrix composites possess some attractive properties, when compared with organic matrices. These include (i) strength retention at higher temperatures, (ii) higher transverse strength, (iii) better electrical and superior thermal conductivity, (iv) higher erosion resistance etc. However, the major disadvantage of metal matrix composites is their higher densities and

consequently lower specific mechanical properties compared to polymer matrix composites. Another notable difficulty is the high-energy requirement for fabrication of such composites.

(2) Polymer Matrices

Polymer matrix composites (PMC) are comprised of a variety of short or continuous fibers bound together by an organic polymer matrix. Polymer matrix composites are much easier to fabricate than MMC and CMC. This is due to the relatively low processing temperature required for fabricating polymer matrix composite. PMC generally consist of synthetic fibers like carbon, nylon, rayon or glass embedded in a polymer matrix, which surrounds and tightly binds the fibers. The reinforcement in a PMC provides high strength and stiffness. The PMC is designed so that the mechanical loads to which the structure is subjected in service supported by the reinforcement. Typically, the fibers make up about 60% of a polymer matrix composite by volume. A very large number of polymeric materials, both thermosetting and thermoplastic, are used as matrix materials for the composites. Some of the major advantages and limitations of resin matrices are shown in table 1.1.

Table 1.1: Advantages and limitations of polymeric matrix materials

Advantages	Limitations
Low densities	Low transverse strength
Good corrosion resistance	Low operational temperature limits
Low thermal conductivities	
Low electrical conductivities	
Translucence	
Aesthetic colour effects	

(3) Ceramic Matrices

Ceramic fibers, such as alumina and SiC (Silicon Carbide) are advantageous in very high temperature applications, and also where environment attack is an issue. Since ceramics have poor properties in tension and shear, most applications as reinforcement are in the

particulate form (e.g. zinc and calcium phosphate). Ceramic Matrix Composites (CMC) are used in very high temperature environments, these materials use a ceramic as the matrix and reinforce it with short fibers, or whiskers such as those made from silicon carbide and boron nitride.

1.4.2.2 Reinforcement

The role of the reinforcement is to strengthen and stiffen the composite through prevention of matrix deformation by mechanical restraint. The function of the reinforcement depends upon its type in structural composites. All of the different fibers, fillers and flakes used in composites have different properties and so affect the properties of the composite in different ways. For most of the applications, the fibers need to be arranged into some form of sheet, known as fabric, for easy handling. Different ways for assembling fibers into sheets and the variety of fibre orientations are possible to achieve separate characteristics. The careful selection of reinforcement type enables finished product characteristics to be customized to almost any specific engineering requirement.

1.4.2.3 Interface

It has characteristics that are not depicted by any of the component in isolation. The interface is a bounding surface or zone where a discontinuity occurs, whether physical, mechanical, chemical etc. The matrix material must “wet” the fibre. Coupling agents are frequently used to improve wet ability. The “wetted” fibers increase the interface surface areas. To obtain desirable properties in a composite, the applied load should be effectively transferred from the matrix to the fibers via the interface. This means that the interface must be large and exhibit strong adhesion between fibers and matrix. Failure at the interface (called debonding) may or may not be desirable.

1.5 Natural fiber composites

Now-a-days, research and engineering interests have been shifting from traditional synthetic fiber composite to lignocellulosic natural fiber composite due to their advantages like high strength to weight ratio, non-carcinogenic and bio-degradability [3,9-11]. Besides the availability of natural fibers and easy of manufacturing have tempted researchers to try locally available inexpensive fiber and to study their feasibility of reinforcement purpose and to what extent they satisfy the required specifications of good reinforced polymer composite for different applications. With low cost and high specific mechanical properties, natural

fiber represents a good renewable and biodegradable alternative to the most common synthetic reinforcement, i.e. glass fiber.

The term “natural fiber” covers a broad range of vegetable, animal and mineral fibers. However in the composite industry, it usually refers to woods, bones, stones, fiber and agro based bast, leaf, seed, and stem fibers are natural composites, as they are either grown in nature or developed by natural processes. These fibers often contribute greatly to the structural performance of plant and when used in plastic composites, can provide significant reinforcement. Wood is a fibrous material consisting of thread like hollow elongated organic cellulose that normally constitutes about 60-70% of wood of which approximately 30-40% is crystalline, insoluble in water, and the rest is amorphous and soluble in water. Cellulose fibres are flexible but possess high strength. The more closely packed cellulose provides higher density and higher strength. The walls of these hollow elongated cells are the primary load bearing components of trees and plants. When the trees and plants are live, the load acting on a particular portion (e.g., a branch) directly influences the growth of cellulose in the cell walls located there and thereby reinforces that part of the branch, which experiences more forces. This self-strengthening mechanism is something unique that can also be observed in the case of live bones. Bones contain short and soft collagen fibers i.e., inorganic calcium carbonate fibers dispersed in a mineral matrix called apatite. The fibers usually grow and get oriented in the direction of load. Human and animal skeletons are the basic structural frame works that support various types of static and dynamic loads. The most remarkable features of woods and bones are that the low density, strong and stiff fibers are embedded in a low density matrix resulting in a strong, stiff and lightweight composite.

Despite the interest and environmental appeal of natural fibers, their use is limited to non-bearing applications due to their lower strength compared with synthetic fiber reinforced polymer composite. The stiffness and strength shortcomings of bio composites can be overcome by structural configurations and better arrangement in a sense of placing the fibers in specific locations for highest strength performance. Accordingly extensive studies on preparation and properties of polymer matrix composite (PMC) replacing the synthetic fiber with natural fiber like Jute, Sisal, Pineapple, Bamboo and Kenaf were carried out [12-17].

These plant fibers have many advantages over glass or carbon fiber like renewable, environmental friendly, low cost, lightweight and high specific mechanical performance.

Increased technical innovation, identification of new applications, continuing political and environmental pressure and government investments in new methods for fiber harvesting and processing are leading to projections of continued growth in the use of natural fibers in composites, use of 150,000 tonnes bio composites (using 80,000 tonnes of wood and natural fibres) in the automotive sector in 2012 could expand to over 600,000 tonnes of biocomposites in 2020, using 150,000 tonnes of wood and natural fibres each along with some recycled cotton[18-19]. The easy availability of natural fibers and manufacturing have motivated researchers worldwide recently to try locally available inexpensive fibers and to study their feasibility of reinforcement purposes and to what extent they satisfy the required specifications of good reinforced polymer composite for various mechanical and tribological applications.

1.5.1 Jute fiber

Jute is an annual plant in the genus *corchorus*. The major types grown are generally known as white jute and tossa jute. Jute, grown mainly in India and Bangladesh, is harvested at 2 to 3 months of growth, at which time it is 3-5 meters tall. Jute has a pithy cover, known as jute stick and the blast fibers grow lengthwise around this core. Jute blast fiber is separated from the pith in a process known as retting. Retting is accomplished by placing cut jute stalks in ponds for several weeks. Microbial action in the pond softens the jute fiber and weakens the bonds between the individual fiber and the pith. The fiber stands are then manually stripped from the jute stick and hung on tracks to dry. Very long fiber stands can be obtained this way. If treated with various oils or conditioners to increase flexibility, the retted jute fiber stands are suitable for manufacturing of textiles.

Jute is multicelled in structure as shown in figure 1.2. The cell wall of a fiber is made up of a number of layers: the so-called primary wall (the first layer deposited during cell development) and the secondary wall (S), which again is made up of the three layers (S₁, S₂ and S₃). As in all lignocelluloses fibres, these layers mainly contain cellulose, hemicelluloses and lignin in varying amounts. The individual fibres are bonded together by a lignin rich region known as the middle lamella. Cellulose attains highest concentration in the S₂ layer

(about 50%) and lignin is most concentrated in the middle lamella (about 90%) which, in principle, is free of cellulose. The S_2 layer is usually by far the thickest layer and dominates the properties of the fibres. Cellulose, a primary component of the fiber, is a linear condensation polymer consisting of D-anhydro-glucopyranose units joined together by β -1,4-glucosidic bonds. The long chains of cellulose are linked together in bundles called microfibrils as in figure 1.3.

Hemicelluloses are also found in all plant fibres. Hemicelluloses are polysaccharides bonded together in relatively short, branching chains. They are intimately associated with the cellulose microfibrils, embedding the cellulose in a matrix. Hemicelluloses are very hydrophilic and have lower molecular masses than both cellulose and lignin. The degree of polymerization is about 50-200. The two main types of hemicelluloses are xylans and glucomannans.

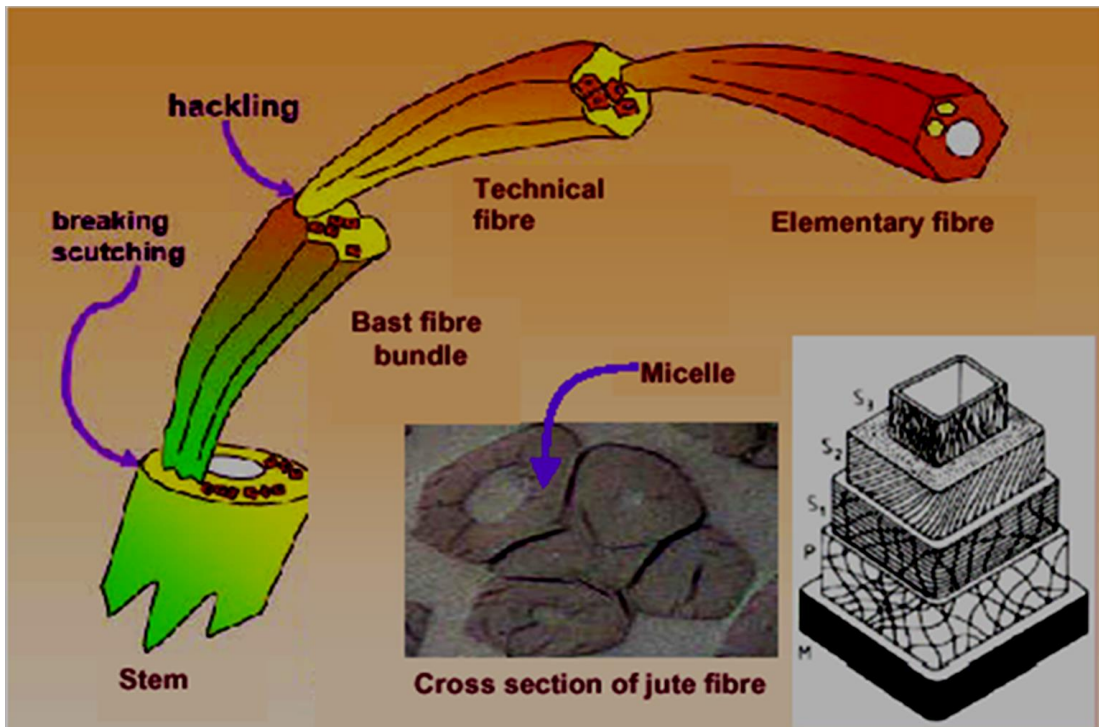


Figure 1.2: Schematic diagram of jute fiber structure

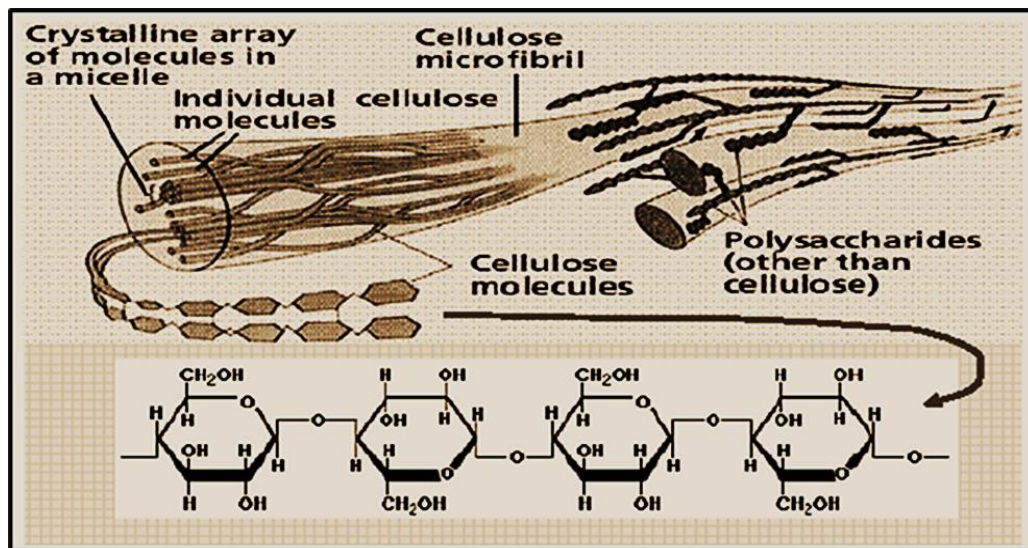


Figure 1.3: Structure of cellulose as it occurs in a plant cell wall

The structure of the jute fiber is influenced by climatic conditions, age and the fermentation process, which also influences the chemical composition [20]. A typical composition of the jute fiber, is shown in table 1.2.

Table 1.2: A typical composition of jute fiber

Substances	Weight percent (%)
Cellulose	61-71.5
Hemicelluloses	13.6-20.4
Pectin	0.2
Lignin	12-13
Moisture content	5-12.6
Wax	0.5

There is a greater awareness of the need for materials with an expanding population and jute based composites provide an opportunity to fill this gap within a cost effective and acceptable environmental framework. Our history using jute in textile applications has limited our expectations of performance, which ultimately limits our ability to accept for improved jute based composite materials. This is interesting as we have accepted completely new material such as material alloys, ceramics, and plastics that have limitations in their performance. But we tend to overlook any deficiencies that may have because our

expectations of these materials are higher than those we have for jute-based composites. It may be because we think we know everything about jute because it is very old familiar fiber used by common people for low cost markets. Jute fiber is a not a low value resource with poor properties and it can be used in a great value added products. Using jute fiber for composites has many advantages. Jute is renewable, versatile, nonabrasive, porous, hygroscopic, viscoelastic, biodegradable, combustible, computable and reactive. The fiber has a high aspect ratio, high strength to weight ratio, low in energy conversion, and has good insulation properties. The jute fiber composites can be very cost-effective material especially for building, construction industries (panels, false ceilings, partition boards etc.), packaging, automobile, railway coach interiors and storage devices.

1.5.2 Glass fiber

Glass fibers are silica based glass compounds that include some metal oxides which can be used to produce different types of glass. A variety of different chemical compositions is commercially available. Common glass fibers are silica based (50-60% SiO_2) and contains a host of other oxides of calcium, boron, sodium, aluminum, and iron. The composition of some common used glass fibers are given in table 1.2. The designation 'E' stands for electrical because E-glass is a good electrical insulator in addition to having good strength and a reasonable Young's Modulus. 'C' stands for corrosion because C-glass has a better resistance to chemical corrosion, 'S' stands for high silica content that makes S-glass withstand higher temperature than other glasses. It should be pointed out that most of the continuous glass fiber produced is of the E-glass type. Electrical use of E-glass fibers are only small fraction of the total market.

Table 1.3: Approximate chemical composition of some glass fibers (wt.%)

Composition	E-glass	C-glass	S-glass
SiO_2	55.2	65.0	65.0
Al_2O_3	8.0	4	25.0
CaO	18.7	14.0	-
MgO	4.6	3.0	10
Na_2O	0.3	8.5	0.3
K_2O	0.2	-	-
B_2O_3	7.3	5.0	-

1.5.3 Limitation of glass fiber

Glass fiber reinforced composites have certain limitations

1. Comparatively low modulus of elasticity (the specific modulus of unidirectional fiber glass composites is of same order as aluminum, titanium, magnesium and steel).
2. Low interlaminar shear strength and compressive properties in relation to tensile strength
3. Poor abrasion resistance causing reduced usable strength
4. Poor adhesion to specific polymer matrix materials in humid environments

1.6 FILLER

The term filler is very broad and encompasses a very wide range of materials which plays an important role for the improvement in performance of polymers and their composites. Fillers are the main ingredient or an additional one in a composite. The filler particles may be irregular structures, or have precise geometrical shapes like polyhedrons, short fibers or spheres. Filler materials are used to reduce the material cost, to improve the mechanical properties to some extent and in some cases to improve process ability. Besides, it also increases properties like abrasion resistance, hardness and reduces shrinkages. Therefore a judicious selection of matrix and the reinforcing phase can lead to a composite with combination of strength and modulus comparable or even better than conventional metallic materials. The physical and mechanical properties can further be modified by addition of a solid filler phase to the matrix body during the composite fabrication.

1.6.1 Conventional Fillers

Particulate fillers have played a vital role in the development of commercial uses for polymers. The primary filler types utilized may be classified as either natural or synthetic fillers. Naturally occurring fillers are generally a pure, crystalline mineral. Common natural filler is calcium carbonate (CaCO_3) which has been used in polyvinyl chloride, polypropylene, elastomers, and unsaturated polyesters. Other filler materials include micron sized clay particulates such as kaolinite and metakaolin. These materials have been used to impart electrical resistivity to polyvinyl chloride for cable insulation applications. Crystalline silicas and calcium sulphate are additional commonly employed, natural fillers.

1.6.2 Micro Fillers

Micro fillers are considered to be some of the most useful fillers. Their specific gravity, stable particle size, strength and controlled density to modify products without compromising on profitability or physical properties are their most favorable assets. Micro fillers are particles between (0.1-100) μm in size. Commercially micro particles are available in a wide variety of materials including ceramics, glass, polymers, and metals. Micro fillers encountered in daily life include pollen, sand, dust, fly ash, flour, and powdered sugar. Microparticles have a much larger surface-to-volume ratio than at the macro scale, and thus their behavior can be quite different. Microspheres are spherical micro filler, and are used where consistent and predictable particle surface area is important. Microspheres vary widely in quality, sphericity, uniformity, particle size and distribution. Microspheres can be manufactured from various natural and synthetic materials primarily used as filler and volumizer for weight reduction, retro-reflector for highway safety, additive for cosmetics and adhesives, with limited applications in medical technology. Glass microspheres, polymer microspheres and ceramic microspheres are commercially available micro fillers. Solid and hollow microspheres vary widely in density and, therefore, are used for different applications. Hollow microspheres are typically used as additives to lower the density of a material. Solid microspheres have numerous applications depending on nature, size and type of materials used.

1.6.3 Nano Fillers

Due to recent developments in the field of nanotechnology, there has been growing interest in polymer matrix composites in which nano-sized fillers are distributed homogeneously due to their unique optical, electric and magnetic properties, as well as their dimensional and thermal stability. The nano composite materials are also potential candidates for catalysts, gas-separation membranes, contact lenses and bioactive implant materials. In nano composites, at least one dimension of the dispersed particles is in the nanometer range. When the three dimensions are in the order of nanometers, called as isodimensional nanoparticles. Carbon black, silica, aluminum oxide, titanium dioxide, zinc oxide, silicon carbide, polyhedral oligomeric silsesquioxanes (POSS) are examples for nanoparticle fillers. Particulate composites reinforced with micron sized particles of various materials are the most widely used composites in today's structures. Particles are typically added to enhance the matrix

elastic modulus and yield strength. By scaling the particle size down to the nanometer scale, it has been shown that novel material properties can be obtained. The infusion of nanoparticles into polymeric and other matrices results in nano composites materials with enhanced multifunctional characteristics. Recently new nano fillers have more demand and increasing in number such as nano clays, carbon nanotubes, nano oxides etc.

1.7 Particulate Filler

Particulate filler is defined as a non-fibrous solid usually in finely divided form which is added in relatively high proportions to a polymer for technical and economical reasons. They provide improved materials as compared with the unfilled matrix and can also be synergistic with a fiber reinforcement to further improve the system performance. There are many good reasons for using particulate filler in plastic, metal, ceramic matrix in addition to the usual reduction of cost of final product. In case of plastic, addition of fillers provides reduction of shrinkage during cure of a thermoset polymer system results in avoidance of cracking in large molded parts. Thermal conductivities of mineral fillers are usually in order of ten times greater than thermal conductivity of polymers.

Different types of particulate fillers classified as mineral, natural or synthetic, organic/inorganic fillers. The mineral fillers are calcium carbonate (CaCO_3), clay, feldspar, talc, Alumina trihydrate, natural silica and mica. Manufactured fillers include products such as glass beads, metal powders and synthetic silicas. Particulate organic fillers include wood flour, carbon black, various starches, Peanut shell, ground rice husk and reclaimed rubber.

Low density particulate fillers are available and include pearlite, hollow microsphere of glass, ceramic or organic polymers such as phenolic and polyvinyl chloride. Specific particulate fillers give composite materials special characteristics such as better electrical and thermal conductivity, biodegradability, thermo chromic and photochromic characteristics, low surface friction and improved mechanical and magnetic properties. The magnitude of the property change observed is not only a function of the filler composition but is strongly influenced by particle size, shape, and surface chemistry. Particle size, shape, and ability to bond with the polymer matrix are all important factors in determining filler performance.

1.7.1 Cenosphere

A cenosphere is a lightweight, inert, hollow sphere made largely of silica and alumina and filled with air or inert gas. It is typically produced as a byproduct of coal combustion at thermal power plants. After recovery, drying and size classification, cenospheres produce a free flowing white or grey white powder. The Chemical composition of cenosphere consists of SiO_2 , Al_2O_3 , Fe_2O_3 , CaO , MgO , K_2O , Na_2O and SO_3 . The density of cenosphere is about $(0.4\text{-}0.8) \text{ g/cm}^3$, which gives them a great buoyancy. Generally the ceramic particles in fly ash have three types of structures. The first type of particles are called as solid precipitator. The second type of particles is hollow and are called cenospheres[21-22]. The third type of particles are called plerospheres, which are hollow particles of large diameter filled with smaller size precipitator and cenosphere. Hence the filler addition into polymer matrix composites leads to great improvement of their properties and increases the demand on fillers.

1.7.2 Need for cenosphere as reinforcing filler material

Since resins are very expensive, it will not be cost effective to fill up the voids in a composite matrix purely with resins. Fillers are added to the resin matrix for controlling material cost and improving its mechanical and chemical properties. These fillers are relatively high price even after giving numerous advantages. This problem can be remitted by exploring the possibility of using some cheaper filler materials such as industrial wastes and slag. Rapid industrial development over the last decade has led to the generation of large amounts of solid waste in the form of ash, mud or slag, which has now come to a stage of environmental threat and needs disposal and/or utilization. Most of these wastes are buried in landfills, which is costly and environmentally unsatisfactory. It is evident from the characteristics of some of these wastes, generated from different processes, that they have good potential for recycling and utilization in developing various value-added products.

In the past two decades, ceramic filled polymer composites have emerged as a subject of extensive research, but due to the high cost of conventional fillers it has become important to explore the potential use of cheap materials like minerals ores and industrial wastes like fly ash and red mud for utilization in preparing particles reinforced polymer composites. Cenosphere is such an industrial waste, the potential of which as a filler material in polymers needs to be explored. It is generated during the combustion of coal in thermal power plant for

energy production and an industrial by-product which is recognized as an environmental pollutant. Now-a-days, as environmental problem is a matter of concern, hence considerable research has been under taken on the subject worldwide [23-24]. The research and development carried out in India for utilization of fly ash derivative in making light weight building materials has proved that cenosphere filler can be successfully used for manufacturing of bricks, blocks, cement and tiles etc. Some areas of cenosphere filler utilization wherein technology projects have been completed or are under way include mine filling, insulation, automobile bodies, fire and heat protection devices, sports equipment and sealants. It can also be used as a feedstock in the formulation of specific types of refractories.

Indigenous technologies for construction of building materials utilizing fly ash derivatives are available and are being practised in a few industries. However, large scale utilization is yet to taken off. Even if the full potential of fly ash utilization through production of cenosphere bricks and blocks is explored, the quantity of cenosphere produced by the thermal power plants is so huge that major portion of it will still remain unutilized. Hence, there is a need to evolve strategies and plans for safe and environmentally sound method of its disposal. This disposal and utilization of fly ash derivative will continue to be an important area of global concern due to dependence of countries like India on coal based power generation. It is true that from the same time from coal utilization perspective, cenosphere is a resource yet to be fully utilized. This is why the producers of thermal electricity keep looking for ways to exploit fly ash derivatives.

Cenosphere as a fly ash derivative is used as particulate reinforcement in composite industry. It has characteristics of fine dispersion and structural homogeneity. It provides enhanced mechanical properties like elastic modulus, toughness, high durability and inertness. It has properties of better surface finish, chemical and dimensional stability, weight reduction and cost effective. However, very little is reported on its potential as filler material in hybrid polymer matrix composites.

Visualizing the increase rate of generation of cenosphere as a waste material, though it has got lot of aesthetic values, its potential use for manufacturing value added products has

not been addressed so far in a large scale. The present research work has been under taken with an objective to explore the use of cenosphere as a potential filler with jute and glass fiber as reinforcing material in polymer matrix composite. The low modulus of glass-reinforced composites has limited their usefulness in applications where buckling stability or high natural frequency is criteria. Both shear and compressive deficiencies have restricted performance in bending. In this present investigation an attempt has been made to prepare woven jute-glass fiber hybrid composite by keeping orientation of jute fiber as $(45^{\circ}\text{-}45^{\circ})$ and that of glass fiber as $(0^{\circ}\text{-}90^{\circ})$ to get the optimum mechanical performance. Efforts are also made to study the effect of hybridization of glass and jute layering sequence on tensile strength, flexural strength, interlaminar shear strength, tensile modulus and flexural modulus of the composites without filler. The improvement in the flexural and tensile strength of the composites is also observed with cenosphere addition and a comparison has been made with the unfilled hybrid glass-jute composite of stacking sequence (GJJG). Experiments were also carried out to study the impact of cenosphere on the mechanical, tribological behaviour and environmental performance by subjecting the developed composites to saline and distilled water condition. Scanning Electron Microscope studies are also made to ascertain the fracture behavior of the developed composites and reported in the thesis.

In the second chapter detailed discussion on reinforcement materials, overview of fabrication processes and work related to present investigation available in literatures are depicted.

In the third chapter the mechanical and flexural behavior of the hybrid jute-glass composites of optimum stacking sequence (GJJG) with and without cenosphere filler has been studied.

In the fourth chapter the effect of environment on the mechanical characterization of cenosphere filled glass-jute reinforced composites along with moisture absorption properties has been presented.

In the fifth chapter the solid particle erosion response of different layering sequences of the glass-jute hybrid epoxy composites has been investigated.

The sixth chapter discusses the effect of particulate filler (cenosphere) on the erosion wear response of the developed composites.

The seventh chapter describes the three-body abrasive wear performance of cenosphere filled glass-jute composite of optimum stacking sequence with microscopic analysis.

In the eighth chapter conclusions have been drawn from the above studies mentioning the scope for the future work.

Chapter 2

Literature Survey

2.1 Introduction

The literature survey is carried out as a part of the thesis work to have an overview of the production processes, properties and tribological behavior of polymer composite. Composite structures have shown universally a savings of at least 20% over metal counterparts and a lower operational and maintenance cost [25]. As the data on the service life of composite structures is becoming available, it can be safely said that they are durable, maintain dimensional integrity, resist fatigue loading and are easily maintainable and repairable. Composites will continue to find new applications, but the large scale growth in the market place for these materials will require less costly processing methods and the prospect of recycling [26] will have to be solved [27].

Composites materials have emerged as a major class of structural elements and are either used or being considered as substitutions for metals/traditional material in aerospace, automotive and other industries. The outstanding features of fiber reinforced polymer composites (FRPs) are their high specific stiffness, high specific strength and controlled anisotropy, which make them very attractive structural materials. Other advantages of composites are light weight, good corrosion resistance, impact resistance, fatigue strength and flexibility in design capabilities. A unique feature of composites is that the characteristics of the finished product can be tailored to a specific engineering requirement by a careful selection of matrix and reinforcement type. FRP composite materials consist of two or more chemically distinct constituents have a distinct interface separating them. It has a unique combination of properties that are noticeably different from the constituent properties.

Generally, a discontinuous phase (reinforcement) is embedded into a continuous phase (matrix). Polymer based composite materials (PMC) or FRP constitutes a major category of composites materials with a wide range of applications. They offer very attractive properties, which can be tailored to the specific requirements by careful selection the fiber,

matrix, fiber configuration (short, long, strength, woven, braided, laminated, etc.) and fiber surface treatment. PMCs exhibit desirable physical and chemical properties that include lightweight coupled with high stiffness and strength along the direction of the reinforcing fiber, dimensional stability, temperature and chemical resistance and relatively easy processing.

The role of matrix in a fiber-reinforced composite is to

- (a) Transfer stresses between the fibers
- (b) Provide a barrier against an adverse environment
- (c) Protect the surface of fibers from mechanical abrasion

2.2 Material selection

Many materials when they are in fibrous form exhibit very good strength properties but to achieve these properties the fiber should be bonded by a suitable matrix. The matrix isolates the fibers from one another in order to prevent abrasion and formation of new surface flaws and acts as a bridge to hold the fibers in place. A good matrix should possess ability to deform easily under applied load, transfer the load on to the fibers and evenly distribute stress concentration.

A study of the nature of bonding forces in laminates indicates that upon initial loading there is a tendency for the adhesive bond between them accounts for the high strength properties of the laminates. The polymer matrix binds the fibers together so as to transfer the load to and between them and protect them from environments and handling. Polymer or resin systems used to manufacture advanced Polymer Matrix Composites (PMCs) are of two basic types, thermosets and thermoplastics (including bio-derived ones).

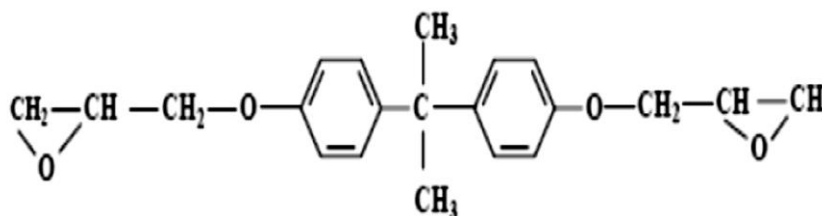
2.2.1 Thermosets

In most of the earlier work, thermosetting resins are used as matrix material for composite production. Products like tufnol which is made from cotton fibers and epoxy resin, have been available for some time, having good stiffness and strength[28]. In the last few years there has been renewed interest in these products for use in automotive applications. To achieve reinforcing effects in composites it is necessary to have good adhesion between the

fibers and resins. Epoxy and phenolic thermosetting resins are known to be able to form covalent cross-links with plant cell walls via -OH groups [29]. Composite manufacture can be achieved using low viscosity epoxy and phenolic resins that cure at room temperature. In addition epoxy resin does not produce volatile products during curing which is most desirable in production of void free composites. Therefore, although epoxy resins are relatively more expensive than polyester, they have potential for the development of high added value plant fiber composites, where long fibers at a high content are required.

The functional group in epoxy resins is called the oxirane, a three-membered strained ring containing oxygen. Epoxy resins, depending on their backbone structure, may be low or high viscosity liquids or solids. In low viscosity resin, it is possible to achieve a good wetting of fibre by the resin without using high temperature or pressure. The impregnation of fibers with high viscosity resins is done by using high temperature and pressure.

A wide range of starting materials can be used for the preparation of epoxy resins thereby providing a variety of resins with controllable high performance characteristics. These resins generally are prepared by reacting to a polyfunctional amine or phenol with epichlorohydrin in the presence of a strong base. The commercially available diglycidyl ether of bisphenol-A (DGEBA) shown in figure 2.1 is characterized by epoxy equivalent weight, which can be determined either by titration or quantitative infrared spectroscopy. The presence of glycidyl units in these resins enhances the process ability but reduces thermal resistance.



The most widely used curing agents for epoxy resins are primary and secondary amines. The overall reaction rate of an amine with an epoxide is influenced by the steric hindrance and the electron withdrawing or electron donating groups present in the amine [30]. During curing, epoxy resins can undergo three basic reactions: Epoxy groups are rearranged and form direct linkages between themselves.

1. Aromatic and aliphatic -OHs link up to the epoxy groups
2. Cross-linking takes place with the curing agent through various radical groups

The advantages of epoxy resins are low polymerization shrinkages unlike polyesters during cure, good mechanical strength, excellent resistance to chemicals and solvents, and excellent adhesion to fibers. The epoxy molecule also contains two ring groups at its center, which are able to absorb both mechanical and thermal stresses better than linear groups, giving epoxy resin very good stiffness, toughness and heat resistance.

The primary disadvantages of the epoxy resins are that they require long curing times and, in general, their mold release characteristics are poor. The epoxy resins are characterized by their high adhesive strengths. This property is attributed to the polarity of aliphatic -OH groups and ether groups that exist in both the initial resin and cured system. The polarity associated with these groups promotes electromagnetic bonding forces between epoxy molecules and the polar fibers.

2.2.2 Bio-derived Thermoplastic Matrices

Cellulose fibers (e.g. hemp, flax, jute) are widely used with conventional thermoplastic polymers (e.g. Polypropylene (PP), polyether (PE)) as reinforcement in composite production to improve mechanical properties. In fact, the history of composites from renewable resources is far longer than conventional polymers. The study and utilization of natural polymers is an ancient science. Typical examples, such as paper, silk, skin, and bone arts, can easily be found in museum around the world. In the biblical Book of Exodus, Moses's mother built the ark from rushes, pitch and slime a kind of fiber reinforced composite, according to the current classification of material. During the opium war more than 1000 years ago, the Chinese built their castles to defend against invaders using a kind of

mineral particle reinforced composite made from gluten rice, sugar, calcium carbonate and sand [31].

However, the availability of petroleum at a lower cost and the bio-chemical inertness of petroleum based products have proven disastrous for the market of natural polymers. It is only about last two decades when the significance of eco-friendly materials has been realized. Now polymers from renewable resources have started drawing an increasing amount of attention. The two main reasons for that are environmental concerns [32], and the realization that the petroleum resources are limited.

Generally, polymers from renewable resources can be classified into three groups: (1) natural polymers such as starch, protein, and cellulose (2) Synthetic polymers from natural monomers, such as polylactic acid (PLA) and (3) polymers from microbial fermentation, such as polyhydroxy butyrate (PHB). Like numerous other petroleum based polymers, many properties of polymers from renewable resources can be improved through composite production [31].

The development of synthetic polymers like polylactic acid using monomers from natural resources has been a driving force for the development of biodegradable polymers from renewable resources. Therefore, in today's world polylactic acid is the most promising among bio-derivable polymers[32]. Polylactic acid can be processed (e.g.compression molding, pultrusion, extrusion and injection moulding) like petroleum based polyolefins and its mechanical property is better than the widely used polymer PP [33]. On degradation polylactic acid does not emit any carbon dioxide to the environment like other biodegradable materials from renewable resources. The degradation occurs by hydrolysis to lactic acid, which is metabolized by micro-organisms to water and carbon dioxide. If polylactic acid is comprised together with other biomass, the biodegradation occurs within a couple of weeks and the material can fully disappear within a month [34]. Chemically, it is linear aliphatic polyester of lactic acid which can be obtained by fermentation of renewable agricultural materials like corn, sugarcane and sugar beets. Lactic acid is converted to a cyclic lactide dimer which is then polymerized to polylactic acid through a ring opening reaction.

The major applications of polylactic acid products are in household wastes as plastic bags, barriers for sanitary products and diapers, planting, and disposable cups and plates. However, a number of authors reported the possibilities of developing fully bio-degradable composite products by using biodegradable polymers as matrix and natural fibers as reinforcements [35, 36]. Keller *et al.* [37] reported that polylactic acid should produce fiber reinforced composites with high mechanical properties for light weight construction materials. Oksman *et al.* [33] observed that polylactic acid had good potential as a polymer matrix in flax fiber reinforcement for composites production. They reported that the composite strength produced with PLA/flax was about 50% better than that of PP/flax composites. Due to the increasing commercial interest for natural fiber reinforced polymer composites for use in automotive applications and building constructions as well as demands for environmentally friendly materials, the development of fully biodegradable composites for many applications could be an interesting area of research.

2.2.3 Reinforcement

Reinforcement increases the strength, stiffness and the temperature resistance capacity and lowers the density of PMC. In order to achieve these properties the selection depends on the type of reinforcement, its method of production and chemical compatibility with the matrix and the following aspects must be considered while selecting the reinforcement material.

- Size - diameter and aspect ratio
- Shape - Chopped fiber, whisker, spherical or irregular particulate, flake etc.
- Surface morphology - smooth or corrugated and rough:
- Poly or single crystal
- Structural defects - voids, occluded material, second phase
- Surface chemistry
- Impurities
- Inherent properties - strength, modulus and density.

2.2.4 Reinforcement Materials

Particles used for reinforcing include ceramics and glasses such as small mineral particles, metal particles such as aluminum and amorphous materials, including polymers and carbon black. Particles are used to increase the modules of the matrix and to decrease the ductility of the matrix. Particles are also used to reduce the cost of the composites. Reinforcements and matrices can be common, inexpensive materials and are easily processed. Some of the useful properties of ceramics and glasses include high melting temperature, low density, high strength, stiffness, wear resistance, and corrosion resistance. Many ceramics are good electrical and thermal insulators. Some ceramics have special properties, some ceramics are magnetic materials, some are piezoelectric materials, and a few special ceramics are even superconductors at very low temperatures. Ceramics and glasses have one major drawback: they are brittle. An example of particle reinforced composites is an automobile tire, which has carbon black particles in a matrix of poly-isobutylene elastomeric polymer.

Polymer composite materials have generated wide interest in various engineering fields, particularly in aerospace applications. Research is underway worldwide to develop newer composites with varied combinations of fibers and fillers so as to make them useable under different operational conditions.

2.3 Fabrication methods of polymer matrix composites

There are two general divisions of composites manufacturing processes: **open molding** and **closed molding**. With open molding, the gel coat and laminate are exposed to the atmosphere during the fabrication process. In closed molding, the composite is processed in a two-part mold set, or within a vacuum bag. There are a variety of processing methods within the open and closed molding categories.

(a) Open Molding Method:

1. Hand Lay-Up
2. Spray-Up
3. Filament Winding

(b) Closed Molding Method:

1. Compression molding
2. Pultrusion
3. Vacuum Bag Molding
4. Vacuum Infusion Processing
5. Resin Transfer Molding (RTM)

2.3.1 Open Molding Method

Open molding process is saturating fiber reinforcement with resin, using manual rollout techniques to consolidate the laminate and removing the entrapped air. A major factor in this operation is the transfer of resin from a drum or storage tanks to the mold. The means used to transport the resin, in many cases, characterizes the specific process method.

(a) Hand Lay-Up

Hand lay-up is an open molding method suitable for making a wide variety of composites products including: boats, tanks bath ware, housings, truck/auto components, architectural products and many other products ranging from very small to very large. Production volume per mold is low; however, it is feasible to produce substantial production quantities using multiple molds. Simple single cavity molds of fiberglass composites construction are generally used. Molds can range from very small to very large and are low cost in the spectrum of soft composites molds.

Gel coat is first applied to the mold using a spray gun for a high-quality surface. When the gel coat has cured sufficiently, roll stock fiberglass reinforcement is manually placed on the mold. The lamination resin is applied by pouring, brushing, spraying, or using a paint roller. Fiber reinforced plastic rollers, paint rollers, or squeegees are used to consolidate the laminate, thoroughly wetting the reinforcement, and removing entrapped air. Subsequent layers of fiber glass reinforcement are added to build laminate thickness as in figure 2.2.

Simplest method offering low-cost tooling, simple processing and wide range of part sizes are the major advantages of this process. Design changes are readily made. There is a minimum investment in equipment with skilled operators, good production rates consistent quality is obtainable.

(b) Spray Lay-Up

Spray-up or chopping is similar to hand lay-up in its suitability for making boats, tanks, transportation components and tub/shower units in a large variety of shapes and sizes. A chopped laminate has good conformability and is sometimes faster than hand lay-up in molding complex shapes. In the spray-up process the operator controls thickness and consistency, therefore the process is more operator dependent than hand lay-up. Although production volume per mold is low, it is feasible to produce substantial production quantities using multiple molds. As with hand lay-up, gel coat is first applied to the mold prior to spray-up of the substrate laminate.

Continuous strand glass roving and catalyzed resin are fed through a chopper gun, which deposits the resin-saturated “chop” on the mold as shown in figure 2.3. The laminate is then rolled to thoroughly saturate the glass strands and compact the chop. Additional layers of chop laminate are added as required for thickness.

(c) Filament Winding

Filament winding is an automated open molding process that uses a rotating mandrel as the mold. The male mold configuration produces a finished inner surface and a laminated rough surface on the outside diameter of the product. Filament winding results in a high degree of fiber loading which provides high tensile strengths in the manufacture of hollow, generally cylindrical products such as chemical and fuel storage tanks, pipes, stacks, pressure vessels, and rocket motor cases. Mandrels of suitable size and shape, made of steel or aluminum form the inner surface of the hollow part. Some mandrels are collapsible to facilitate part removal.

Figure 2.4 shows the schematic picture of a typical filament winding process. Continuous strand roving is fed through a resin bath and mould onto a rotating mandrel. The roving feed runs on a trolley that traverses the length of the mandrel. The filament is laid down in a predetermined geometric pattern to provide maximum strength in the directions required. When sufficient layers have been applied, the laminate is cured on the mandrel. The molded part is then stripped from the mandrel. Equipment is available for filament winding on a continuous basis with two axes winding for pressure cylinders. This process makes high

strength-to-weight ratio laminates and provides a high degree of control over uniformity and fiber orientation.

The filament winding process can be used to make structures, which are highly engineered and meet strict tolerances. Because filament winding is automated, the labour factor for filament winding is lower than other open molding processes.

2.3.2 Closed Molding Method

(a) Compression Molding

Compression molding is a high-volume, high-pressure method suitable for molding complex, fiberglass-reinforced plastic parts on a rapid cycle time. There are several types of compression molding including: sheet molding compound (SMC) which are, bulk molding compound (BMC), thick molding compound (TMC), and wet lay-up compression molding. Compression molding tooling consists of heated metal molds mounted in large presses. Tooling is usually machined steel or cast alloy molds that can be in either single or multiple cavity configurations. Steel molds are hardened and sometimes chrome plated for enhanced durability. The molds are heated using steam, hot oil, or electricity. Side cores, provisions for inserts and other refinements are often employed. Mold materials include cast or forged steel, cast iron, and cast aluminum.

The mold set is mounted in a hydraulic or mechanical molding press. The molds are heated to 2500 to 4000°F. A weight charge of molding compound is placed in the open mold as shown in figure 2.5. The two halves of the mold are closed and pressure is applied. Depending on thickness, size, and shape of the part, curing cycles range from less than a minute to about five minutes. The mold is opened and the finished part is removed. Typical parts include: automobile components, appliance housings, structural components, furniture, electrical components, and business machine housings and parts. Compression molding produces fast molding cycles and high part uniformity. The process can be automated. Good part design flexibility and features such as inserts, ribs, bosses and attachments can be molded in. Good surface finishes are obtainable, contributing to lower part finishing cost. Subsequent trimming and machining operations are minimized in compression molding.

(b) Pultrusion

Pultrusion is a continuous process for the manufacture of products having a constant cross section, such as rod stock, structural shapes, beams channels, pipe, tubing, fishing rods, and golf club shafts. Pultrusion produces profiles with extremely high fiber loading, thus pultruded products have high structural properties. Hardened steel dies are machined and include a perform area to do the initial shaping of the resin saturated roving. The dies include heating which can be electric or hot oil. The latest pultrusion technology used direct injection dies, in which the resin is introduced inside the die, rather than through an external resin bath, which may be called as partial resin transfer molding.

Continuous strand fiber glass roving, mat, cloth, or surfacing veil is impregnated in a resin bath, then pulled (pultrusion) through a steel die, by a powerful tractor mechanism (Figure 2.6). The steel die consolidates the saturated reinforcement, sets the shape of the stock and controls the fiber/resin ratio. The die is heated to rapidly cure the resin. Many creels (balls) of roving are positioned on a rack, and a complex series of tensioning devices and roving guides direct the roving into the die. The process is a continuous operation that can be readily automated. It is adaptable to both simple and complex cross-sectional shapes. Very high strengths are possible due to the fiber loading and labor costs are low.

c) Vacuum Bag Molding

The mechanical properties of open-mold laminates can be improved with vacuum bagging. By reducing the pressure inside the vacuum bag, external atmospheric pressure exerts force on the bag. The pressure on the laminate removes entrapped air, excess resin and compact the laminate. Vacuum bagging can be used with wet lay laminates and prepreg advanced composites. In wet lay-up bagging the reinforcement is saturated using hand lay-up, then the vacuum bag is mounted on the mold and used to compact the laminate and remove air voids. In the case of prepreg advanced composites molding, the prepreg material is laid up on the mold, the vacuum bag is mounted and the mold is heated or the mold is placed in an autoclave that applies both heat and external pressure, adding to the force of atmospheric pressure. The prepreg vacuum bag autoclave method is most often used to create advanced composites used in aircraft and military products. Molds are similar to those used for conventional open mold processes.

In the simplest form of vacuum bagging, a flexible film (PVA, Nylon, Mylar, or Polyethylene) is placed over the wet lay-up, the edges sealed, and a vacuum drawn. A more advanced form of vacuum bagging places a release film over the laminate, followed by a bleeder ply of fiber glass cloth, non-woven nylon, polyester cloth, or other material that absorbs excess resin from the laminate. Figure 2.7 shows the schematic picture of vacuum bag molding process. A breather ply of a non-woven fabric is placed over the bleeder ply, and the vacuum bag is mounted over the entire assembly. Pulling a vacuum from within the bag uses atmospheric pressure to eliminate voids and force excess resin from the laminate. The addition of pressure further results in high fiber concentration and provides better adhesion between layers of sandwich construction. When laying non-contoured sheets of PVC foam or balsa into a female mold, vacuum bagging is the technique of choice to ensure proper secondary bonding of the core to the outer laminate.

Vacuum bag processing can produce laminates with a uniform degree of consolidation, while at the same time removing entrapped air, thus reducing the finished void content. Structures fabricated with traditional hand lay-up techniques can become resin rich and vacuum bagging can eliminate the problem. Additionally, complete fiber wet-out can be accomplished if the process is done correctly. Improved core bonding is also possible with vacuum bag processing.

(d) Vacuum Infusion Processing

Vacuum infusion is a variation of vacuum bagging where the resin is introduced into the mold after the vacuum has pulled the bag down and compact the laminate. The method is defined as having lower atmospheric pressure in the mold cavity. The reinforcement and core material are laid-up dry in the mold. This is done by hand and provides the opportunity to precisely position the reinforcement. When the resin is pulled into the mold the laminate is already compacted, therefore, there is no room for excess resin. Very high resin to glass ratio is possible with vacuum infusion and the mechanical properties of the laminate are superior. Vacuum infusion is suitable to mold of very large structures and is considered a low volume molding process. Molds are similar to those used for conventional open mold processes.

The mold may be gel coated in the tradition fashion. After the gel coat cures, the dry reinforcement is positioned in the mold. This includes all the plies of the laminate and core

material if required. A perforated release film is placed over the dry reinforcement. Next a flow media consisting of a course mesh or a “crinkle” ply is positioned, and perforated tubing is positioned as a manifold to distribute resin across the laminate. The vacuum bag is then positioned and sealed at the mold perimeter. A tube is connected between the vacuum, bag and the resin container. A vacuum is plied to consolidate the laminate and the resin is pulled into the mold (Figure 2.8).

Vacuum infusion can produce laminates with a uniform degree of consolidation, producing high strength, lightweight structures. This process uses the same low cost tooling as open molding and requires minimal equipment. Very large structures can be fabricated using this method. Vacuum infusion offers a substantial emissions reduction compared to either open molding or wet lay-up vacuum bagging.

(e) Resin Transfer Molding

Resin transfer molding is an intermediate volume molding process for producing composites. The RTM process is used to inject resin under pressure into a mold cavity. Vacuum assist can be used to enhance resin flow in the mold cavity. RTM can use a wide variety of tooling, ranging from low cost composite molds to temperature controlled metal tooling. RTM can utilize either “hard” or “soft” tooling, depending upon the expected duration of the run. Soft tooling would be either polyester or epoxy molds, while hard tooling may consist of cast machined aluminum, electroformed nickel shell, or machined steel molds. RTM can take advantage of the broadest range of tooling.

Figure 2.9 shows the resin transfer molding process of polyester resin with peroxide catalyst. The mold set is gel coated conventionally, if required. The reinforcement (and core material) is positioned in the mold and the mold is closed and clamped. The resin is injected under pressure, using mix/meter injection equipment, and the part is cured in the mold. The reinforcement can be either performs or pattern cut roll stock material. Performs are reinforcement that is pre-formed in a separate process and can be quickly positioned in the mold. RTM can be done at room temperature; however, heated molds are required to achieve fast cycle times and product consistency. This closed molding process produces parts with

two finished surfaces. By laying up reinforcement material dry inside the mold, any combination of materials and orientation can be used, including three dimensional reinforcements. Part thickness is determined by the tool cavity.

2.4 Natural fiber reinforced polymer composites

Natural fiber reinforced polymer composites are hybrid with their properties, with characteristics of both natural fibers and polymers. In the beginning of the 20th century wood or cotton fiber reinforced phenol or melamine formaldehyde resins were fabricated and used in electrical applications for their non-conductive and heat-resistant properties. Incorporation of natural fibers into polymer is now a standard technology to improve the mechanical properties of polymer. Mechanical properties like tensile strength and young's modulus are enhanced in the end product as the fibers in the composites determine the tensile strength and young's modulus of the materials [38].

One of the largest areas of recent growth in natural fiber plastic composites in worldwide is the automotive industry, where natural fibers are advantageously used as a result of their low density and increasing environmental pressures. Natural fibers composites found application where load bearing capacity and dimensional stability under moist and high thermal conditions are of second order importance. For example, flax fiber reinforced polyolefin are extensively used today in the automotive industry, but the fiber acts mainly as filler material in non-structural interior panels [39]. Natural fiber composites used for structural purposes exist, but then usually with synthetic thermoset matrices which of course limit the environmental benefits [40, 41].

Plant fibers, such as hemp, flax and wood, have large potential as reinforcement in structural materials due to the high aspect ratio and high specific strength and stiffness of the fibers [21,42-44]. Apart from good specific mechanical properties and positive environmental impact, other benefits from using natural fibers worth mentioning are low cost, friendly processing, low tool wear, no skin irritation and good thermal and acoustic insulating properties [44].

A complete biodegradable system may be obtained if the matrix material also comes from a renewable resource. Examples of such materials are lignophenolics, starch and polylactic acid. Some of these systems show encouraging results. For example Oksman *et al.* [33] have reported that flax fiber composites with polylactic acid matrix can compete with

and even outperform flax/polypropylene composites in terms of mechanical properties. In a recent study [45] it was found that composites of poly-L-Lactide Acid (PLLA) reinforced by flax fibers can show specific tensile modulus equivalent to that of glass/polyester short fiber composites. The specific strength of flax/PLLA composites was lower than that of glass/polyester, but higher than that of flax/polyester.

The limited use of natural fiber composites is also connected with some other major disadvantages still associated with these materials. The fibers generally show low ability to adhere to common non-polar matrix materials for efficient stress transfer. Furthermore, the fibers inherent hydrophilic nature makes them susceptible to water uptake in moist conditions. Natural fiber composites tend to swell considerably with water uptake and as a consequence mechanical properties, such as stiffness and strength, are negatively influenced. However, the natural fiber is not inert. The fiber-matrix adhesion may be improved and the fiber swelling reduced by means of chemical, enzymatic or mechanical modifications [21].

There are many application of natural fiber composite in everyday life. For example, jute is a common reinforcement for composites in India. Jute fibers with polyester resins are used in buildings, elevators, pipes, and panels [46]. Natural fiber composites can also be very cost effective material for application in building and construction areas (e.g. walls, ceiling, partition, window and door frames), storage devices (e.g. bio-gas container, post boxes, etc.) furniture (e.g. chair, table, tools, etc.), electronic devices (outer casting of mobile phones), automobile and railway coach interior parts (inner fenders and bumpers), toys and other miscellaneous applications (helmets, suitcases).

During the last few years, a series of works have been done to replace the conventional synthetic fiber with natural fiber composites [46-53]. For instant, hemp, sisal, jute, cotton, flax and broom are the most commonly fibers used to reinforce polymers like polypropylene [54], polystyrene [55], and epoxy resins [29]. In addition, fibers like sisal, jute, coir, oil palm, bamboo, bagasse, wheat and flax straw, waste silk and banana [48, 49, 54-64] have proved to be good and effective reinforcement in the thermoset and thermoplastic matrices. Nevertheless, certain aspects of natural fiber reinforced composite behavior still poorly understood such as their viscoelastic, viscoplastic or time-dependent behavior due to creep and fatigue loadings [65], interfacial adhesion [66, 67] and tribological properties. Little information concerning the tribological performance of natural fiber

reinforced composite material [58-62, 67] has been available in the literatures. In this context, long plant fibers, like hemp, flax [69, 70] and bamboo [61, 62] have considerable potential in the manufacture of composite materials for tribo applications.

Among these fibers, Jute is the one of the most common agro fibers which has high tensile modulus and low elongation at break. If the low density (1.4gm/cm^3) of this fiber is taken into consideration, then its specific stiffness and strength are comparable to those of glass fiber [68-70]. There are many reports available about the use of jute as reinforcing fibers for thermoset polymers [71,72].

A.K Rana and Jayachandran [73] made a comparison of the jute fiber as reinforcing material compared to glass fiber and concluded that this natural fiber possesses some drawbacks and needs chemical modification for improvement in properties.

Ray, Sarkar *et al.*[74] studied the thermal behavior of vinyl ester resin matrix composite reinforced with jute fibers treated for 2, 4, 6, and 8h with 5% NaOH. They reported that the modulus of jute fibers improved by 12, 68 and 79% after 4, 6 and 8h of treatment, respectively. The tenacity of fibers improved by 46% after 6 and 8h treatment and the percent breaking strain is reduced by 23% after 8h treatment.

Dash *et al.*[75] studied on the improved mechanical performance of jute composite by using unidirectional oriented jute silvers as the reinforcements and general purpose polyester resin as the matrix. The primary objective of their work to develop surface modification through the bleaching process in an economical way unlike the conventional grafting and surface coating used by previous workers. Composites having 60 wt.% of jute fiber yielded the best results. The flexural storage modulus was found to be 12.3GPa at 30°C and decreased slowly with temperature. The major finding in this work is the attainment of high mechanical properties of composite specimens with 60 wt.% fiber loading. On a weight and cost basis, bleached jute fibers were found to be better reinforcements than other fibers with usual surface modification by coating or grafting processes.

Giridhar and Rao[76] made a comparative study in which raw jute fiber has been incorporated in a polyester resin matrix to form uniaxial reinforced composite containing up to 60 volume percent fiber. The tensile strength and young's modulus work of fracture determined by charpy impact and inter-laminar shear strength have been measured as a function of fiber volume fraction.

Ray *et al.*[77] studied the effect of 5% NaOH treatment for short duration on jute reinforcing fiber material to vinylester resin. Their reports showed improved mechanical properties. The Flexural strength improved by 20% and modulus by 23%.

Mitra *et al.*[78] tried to improve the fiber matrix bonding by treating the surface of the jute fibers with pre-condensate like phenol formaldehyde and melamine formaldehyde and cashew nut shell formaldehyde before impregnating with the PF resin for composite fabrication.

Md. Rezaur Rahman *et al.*[79] while studying the strength behavior of jute fiber found that young's modulus, flexural modulus and hardness of the composites increases with increase in the fiber loading and also showed that 30% jute fiber reinforcement had the optimum set of mechanical properties.

K. Sabeel Ahmed and S. Vijayarangan [80] investigated on tensile, flexural and interlaminar shear properties of woven jute and jute-glass fabric reinforced polyester hybrid composites experimentally. All the laminates were made with a total of ten plies, by varying the number and position of glass layers so as to obtain six different stacking sequences. The results indicated that the properties of jute composites can be considerably improved by incorporation of glass fibre as extreme glass plies. The layered sequence has greater effect on flexural and interlaminar shear properties than tensile properties. An overall comparison between the properties of all the laminates revealed that the hybrid laminate with two extreme glass plies on either side is the optimum combination with a good balance between the properties and cost.

Recently C. Santulli and A.P. Caruso [81] studied the comparison between two composite architectures namely a hemp/epoxy random mat and a jute/epoxy plain weave laminate, both with $45 \pm 2\%$ volume fraction and their work reported that manufacturing a hybrid laminate, using jute/epoxy plain woven and hemp/epoxy random mat, most preferably

the latter (inherently stronger) as skins and the former as core, would be able to reduce the scattering in impact resistance values and lead to a better predictability of its impact behavior.

P. Kanakasabai, *et al.* [82] studied the effect of fabric treatment and filler content on jute polymer composites and their result found that fabric treatment significantly improved mechanical property of composite and the filler (calcium carbonate up to 40%) had no significant improvement on the mechanical property or say decreased the mechanical property of composite and so that, we can use filler of 10% for reducing the moisture absorption of the composite.

S.K. Acharya *et al.* [83] processed a composite using fly ash, jute with epoxy and investigated its weathering behaviour on mechanical properties such as flexural strength. Their reports state that three layered jute composite shows maximum stress value with 15% fly ash reinforcement.

M. Ramesha and K. Palanikumar [84] investigated the comparative evaluation on properties of hybrid glass fiber-sisal/jute reinforced epoxy composites. Their results indicated that the incorporation of sisal fiber with glass fiber reinforced plastic (GFRP) exhibited superior properties than the jute fiber reinforced glass fiber reinforced plastic composites in tensile properties and jute fiber reinforced GFRP composites performed better in flexural properties.

Thi-Thu-Loan Doan *et al.* [85] treated the surface of jute fiber with alkaline to enhance the interfacial interaction between jute natural fibers and experimented single fiber pull-out test combined with SEM and AFM characterization of the fracture surfaces were used to identify the interfacial strengths and to reveal the mechanism of failure and an epoxy matrix.

After reviewing the existing literature available on jute fiber it is clear that the interfacial bond between the reinforcing fiber and the resin matrix is an important element to realize the mechanical properties of the composite. It is also found that mechanical properties of jute fiber composite are much lower than those of synthetic fiber composite. Another disadvantage which makes jute fiber less attractive is the poor resistance to moisture absorption. Hence use of jute fiber alone in polymer matrix is inadequate in satisfactorily

tackling all the technical needs of a fiber reinforced composite. In addition, to obtain the desired properties from a composite system reinforcement and filler are added for polymer materials. The additional improvement in mechanical and tribological properties in many cases attained by filling particulate matters.

As explained earlier cenosphere (particulate filler), can lead to special effects which cannot be reached so easily with conventional/traditional fillers. Accordingly lot of research has been carried out in recent past with cenosphere filler. Table 2.1 shows the list of research work carried out with composites having cenosphere fillers.

Table 2.1: List of researchers worked on cenosphere filler composites

Authors	Year	Reinforcement	Matrix type	Studies	Ref.
Scott W. Davey	2005	Cenosphere powder	Vinylester	Civil and Structural Engineering	86
B.Suresh and G. Chandra mohan	2008	Glass Fiber and cenosphere	Epoxy resin (LAPOX L-12)	Three-Body Abrasive Wear Behavior	87
Jian Gu <i>et al.</i>	2009	Surface-modified γ -aminopropyl triethoxy silane cenosphere	Epoxy resin	Dynamic behaviours	88
M.V. Deepthi <i>et al.</i>	2010	Cenosphere	High density polyethylene	Mechanical and thermal characteristics	89
Navin Chand	2010	Silane treatment cenosphere	polyethylene	Mechanical and tribological properties	90
A. Das and B.K. Satapathy	2011	Cenosphere (CS-300)	polypropylene (PP) REPOL H110MA	Structural, thermal, mechanical and dynamic mechanical properties	91
Abdullah M.A. <i>et al.</i>	2011	Fly ash and Cenosphere	Amine Containing Silicone(ACS) modified epoxy	Mechanical and microstructural properties	92

Parag A.Wasekar and Pravin G.Kadam	2012	Cenosphere	Nylon 6	Mechanical, Thermal, Rheological and Morphological Properties	93
Mohammed Ismail <i>et al.</i>	2012	Carbon fabric reinforced cenosphere	Epoxy	Mechanical and Erosive wear behaviour	94
P. Arivalagan <i>et al.</i>	2012	Carbon fabric and cenosphere	Epoxy	Mechanical and abrasive wear behavior	95
Janu Sharma and Navin Chand	2012	Agro-waste rice husk and cenosphere	Polypropylene	Dynamic mechanical analysis and dielectric studies	96
S.R. Chauhan and S.Thakur	2013	cenosphere	Vinylester	Friction and wear properties	98
H. Jena and A.K. Pradhan <i>et al.</i>	2013	Cenosphere and Bamboo fiber	Epoxy	Mechanical behavior	99
M.B. Kulkarni <i>et al.</i>	2014	Cenosphere	Acrylonitrile butadiene styrene	Tensile and impact properties	100
Sunil Thakur and S. Chauhan	2014	Cenosphere	Vinylester resin	Mechanical and tribological characteristics	101
S.Thakur <i>et al.</i>	2014	Cenosphere	Vinyl ester	Friction and sliding wear characteristics	97
Aashis S. Roy <i>et al.</i>	2014	Amino silane functionalized cenosphere	Polyvinylbutyral	Dielectric performance of the composite films	102
Parisa Khoshnoud <i>et al.</i>	2015	TG-cenosphere	Rigid PVC resin	Thermal, Mechanical, and Morphological Properties	103

B. Suresha <i>et al.</i>	2015	Cenosphere	Epoxy	Mechanical and Three-body Abrasive Wear Behaviour	104
Sukanya Satapathy and Raju V. S. Kothapalli	2015	Coir fiber and cenosphere	Polyethylene	Mechanical properties and water absorption	105

Basing on the above the priority of this work is twofold.

(1) To develop a polymer matrix hybrid composite taking jute and glass fiber as reinforcement material. The angle ply orientation of jute (45° - 45°) and glass (0° - 90°) fibers are kept as such for significant improvement in mechanical properties of composites. It is also planned to add particulate filler to the composite for further improvement in different properties of the composites. Fillers like cenosphere of different weight percentages (5, 10, 15 and 20%) are incorporated to the fibers. These fillers are cheap and non-toxic and can be obtained from renewable resources and are easily recyclable. The mechanical properties like tensile, flexural, interlaminar shear strength and modulus with and without fillers are evaluated and reported in this thesis. The fiber and filler characterization are also carried out by Fourier Transform Infrared (FTIR) spectroscopy, X-Ray Diffraction (XRD) and TGA analysis technique. The developed composites were also subjected to different weathering condition like saline and distilled water condition. The mechanical properties and moisture absorption kinetics of the hybrid jute-glass epoxy composites has also been evaluated with cenosphere filler.

(2) The potential of the developed hybrid composites for tribological application (solid particle erosion and three-body abrasion test) with and without waste fillers have also been carried out and reported in this thesis.

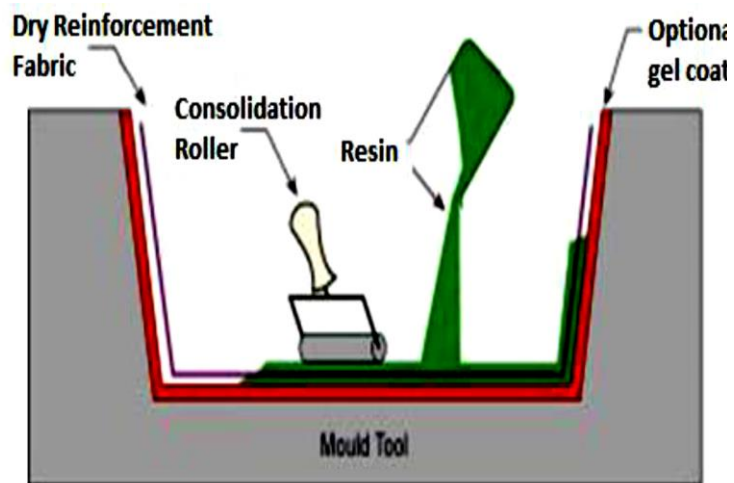


Figure 2.2: Hand Lay-Up Techniques

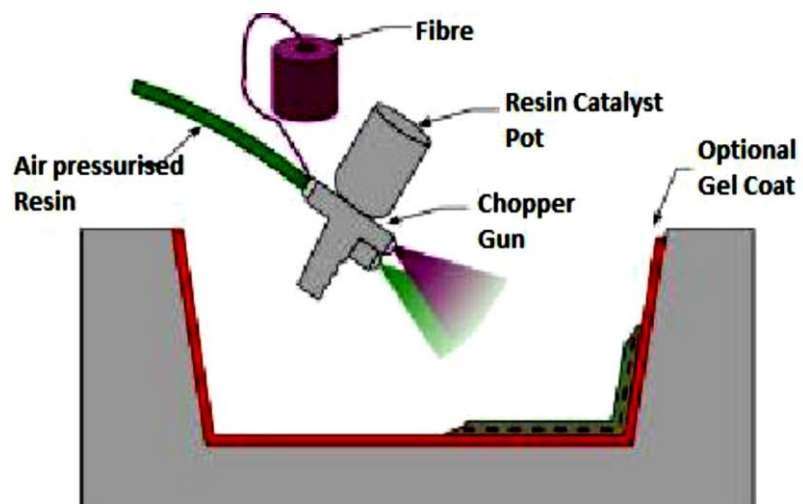


Figure 2.3: Spray up Technique

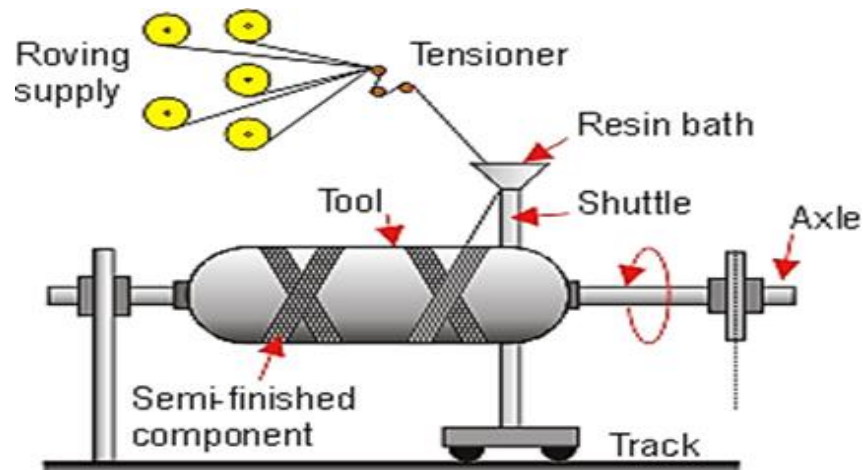


Figure 2.4: Filament Winding Process

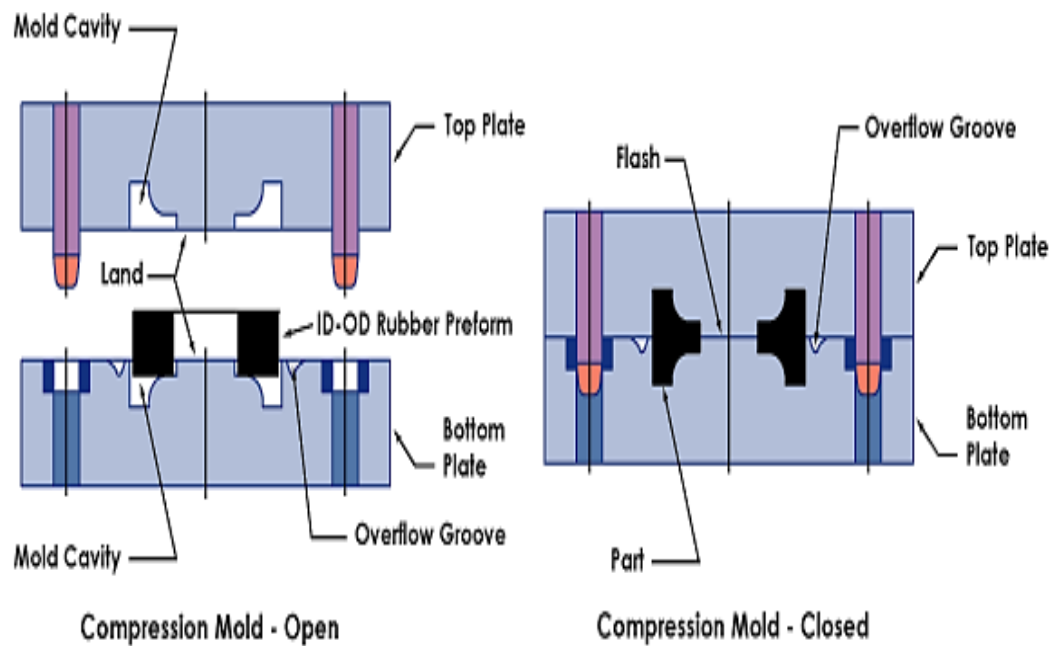


Figure 2.5: Compression Molding Technique

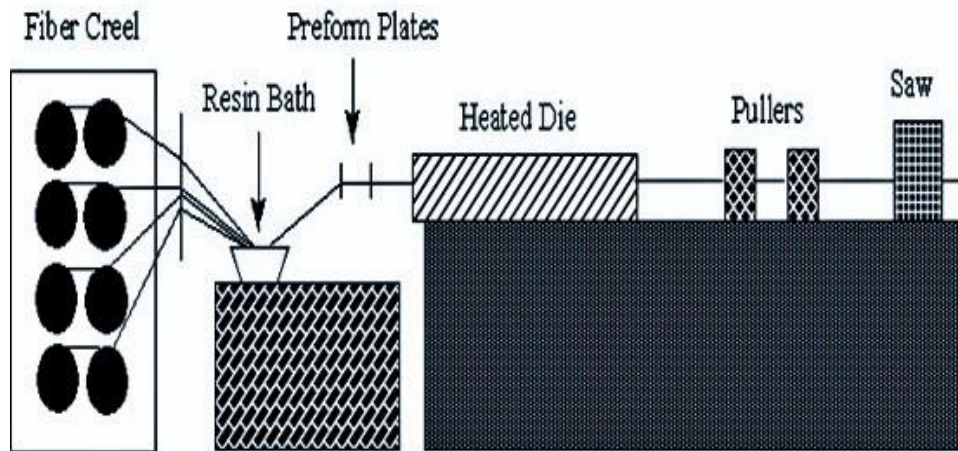


Figure 2.6: Pultrusion Process

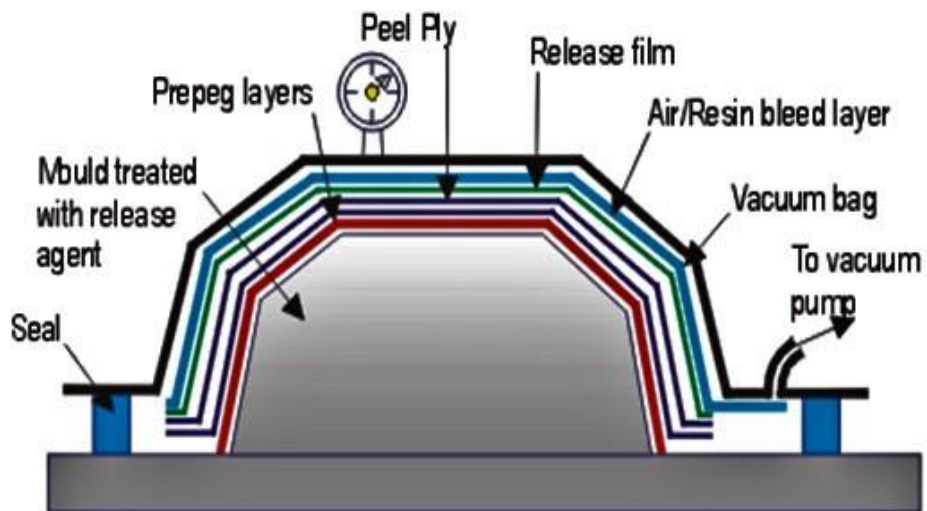


Figure 2.7: Vacuum Bag Molding

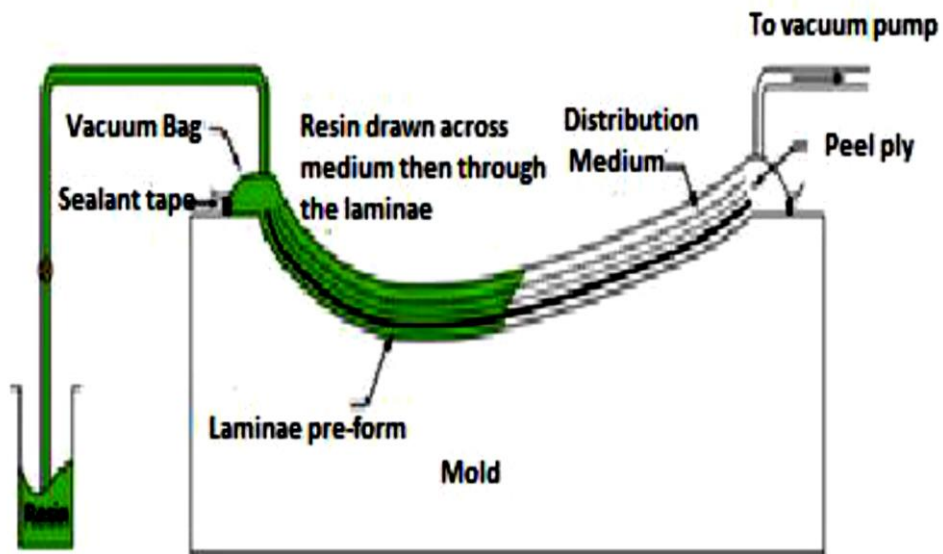


Figure 2.8: Vacuum Infusion Process

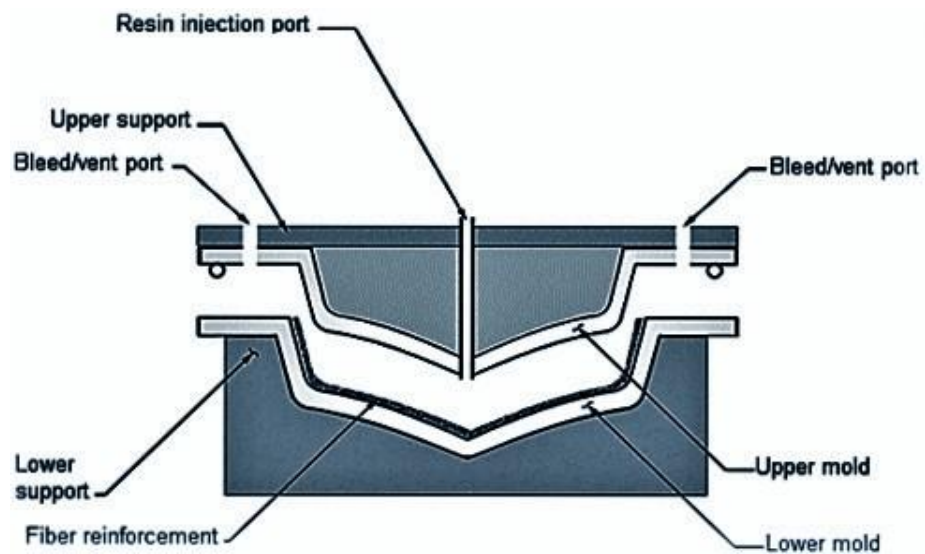


Figure 2.9: Resin Transfer Molding

Chapter 3

Mechanical properties of hybrid Jute-Glass fiber epoxy composites with and without cenosphere filler

3.1 Introduction

The polymers have replaced many of the conventional materials in various applications over the past few decades. This is owing to the advantages of polymers over conventional materials such as ease of processing, productivity, cost reduction etc. Research is underway worldwide to develop newer composites with varied combinations of fibers and fillers so as to make them useable under different operational conditions. In most of these applications, the properties of polymers are modified using fillers and fibers to suit high strength/high modulus requirements. A notable advance in the polymer industry has been the use of fiber and particulate fillers as reinforcements in polymer matrix. Particulate fillers are of considerable interest, not only from an economic viewpoint, but as modifiers especially the physical properties of the polymer. It is well documented in the literature that majority fillers have a positive influence on mechanical properties.

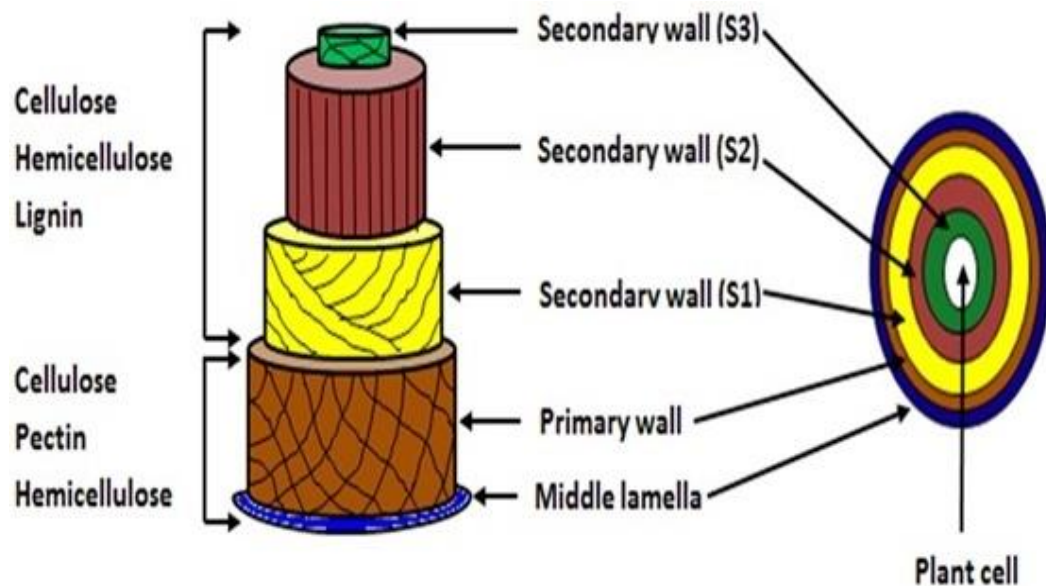


Figure 3.1: Cell wall structure of natural fiber

The cell wall structure of natural fibers (Figure 3.1) contains many micropores. Also, some of the lignin and hemicellulose of natural fibers are usually removed during chemical treatments or pulping, which created additional micropores [106]. The presence of these micropores in the cell wall could cause manufacturing defects in composites, such as interfacial failure and air pockets. In order to reduce the air pocket defect, one can incorporate a vacuum assist system in the natural fiber polymer composites processing to reduce the air bubble to some extent. Another efficient method is to introduce nano-particles into the micropores of the fiber cell wall structure through an impregnation process to fill those voids. Compatibility between the hydrophilic natural fibers and the hydrophobic polyolefin has been a major issue for the natural fiber polymer composite [107,108]. Lee *et al.* [109] indicated that the deposited nano-scale particles on the natural fiber surface may serve as heterogeneous nucleation sites to initiate the crystalline orientation of the molten polymer matrix. These results suggested that nanoparticles might control the heterogeneous nucleation of a semi crystalline polymer on the natural fiber surface. The natural fiber itself cannot initiate nuclei due to extremely unbalanced free energy between the cellulosic fibers and molten polyolefin matrices [109-111]. Therefore, the nanoparticle impregnation could not only fill the micropores of the fiber cell wall structure minimizing the air bubble defects of the natural fiber polymer composite, but also introduce nanoparticles onto the fiber surfaces serving as attraction force manipulators to polymer matrixes to improve the compatibility at the fiber and polymer interfaces.

Hard particulate fillers consisting of ceramic or metal particles and fiber made of glass are being used these days to dramatically improve the properties of composite materials, even up to three orders of magnitude [112]. Various kinds of polymers and polymer matrix composites reinforced with metal particles have a wide range of industrial applications such as heaters, electrodes [113], composites with thermal durability at high temperature[114] etc. These engineering composites are desired due to their low density, high corrosion resistance, ease of fabrication and low cost [115-117]. Similarly, ceramic filled polymer composites have been the subject of extensive research in last two decades. The inclusion of inorganic fillers into polymers for commercial applications is primarily aimed at the cost reduction and stiffness improvement [118,119]. Along with fiber-reinforce

Chapter 3 Mechanical properties of jute-glass composite with and without cenosphere

composites, the composites made with particulate fillers have been found to perform well in many real operational conditions. When silica particles are added into a polymer matrix to form a composite, they play an important role in improving electrical, mechanical and thermal properties of the composites [120,121]. Currently, particle size is being reduced rapidly and many studies have focused on how single-particle size affects mechanical properties [122-129]. The shape, size, volume fraction, and specific surface area of such added particles have been found to affect mechanical properties of the composites greatly. In this regard, Yamamoto *et al.* [129] reported that the structure and shape of silica particle have significant effects on the mechanical properties such as fatigue resistance, tensile and fracture properties. Nakamura *et al.* [130-132] discussed the effects of size and shape of silica particle on the strength and fracture toughness based on particle matrix adhesion and also found an increase of the flexural and tensile strength as specific surface area of particles increased.

In the literature, many works devoted to the mechanical properties of natural fibers from micro to nano scales are available. In these, the effects of reinforcement of matrix (thermoplastic starch) by using cellulose whiskers, commercial regenerated cellulose fibers are also proposed. A number of investigations have been conducted on several types of natural fibers such as kenaf, hemp, flax, bamboo, and jute to study the effect of these fibers on the mechanical properties of composite materials [133-139]. K. Sabeel Ahmed and S. Vijayarangan [140] investigated on the effect of hybridization on the mechanical properties of untreated woven jute and jute-glass fabric-reinforced isothalic polyester composites. They found that tensile properties such as tensile strength and tensile modulus and impact properties of jute-polyester composites were found to improve by the incorporation of glass fibers showing a positive hybrid effect. Addition of 16.5 wt.% glass fiber, in a total fiber weight fraction of 42% enhances the tensile, flexural, and interlaminar shear strength (ILSS) by 37, 31.23, and 17.6% respectively.

Few researches about the influence of the filler and its size over the mechanical and physical properties of wood-flour reinforced thermoplastics [141] has been observed that the elongation at break and the impact strength of the composites decrease with the addition of filler independently of its size. The behavior of the tensile modulus and the tensile strength

Chapter 3 Mechanical properties of jute-glass composite with and without cenosphere

seems to depend on the shape of the particles. This behaviour can improve with the load as the aspect ratio does so. There are several reports available in the literature which discusses the different types of natural fibers composites and their mechanical behavior, very limited work has been done on study of mechanical behaviour of hybridization of natural fiber and synthetic fiber reinforced polymer composites.

Pavithran *et al.* [142] evaluated the enhancement in the properties of coir-polyester composites by incorporating glass as intimate mix with coir. Mohan and Kishore [143] reported that jute provided a reasonable core material in jute-glass hybrid laminates. They evaluated flexural and compressive properties of the jute-glass reinforced epoxy laminates fabricated by filament winding technique using flat mandrel. Four different hybrid combinations were studied with different glass fiber volume fractions and the results were compared with jute reinforced plastic. They found substantial increase in flexural and compressive properties with hybridization.

Pavithran *et al.* [144] determined the work of fracture by impact testing on sisal-glass hybrid composites with two arrangements, one with sisal shell and glass core and the other with glass shell and sisal core. They showed that the sisal shell laminate had the higher work of fracture compared with glass shell hybrid laminates of equivalent volume fraction of sisal and glass fibers. Mishra *et al.* [145] studied the effect of glass fiber addition on tensile and flexural strength and izod impact strength of pine apple leaf fiber (PALF) and sisal fiber reinforced polyester composites. K. John *et al.* [146-148] have studied the unsaturated polyester based sisal glass composites with 5% and 8% volume fraction and found a considerable enhancement in impact, compression, flexural and tensile properties.

In this chapter, effect of hybridization of glass and layering sequence on tensile and flexural properties of woven jute-glass hybrid epoxy composites is studied. The orientation of jute fiber has been kept as $(45^{\circ}-45^{\circ})$ and that of glass as $(0^{\circ}-90^{\circ})$ while making the hybrid composites. The experiment has been conducted in two parts. One without cenosphere for all possible stacking sequences and secondly with particulate filler cenosphere for the optimum stacking sequence obtained from the first experiment has been reported in this chapter.

3.2 Materials and methods

3.2.1 Raw materials used

Raw materials used in this experimental work are listed below:

1. Jute fiber
2. E-glass fiber
3. Epoxy resin
4. Hardener

3.2.1.1 Jute fiber

As explained earlier natural vegetable fibers have attracted worldwide attention as a potential reinforcement for composite because of their easy availability as a renewable resource, easy process ability, low density, light weight, nonabrasive, low cost and above all for their bio friendly characteristics. The woven jute fiber used for the present investigation is shown in figure 3.2. It is an important bast fiber and comprises bundle of ultimate cells, each containing spirally oriented micro fibrils bound together. The main component of jute fiber is cellulose which leads to higher stiffness. Other components of jute fiber are hemi-cellulose, lignin, pectin, waxy and water soluble substances. In the present work, bi-directional jute fibers have been used for experimentation.



Figure 3.2: Woven Jute fiber mat

3.2.1.2 E-glass fiber

Glass is the most common fiber used in polymer matrix composites is shown in figure 3.3. Its advantage includes its high strength, low cost, high chemical and corrosion resistance, good insulation properties and non-flammable. In the present investigation E-glass fiber 360 roving

supplied by saint Gobian limited is used. The fibers sheets were cut to sizes of (150×60) mm from the long sheet.

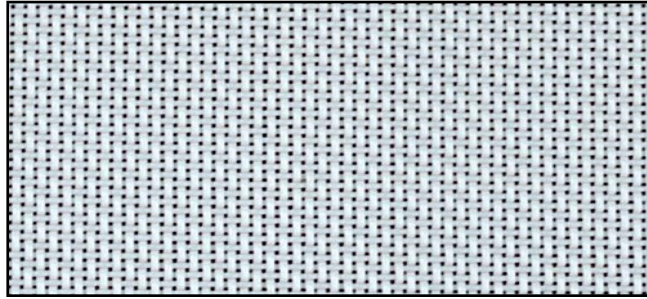


Figure 3.3: E-Glass fiber mat

3.2.1.3 Epoxy resin and Hardener

Epoxy resins are relatively low molecular weight pre-polymers capable of being processed under a variety of conditions. Two important advantages of these over unsaturated polyester resins are: first, they can be partially cured and stored in that state, and second they exhibit low shrinkage during cure. However, the viscosity of conventional epoxy resins is higher and they are more expensive compared to polyester resins. The cured resins have high chemical, corrosion resistance, good mechanical and thermal properties, outstanding adhesion to a variety of substrates and good electrical properties. Approximately 45% of the total amount of epoxy resins produced is used in protective coatings while the remaining is used in structural applications such as laminates composites, tooling, molding, casting, construction and adhesives etc.

The type of epoxy resin used in the present investigation is Araldite LY-556 which chemically belongs to epoxide family. Epoxy resins are characterized by the presence of a three membered ring containing two carbons and an oxygen (epoxy group or epoxide or oxirane ring). Epoxy is the first liquid reaction product of Bisphenol-A with excess of epichlorohydrin and this resin is known as Diglycidyl-Ether of Bisphenol-A(DGEBA). DGEBA is used extensively in industry due to its high fluidity, ease processing and good physical properties of the cured resin. The hardener with IUPAC name NNO-bis (2amino ethyl ethane -1,2 diamin) has been used with the epoxy designated as HY 951. This has a

viscosity of (10-20) MPa at 25°C. Both the epoxy and hardener were supplied by Ciba-Geigy of India Ltd.

3.2.2 Preparation of Hybrid composites

Hybrid laminates of jute and glass composite were prepared by usual hand lay-up technique. The layout of fiber for glass was kept at (0-90°) and for jute it was changed to (45°-45°) orientation instead of (0-90°) orientation. A wooden mold of (150×60×5) mm³ was used for composite fabrication. For quick and easy removal of the composite a mold release sheet is placed on the top and bottom of the wooden mold. The mold release spray is also applied to the inner surface of the mold wall to facilitate easy removal of the composite specimen. A calculated amount of epoxy resin and hardener (of 10:1 by weight) was thoroughly mixed with a mechanical stirrer. After 5 min stirring, some mixture was poured into the mold uniformly, jute fiber mat was placed and then the required amount of epoxy resin was poured over it. The process was continued to fabricate four layers of jute-mat composite. After putting all the layers in the mold, a roller was used to roll over the fiber to remove air bubbles if any present. The mold was then pressed from the top with dead weight to put pressure on the mold. It was kept like that for 72h for proper curing. After 72 h the mold was removed to take out the composite slab. The same procedure was continued to fabricate hybrid composites with different stacking sequences of jute and glass fiber. In all the fabricated samples, care was taken to keep the thickness as 5mm. The specimen for tensile and flexural tests were then cut to required shape and size for mechanical tests by a diamond cutter from the composite slab as shown in figures 3.4 (a-d). The stacking sequences used are shown in table 3.1.

Table 3.1: Laminate stacking sequence of hybrid jute-glass epoxy composites

Symbol	Stacking sequence	Wt. % of fibers		Total fiber		Thickness (mm)
		Jute	Glass	Volume fraction %	Weight fraction %	
S1	JJJJ	100	0	15.12	20.63	5
S2	GJGJ	50	50	14.12	25.09	5
S3	JGGJ	50	50	14.02	25.00	5
S4	GJJG	50	50	14.0	25.00	5

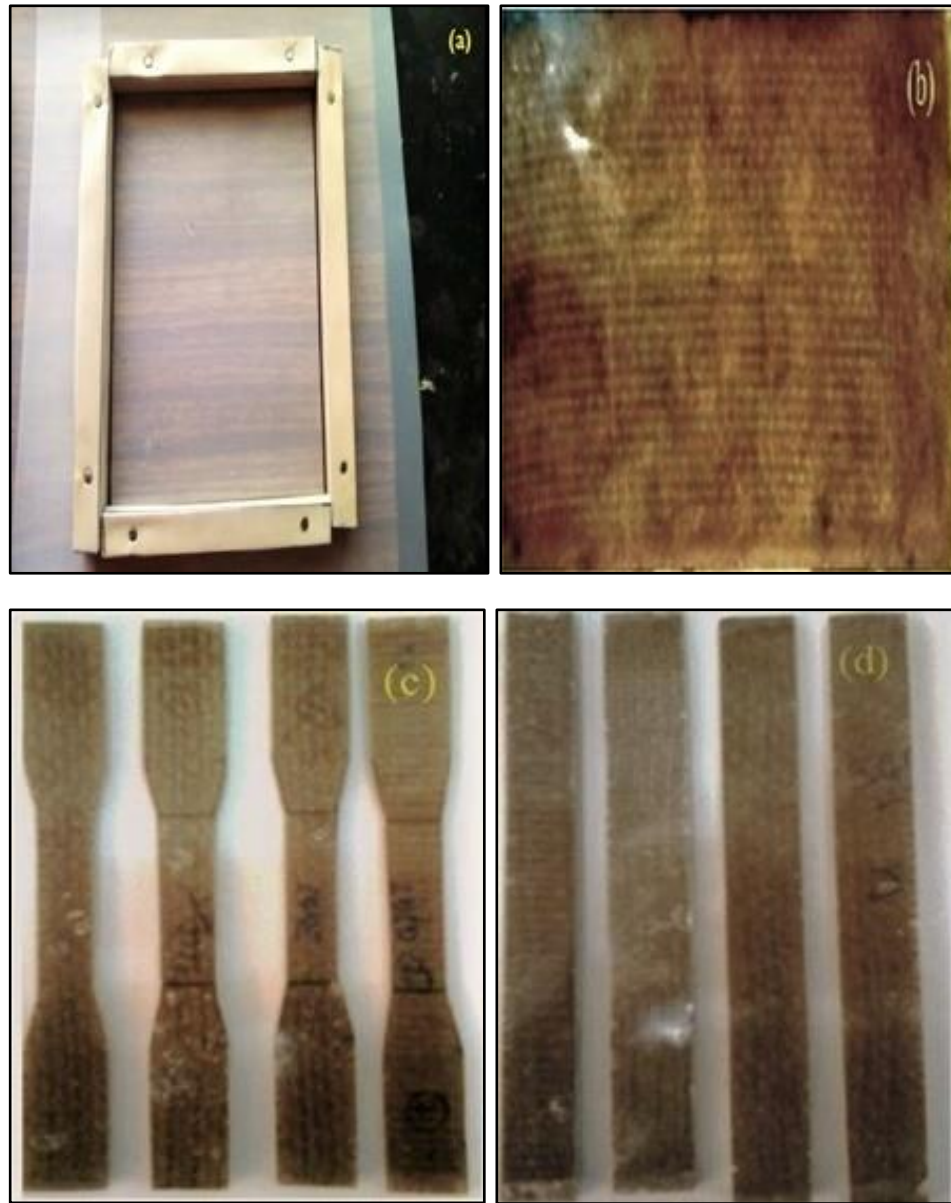


Figure 3.4: (a) Mold used for composite preparation (b) Photograph of composite slab (c) Specimen for tensile test and (d) Flexural test

The total fiber volume fraction of the hybrid composites was calculated using equation.

$$V_f = \frac{\left(\frac{W_j}{\rho_j}\right) + \left(\frac{W_g}{\rho_g}\right)}{\left(\frac{W_j}{\rho_j}\right) + \left(\frac{W_g}{\rho_g}\right) + \left(\frac{W_r}{\rho_r}\right)} \quad (3.1)$$

Chapter 3 Mechanical properties of jute-glass composite with and without cenosphere

Where W_j, W_g and W_r are the known weights of the jute, glass, resin respectively and ρ_j, ρ_g, ρ_r are the densities of jute, glass and resin respectively. The density of epoxy resin, jute and glass fiber is found to be 1.1 g/cm³, 1.5 g/cm³ and 2.5 g/cm³ respectively.

3.2.3 Density and void fraction measurement

In terms of weight fraction the theoretical density of the hybrid composite materials can be found out from Agarwal and Broutman [149] equation.

$$\rho_{ct} = \frac{1}{(W_f / \rho_f) + (W_m / \rho_m)} \quad (3.2)$$

Where 'W' and 'ρ' represent the weight fraction and density respectively. The suffix 'f', 'm' and 'ct' stand for the fiber, matrix and theoretical density of composite materials, respectively.

3.2.3.1 Experimental density of composite samples

The actual density of materials in terms of weight fraction is found out from the equations.

$$S_m = \frac{w_o}{(w_o) + (w_a - w_b)} \quad (3.3)$$

Where S_m represents specific gravity of the material, w_o represents the weight of the sample w_a represents the weight of the bottle + kerosene, w_b represents the weight of the bottle + kerosene + sample.

$$\text{Density} = S_m * \text{Density of kerosene} \quad (3.4)$$

The void content of composite sample has been determined as per ASTM D-2734-70 standard procedure. The volume fraction of voids (V_v) in the hybrid composites is calculated by using equation.

$$V_v = \frac{\rho_{ct} - \rho_{ca}}{\rho_{ct}} \quad (3.5)$$

Where ρ represents the density of the composite. The suffix *ct* and *ca* stand for the theoretical and actual density of the composite materials. For the present investigation the theoretical density, actual density and the void fraction so obtained for hybrid glass-jute composites of different stacking sequences are presented in table 3.2.

Table 3.2: Density and void content of hybrid jute-glass epoxy composites

Stacking Sequence	Theoretical density (g/cm³)	Measured density (g/cm³)	Volume fraction of Voids (%)
JJJJ	1.16	1.152	0.646
GJGJ	1.19	1.180	0.784
JGGJ	1.20	1.189	0.916
GJJG	1.20	1.193	0.566

3.2.4 Tensile Strength

The tension test is generally performed on flat specimens. The most commonly used sample geometries are the dog-bone shape and straight-sided specimen with end tabs as shown in figure 3.5. The standard test method used is as per ASTM D 3039-76. The length of the test specimen used was 140 mm. The tensile test was performed in universal testing machine INSTRON H10KS. The tests were performed with a cross head speed of 10mm/min. The tensile stress is found out by dividing total load exerted on specimen by actual cross sectional area through which the force is applied. The tensile modulus is calculated by using following equation.

$$\text{Tensile modulus}(E) = \frac{\text{Tensile stress}(\sigma)}{\text{Extensional strain}(\epsilon)} \quad (3.6)$$

For each stacking sequence, five identical specimens were tested, and average result was obtained. Figures 3.6 (a-c) show the machine used for the test and the sample in loading condition. The results obtained from the tests are presented in table 3.3.

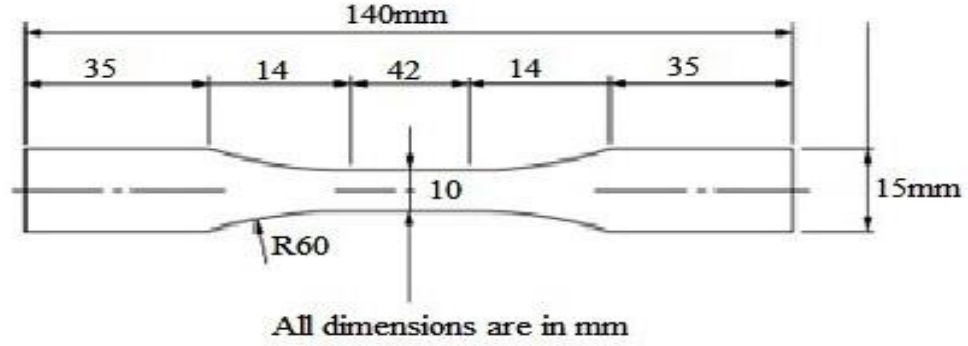


Figure 3.5: Tensile specimen



Figure 3.6: Photograph of (a) INSTRON H10KS testing machine (b) Sample in loading condition (c) Tested samples

3.2.5 Flexural Strength

Flexural test was conducted on INSTRON H10KS machine in accordance with ASTM D2344-84. Specimens of 150 mm length and 20 mm wide were cut and were loaded in three point bending with a recommended span to depth ratio of 16:1 as shown in figure 3.7(a-c). The test was conducted on the same machine used for tensile testing using a load cell of 10 KN at 2 mm/min rate of loading. The flexural stress in a three point bending test is found out by using following equation.

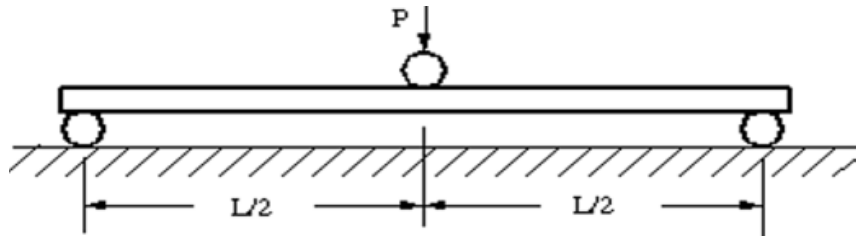
$$\sigma_{max} = \frac{3P_{max}L}{bh^2} \quad (3.7)$$

Chapter 3 Mechanical properties of jute-glass composite with and without cenosphere

Where P_{\max} is the maximum load (N) at failure, L is the span (mm), b and h is the width and thickness of the specimen (mm), respectively. The flexural modulus is calculated from the slope of the initial portion of the load-deflection curve which is found out by using by using following equation.

$$E = \frac{mL^3}{4bh^3} \quad (3.8)$$

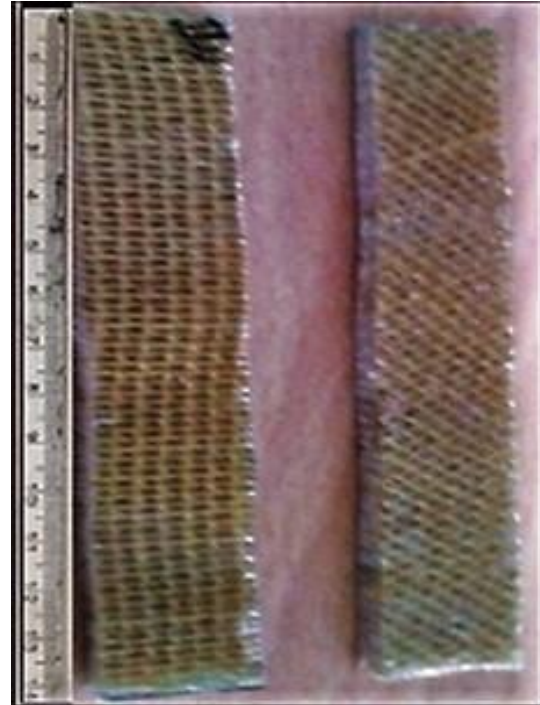
Where m is the initial slope of the load deflection curve. For each stacking sequence, five specimens were tested and average result was obtained and are presented in table 3.3.



(a) Flexural specimen



(b) Sample in loading position



(c) Testing samples

Figure 3.7: Photograph of (a) Flexural specimen (b) Sample in loading position (c) Testing samples

3.2.6 Interlaminar shear Strength (ILSS)

ILSS was found out in accordance with ASTM D2344-84. The data recorded during the three-point bend test was used to evaluate the interlaminar shear strength (ILSS). The test was conducted using the same UTM used for flexural test with bend test fixtures. The crosshead speed of 2 mm/min was maintained. The force applied at the time of failure was recorded, and the stresses were determined using the following equation.

$$ILSS = \frac{3F}{4bt} \quad (3.9)$$

Where F is the maximum load in (N) and b and t are the width and thickness of the specimen (mm), respectively. The ILSS calculated are presented in table 3.3.

3.2.7 Impact Test

Impact tests are designed to measure the resistance to failure of a material to a suddenly applied force. The test measures the energy absorbed prior to fracture. The impact test of the composites was performed by Izod impact tester as in figure 3.8(a) according to ASTM D 256.

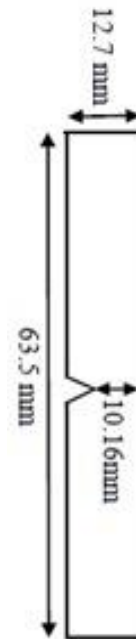


Figure 3.8 (a): Impact test machine **(b):** Configuration of impact test specimen

The size of the test specimen is 63.5mm long and 12.7mm width as shown in figure 3.8(b). A ‘V’ notch (2.54 cm depth and 45° notch angle) is created at the centre of the

specimen. To perform the test, hammer release angle of 150° with hammer range of 5.4J was used. The impact strength of all hybrid jute-glass epoxy composite samples of different stacking sequences was recorded directly from the dial indicator and noted in table 3.3. All the results were taken as the average value of five samples.

3.3 Results and discussion

3.3.1 Hybrid Composites

3.3.1.1 Effect of tensile strength on hybrid jute-glass epoxy composites

The variation of tensile strength and modulus for various laminate stacking sequences of hybrid jute-glass fiber epoxy composites is given in table 3.3 and shown in figures 3.9-3.10. From the table the tensile strength of unreinforced epoxy resin is found to be 13.34 MPa. The maximum tensile strength is observed for the composite of stacking sequence GJJG of 42MPa. It is also found that there is a sharp increase in the tensile strength of the composites with the incorporation of glass fibers at extreme end positions. Wambua *et al.* [150] reported in their research article that jute fiber has 1.8% elongation of failure whereas glass fiber has 3%. When comparing the tensile strength of the jute fiber epoxy composite with glass fiber epoxy composites, it gives about 50% strength of glass fiber composites. It is also observed that an increase in the tensile strength of 50, 38, and 60% is achieved for 50:50 jute-glass fiber reinforced hybrid laminate (GJGJ, JGGJ and GJJG) composites when compared to that of only jute laminate (JJJJ) composite. The variation in mechanical properties is due to the different weight and volume fraction of jute and glass fiber with respect to their position and orientation in different stacking sequences.

Table 3.3: Mechanical properties of hybrid Jute-glass epoxy composites

Stacking Sequence	Flexural Strength (MPa)	Tensile Strength (MPa)	Interlaminar shear strength(ILSS) (MPa)	Flexural Modulus (GPa)	Tensile Modulus (GPa)	Impact strength (KJ/m²)
Epoxy	25	13.34	2	0.85	1.08	78.33
JJJJ(S1)	117	21.0	5	9.92	1.91	11.80
GJGJ(S2)	170	40.04	4	4.02	2.95	53.95
JGGJ(S3)	210	36.0	7	9.08	2.41	58.70
GJJG(S4)	241.3	42.0	8	13.54	2.95	67.60

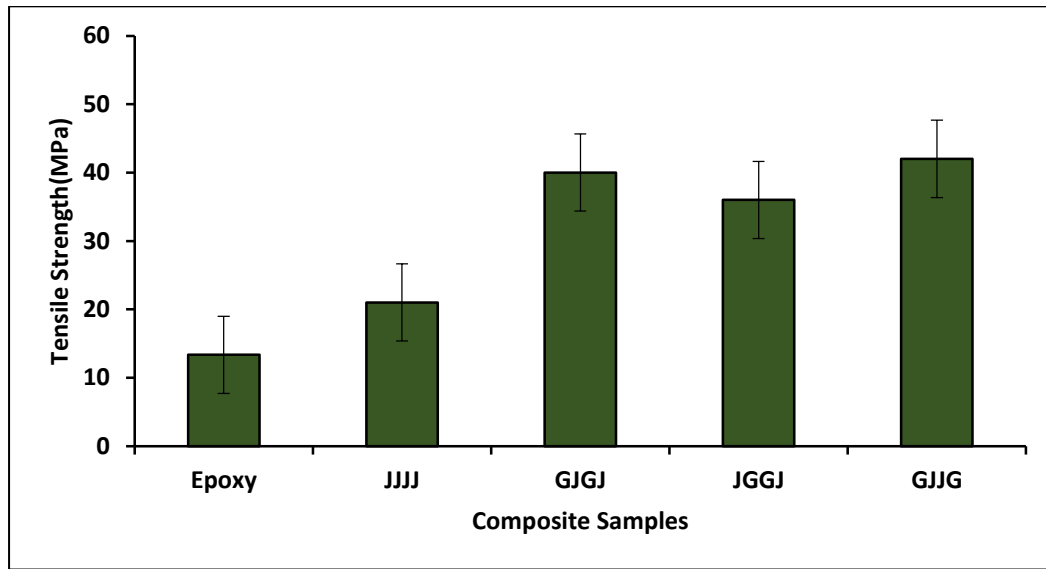


Figure 3.9: Tensile strength of hybrid jute-glass fiber reinforced epoxy composites

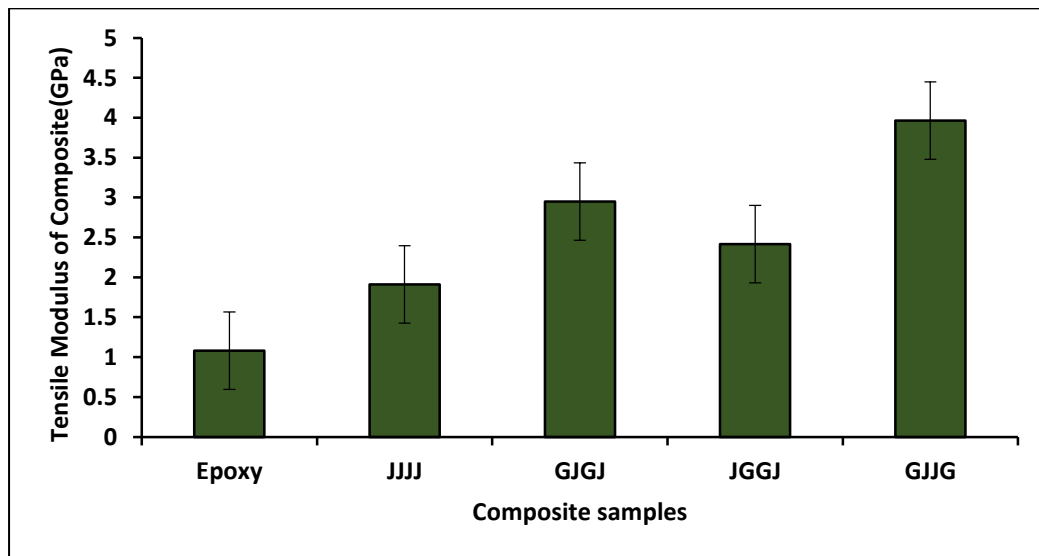


Figure 3.10: Tensile modulus of hybrid jute-glass fiber reinforced epoxy composites

3.3.1.2 Effect of Flexural strength on hybrid jute-glass epoxy composites

Flexural strength and flexural modulus for various laminate stacking sequences of jute-glass fiber epoxy composites are given in figures 3.11-3.12 respectively. Due to the incorporation of glass and jute fibers into the epoxy resin, the strength of the composites increases to a great extent. From the table 3.3 the flexural strength of the unreinforced epoxy is found to be 25

Chapter 3 Mechanical properties of jute-glass composite with and without cenosphere

MPa whereas the flexural strength of only JJJJ and GGGG laminate composites is found to be 117 MPa and 270 MPa, respectively which is greater than that of the neat epoxy. From the graph the maximum flexural strength is observed for composite of stacking sequence GJJG in hybrid glass-jute epoxy composite (i.e.) when the glass fibers are placed at the outer layer of composites providing better strength results (241.3MPa). Also it is found that the flexural strength of hybrid composite GJGJ is less than that of GJJG due to layering effect.

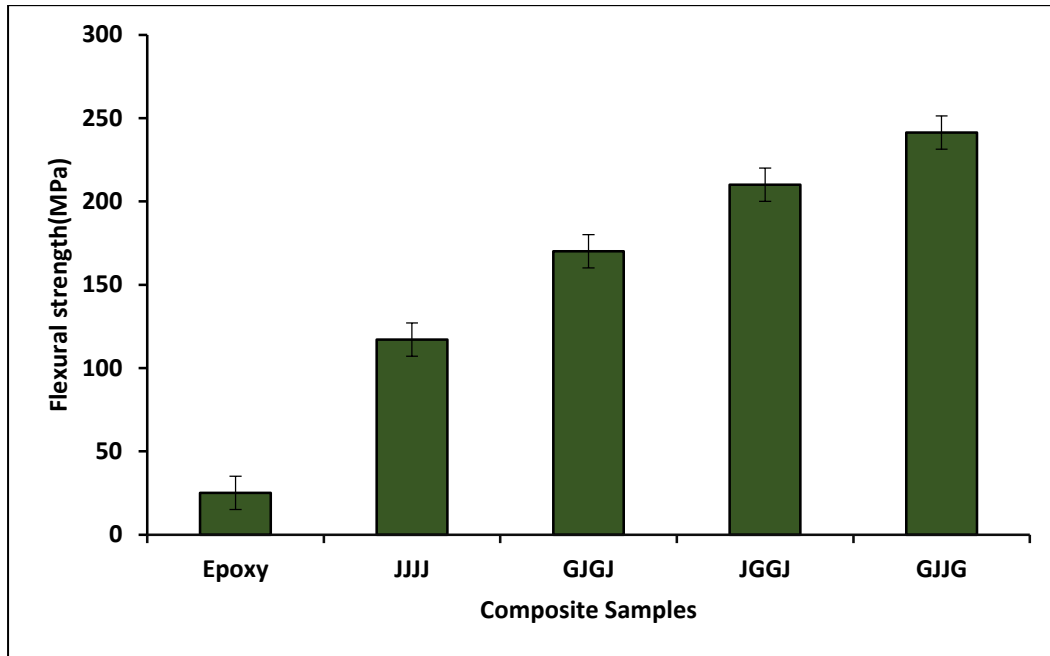


Figure 3.11: Flexural strength of jute-glass fiber reinforced epoxy composites

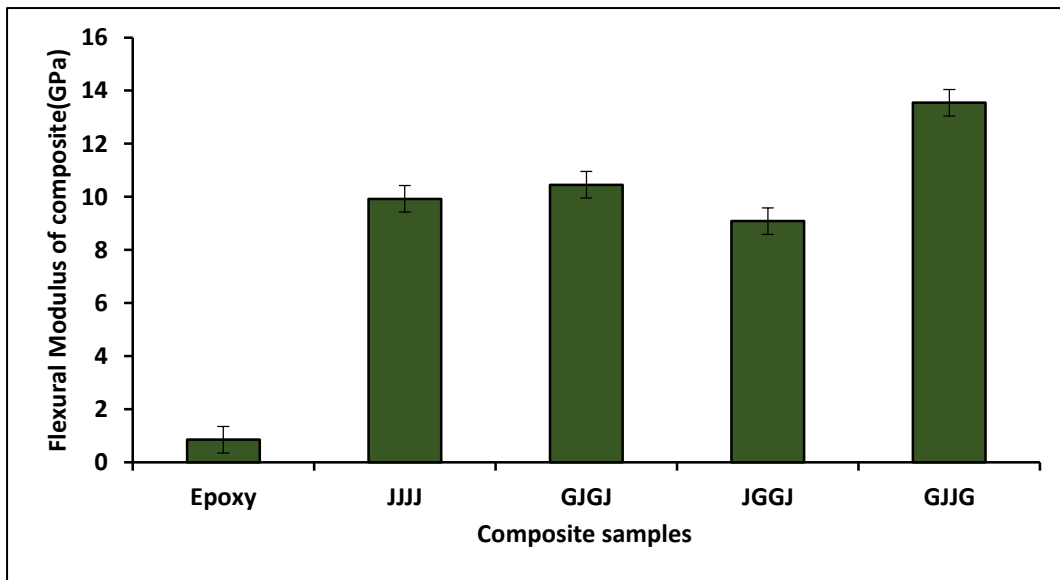


Figure 3.12: Flexural modulus of jute-glass fiber reinforced epoxy composites

3.3.1.3 Effect of Interlaminar shear strength (ILSS) on hybrid jute-glass epoxy composites

Interlaminar shear strength for various laminate stacking sequences of hybrid jute-glass fiber epoxy composites is given in figure 3.13. The ILSS value increases due to glass-jute layering sequence on hybrid epoxy composites. From the table 3.3, the ILSS of the unreinforced epoxy is found to be 2MPa whereas the ILSS of hybrid glass-jute composites for the sequence (GJJG) is found to be 8MPa, which is greater than that of the neat epoxy. The higher value of ILSS is due to presence of glass fiber at the outer surface of the hybrid jute-glass epoxy composites. The value of interlaminar shear strength is found to be 60% higher for the sequence GJJG as compared to only jute fiber composite.

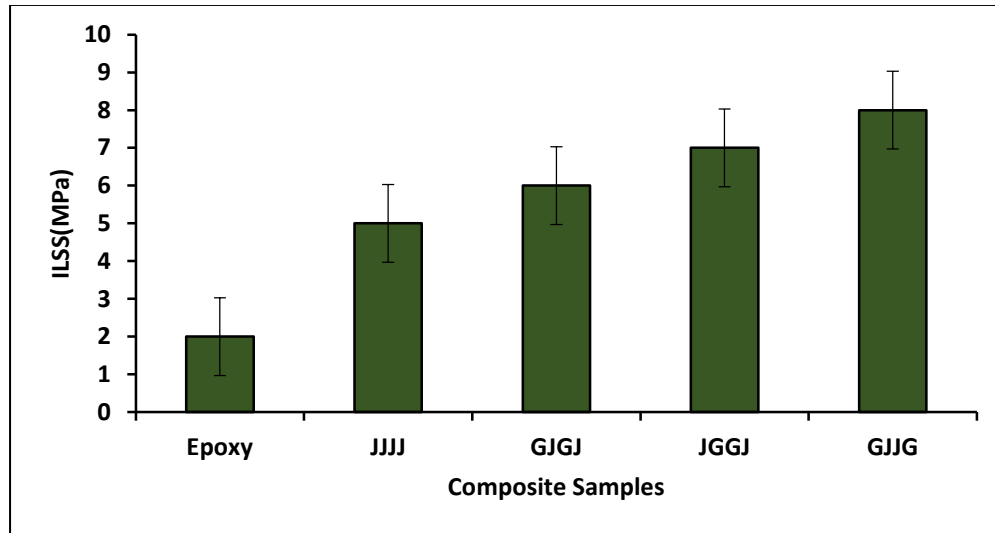


Figure 3.13: Interlaminar shear strength of hybrid jute-glass laminate epoxy composites

3.3.1.4 Effect of Impact strength on hybrid jute-glass epoxy composites

The impact properties of composite materials depend on overall toughness which is highly influenced by the nature of the constituent materials, fiber-matrix interface, construction, geometry of the composites and test conditions. The objective of Izod impact test is to measure the relative susceptibility of a standard test specimen to the pendulum type impact load. The results are expressed in terms of kinetic energy consumed by the pendulum in order to break the specimen. The impact strength of hybrid jute-glass fiber reinforced epoxy composites for various stacking sequences is given in figure 3.14. From the graph it was observed that impact strength of all hybrid composites are less than that of neat epoxy. The highest impact strength is found to be for glass-jute composite (GJJG) of value

67.6KJ/m². The lower value is observed for JJJJ composite of 12 KJ/m². This might have happened due to good adhesion between the fiber and matrix and orientation of fibres which are responsible for resistance to crack propagation during impact test. This indicates that woven fabric plays an important role in the impact resistance of the composite as they interact with the crack formation in the matrix and act as stress-transferring medium. Generally the polymer based composite materials when subjected to impact type of loading conditions, energy is absorbed in the process of plastic deformation of matrix material, debonding at matrix/reinforcement interface and in the fracture of reinforcing material. The phenomenon that absorbs least energy for its occurrence become prominent and leads to fracture [151]. In the present study, plastic deformation of epoxy matrix and debonding at interface could be the reason for decrease in impact properties of hybrid developed composites. Similar types of results are also reported in literatures [48,144,152-153].

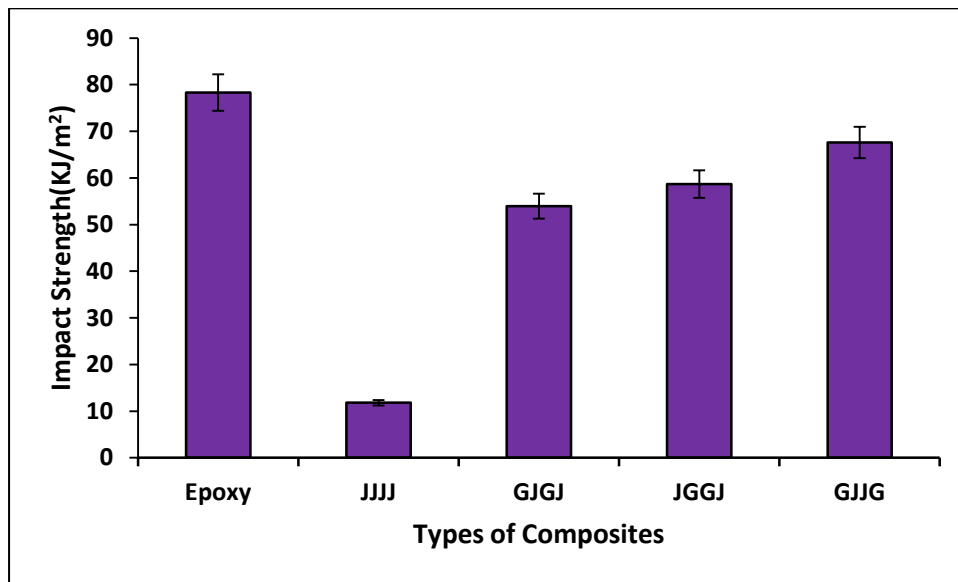


Figure 3.14: Impact strength of hybrid jute-glass epoxy composites

3.3.2 Morphological studies of hybrid jute-glass epoxy composite

The morphology of the hybrid composite due to tensile load is presented in figure 3.15(a). The stretching out of the jute fiber from the matrix is clearly visible. There is no indication of matrix cracking or tearing of surfaces. Figure 3.15(b) shows the morphology of the flexural specimen. Observation of failed specimens revealed that failure in jute laminates is sudden with pull out of jute fibers; however there is no damage seen for the glass fibers. This can be attributed to the fact that, glass fibers are stronger and stiffer than jute fibers.

Thus it can be concluded that, the flexural strength and stiffness for the present case are controlled by extreme layers of reinforcement.

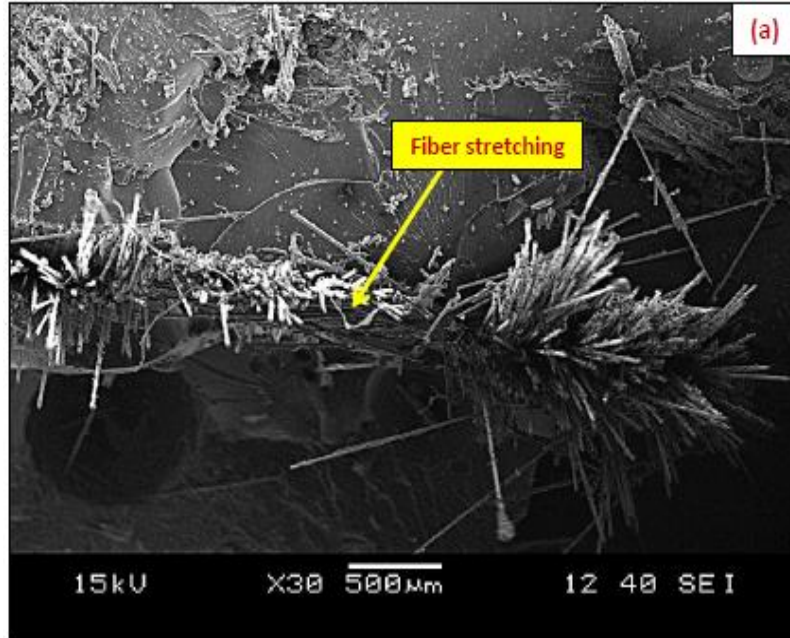


Figure 3.15 (a): SEM image of tensile fractured surface of hybrid GJJG epoxy composite

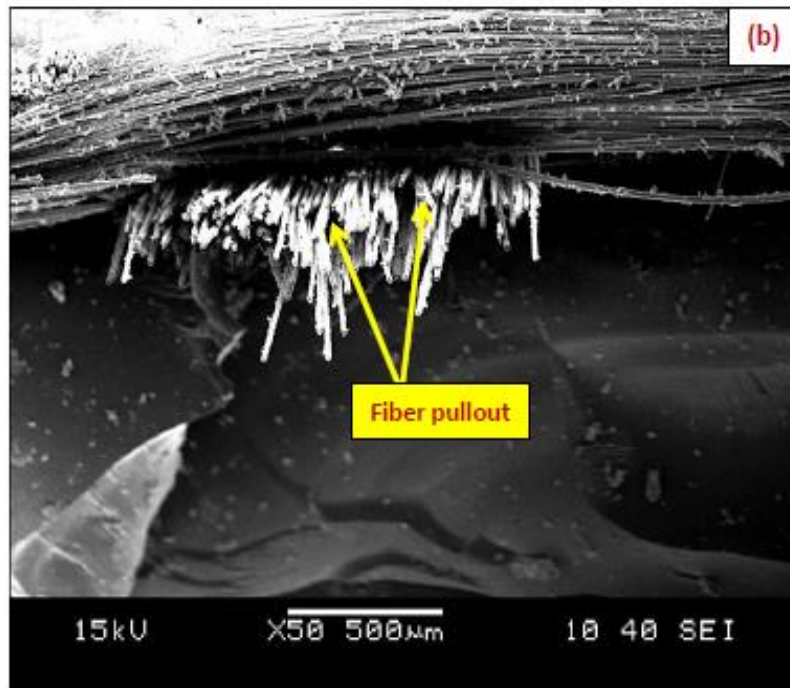


Figure 3.15 (b): SEM image of flexural fractured surface of hybrid GJJG epoxy composite

3.4 Micro Filler Hybrid Composites

In this section it is tried to improve the strength of the hybrid composite GJJG by incorporating particulate filler cenosphere with different doses (5, 10, 15 and 20wt.%).The results obtained from different tests are explained in the next sections.

3.4.1 Density and void fraction measurement

In the present study the composite consists of matrix, fiber and particulate filler. Hence the modified form of equation(3.2) for the density of the composites can be rewritten as

$$\rho_{ct} = \frac{1}{(W_m/\rho_m) + (W_f/\rho_f) + (W_p/\rho_p)} \quad (3.9)$$

Where W_p and ρ_p are weight fraction and density of particulate filler respectively.

For finding out void fraction of GJJG composites for various wt. percentages of cenosphere particles, the same procedure is followed as explained earlier in section no. 3.2.3 and article no. 3.2.3.1. The theoretical density, actual density and the void fraction obtained for cenosphere filled developed GJJG composites are shown in table 3.5.

3.5 Materials and methods

3.5.1 Raw materials used

Raw materials used in this experimental work are listed below:

1. Jute fiber
2. E-glass fiber
3. Epoxy resin
4. Hardener
5. Cenosphere

3.5.1.1 Jute fiber

The details of the jute fiber, its chemical constituents used for the present investigation are explained in chapter 1 art. 1.5.1.

3.5.1.2 E-glass fiber

The details of the glass fiber, its chemical constituents used for the present investigation are explained in chapter 3 art. 3.2.1.2.

3.5.1.3 Epoxy resin and Hardener

The details of the epoxy resin and hardener used for the mechanical tests are same as explained in chapter 3 art. 3.2.1.3.

3.5.1.4 Cenosphere filler

As cenosphere is a hollow microsphere produced during phase transformation and thermochemical reaction during combustion of coal in thermal power plant. It is obtained from National Power Engineers Kolkata.

3.5.2 Preparation of Composites

Preparation of the hybrid composites with the filler addition is same as explained in chapter 3 article 3.2.2. The only difference is the addition of cenosphere particles with varying weight percentages (5, 10, 15 and 20wt.%) to the developed composites. The required amount were calculated and put in the epoxy hardener mix and then were poured in to the mould during fabrication. In all the fabricated samples care was taken to keep the thickness as 5mm. The stacking sequences used are shown in table 3.4.

Table 3.4: Laminate stacking sequence of cenosphere filled hybrid glass-jute epoxy composites

Symbol	Stacking sequence	Cenosphere Wt. (%)	Total fiber		Thickness (mm)
			Volume fraction %	Weight fraction %	
S5	GJJG	5	16.43	29.34	5
S6	GJJG	10	18.28	32.66	5
S7	GJJG	15	20.83	37.11	5
S8	GJJG	20	23.33	41.46	5

3.5.3 Tensile strength

The tensile tests for the filled developed hybrid composites were carried out as per the procedure given in chapter 3 article 3.2.4. For each stacking sequence of different cenosphere weight percentage, five identical samples were tested, and the average result was obtained.

Figures 3.16 (a-b) shows the specimen used for the testing and the fractured samples. The results obtained from the tests are presented in table 3.6.

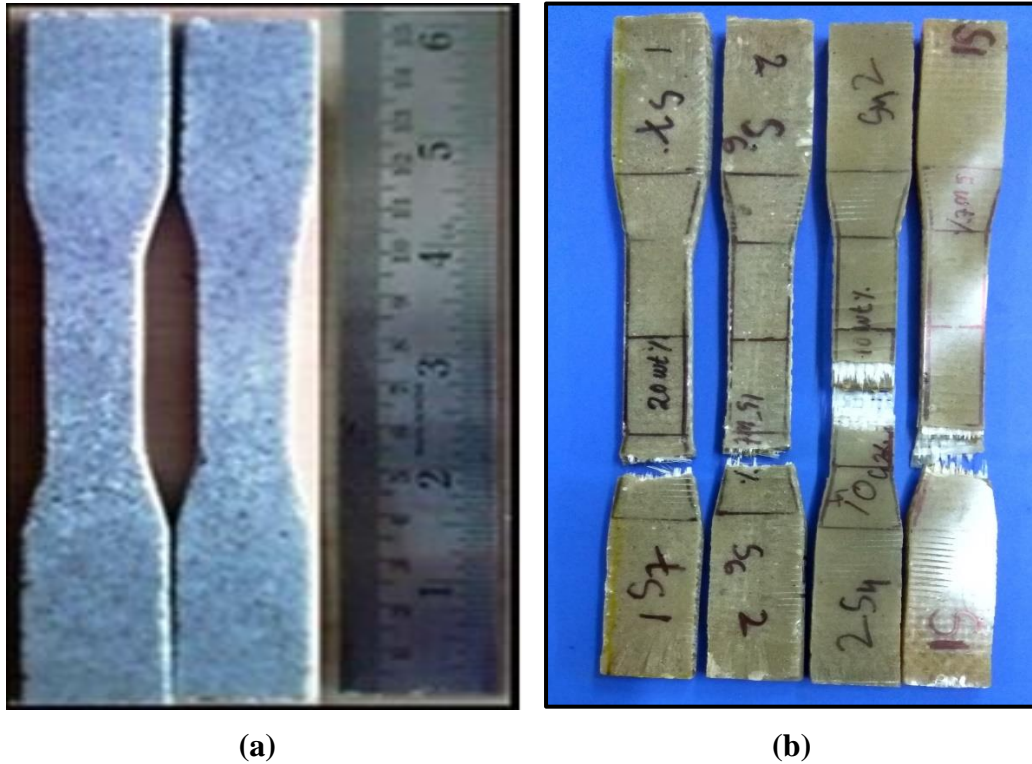


Figure 3.16: Photograph of (a) Specimen for testing (b) Tensile fractured samples

3.5.4 Flexural strength

Flexural tests of cenosphere filled composites were also conducted on the same machine figure 3.7(b) used for hybrid jute-glass epoxy composites. The detail procedure and calculation is explained in chapter 3 article 3.2.5. Few flexural tested samples are shown in figures 3.17 (a-b). Five specimens of each sample were tested for accuracy.

3.5.5 Interlaminar shear strength

The procedure of ILSS test for different cenosphere weight percentage of developed hybrid jute-glass(GJJG) composite is explained in chapter 3 article 3.2.6. The ILSS calculated are presented in table 3.6.

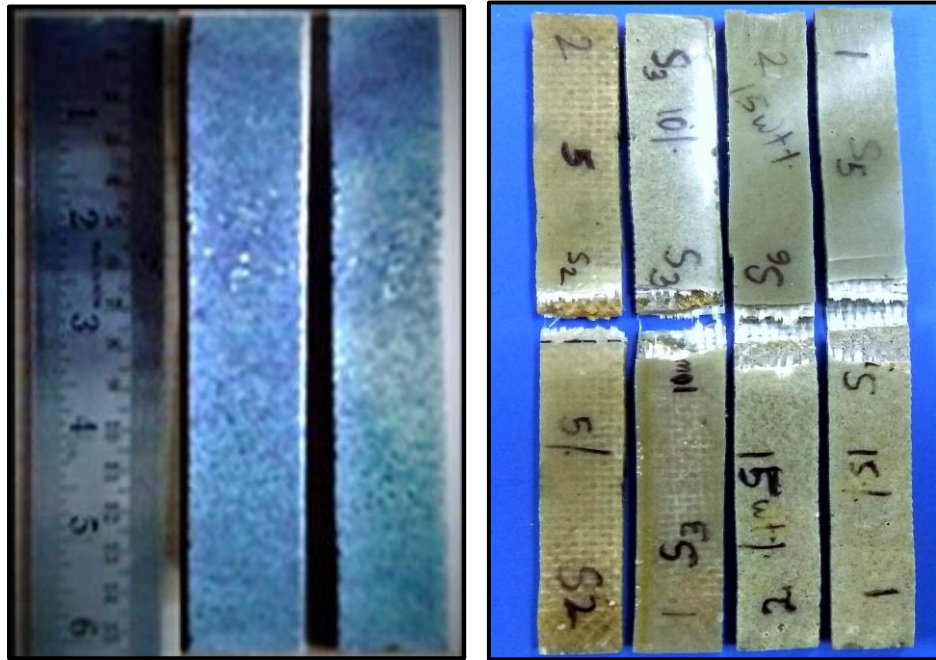


Figure 3.17: Photograph of (a) Flexural testing samples (b) Few fractured samples

3.6 Results and discussion

3.6.1 Density and void fraction of composites

The density and void fractions of the hybrid jute-glass fiber reinforced epoxy composites with cenosphere addition for different stacking sequences are shown in table 3.5. The volume fraction of voids for the particulate filled composites are found to be within the limit of 2% [154]. It is interesting to note here that the void fractions are found to be reduced drastically for different weight fraction of particulate filler (cenosphere). This might have happened due to good packing characteristic of the composites. The same type of result was reported by Satapathy *et.al* [154] while working with jute-epoxy composites reinforced with SiC derived from rice husk. Generally density of a composite depends on the relative proportion of matrix and reinforcing materials and this is one of the most important factors determining the properties of the composites. The voids significantly affect some of the mechanical properties and even the performance of composites. Higher void contents usually mean lower fatigue resistance, greater susceptibility to water penetration and weathering

[149]. However, the presence of void is unavoidable in composites making particularly through hand-lay-up route.

Table 3.5: Density and void content of cenosphere filled hybrid jute-glass epoxy composites

Stacking sequence	Cenosphere(CS) wt. %	Theoretical density (g/cm ³)	Experimental density (g/cm ³)	Volume fraction of voids (%)
GJJG(S4)	0	1.20	1.193	0.566
GJJG(S5)	5	1.196	1.194	0.167
GJJG(S6)	10	1.181	1.180	0.084
GJJG(S7)	15	1.087	1.086	0.091
GJJG(S8)	20	1.144	1.143	0.087
G-Glass fiber, J-Jute fiber, CS-Cenosphere				

3.6.2 Effect of cenosphere on mechanical properties of hybrid glass-jute epoxy composite for stacking sequence (GJJG)

The variation of tensile strength, flexural strength, their modulus and ILSS (Interlaminar shear strength) values for different amounts of cenosphere filled composite laminates is shown in table 3.6 and in figures 3.18-3.22. It is found that the tensile strength of the composite increases due to the incorporation of third phase particulate cenosphere from 5 to 15wt. %. Further addition of cenosphere (i.e.) 20wt. %, the tensile strength decreases and same type of result was reported by [155-156] while they worked with oil palm empty fruit bunches/jute fiber reinforced epoxy hybrid composites and ceramic filled woven jute fabric epoxy composites respectively. This might have happened due to the chemical reaction at the interface between the filler particles (cenosphere) and the matrix which might be too weak to transfer the loads. The other factor might be due to the irregular shaped particulates which gives rise to uneven stress concentration in the epoxy matrix. Similarly for the case of

Chapter 3 Mechanical properties of jute-glass composite with and without cenosphere

flexural strength, their modulus and interlaminar shear strength the same trend is observed. The increase in tensile strength, flexural strength and ILSS (interlaminar shear strength) is about 90.47%, 24.32% and 16.75% higher for 15wt. % cenosphere filled composite as compared to the strength of only glass-jute (GJJG) composite. This indicates the advantage of adding third phase (cenosphere particles) in the composite for suitable applications.

Table 3.6: Mechanical properties of cenosphere filled hybrid jute-glass epoxy composites

Stacking Sequence	Cenosphere Wt. %	Flexural Strength (MPa)	Tensile Strength (MPa)	Interlaminar shear strength (MPa)	Flexural Modulus (GPa)	Tensile Modulus (GPa)
GJJG(S4)	0	241.3	42	8	13.543	2.95
GJJG(S5)	5	246.75	45	8.1	15.996	3.806
GJJG(S6)	10	265	54.6	8.32	20.93	4.481
GJJG(S7)	15	300	80	9.34	30.324	6.656
GJJG(S8)	20	282.04	65	8.8	21.6	4.418

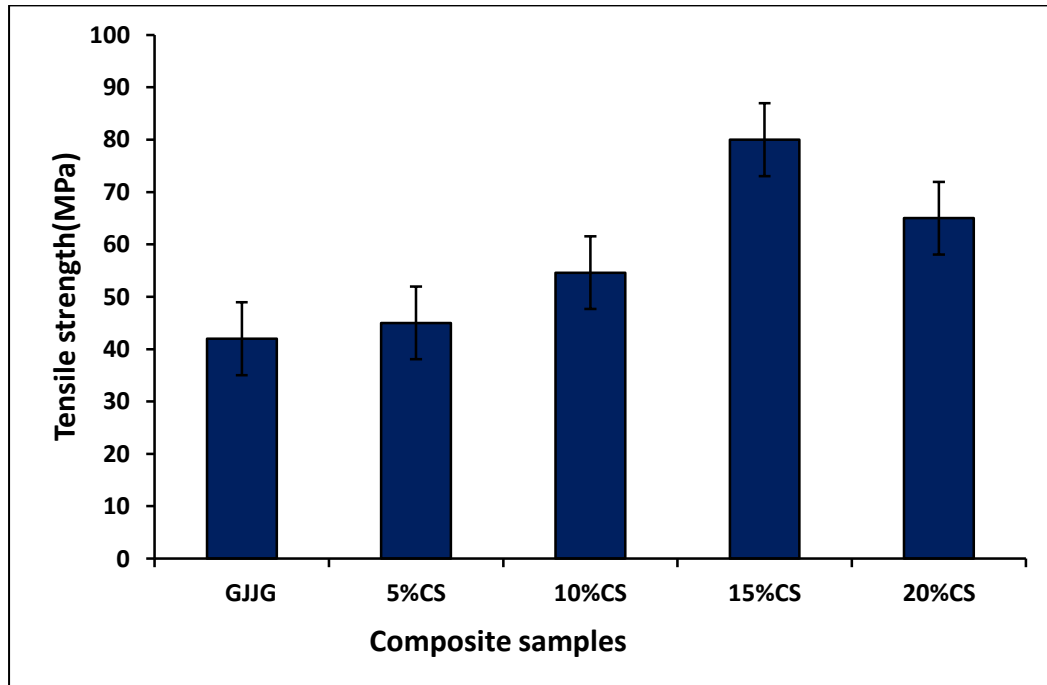


Figure 3.18: Tensile strength of cenosphere filled hybrid jute-glass epoxy composites

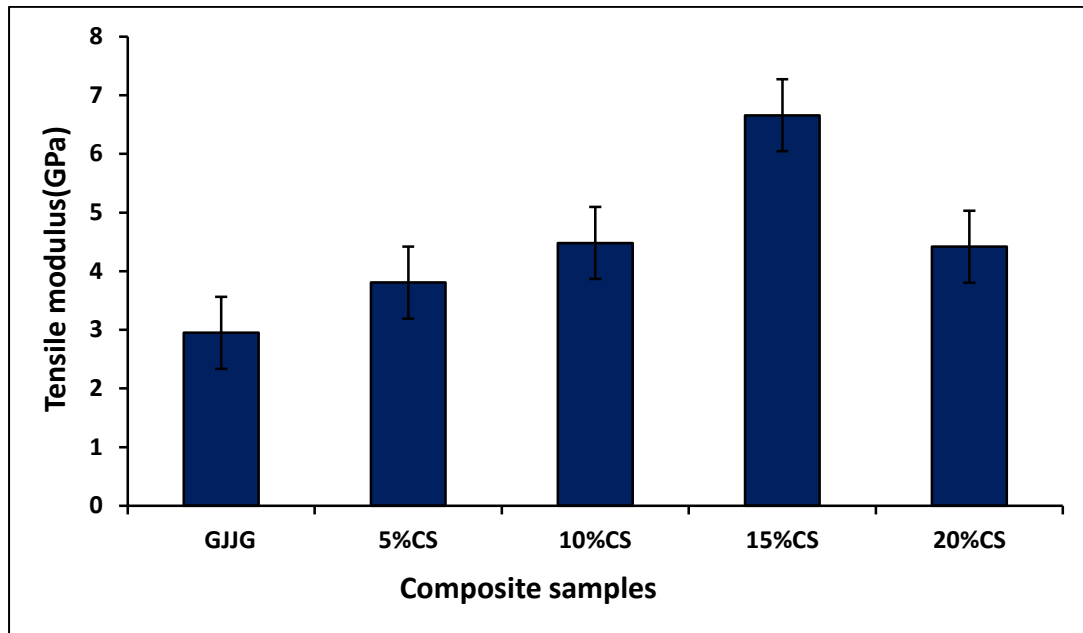


Figure 3.19: Tensile modulus of cenosphere filled hybrid jute-glass epoxy composites

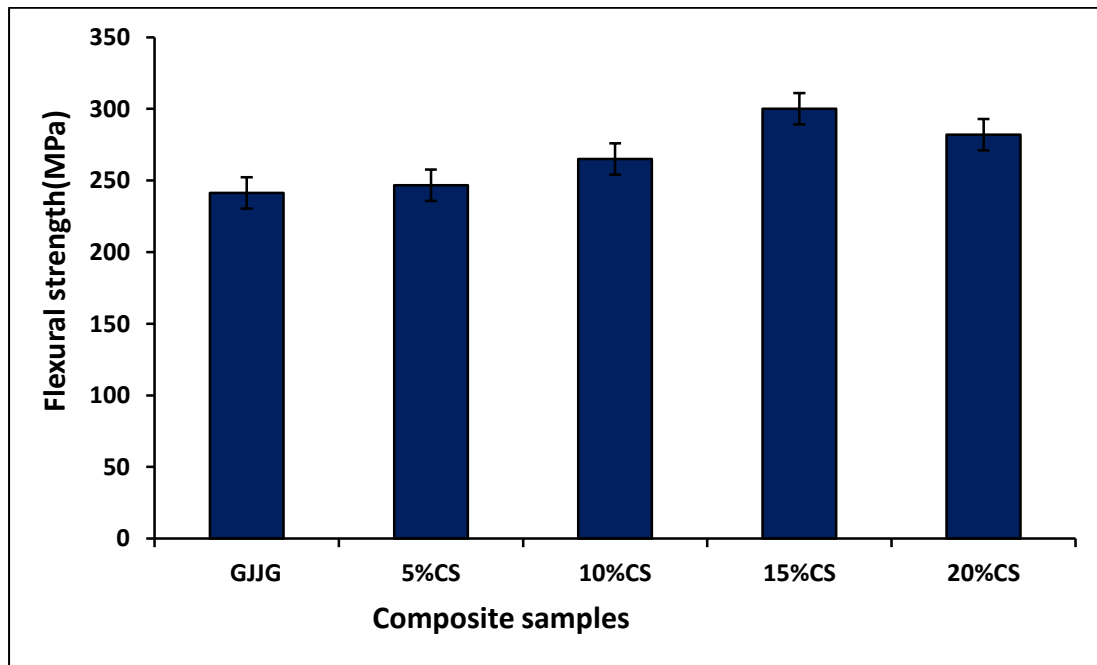


Figure 3.20: Flexural strength of cenosphere filled hybrid jute-glass epoxy composites

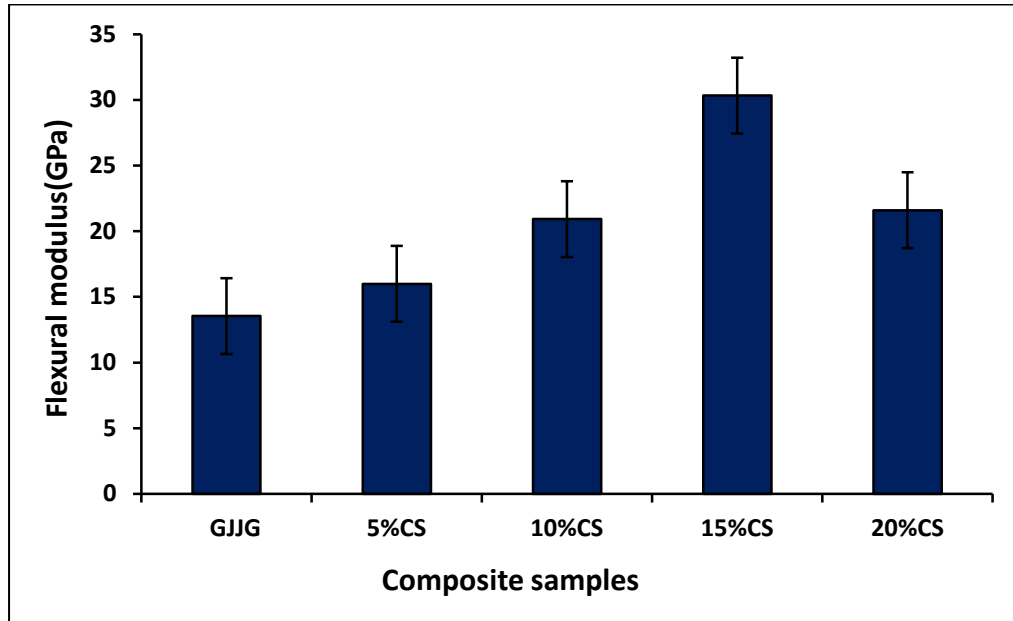


Figure 3.21: Flexural modulus of cenosphere filled hybrid jute-glass epoxy composites

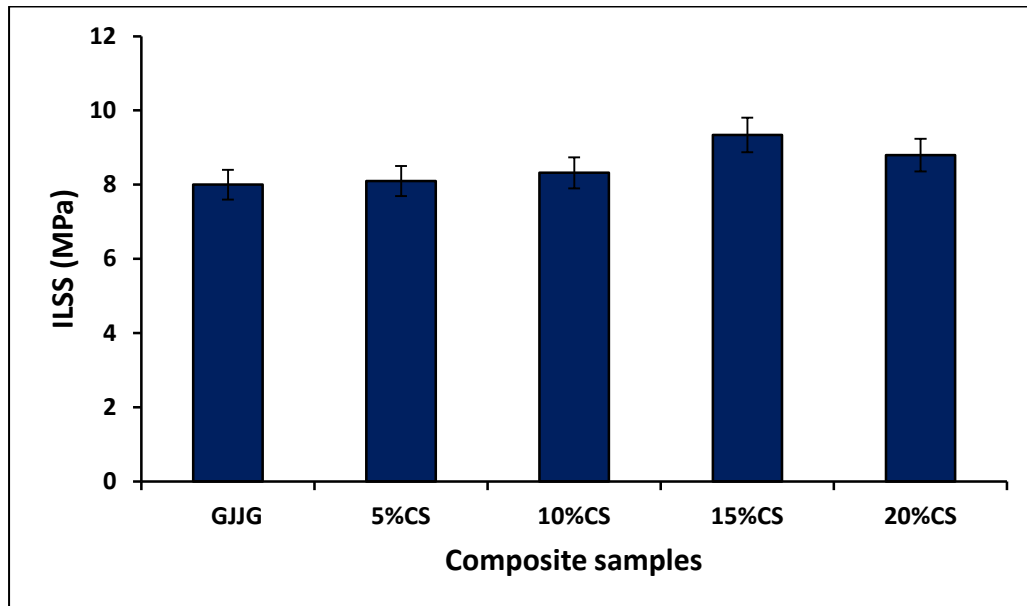
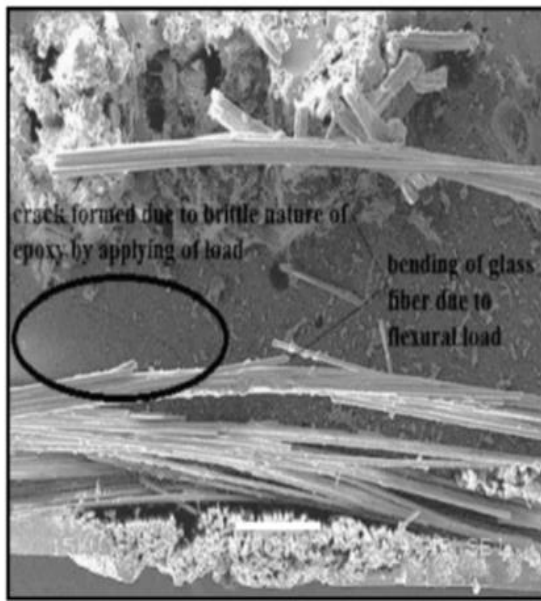


Figure 3.22: Interlaminar shear strength of cenosphere filled hybrid jute-glass epoxy composites

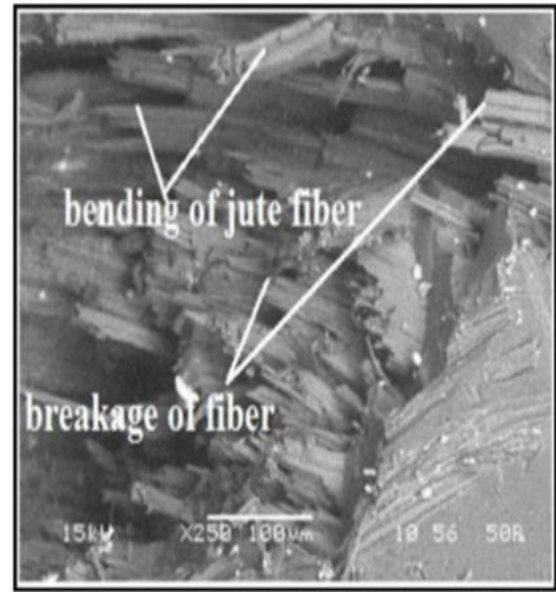
3.6.3 Morphological Studies of hybrid glass-jute epoxy composites with and without filler

The morphology of the flexural tested composites of the jute-glass fiber hybrid composites with and without cenosphere are shown in figures 3.23 and 3.24. Bending of glass fiber due to flexural load is clearly visible in figure 3.23(a) whereas bending as well as breakage of jute fiber is found for the jute fiber composite when flexural load is being applied as in figure 3.23(b). Sharp cut were also observed for the jute fiber which indicates brittle nature of the jute fiber. For the hybrid composites when flexural load is applied matrix cracking occurs much before the failure as shown in figure 3.23(c). But when cenosphere of 15 wt. percentage was added to hybrid composite it was found that stretching of glass fiber is minimum with bending of jute fiber without breaking as in figure 3.23(d). Matrix cracking is also not visible. This indicates the increase in the strength of the hybrid composite due to addition of cenosphere particles.

For tensile tested specimen also breakage of jute fiber figure 3.24(a) and stretching out of glass fiber from the matrix in figure 3.24(b) are clearly seen. For the hybrid composite breaking of glass fiber on the outer layer without any effect on the jute fiber is found in figure 3.24(c). When cenosphere of 15 wt.% was added to the hybrid composite it was found that breaking of glass fiber is restricted with little stretching of jute fiber in figure 3.24(d). Since glass fiber breaking is avoided which is at the outer layer, increase in the strength of the composite is found. This happened due to addition of cenosphere particles into the matrix.



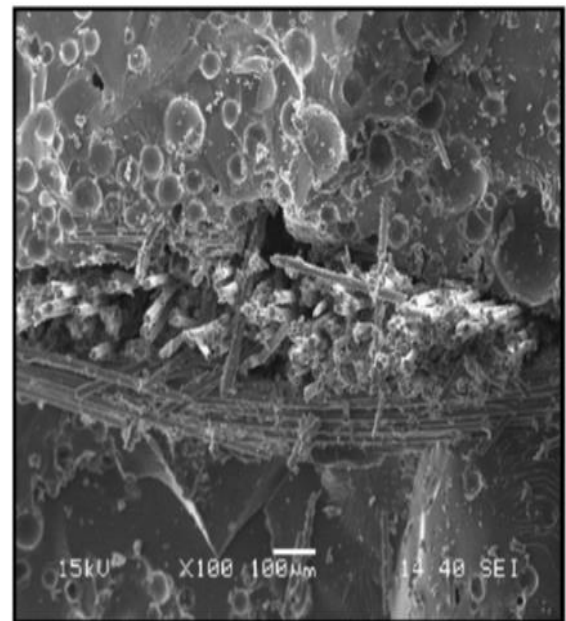
(a)



(b)



(c)



(d)

Figure 3.23 SEM images of flexural fractured surface of (a) Glass fiber composite (b) Jute fiber composite (c) Jute-glass hybrid composite (d) Cenosphere filled GJJG hybrid composite

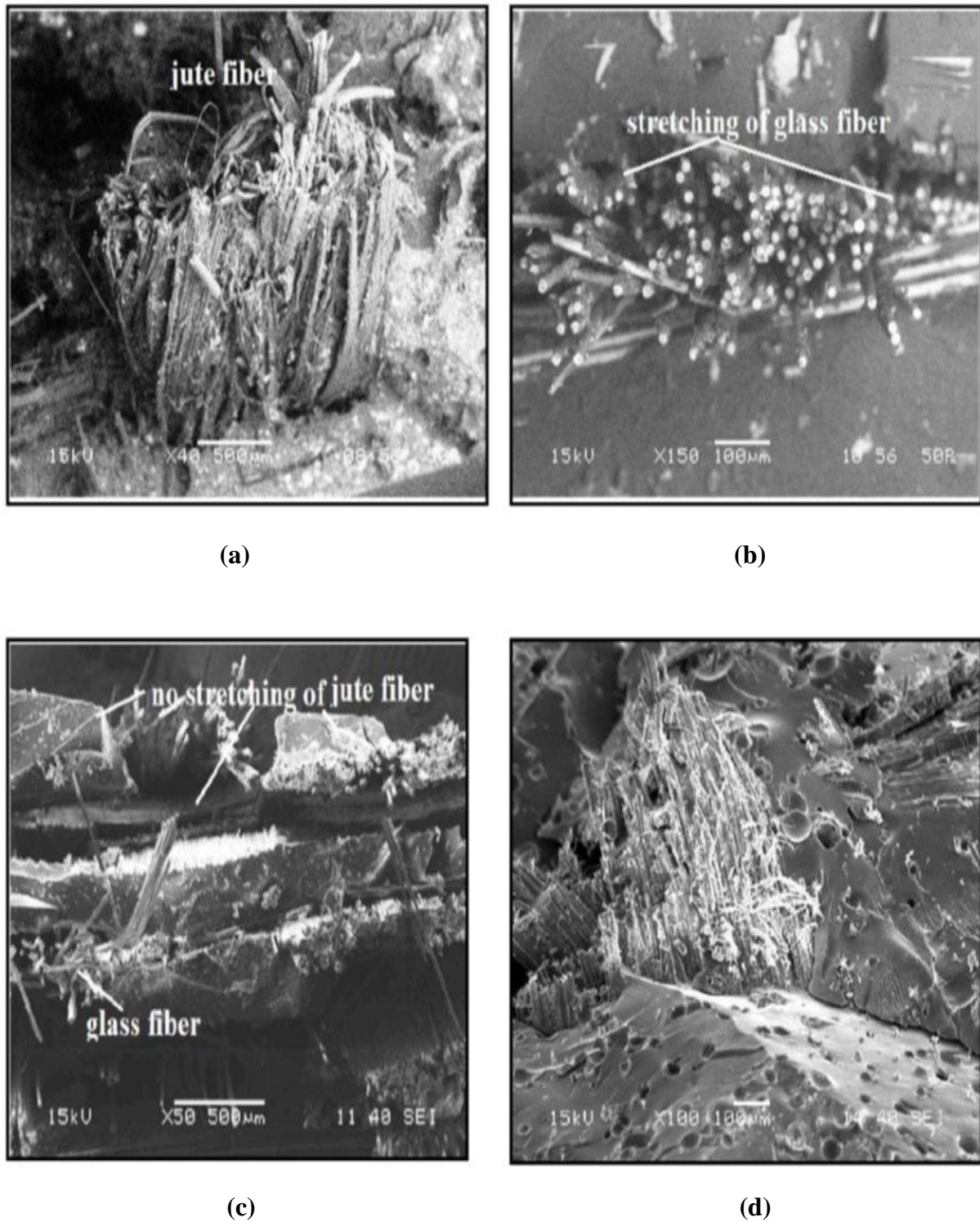


Figure 3.24: SEM images of tensile fractured surface of (a) Jute fiber composite (b) Glass fiber composite (c) Jute-glass hybrid composite (d) Cenosphere filled GJJG hybrid composite

3.7 Conclusions

1. By incorporation of natural and synthetic fibers into the polymer matrix, the mechanical properties enhanced to a greater extent with different stacking sequences.
2. The maximum flexural and tensile strength is observed in hybrid glass-jute epoxy composites with the sequence GJJG.
3. The maximum ILSS is observed for the composite prepared with glass fiber at extreme layers.
4. Effect of cenosphere filler on tensile and flexural properties of jute-glass fabrics reinforced epoxy composites indicates that, that incorporation of filler enhanced the mechanical properties with their modulus.
5. Maximum tensile, flexural and ILSS are observed for the composite with inclusion of 15wt% cenosphere filler.
6. The increase in tensile, flexural and ILSS with 15wt. % of cenosphere filled composite is found to be 90.47%, 24.32% and 16.75% higher than that of GJJG composite without filler.
7. The SEM studies confirm that bending of glass fiber for flexural strength and breaking of glass fiber in case of tensile strength is restricted due to addition of third phase i.e. cenosphere which increases the strength of the developed composites.

Chapter 4

Moisture absorption behaviour of cenosphere filled hybrid jute-glass fiber epoxy composites

4.1 Introduction

In general natural fibers are hygroscopic in nature and they absorb or release moisture depending on environmental conditions. Amorphous cellulose and hemicellulose that present in the natural fiber are mostly responsible for the high moisture absorption, since they contain numerous easily accessible hydroxyl groups which give a high level of hydrophilic character to fibers. The high moisture absorption of the fiber occurs due to hydrogen bonding of water molecules to the hydroxyl groups within the fiber cell wall. This leads to a moisture build-up in the fiber cell wall (fiber swelling) and also in the fiber-matrix interface. This in turn becomes responsible for changes in the dimensions of cellulose-based composites, particularly in the thickness and the linear expansion due to reversible and irreversible swelling of the composites[157]. Another problem associated with fiber swelling is a reduction in the adhesion between the fiber and the matrix, leading to deterioration in the mechanical properties of the composite [158]. A good fiber-matrix bonding can decrease the rate and amount of moisture absorbed by the composite as well as improving the mechanical properties [159]. However in order to overcome this problem, chemical treatment has been considered as a good technique to reduce the hydroxyl group in the fibers. Different chemical treatments such as mercerization or alkali treatment, isocyanate treatment, acrylation, benzylation, permanganate treatment, acetone treatment, acetylation, silane treatment etc. are reported by several researchers [160-163].The moisture absorption by composites containing natural fibers with fillers has several adverse effects on their properties and thus affecting their long-term performance. In view of the severity of moisture absorption and its effects on composite properties, numerous efforts have already been made by several researchers to address this issue.

Chapter 4 Moisture absorption behaviour of cenosphere filled jute glass epoxy composites

George *et al.* [164] investigated the relationship between the moisture absorption of pineapple-leaf fiber reinforced low density polyethylene (LDPE) composites with different fiber loadings. They found that the moisture absorption increases almost linearly with the fiber loading.

Joseph *et al.* [165] studied the environmental effects on sisal fiber reinforced PP composites. Water uptake of the composite was found to increase with fiber content and leveled off at longer periods. The chemically modified fiber composites showed a reduction in water uptake because of better interfacial bonding. Water uptake of the composite was found to increase with temperature since temperature activates the diffusion process. Reduction in tensile properties was observed due to the plasticization effect of water. The fiber/matrix bonding becomes weak with increasing moisture content, resulting in interfacial failure.

Stark [166] found that wood flour-polypropylene (PP) composites with 20 wt.% wood flour reached equilibrium after 1500 hrs in a water bath and absorbed only 1.4% moisture while composites with 40 wt.% loading reached equilibrium after 1200 h water submersion and absorbed approximately 9.0% moisture. After the analysis, she concluded that the wood flour is inhibited from absorbing moisture due to encapsulation of the wood flour by the PP matrix and that the degree of encapsulation is greater for the 20% wood flour composite than that for the 40% wood flour composite.

Thomas *et al.* [167], while studying water absorption characteristics of sisal fiber polyester composites found that diffusion coefficient decreases with chemical treatment of fiber. In addition to this the chemical treatment also decreases water absorption capacity of the composite. They also showed that the composite with benzoyl-chloride treated sisal fiber composite exhibited lower water absorption capacity.

Masoodi R. and Pillai KM. [168] studied on six different sets of composite specimen using different percentages of jute fibers and two types of epoxy (traditional and bio-based) resin. It is observed that the moisture diffusion rate into composites increases with an increase in the jute fiber to epoxy ratio. The type of epoxy used as the matrix appeared to have an influence on the moisture absorption percentages of the composites. They showed that both the water absorption and swelling measurements were higher for the bio-epoxy composites compared to the epoxy composites, possibly due to the use of cellulose and

Chapter 4 Moisture absorption behaviour of cenosphere filled jute glass epoxy composites

hydroxyl group in bio-epoxies. The swelling of composites was correlated with an increase in diameters of jute fiber in water and possibilities for the appearance of micro-cracks around fibers in composites were also observed. Addition of more jute fibers to the composites parts leads to higher rates of swelling and water absorption in all the composites.

Osman Ekhlas A. *et al.* [169] investigated the effects of moisture absorption on the flexural properties of kenaf-unsaturated polyester composites and kenaf/recycled jute-unsaturated polyester composites. Their result demonstrated that the water absorption and the thickness swelling increased with increase in immersion time. They also showed that generally kenaf/recycled jute composites had considerably lower water absorption and thickness swelling as compared with original kenaf composites which were attributed to changes in physical and chemical properties of composites. The effects of water absorption on flexural properties of kenaf fiber composites can also be reduced significantly with incorporation of recycled jute in composites formulation. The process of absorption of water was found to approach Fickian diffusion behavior for both kenaf composites and hybrid composites.

Zamri Mohd. Hafiz *et al.* [170] reported the results on the moisture absorption of pultruded jute/glass fiber-reinforced unsaturated polyester hybrid composites, which was subjected to various water conditions and their effects on its mechanical properties. They found that hybridization of natural fibers with synthetic fibers decreases the maximum moisture absorption and increases the mechanical properties of the composites. The water absorption behavior of the glass/jute fiber-reinforced unsaturated polyester hybrid composite was found to follow a non-Fickian behavior. The highest values of diffusion coefficient (D_x) and maximum moisture content value (M_m) were recorded for specimens immersed in distilled water, then followed by the acidic solution, and finally sea water.

Jena *et al.* [171] studied the water absorption pattern of bamboo-epoxy composites with fibre and filler loading subjected to sea and distilled water conditions. They found that moisture absorption and thickness swelling increase with increase in number of layers for both environmental conditions. The maximum weight gain and thickness swelling per cent is

Chapter 4 Moisture absorption behaviour of cenosphere filled jute glass epoxy composites

higher in the case of distilled water as compared to that of sea water for both fibre and filler loading. The addition of cenosphere improves the water absorption resistance of the composites, but it depends upon the amount of cenosphere which is limited to 3.0 wt. %.

For potential application of natural fiber polymer composites a comprehensive study on the moisture absorption characteristic and its effect on mechanical properties are required. In this chapter, the characteristics of moisture absorption kinetics and effect of water absorption on the mechanical performance of untreated woven jute-glass fiber hybrid epoxy composites with cenosphere as filler material under different environmental conditions are investigated and reported.

4.2 Characterization studies

4.2.1 EDX analysis of cenosphere filler and raw jute fiber

Cenosphere is a ceramic rich industrial waste produced during burning of coal in thermal power plants. This is also known as aluminosilicate hollow microsphere. The micrograph of filler shows surface morphology and the particle size in the range of (20-200) μm as in figure 4.1(a).

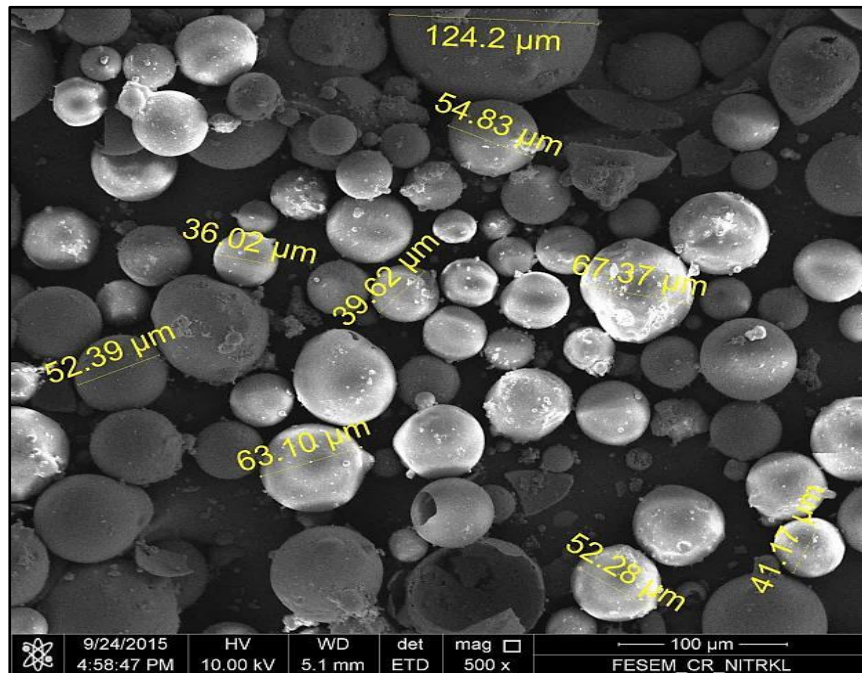


Figure 4.1(a) SEM micrograph Cenosphere

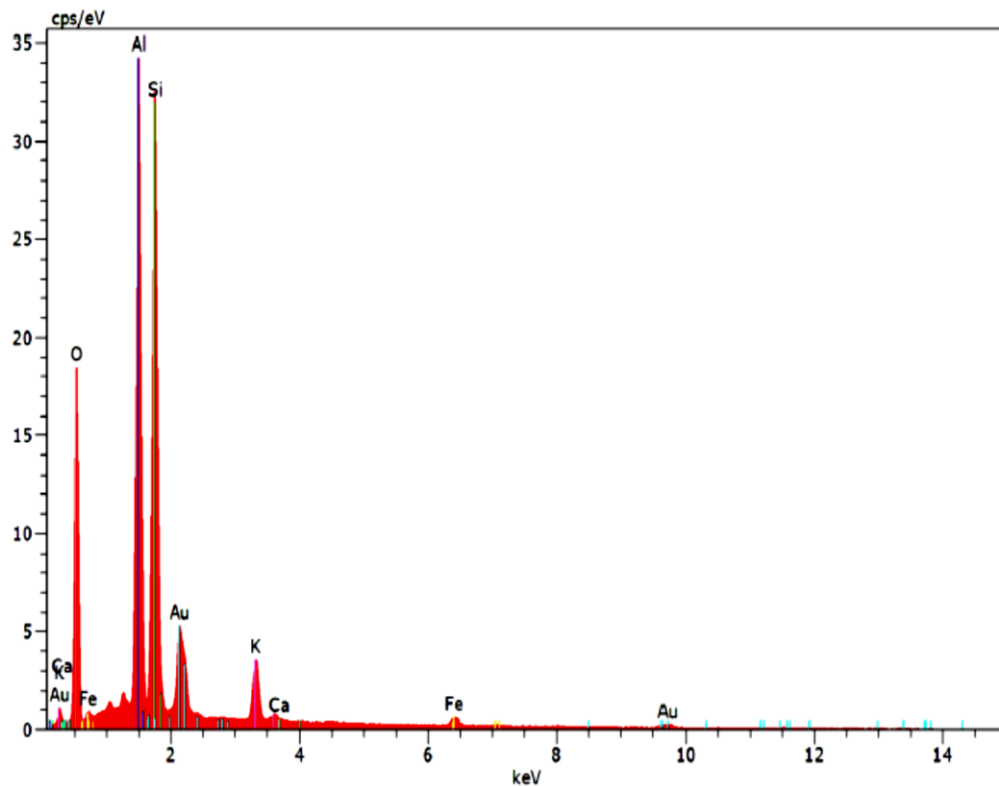


Figure 4.1(b) EDX analysis of cenosphere

The figure 4.1(b) shows the EDS analysis of cenosphere particles. Energy dispersive x-ray spectroscopy (EDS) was used for elemental analysis of cenosphere filler. The EDS spectrum showed the peaks for aluminium, silicon and oxygen corresponding to their binding energies. As indicated in EDX analysis the particles are mainly composed of mixtures of oxides such as SiO_2 , Al_2O_3 and Fe_2O_3 . The chemical composition of cenosphere powder consists of 48.62% of silicon, 27.79 % of aluminium and 3.75 % of iron in oxide form. Various trace elements such as K, Ca and Au are also present. It is a unique class of filler suitable for polymer matrix because of its fine dispersion, homogeneity, inertness, low water absorption and chemical stability.

Figure 4.2 (a) shows the SEM micrograph of jute fiber and the figure 4.2 (b) shows the energy dispersive x-ray spectroscopy (EDS) for elemental analysis of jute fiber. The micrograph shows the morphological structure and the size of jute fiber in between (7-140) μm .



Figure 4.2 (a) SEM micrograph of Jute Fiber

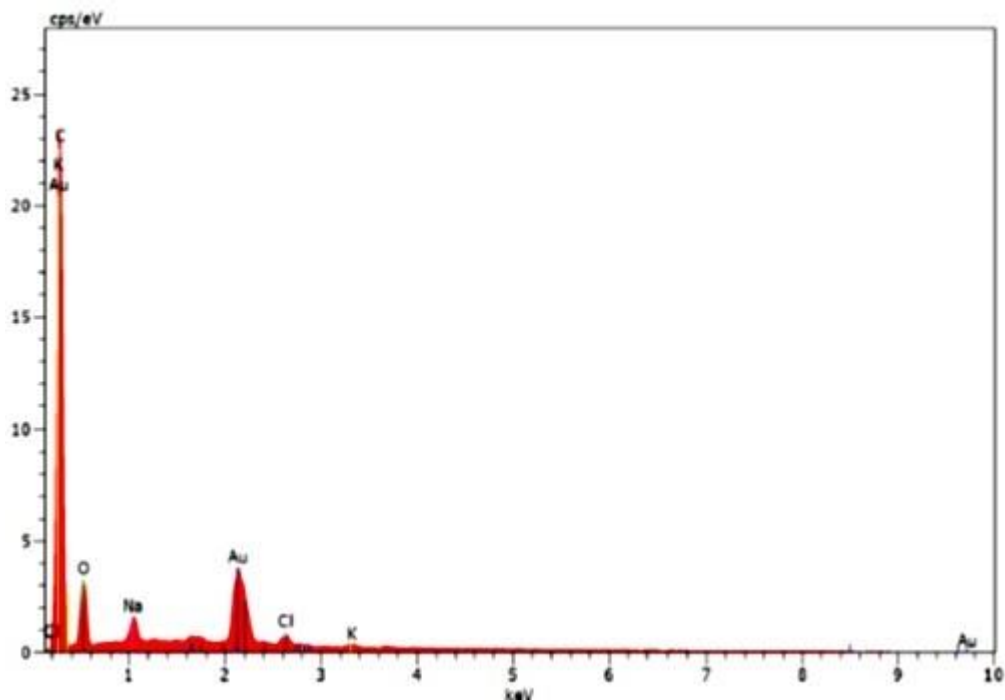


Figure 4.2 (b) EDX analysis of jute fiber

The EDS spectrum showed the peaks for elements carbon, oxygen and sodium corresponding to their binding energies. From the graph it has clearly shown that jute fiber

Chapter 4 Moisture absorption behaviour of cenosphere filled jute glass epoxy composites

consists of 74.01% of carbon(C), 20.32% of oxygen (O), 2.76% of sodium (Na) and minor traces of chlorine (Cl) and potassium (K) are also present.

4.2.2 FTIR Spectroscopy

The chemical structure and identification of the surface functional groups of jute fiber and cenosphere powder were studied by using FTIR spectroscopy method and is shown in figure 4.3. The infrared spectrum analysis was performed on Perkin-Elmer spectrum GXA Fourier transform infrared spectrometer with a resolution of 4cm^{-1} . The samples for FTIR analysis were mixed with KBr dried powder and pressed into pellets under pressure and then scanned. The scanning speed was 2cm s^{-1} with total 20 no. of scans and the samples were measured in an optical range of $(400\text{--}4000)\text{ cm}^{-1}$ as KBr pellets.

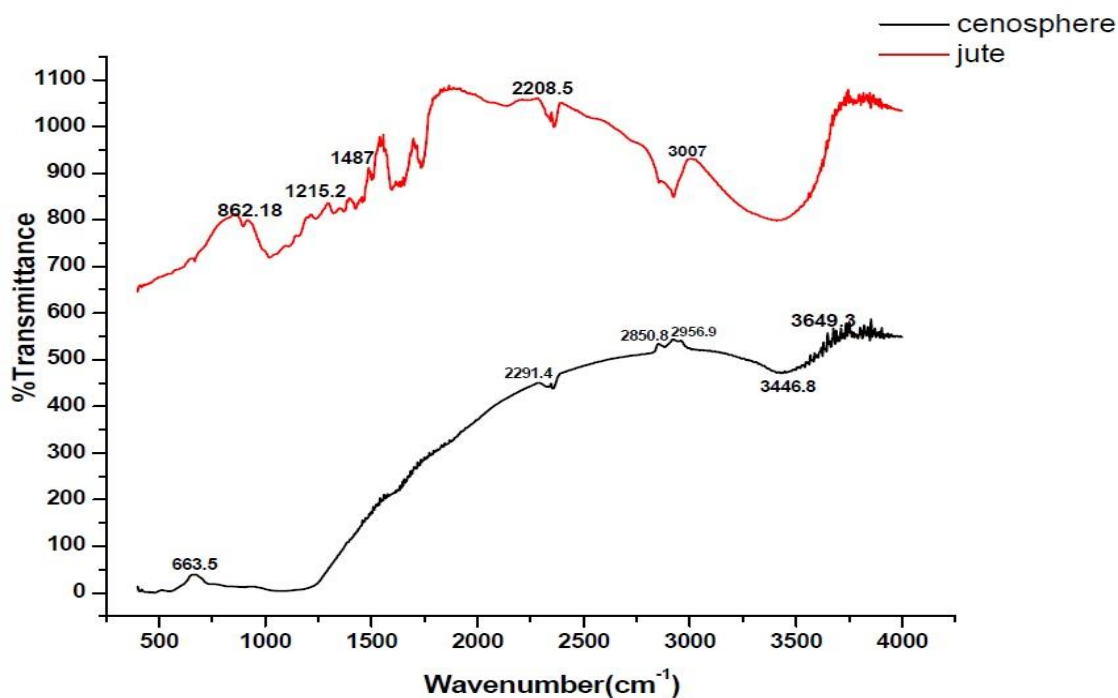


Figure 4.3: Percentage Transmittance of cenosphere powder and jute fiber

From spectrum analysis it can be observed that the cenospheres have very intensive band related to the vibration absorbing peak of the C-Br (alkyl) group at lower wavenumber of 663.5cm^{-1} . The peak lying in the spectrum 2291.4cm^{-1} and 2345.4cm^{-1} indicates the presence of N-H bond and the lower wavenumber results due to the transmission of amine group ($-\text{NH}_2$) to ammonium ion (NH_4^+) as reported[172]. The peaks lying between wavenumber

Chapter 4 Moisture absorption behaviour of cenosphere filled jute glass epoxy composites

2850.8cm⁻¹ and 2956.9cm⁻¹ represents the characteristic peaks of C-H bond which belongs to methyl(-CH₃) group. Additionally the peak lying in wavenumber 3446.8cm⁻¹ is weakened due to the reduction of N-H bond and the formation of H-bridge at wavenumber of 3587.6cm⁻¹ in solvated environment. The peak of 3649.3cm⁻¹ produces the free hydroxyl (-OH) group showing the hydrophilic nature of cenosphere powder.

From spectrum analysis of jute fiber it is found that at lower transmittance of wavenumber of 862.18cm⁻¹, there is presence of isolated aromatic(C-H) group. The wavenumber of 1097.5cm⁻¹ and 1215.2cm⁻¹ indicates the occurrence of aromatic group(C-Cl) and (C-F) in fiber structure. At peak of 1296.2cm⁻¹ there is presence of free hydroxyl (-OH) group leading to the formation of C-F(alkyl) group at wavenumber corresponds to 1348.2cm⁻¹. At higher wavenumber of 3007cm⁻¹ denotes the presence of broad -OH (hydroxyl) stretching vibration with a hydrogen bond in fiber structure integration.

4.2.3 X-ray Diffraction studies

XRD is an useful method for characterizing the crystallinity, phase composition, orientation in the sample and crystallographic structure of semi crystalline material for jute fiber and ceramic rich cenosphere powder. A philips X-Ray diffractometer employing CuK α ($\lambda=1.54\text{\AA}$) radiation and a graphite monochromator with a current of 20A and voltage of 30V was used with a diffraction intensity in the range of 10°-80° (2 θ -angle range). The crystallinity was evaluated by applying the peak-area integration method in the range of 2 θ = (10°-80°) by applying an amorphous scattering curve that was realized by experimental and theoretical experiences. The phase composition of received cenosphere particles are metal oxide and non-metal oxide and the main phase composition are α -SiO₂ and 3Al₂O₃.2SiO₂. The X-Ray diffractograms of cenosphere powder and jute fiber are shown in figures 4.4 (a) and (b).

Chapter 4 Moisture absorption behaviour of cenosphere filled jute glass epoxy composites

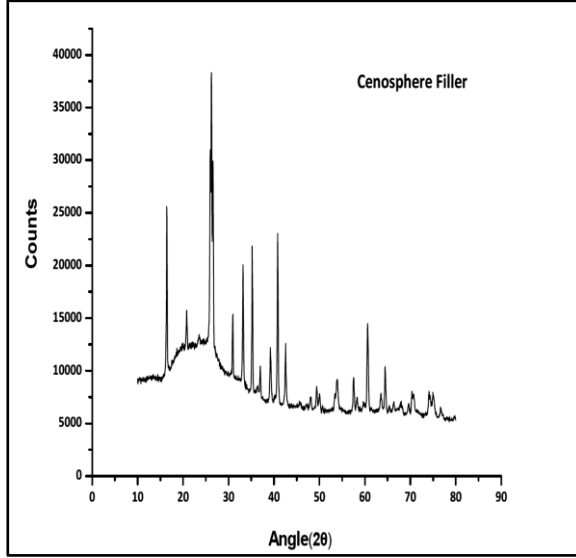


Figure 4.4(a) X-Ray diffractograms of cenosphere powder

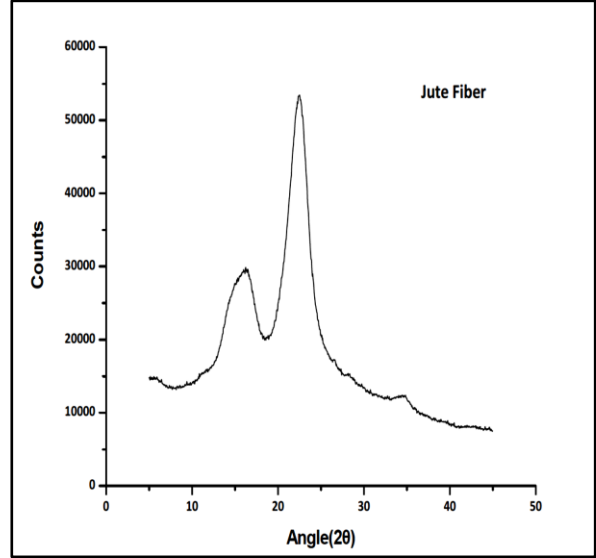


Figure 4.4(b) X-Ray diffractograms of jute fiber

It was observed that the major crystallinity peak of each profile occurred at around angle $(2\theta) = 26.293^\circ$ for amorphous powder and $(2\theta) = 22.3^\circ$ for semi crystalline jute fiber. The results so obtained are in table 4.1.

The crystallinity index (I_c) of both fiber and powder were calculated by using equation.

$$I_c = \left[\frac{I_{crystalline} - I_{amorphous}}{I_{crystalline}} \right] \quad (4.1)$$

Where $I_{crystalline}$ = Maximum intensity of diffraction of the sharp lattice peak at angle 2θ between 20° and 30°

$I_{amorphous}$ = Minimum intensity of diffraction of the smooth lattice peak taken at angle 2θ between 70° and 80°

Table 4.1: Crystallinity Index of Jute fiber and Cenosphere powder

Sample Name	Angle 2θ for $I_{amorphous}(^\circ)$	Angle 2θ for $I_{crystalline}(^\circ)$	$I_{amorphous}$	$I_{crystalline}$	Crystallinity Index $I_c(\%)$
Jute fiber	73.311	22.3	0.7499	13.75	94.54
Cenosphere	79.951	26.293	0.7086	8.451	91.61

Chapter 4 Moisture absorption behaviour of cenosphere filled jute glass epoxy composites

It was observed that fiber shows higher crystallinity index as compared to amorphous powder as reported [173-174]. Jute fiber shows higher crystalline behaviour indicating the higher strength of the polymer composite due to compactness of cellulose content in the fiber bundle integration. From the figures as the angle of crystallization increases, the intensity decreases denoting the non-crystalline behaviour of the samples. Crystallinity decreases progressively with addition of cenosphere content and thereby enhancing the amorphous volume fraction in the structural form of the composites.

4.2.4 Thermogravimetric analysis (TGA) of cenosphere filled hybrid glass-jute epoxy composite

Thermal analysis is the concept that purely reflects the decomposition reactions that occur at the molecular level of the materials with variation in temperature. The analysis was done to know the thermal degradation behaviour of particulate (cenosphere) filled jute-glass reinforced composite of optimum sequence (GJJG) at higher temperature. The test was conducted on Perkin-Elmerpyris-7 TG analyzer at heating rate of 10°C/min from (40°-600°)C under nitrogen atmosphere. The thermal degradation temperature was taken as the minimum of the first derivative of the weight loss with respect to time as given in table 4.2 below.

Table 4.2: Thermal characterization of cenosphere filled hybrid glass-jute epoxy composites

Sample Type	IDT(°C)	FDT(°C)
Epoxy	303	575
GJJG	305	469
5% CSGJJG	313	481
10%CSGJJG	240	513
15%CSGJJG	302	528
20%CSGJJG	293	540

Where IDT - Initial Degradation Temperature

FDT - Final Degradation Temperature

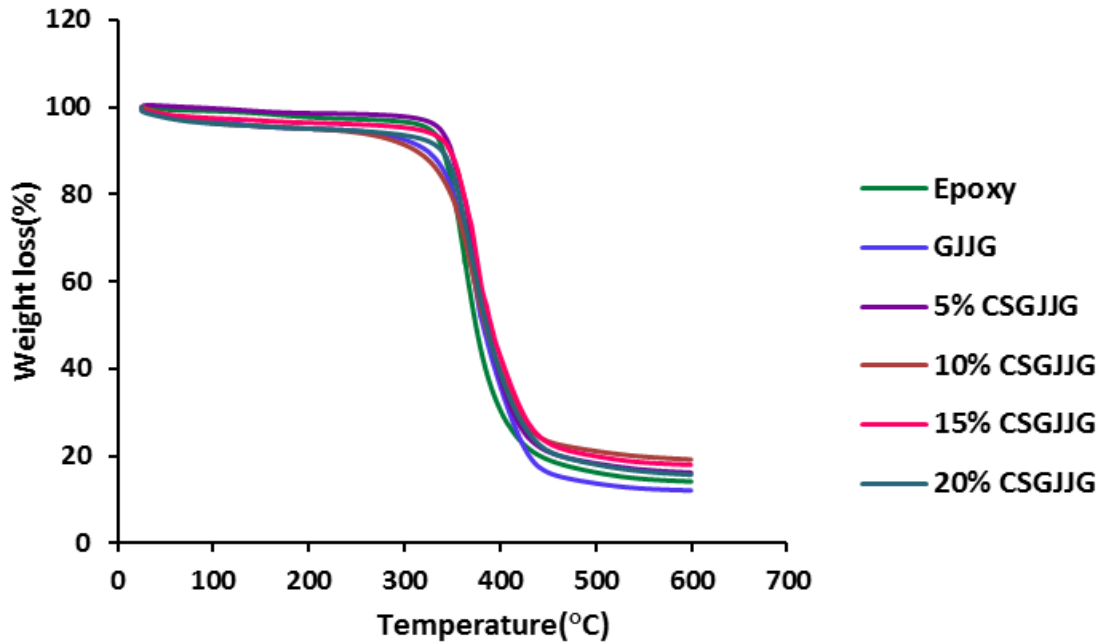


Figure 4.5: TGA Thermograms of cenosphere filled glass-jute reinforced composites

From the figure 4.5 the maximum decomposition of neat epoxy occurs at 575°C with 14.20% residue formation with initial degradation temperature of 303°C. The onset of thermal degradation for 5wt% cenosphere filled GJJG reinforced composite occurs at 313°C and degradation completes at 481°C with 16.03% residue formation. For higher wt. percentage (20%) cenosphere filler loading, the onset degradation temperature is at 293°C and complete degradation occurs at 540°C with 15.82% residue left owing to improved interfacial adhesion. Hence TGA analysis indicates the thermal stability of the polymer matrix increases with the incorporation of particulate filler i.e. (cenosphere) to the glass-jute hybrid composite. Higher weight percentage of filler shows better thermal stability as compared to only hybrid composites as reported by different authors[89,175]. It also confirms the presence of intermolecular bonding between the fiber and matrix due to formation of ester linkage[176-177]. From the literature [93], it has also been found that due to addition of treated cenosphere particle into the epoxy, an increase in the thermal resistance due to high temperature was achieved. The thermal stability of jute-glass epoxy composites also increases due to addition of jute fiber, which has high content of lignin, hemicelluloses and

Chapter 4 Moisture absorption behaviour of cenosphere filled jute glass epoxy composites

cellulose having decomposition temperature ranges of (180-240) °C, (230-310) °C and (300-400) °C, respectively reported by Zeriouh *et al.*[178].

4.3 Composite fabrication

For preparation of the composites for moisture absorption test the following raw materials have been used.

1. Jute Mats and Glass Fiber
2. Cenosphere
3. Epoxy resin
4. Hardener

4.3.1 Jute and Glass fiber

As explained earlier natural vegetable fibers have attracted worldwide attention as a potential reinforcement for composites because of their easy availability as a renewable resource, easy processability, low density, light weight, nonabrasive, low cost and above all for their bio friendly characteristics. The jute fiber is an important bast fiber and comprises bundled of ultimate cells, each containing spirally oriented microfibrills bound together. The main component of jute fiber is cellulose which leads to higher stiffness. Other components of jute fiber are hemicellulose, lignin, pectin, wax and water soluble substances. Similarly glass fiber used as synthetic fiber provides high strength and resistance to the polymer matrix composites. In the present work, jute and glass fibers have been used for experimentation.

4.3.2 Cenosphere

The details of cenosphere collected are given in chapter 3 article 3.5.1.4. The size of powder was measured by sieve. As per sieve analysis average size of the powder was 150 microns.

4.3.3 Epoxy Resin and Hardener

The type of epoxy resin and hardener used is same as explained in chapter 3 article 3.2.1.3.

4.3.4 Composite preparation

The fabrication for the moisture absorption test specimens were carried out as per the procedure explained in chapter 3 article 3.5.2. The composites after preparation with their designation, volume fraction of fiber and thickness calculated are presented in table 4.3.

Chapter 4 Moisture absorption behaviour of cenosphere filled jute glass epoxy composites

Figure 4.6 shows the photograph of the composite specimen used for moisture absorption test. After cutting they were kept in airtight container for further experimentation.

Table 4.3: Laminate stacking sequence of cenosphere filled glass-jute (GJJG) epoxy composite

Symbol	Stacking sequence	Cenosphere Wt. (%)	Total fiber		Thickness (mm)
			Volume fraction %	Weight fraction %	
S ₉	GJJG	5	16.4	29.3	5
S ₁₀	GJJG	10	18.2	32.6	5
S ₁₁	GJJG	15	20.8	37.1	5
S ₁₂	GJJG	20	23.3	41.4	5

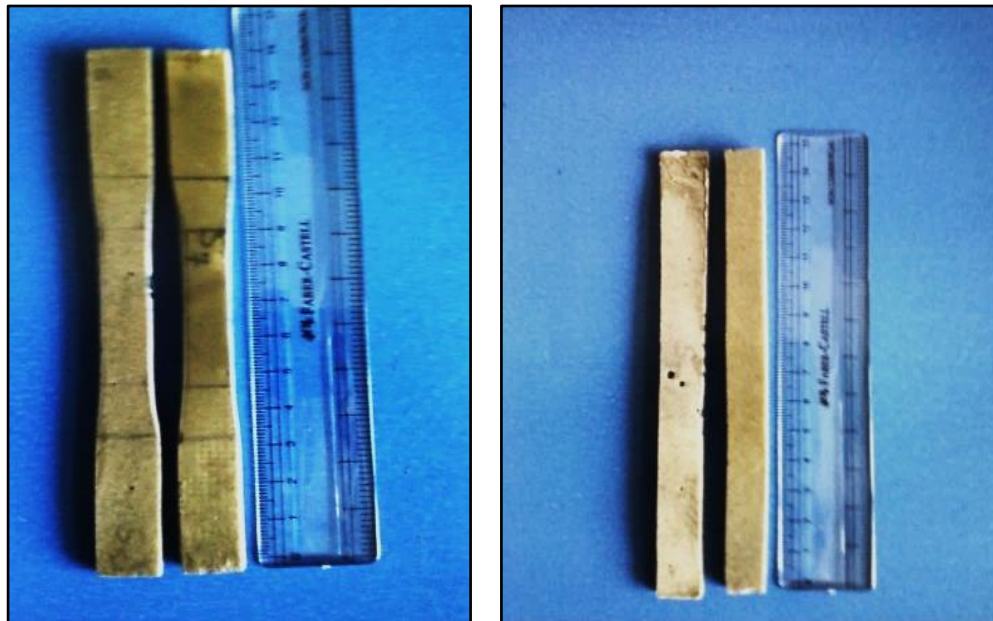


Figure 4.6: Specimen for (a) Tensile and (b) Flexural test subjected to different environmental condition

4.4 Study of environmental effect

To study the effect of environment on performance of cenosphere filled woven jute-glass hybrid epoxy composites of sequences (S₉-S₁₂), the prepared composite samples were subjected to various environments such as:

- (a) Distilled Water
- (b) Saline Water

4.4.1 Moisture absorption test

Moisture absorption and thickness swelling tests were conducted in accordance with ASTM D570-98. Three specimens for each composite system were cut with dimensions of (140×15×5) mm and the experiment was performed using test samples. The specimens prior to testing were dried in an oven at 80⁰ C and then were allowed to cool to room temperature and kept in a desiccator. The weights of the samples were taken before subjecting them to distilled and saline water environments. After exposure for 24 h, the specimens were taken out from the moist environment and all surface moisture was removed with a clean dry cloth or tissue paper. The specimens were reweighed to the nearest 0.001 mg within 1 minute of removing them from the environment chamber. The specimens were weighed regularly with a gap of 24h exposure for a total time period of 216h (9 weeks). The moisture absorption was calculated by the weight difference. The percentage weight gain of the samples was measured at different time intervals by using the following equation:

$$\%M = \frac{W_t - W_0}{W_0} \times 100 \quad (4.2)$$

Where ‘W₀’ and ‘W_t’ denote the oven-dry weight and weight after time ‘t’, respectively. Equilibrium Moisture Content (EMC) of the sample is the moisture content when the periodic weight change of the sample was less than 0.1% and thus it can be assumed that equilibrium state has been reached. The thickness swelling is determined by the same procedure using the following relation.

$$\%T = \frac{T_t - T_0}{T_0} \times 100 \quad (4.3)$$

Where T_t and T₀ are the composite thickness after and before immersion in water, respectively.

4.4.2 Mechanical Tests

Tensile and flexural test were performed on the specimen immediately after they were removed from the environmental baths to know the effect of the environment on these values. These tests were carried out as per the procedure given in chapter 3 articles 3.2.4 and 3.2.5. For each stacking sequence of different cenosphere weight percentage, three identical samples were tested, and the average result was obtained.

4.4.3 Fractography Studies

To investigate the effect of moisture absorption on the microstructure of cenosphere filled jute-glass fiber hybrid epoxy composite of varying weight percentages (5, 10, 15 and 20%) and to know the mode of failure, few selected samples were subjected to scanning electron microscopy (SEM).

4.4 Results and discussions

4.4.1 Effect of filler loading on moisture absorption behaviour

The results of cenosphere filled hybrid jute-glass epoxy composites samples exposed to different environments are shown in table 4.4 to 4.7. Figures 4.7 to 4.10 shows the percentage of moisture absorption characteristics of composite samples for different mechanical tests exposed to distilled and saline water environment with time. It is clear from the figure that the initial rate of moisture absorption and the maximum moisture uptake in all environments increases for all composite specimens as filler content increases. With addition of 5 wt. % and 20 wt. % filler to the developed composite the maximum absorption increases from 1.815% to 3.252% in distilled water and from 1.352% to 2.094% for saline water respectively. Presence of filler particles in the matrix produces voids at the interface and increases the ability of water molecules to piercing the composite through capillary transport and causes disorder in the structural homogeneity of the material. As the filler loading increases, the weak interfacial bonding between the filler and matrix resulted in the increased number of micro voids, causing more water absorption as reported by authors[179].

Again it is observed that, the moisture absorption increases with time, and got saturated after certain time period. Time to reach the saturation point is not same for all the environments. The saturation time is approximately 216h for distilled water and 168h for saline water

Chapter 4 Moisture absorption behaviour of cenosphere filled jute glass epoxy composites

environment for all weight percentages of cenosphere filled hybrid glass-jute(GJJG) composites. It is also noticed that the absorption rate in case of saline water is less than that of distilled water. This happens because of the accumulation of NaCl ions in the fiber's surface immersed in saline water, which increases with time and hinders subsequent moisture diffusion[180].

4.4.2 Thickness swelling behaviour

The thickness swelling processes for cenosphere filled jute-glass hybrid epoxy composites at different ambient environments has been studied by considering the thickness swelling (TS) and swelling rate parameter (K_{SR}). Figures (4.11-4.14) shows the thickness swelling behaviour of cenosphere filled hybrid jute-glass epoxy composites at various environments for different specimens. It was observed that in both environmental conditions the thickness swelling (TS) increases with an increase in filler content and immersion time. The results showed that with addition of 5 wt. % and 20 wt. % filler to the developed glass-jute composite, the thickness swelling increases from 8.734% to 16.63% and from 2.886% to 6.9% in both saline and distilled water conditions respectively. This might have happened because of the increased number of micro voids caused by the larger amount of poorly bonded area between the hydrophilic filler and the hydrophobic polymer matrix. From the test it was confirmed that the long-term immersion in water causes the dimensional instability of the composites.

The value of K_{SR} was evaluated through a non-linear regression curve fitting method to fit the experimental data (table- 4.4 to 4.7) in equation 4.5 [181], using computer software with curve fitting routines.

$$TS(t) = \left(\frac{H_{\infty}}{H_0 + (H_{\infty} - H_0)e^{-K_{SR}t}} - 1 \right) \times 100 \quad (4.5)$$

Where ' $TS(t)$ ' is the thickness swelling at specific time (t), ' H_0 ' and ' H_{∞} ' are the initial and equilibrium thickness respectively.

Chapter 4 Moisture absorption behaviour of cenosphere filled jute glass epoxy composites

The experimental data was used to obtain the swelling rate parameter (K_{SR}) by using equation 4.5. Table 4.8 summarizes the respective values of K_{SR} obtained through non-linear curve fitting. The swelling rate parameter (K_{SR}) quantifies the rate of the composites approaching the equilibrium value for thickness swelling after sufficient time of moisture immersion. The higher value of K_{SR} indicates, the higher rate of swelling along with reaching of equilibrium thickness swelling in a shorter period of time. As per the literature the swelling rate parameter of the composites increases with increase in filler content but it reduces significantly with chemical treatment of fiber surface which was due to the improved compatibility between polymer and fiber [182].

4.4.3 Measurement of Diffusivity

The moisture absorption kinetics in cenosphere filled glass-jute (GJJG) hybrid epoxy composite has been studied through the diffusion constants k and n . The behaviour of moisture absorption in the composites was studied by the shape of the absorption curve represented by the following equation [183].

$$\frac{M_t}{M_m} = kt^n \quad (4.6)$$

The above equation can be written in following form as follows.

$$\log\left(\frac{M_t}{M_m}\right) = \log(k) + n \log(t) \quad (4.7)$$

Where M_t : Moisture absorption at specified time ' t '

M_m : Moisture absorption at the saturation point or the Equilibrium moisture content (EMC)

The value of k and n were determined from the slope and the intercept of M_t / M_m versus ' t ' in the log plot which was drawn from experimental data of moisture absorption with time. The value of n indicates the type of transport mechanism and k indicates the interaction between the sample and water in addition to its structural characteristics of the polymer network. Figures (4.15-4.18) showed the typical curve of $\log (M_t/M_m)$ as a function

Chapter 4 Moisture absorption behaviour of cenosphere filled jute glass epoxy composites

of $\log(t)$ for cenosphere filled jute-glass(GJJG) hybrid composites in both distilled and saline environment for different specimens used to determine these constants. They are determined by linear regression analysis and the values are given in table 4.9 for different doses (5, 10,15and 20%) of cenosphere filled glass-jute (GJJG) epoxy composites. It was observed that the value of n is close to 0.5 for all of the composites. This confirms that the fickian diffusion can be used to adequately describe moisture absorption in the composites, which is consistent with previous studies [184,185]. A higher value of n and k indicates that the composite needs shorter time to attain equilibrium water absorption. For a Fickian diffusion mechanism, n has a value of 0.5. When $n = 1$, the mechanism is non-fickian and when it lies between 0.5 and 1, the diffusion is anomalous [186]. If the value of coefficient n gets smaller than 0.5, then water absorption behaviour follows the fickian diffusion process [187]. From table 4.9, the value of n falls below 0.5 indicating the transport mechanism as fickian for all composite types. Similarly the value of k tends to be less for the cenosphere filled jute-glass (GJJG) composites, confirming the reduction in water consumption in saline water as compared to distilled environment.

The diffusion coefficient (D_x) is one of the important parameters of Fick's model and shows the ability of water molecules to penetrate inside the composite structures. The diffusion coefficient or diffusivity (D_x) of moisture absorption was calculated using the following equation [188].

$$D_x = \pi \left[\frac{h}{4M_m} \right]^2 \left[\frac{M_2 - M_1}{\sqrt{t_2} - \sqrt{t_1}} \right]^2 \quad (4.8)$$

Where M_m : The maximum percentage of moisture content

h : Thickness of the sample.

t_1 and t_2 : Selected points in the initial linear portion of the plot of moisture absorption (M_t) versus \sqrt{t} as shown in (Figure-3.18)

M_1 and M_2 : Respective Moisture content at time t_1 and t_2

Chapter 4 Moisture absorption behaviour of cenosphere filled jute glass epoxy composites

From the plot of M_t verses square root of time (t) shown in figures 4.19 to 4.23 the value of D_x has been evaluated and summarized in table 4.10. It has been observed that D_x value increases with the cenosphere filler content for the developed composites examined. The maximum diffusivity value is found for 20wt. % cenosphere filled glass-jute (GJJG) composite as compared to 5wt. % in both environmental conditions. These results are consistent with previous findings on wood and natural fiber composites [185-187,189]. The direct comparison of the diffusion coefficient obtained from this work with previous is difficult due to variation in filler content, manufacturing methods and test conditions. With better adhesion between matrix and filler, the velocity of the diffusion process decreases due to fewer gaps in interfacial region and presence of more hydrophilic groups as OH, that are blocked by the filler content. The presence of glass fiber at outer layers of composites also shows lower diffusion coefficient. It is possible due to lower hydrophilicity of the glass fiber as compared to jute fiber. In case of “non-Fickian” transport, observed at high temperature, there is no cracking in the initial stage of the moisture absorption in the material and Fick’s law is obeyed. When cracking occurs, the experimental data deviates from the Fickian behaviour, resulting in increasing water intake. According to Fujita [190], the “non-Fickian” absorption process is one of the most general absorption features of glassy polymers. It is generally acquired that the penetrant diffuses rapidly into the polymer, accompanied by reversible elastic swelling of the matrix. The stress developed is then slowly relieved by molecular relaxation process such that the chemical potential of the absorbed water is decreased, leading to further absorption [191].

4.4.4 Effect of moisture absorption on Mechanical properties

The moisture absorption has a significant influence on the mechanical properties of the cenosphere filled jute-glass composites after exposure to different moist environment for a period of 216h. It has been observed that both strength and stiffness of all composite decrease after moisture absorption. This reduction in the strength and stiffness is attributed to the changes occurring in the fiber, and the interface between fiber, filler and matrix. When fiber/matrix interface is accessible to moisture from the environment, the cellulosic fibers tend to swell, thereby developing shear stresses at the interface, which favours ultimate debonding of the fibers, which in turn causes a reduction in strength [164]. It is also observed that the reduction in properties was greatly influenced by the fiber and filler loading and nature of environment.

Chapter 4 Moisture absorption behaviour of cenosphere filled jute glass epoxy composites

From the figures 4.24 and 4.25, it is observed that flexural strength increases in 20wt.% cenosphere filled hybrid glass-jute (GJJG) epoxy composite and tensile strength is higher in 10wt.% cenosphere filled composite with distilled water as the immersion time increases. The results indicate that the material has practised some forms of physical damage or chemical degradation. The deterioration of bonding between fibre and matrix is also the reason for the decreased composite strength. The orientation of fiber also produces lower mechanical properties. This fibre mix-up creates resin rich areas, which can accord to the formation of voids and porosity. Voids and porosity can act as stress concentrator leading to failure of hybrid composite samples. The decrease of flexural strength after immersion can also be related to the weak fibre matrix interface due to moisture absorption[191-192].

4.5 SEM studies of fractured surface of moisture absorption

Figures 4.26(a-d) presents the morphology of the tensile tested fractured surface of 20wt.% of cenosphere filled glass-jute(GJJG) epoxy composites exposed to both distilled and saline water environment at lower and higher magnification. Generally the mechanical properties of fiber reinforced composites depend on the nature of the polymer matrix, distribution and orientation of the reinforcing fibres with fillers, the nature of the fiber-matrix interfaces. Figures 4.26(a) presents the morphology of the fractured surface of cenosphere filled GJJG epoxy composites exposed to distilled water environment at lower magnification. From the figure the pull out of both jute and glass fiber is clearly visible. The same figure at higher magnification is shown in fig. 4.26(b). The pull out of fiber is clearly visible due to tensile load along with cavity formation. The immersion of cenosphere filled developed composites in water results in development of poor interfacial adhesion between fiber and matrix when subjected to tensile loading. This might have happened due to swelling of fiber which leads to breakage of jute fiber. However glass fibers are seen to be intact indicating no effect of swelling of glass fiber.

Figure 4.26(c) shows fractured surface of the same composite exposed to saline water environment. Fiber breakage and swelling of fiber is observed for the composite under tensile loading. Small voids are being created in the fiber structure. This void gives space for water absorption due to which swelling of composites occurs that finally leads to deterioration of fiber strength. Figure 4.26(d) shows the same morphology of cenosphere filled hybrid glass-

Chapter 4 Moisture absorption behaviour of cenosphere filled jute glass epoxy composites

jute composite under saline water at higher magnification. Delamination and fiber pull out from the composite matrix surface is clearly visible in the figures. This is due to fact that when the fiber/matrix interface was subjected to moisture under saline water environment, the cellulose fibers got swelled. This resulted in the development of shear stress at the interface, which led to the ultimate debonding of the fibers, delamination and loss of structural integrity of filled hybrid composites.

Figures 4.27(a-d) shows the SEM micrograph of the bending fractured surface of 20wt.% cenosphere filled hybrid glass-jute(GJJG) epoxy composites exposed to both distilled and saline water environment at lower and higher magnification. Figures 4.27 (a) shows the pull out of glass fiber from the matrix surface along with jute fiber exposure during flexural failure under distilled water at lower magnification. The image analysis also shows the formation of voids due to the pulling out of the fiber. Figure 4.27 (b) shows the same micrograph at higher magnification. Fiber bending and swelling is also clearly seen in the fractured surface due to flexural load under distilled water.

When the cenosphere filled hybrid glass-jute (GJJG) composite is subjected to saline environment, crack formation takes place between fiber matrix interfaces along with bending of fiber as shown in figure 4.27 (c).This might have happened due to the poor compatibility between fiber and the matrix surfaces. The same figure with higher magnification as shown in figure 4.27(d), the breakage of fiber along with fiber matrix debonding is clearly visible on the composite surface. Debonding between fiber and matrix and empty space between fibers and filler due to insufficient wetting are also clearly visible. This reveals that at higher filler loading poor fiber wetting occurs due to insufficient matrix material results in lower strength and modulus. This has also been seen in the experimental results shown in figures (4.24-4.25).This debonding at fiber-matrix interface is mainly responsible for degradation in mechanical properties. The decrease in mechanical properties with increase in moisture content was due to the formation of hydrogen bond between the water molecules and cellulose fiber leading to dimensional variation of composites products and poor interfacial bonding between the fiber and matrix.

4.6 Conclusions

Based on experimental results, this study led to the following conclusions:

1. The jute and glass fiber can successfully be used as reinforcing agent along with cenosphere (particulate filler) to fabricate composites by suitably bonding with epoxy resin.
2. TGA analysis of cenosphere filled hybrid jute-glass epoxy composites revealed an improvement in thermal stability over that of neat epoxy and is accompanied by char formation. Thus these lightweight inexpensive particulate composites can be used as potential fire retardants materials.
3. The maximum weight gain and thickness swelling increases in 20wt. % and decreases in 5wt. % cenosphere filled glass-jute (GJJG) composite in both environmental conditions. It is due to the biodegradable filler particles generating voids at the interface increasing water uptake in the composite through capillary transport.
4. The water absorption trend is found to follow Fickian behaviour and is predictable over a period. The highest values of diffusion coefficient (D_x) and equilibrium moisture content values (EMC) were recorded for specimens immersed in distilled water as compared to saline water.
5. Exposure to moisture results in significant drops in mechanical properties. The presence of porosity and degradation of fiber-matrix interface can be imputed to fiber-fiber interaction and proposed to have strong influence on flexural properties of composites for long time exposure in the hygrothermal environment.
6. SEM morphology confirms the fiber swelling, fiber pull out and poor interfacial bonding between fiber and matrix leading to variation in mechanical properties of composites.

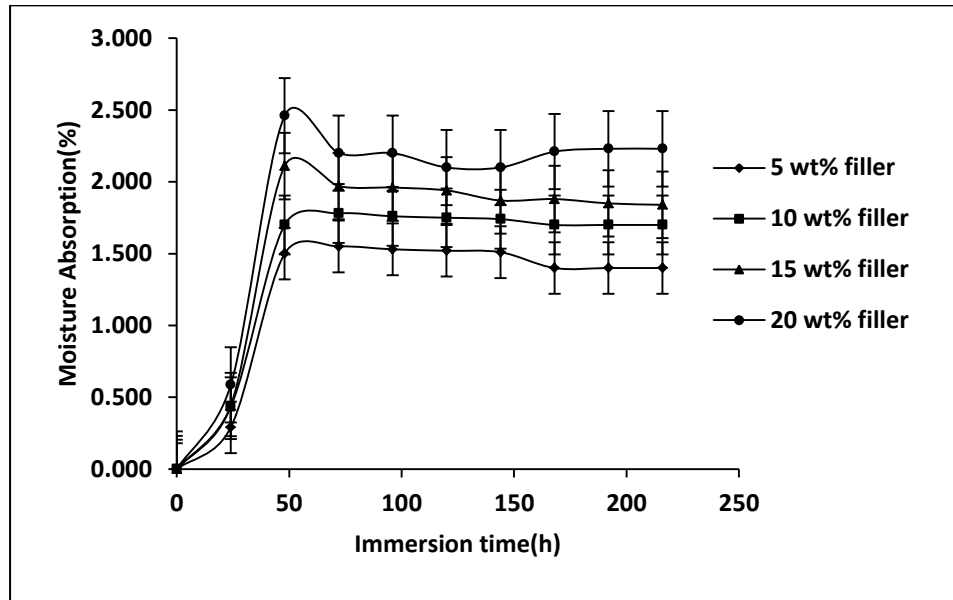


Figure 4.7: Variation of moisture absorption of cenosphere filled jute-glass (GJJG) composites with immersion time in distilled water for tensile specimens

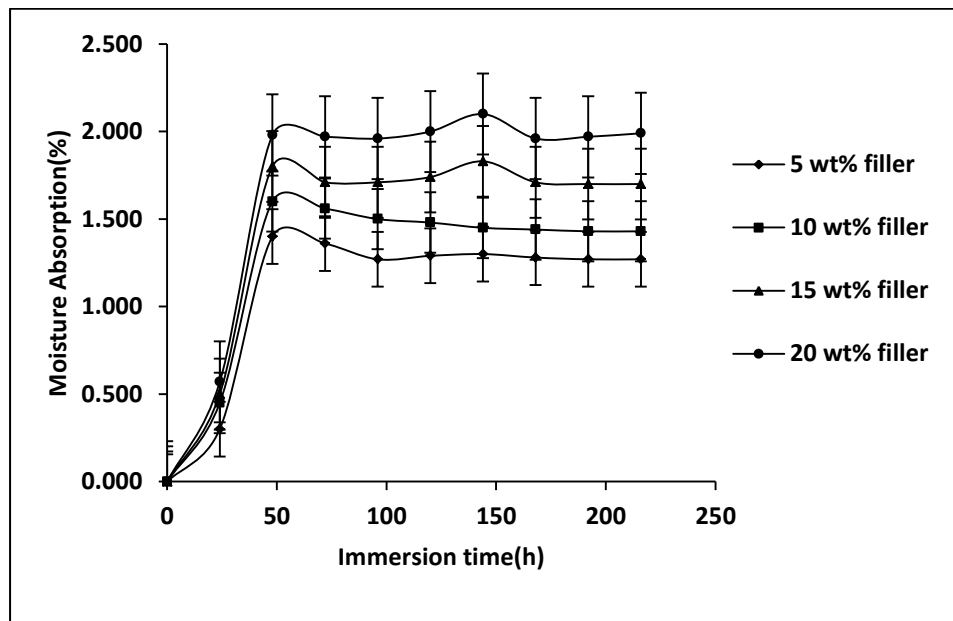


Figure 4.8: Variation of moisture absorption of cenosphere filled jute-glass (GJJG) composites with immersion time in saline water for tensile specimens

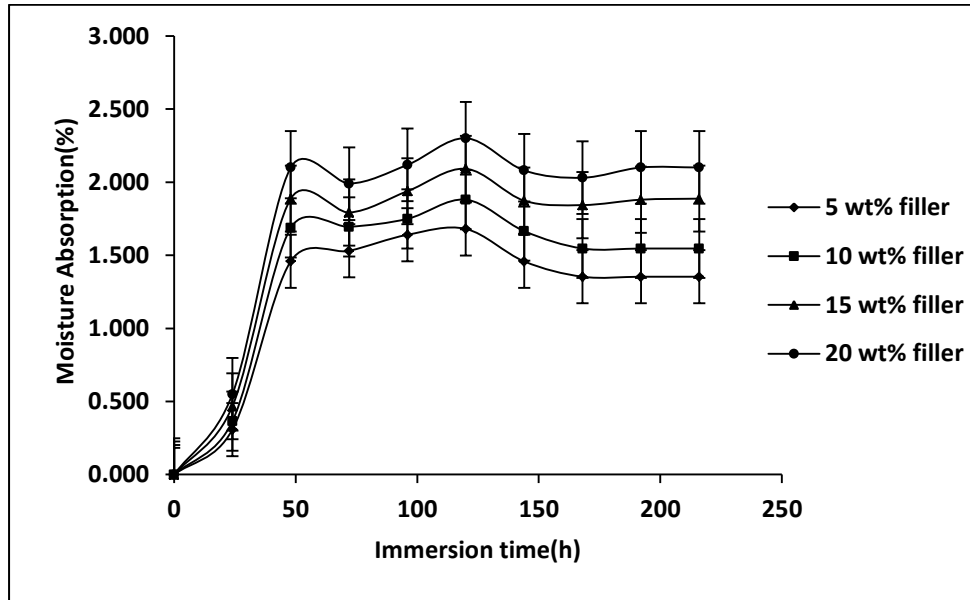


Figure 4.9: Variation of moisture absorption of cenosphere filled jute-glass (GJJG) composites with immersion time in saline water for flexural specimens

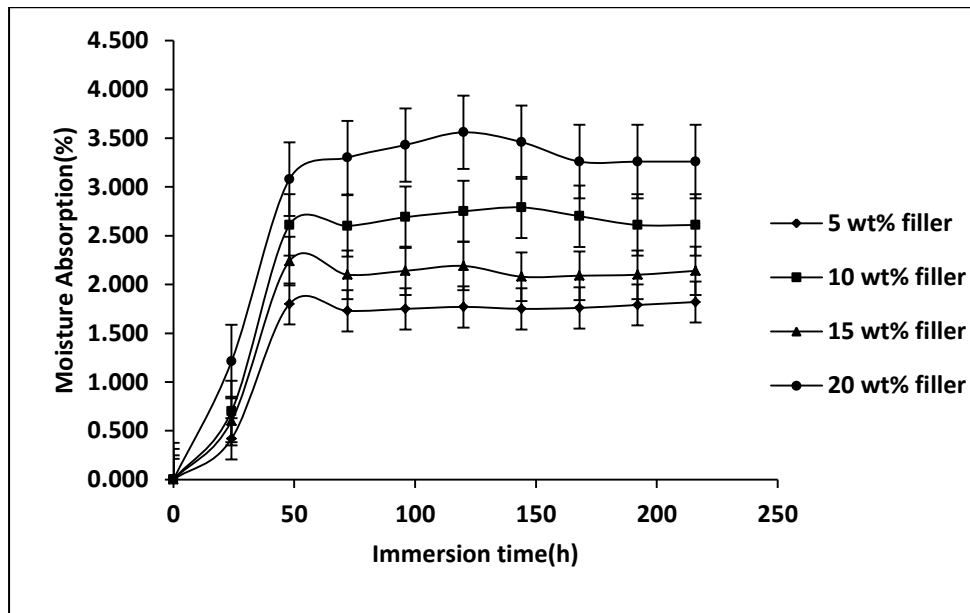


Figure 4.10: Variation of moisture absorption of cenosphere filled jute-glass (GJJG) composites with immersion time in distilled water for flexural specimens

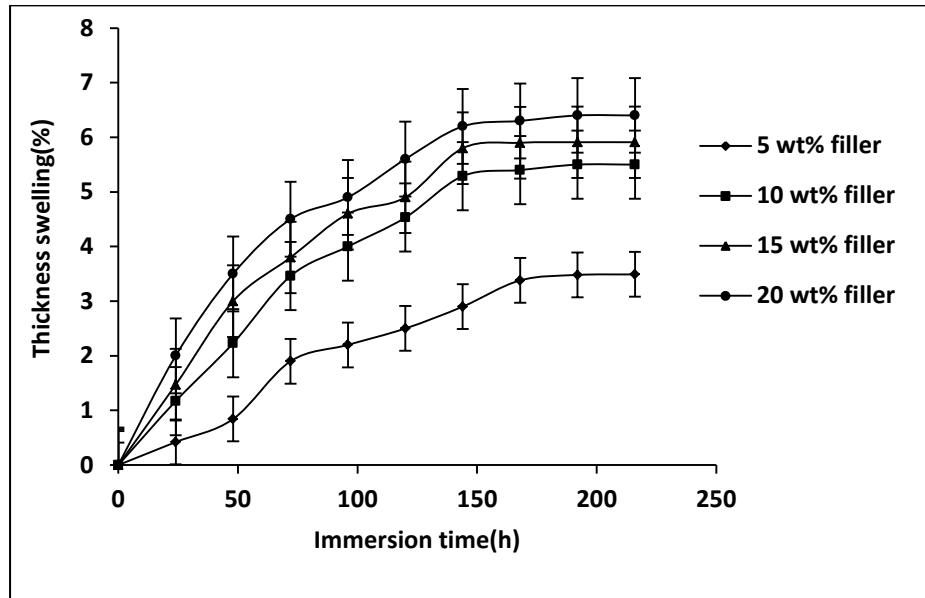


Figure 4.11: Variation of thickness swelling of cenosphere filled jute-glass (GJJG) composites with immersion time in distilled water for tensile specimen

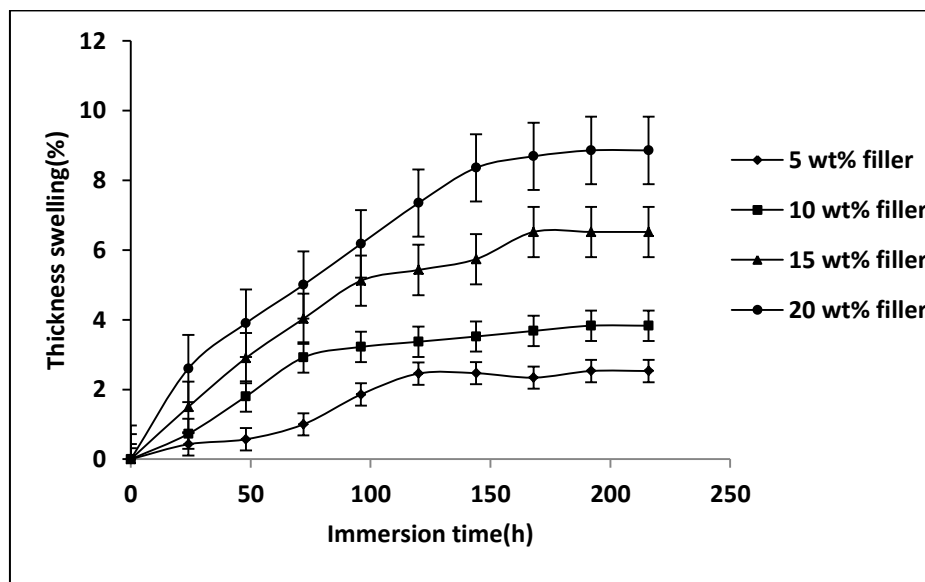


Figure 4.12: Variation of thickness swelling of cenosphere filled jute-glass (GJJG) composites with immersion time in saline water for tensile specimen

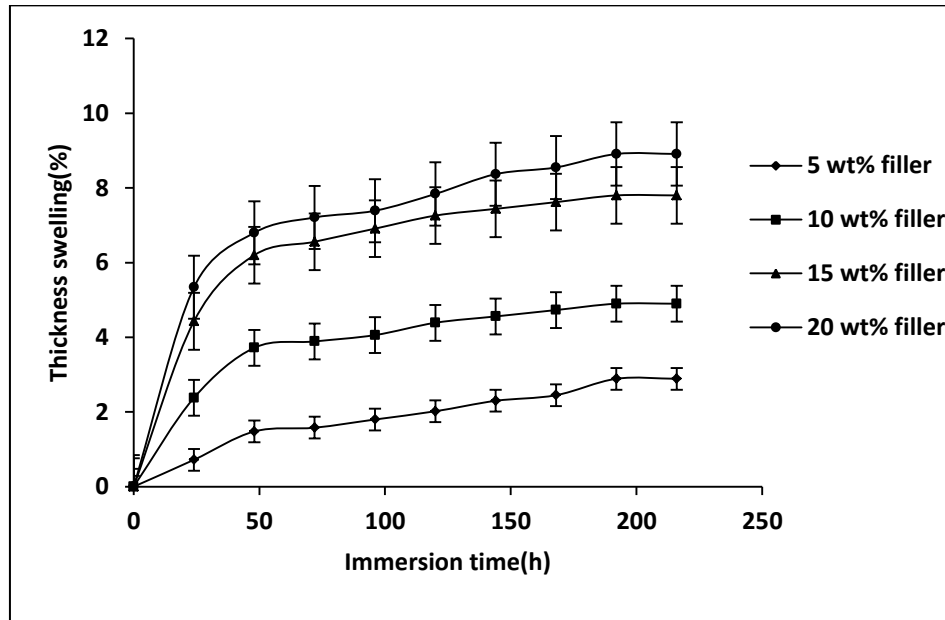


Figure 4.13: Variation of thickness swelling of cenosphere filled jute-glass (GJJG) composites with immersion time in distilled water for flexural specimen

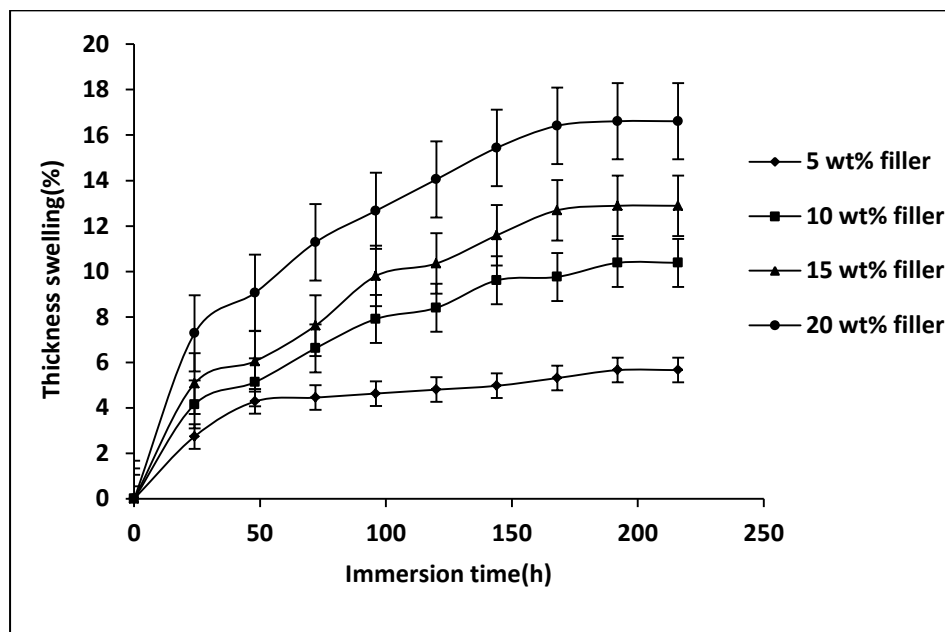


Figure 4.14: Variation of thickness swelling of cenosphere filled jute-glass (GJJG) composites with immersion time in saline water for flexural specimen

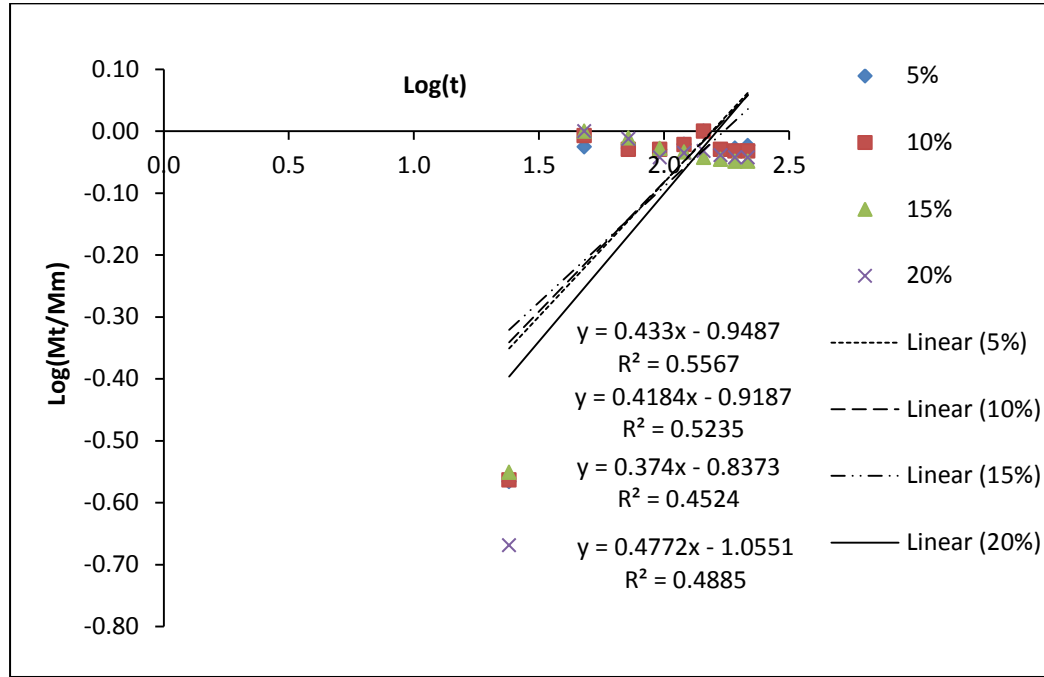


Figure 4.15: Diffusion curve fitting for cenosphere filled hybrid jute-glass (GJJG) epoxy composites under saline environment for tensile specimen

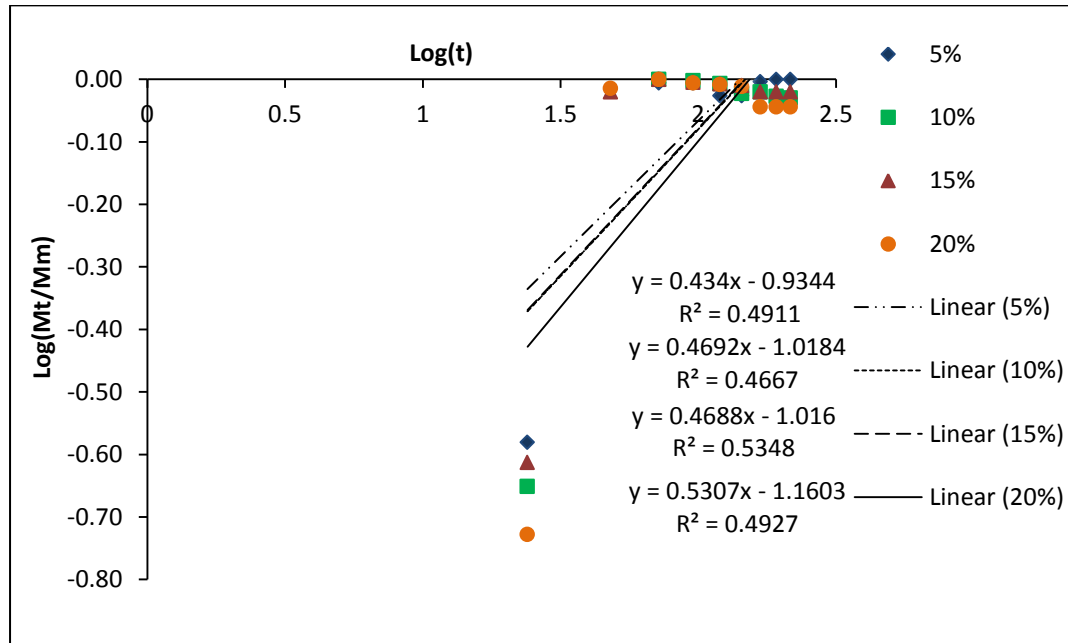


Figure 4.16: Diffusion curve fitting for cenosphere filled hybrid jute-glass (GJJG) epoxy composites under distilled environment for tensile specimen

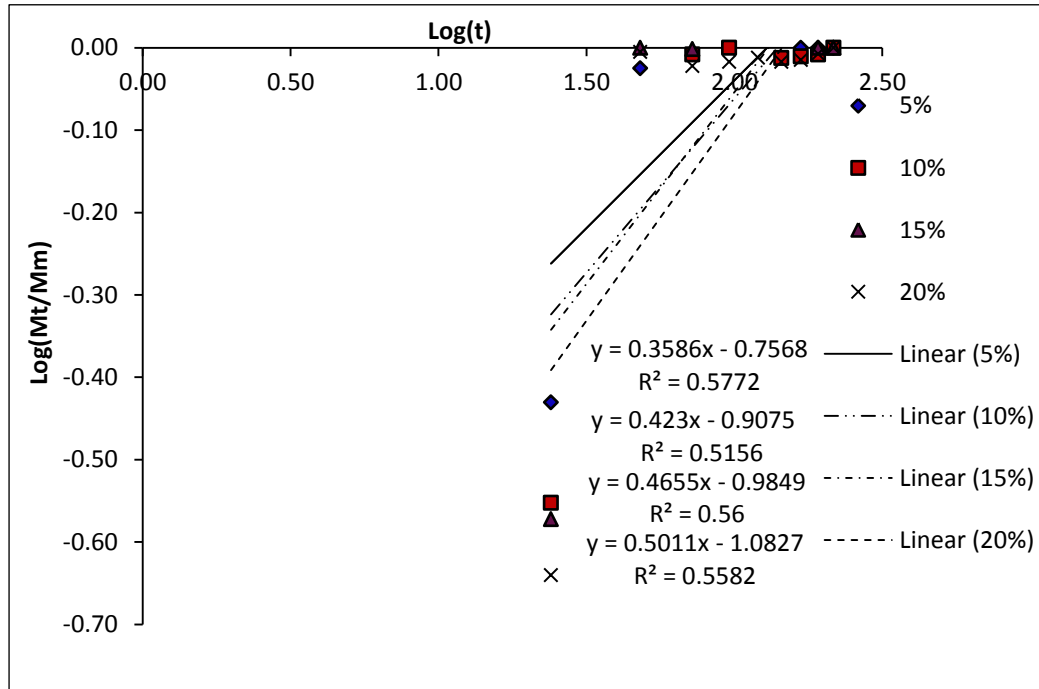


Figure 4.17: Diffusion curve fitting for cenosphere filled hybrid jute-glass (GJJG) epoxy composites under distilled environment for flexural specimen

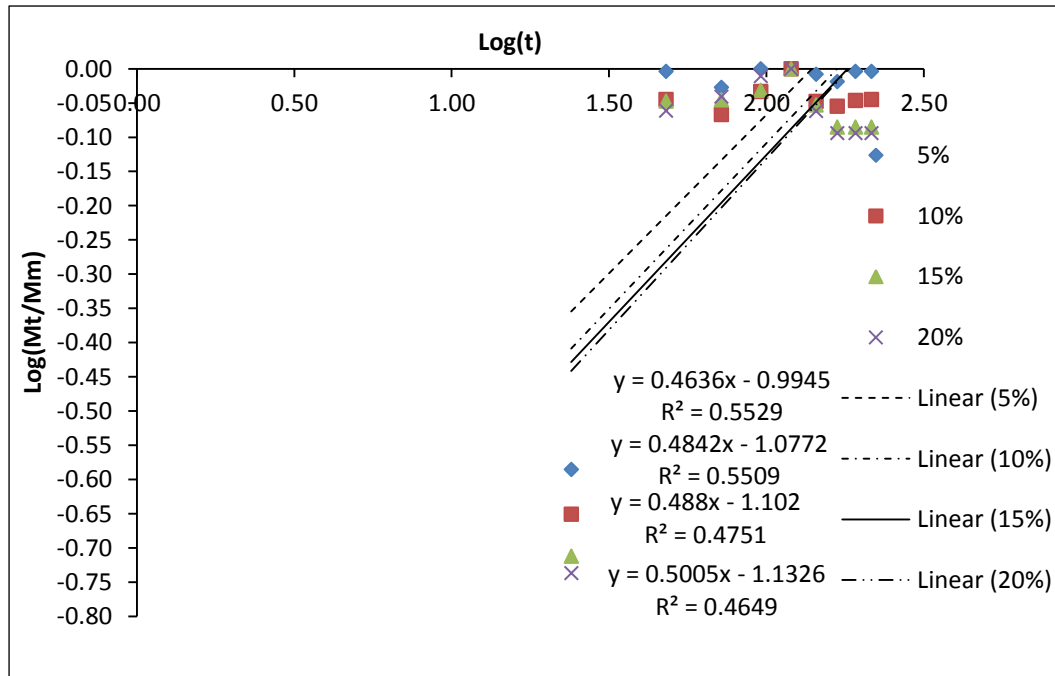


Figure 4.18: Diffusion curve fitting for cenosphere filled hybrid jute-glass (GJJG) epoxy composites under saline environment for flexural specimen

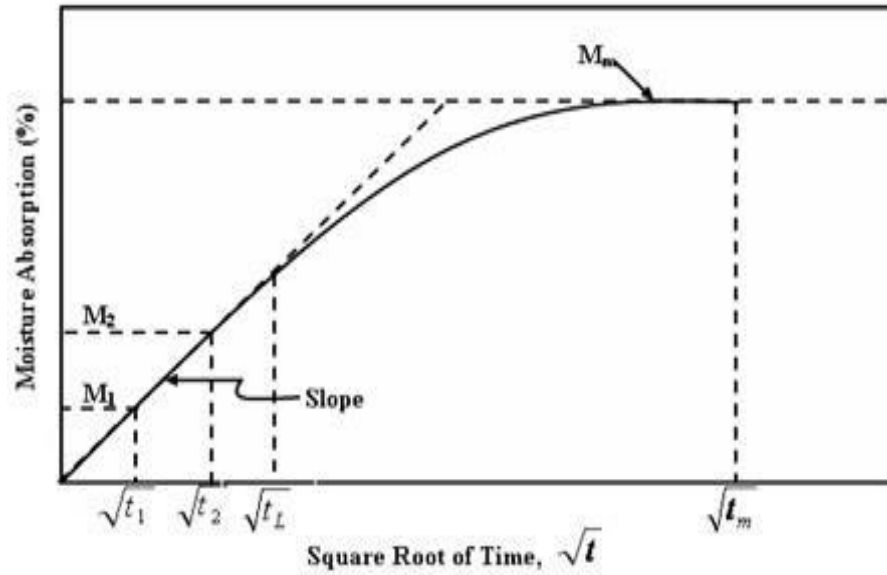


Figure 4.19: Example Plot of percentage of moisture absorption versus square root of time for calculation of diffusivity

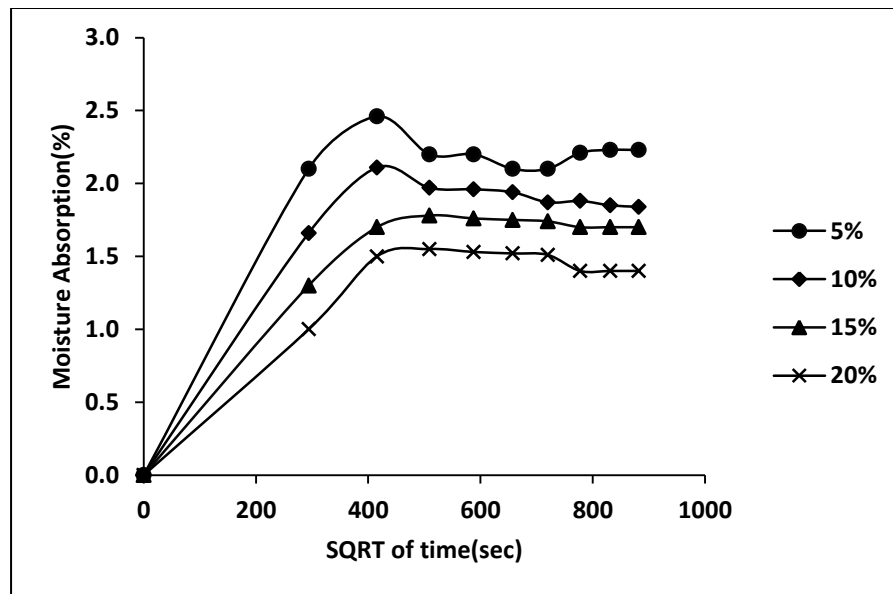


Figure 4.20: Variation of moisture absorption of cenosphere filled glass-jute (GJJG) composites with square root of immersion time at distilled water for tensile specimen

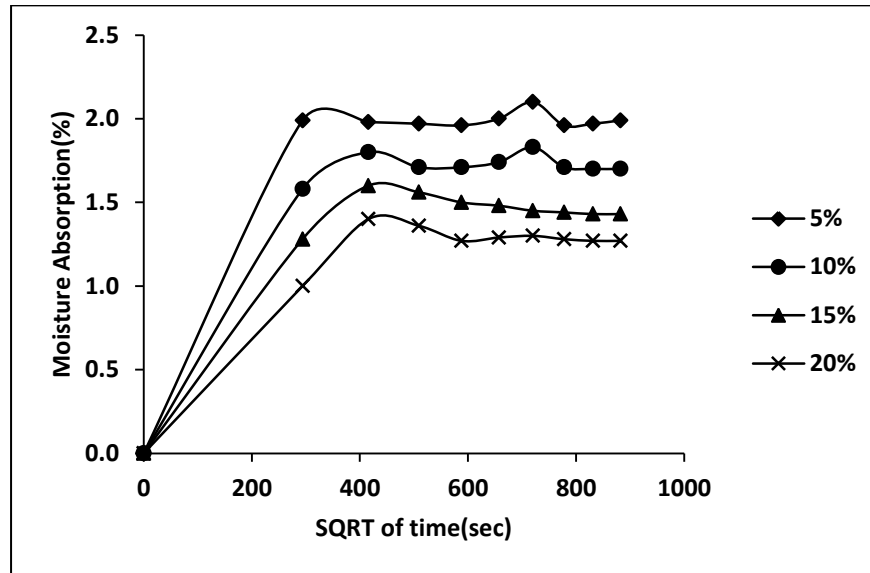


Figure 4.21: Variation of moisture absorption of cenosphere filled glass-jute (GJJG) composites with square root of immersion time at saline water for tensile specimen

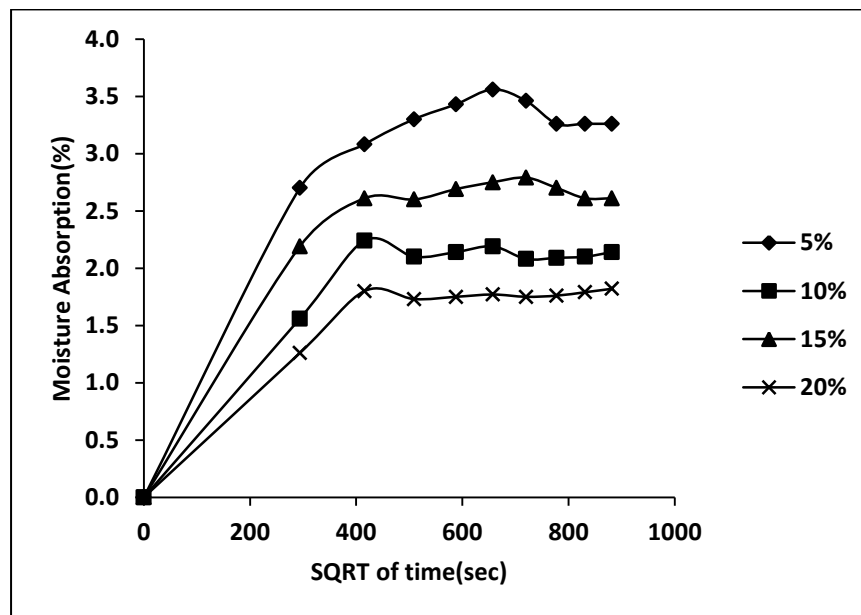


Figure 4.22: Variation of moisture absorption of cenosphere filled glass-jute (GJJG) composites with square root of immersion time at distilled water for flexural specimen

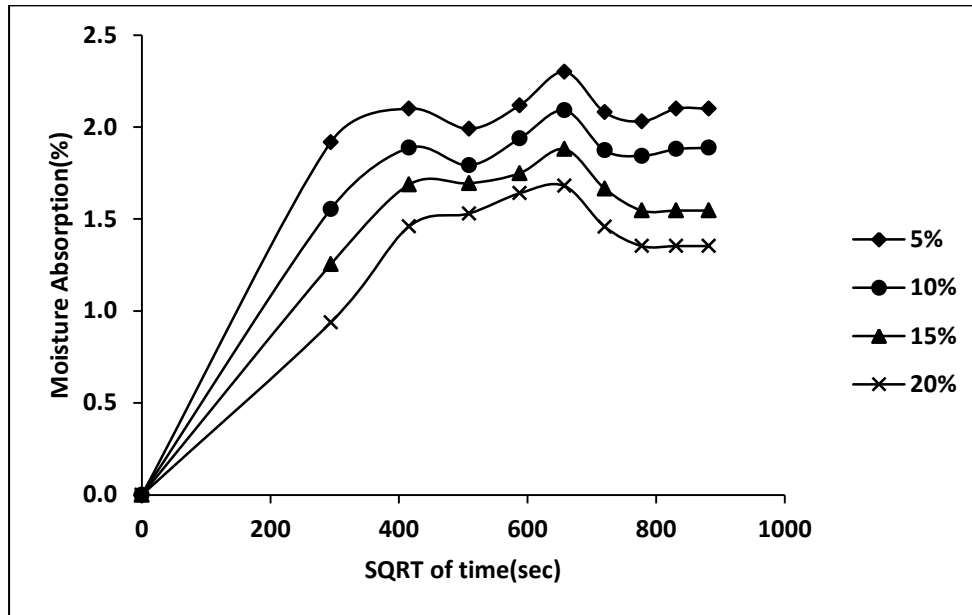


Figure 4.23: Variation of moisture absorption of cenosphere filled glass-jute (GJJG) composites with square root of immersion time at saline water for flexural specimen

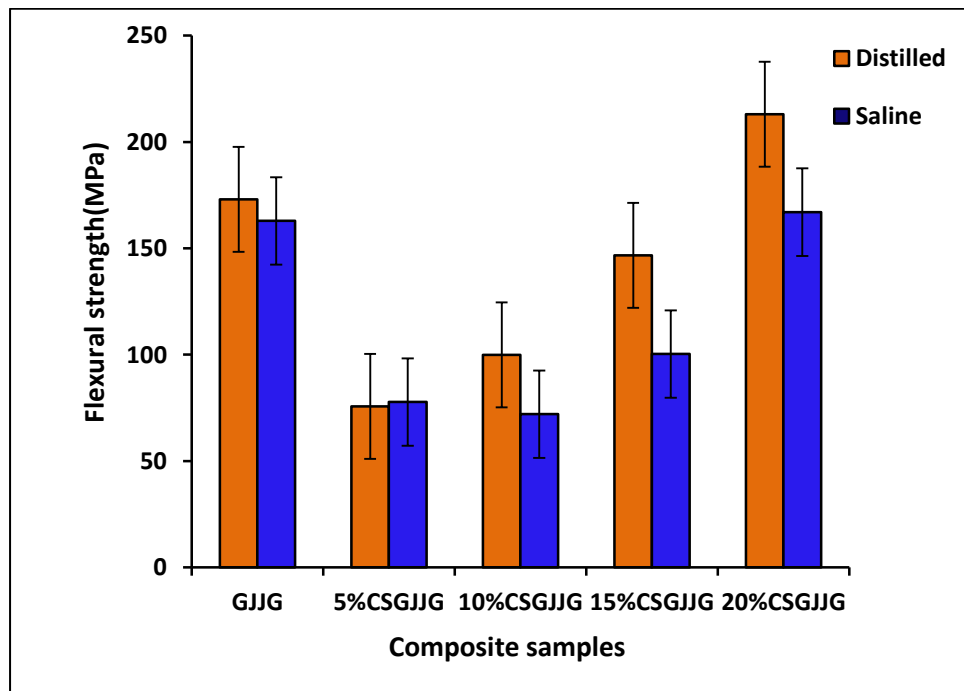


Figure 4.24: Flexural strength of cenosphere filled hybrid glass-jute (GJJG) epoxy composite after exposure to different environmental conditions

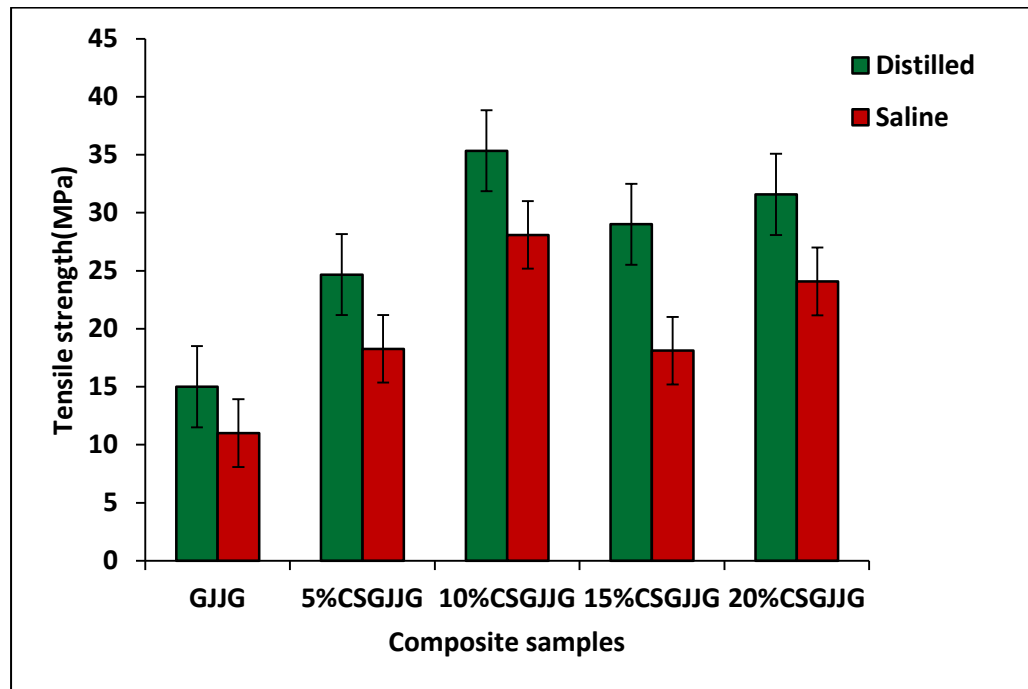


Figure 4.25: Tensile strength of cenosphere filled hybrid glass-jute (GJJG) epoxy composites after exposure to different environmental conditions

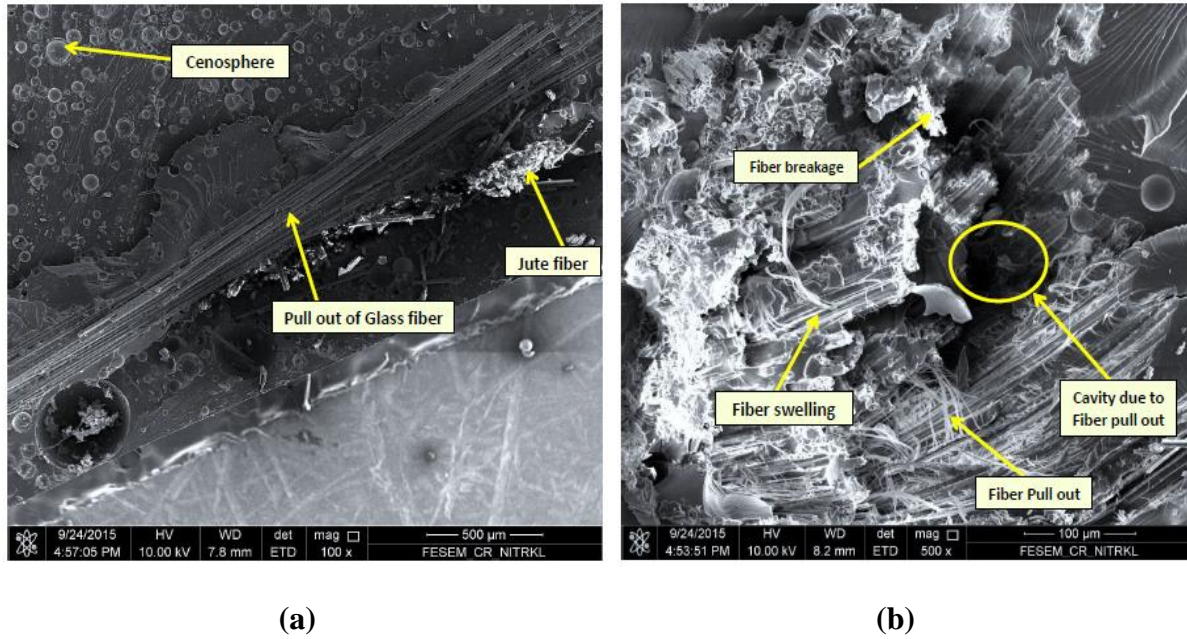


Figure 4.26 (a-b): SEM images of tensile fractured surfaces of 20wt.% cenosphere filled hybrid glass-jute (GJJG) epoxy composites in distilled water environment at lower (100x) and higher (500x) magnification

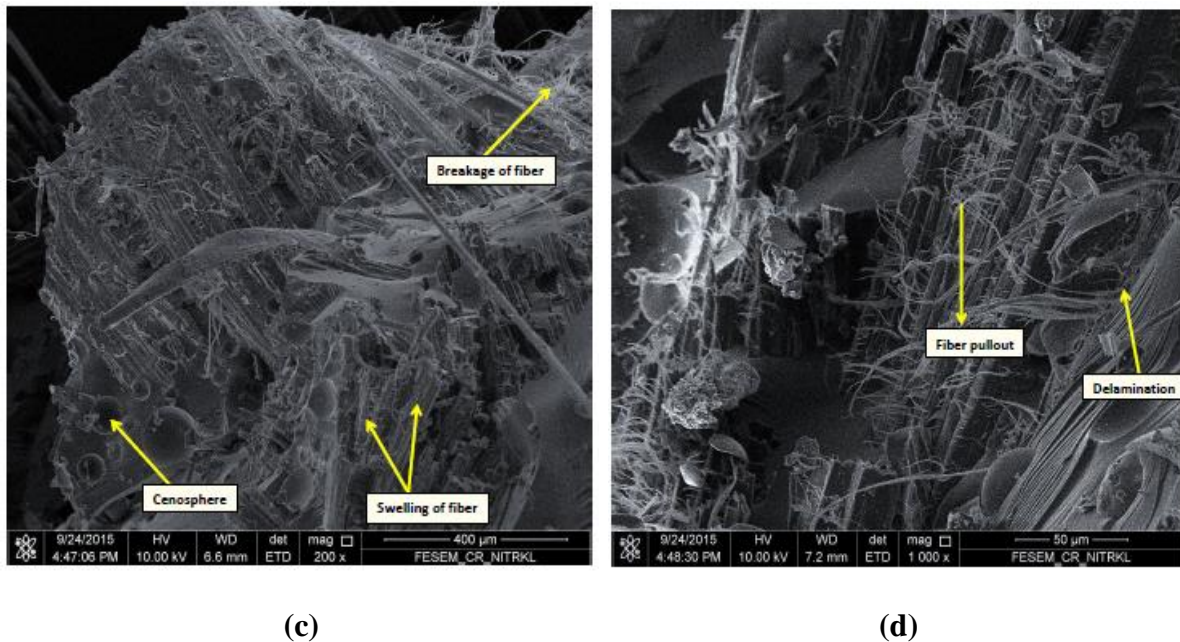


Figure 4.26 (c-d): SEM images of tensile fractured surfaces of 20wt.% cenosphere filled hybrid glass-jute (GJJG) epoxy composites in saline water environment at lower (200x) and higher (1000x) magnification

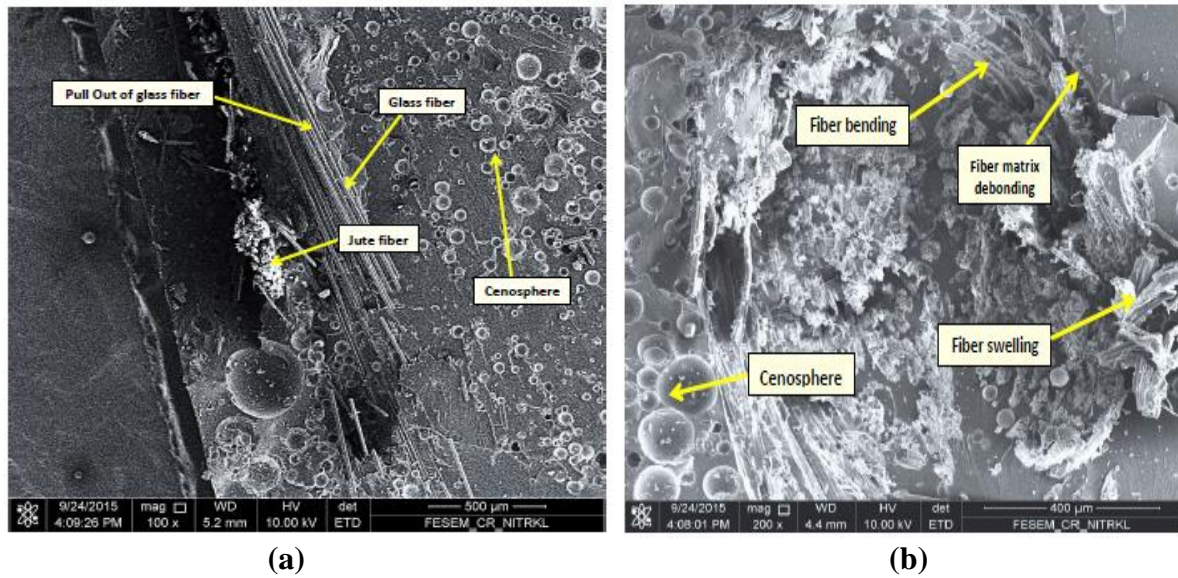


Figure 4.27 (a-b): SEM images of flexural fractured surfaces of 20wt.% cenosphere filled hybrid glass-jute(GJJG) epoxy composites in distilled water environment at lower (100x) and higher (200x) magnification

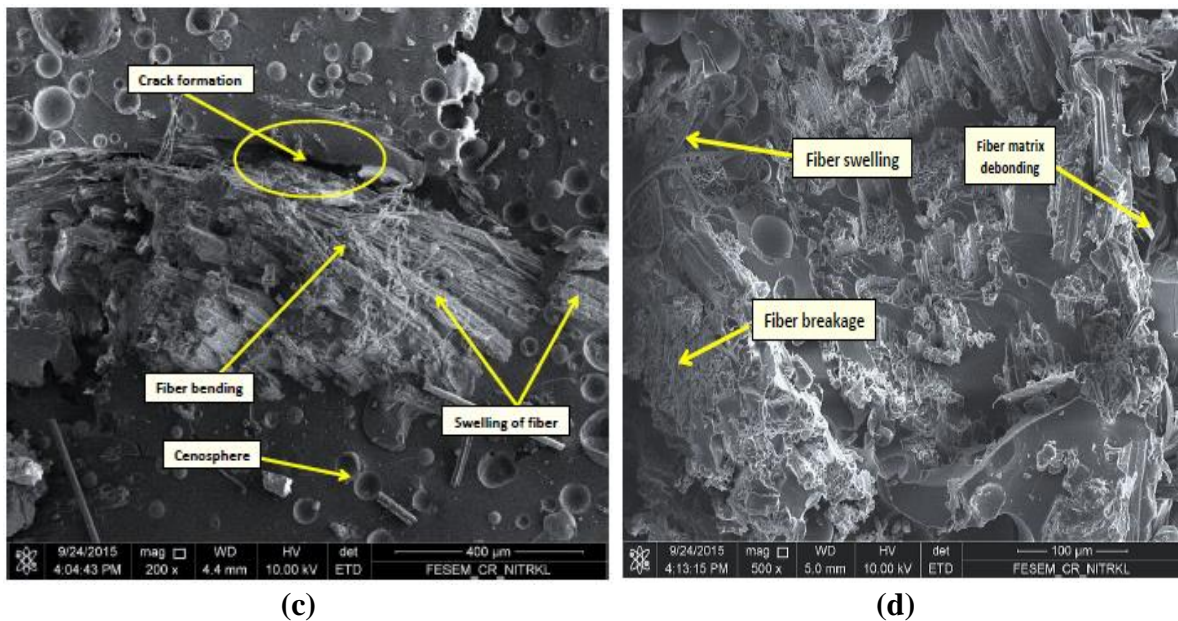


Figure 4.27 (c-d): SEM images of flexural fractured surfaces of 20wt. % cenosphere filled hybrid glass-jute (GJJG) epoxy composites in saline water environment at lower (200x) and higher (500x) magnification

Chapter 4 Moisture absorption behaviour of cenosphere filled jute glass epoxy composites**Table 4.4:** Variation of weight gain and thickness swelling of cenosphere filled hybrid jute-glass(GJJG) epoxy composite with immersion time exposure at distilled water environment for flexural specimens

% of Filler	Immersion time 't' (hrs)	Weight of the sample (w_t) g	Percentage of weight gain(%M)	Thickness at time 't' H(t)	Thickness swelling TS (t) (%)
5	0	10.822	0.000	6.93	0
	24	10.953	2.700	6.97	0.721
	48	11.155	3.080	7.03	1.48
	72	11.179	3.300	7.04	1.58
	96	11.193	3.430	7.05	1.8
	120	11.207	3.560	7.06	2.02
	144	11.196	3.460	7.08	2.3
	168	11.174	3.260	7.09	2.45
	192	11.174	3.260	7.13	2.89
	216	11.174	3.260	7.13	2.89
10	0	13.796	0.000	5.64	0
	24	13.879	1.560	5.77	2.38
	48	14.105	2.240	5.84	3.72
	72	14.085	2.100	5.85	3.89
	96	14.091	2.140	5.86	4.06
	120	14.098	2.190	5.88	4.39
	144	14.082	2.080	5.89	4.56
	168	14.084	2.090	5.90	4.73
	192	14.085	2.100	5.91	4.9
	216	14.091	2.140	5.91	4.9
15	0	14.457	0.000	5.91	0
	24	14.558	2.190	6.17	4.43
	48	14.834	2.610	6.27	6.2
	72	14.832	2.600	6.29	6.56
	96	14.845	2.690	6.31	6.91
	120	14.854	2.750	6.33	7.26
	144	14.860	2.790	6.34	7.44
	168	14.847	2.700	6.36	7.62
	192	14.834	2.610	6.37	7.8
	216	14.834	2.610	6.37	7.8
20	0	15.536	0.000	5.61	0
	24	15.601	1.260	5.90	5.34
	48	15.815	1.800	5.99	6.8
	72	15.804	1.730	6.01	7.21
	96	15.807	1.750	6.02	7.39
	120	15.810	1.770	6.04	7.84
	144	15.807	1.750	6.07	8.37
	168	15.809	1.760	6.08	8.55
	192	15.814	1.790	6.10	8.91
	216	15.818	1.820	6.10	8.91

Chapter 4 Moisture absorption behaviour of cenosphere filled jute glass epoxy composites

Table 4.5: Variation of weight gain and thickness swelling of cenosphere filled hybrid jute-glass(GJJG) epoxy composite with immersion time exposure at saline water environment for flexural specimens

% of Filler	Immersion time 't' (hrs)	Weight of the sample (w_t) g	Percentage of weight gain (% M)	Thickness at time 't' H(t)	Thickness swelling TS (t) (%)
5	0	14.372	0.000	6.45	0
	24	14.451	0.550	6.62	2.74
	48	14.673	2.100	6.72	4.28
	72	14.658	1.990	6.73	4.45
	96	14.676	2.118	6.74	4.63
	120	14.702	2.300	6.75	4.8
	144	14.670	2.080	6.77	4.97
	168	14.663	2.030	6.79	5.31
	192	14.673	2.100	6.81	5.66
	216	14.673	2.100	6.81	5.66
10	0	13.721	0.000	5.83	0
	24	13.785	0.467	6.07	4.15
	48	13.979	1.887	6.12	5.13
	72	13.966	1.792	6.21	6.617
	96	13.986	1.938	6.29	7.91
	120	14.007	2.091	6.31	8.4
	144	13.977	1.873	6.39	9.61
	168	13.973	1.843	6.40	9.76
	192	13.978	1.880	6.43	10.38
	216	13.979	1.887	6.43	10.38
15	0	13.164	0.000	5.12	0
	24	13.212	0.365	5.37	5.07
	48	13.386	1.687	5.42	6.05
	72	13.387	1.694	5.50	7.617
	96	13.394	1.749	5.62	9.803
	120	13.411	1.880	5.64	10.35
	144	13.383	1.665	5.71	11.59
	168	13.367	1.546	5.76	12.69
	192	13.367	1.546	5.77	12.89
	216	13.367	1.546	5.77	12.89
20	0	15.825	0.000	5.05	0
	24	15.874	0.308	5.41	7.28
	48	16.055	1.459	5.50	9.06
	72	16.067	1.530	5.61	11.28
	96	16.084	1.640	5.68	12.67
	120	16.090	1.680	5.75	14.05
	144	16.055	1.458	5.82	15.44
	168	16.039	1.353	5.87	16.41
	192	16.039	1.353	5.89	16.61
	216	16.039	1.353	5.89	16.61

Chapter 4 Moisture absorption behaviour of cenosphere filled jute glass epoxy composites**Table 4.6:** Variation of weight gain and thickness swelling of cenosphere filled hybrid jute-glass(GJJG) epoxy composite with immersion time exposure at distilled water environment for tensile specimens

% of Filler	Immersion Time 't' (hrs)	Weight of the sample (w_t) gm	Percentage of weight gain (% M)	Thickness at time 't' H(t)	Thickness swelling TS (t) (%)
5	0	14.045	0.000	7.11	0
	24	14.127	0.586	7.13	0.42
	48	14.390	2.460	7.16	0.843
	72	14.353	2.200	7.24	1.9
	96	14.353	2.200	7.26	2.2
	120	14.339	2.100	7.28	2.5
	144	14.339	2.100	7.31	2.9
	168	14.355	2.210	7.35	3.38
	192	14.358	2.230	7.357	3.48
	216	14.358	2.230	7.358	3.49
10	0	15.297	0.000	5.61	0
	24	15.364	0.440	5.67	1.17
	48	15.619	2.110	5.73	2.23
	72	15.598	1.970	5.80	3.46
	96	15.596	1.960	5.83	4
	120	15.593	1.940	5.86	4.53
	144	15.583	1.870	5.90	5.29
	168	15.584	1.880	5.912	5.4
	192	15.579	1.850	5.918	5.5
	216	15.578	1.840	5.918	5.5
15	0	12.913	0.000	6.27	0
	24	12.969	0.434	6.36	1.47
	48	13.132	1.700	6.45	3
	72	13.142	1.780	6.50	3.8
	96	13.140	1.760	6.55	4.6
	120	13.138	1.750	6.57	4.9
	144	13.137	1.740	6.63	5.8
	168	13.132	1.700	6.69	5.9
	192	13.132	1.700	6.64	5.91
	216	13.132	1.700	6.64	5.91
20	0	15.971	0.000	7.17	0
	24	16.130	0.290	7.31	2
	48	16.210	1.500	7.42	3.5
	72	16.218	1.550	7.49	4.5
	96	16.215	1.530	7.52	4.9
	120	16.213	1.520	7.57	5.6
	144	16.212	1.510	7.61	6.2
	168	16.194	1.400	7.62	6.3
	192	16.194	1.400	7.63	6.4
	216	16.194	1.400	7.63	6.4

Chapter 4 Moisture absorption behaviour of cenosphere filled jute glass epoxy composites**Table 4.7:** Variation of weight gain and thickness swelling of cenosphere filled hybrid jute-glass (GJJG) epoxy composite with immersion time exposure at saline water environment for tensile specimens

% of Filler	Immersion Time 't' (hrs)	Weight of the sample (w _t) gm	Percentage of weight gain (% M)	Thickness at time 't' H(t)	Thickness swelling TS (t) (%)
5	0	15.025	0.000	7.00	0
	24	15.111	0.570	7.02	0.428
	48	15.322	1.980	7.03	0.571
	72	15.320	1.970	7.07	1.000
	96	15.319	1.960	7.12	1.857
	120	15.325	2.000	7.171	2.457
	144	15.340	2.100	7.172	2.467
	168	15.319	1.960	7.163	2.340
	192	15.320	1.970	7.177	2.530
	216	15.323	1.990	7.177	2.530
10	0	14.912	0.000	6.44	0
	24	14.987	0.500	6.48	0.728
	48	15.180	1.800	6.55	1.800
	72	15.166	1.710	6.628	2.920
	96	15.166	1.710	6.647	3.220
	120	15.171	1.740	6.657	3.370
	144	15.184	1.830	6.660	3.520
	168	15.166	1.710	6.676	3.680
	192	15.165	1.700	6.686	3.830
	216	15.165	1.700	6.686	3.830
15	0	14.770	0.000	6.52	0
	24	14.836	0.450	6.617	1.500
	48	15.006	1.600	6.709	2.900
	72	15.004	1.560	6.782	4.030
	96	14.991	1.500	6.853	5.120
	120	14.988	1.480	6.874	5.430
	144	14.984	1.450	6.894	5.740
	168	14.982	1.440	6.945	6.520
	192	14.981	1.430	6.945	6.520
	216	14.981	1.430	6.945	6.520
20	0	16.190	0	5.98	0
	24	16.239	0.300	6.135	2.600
	48	16.416	1.400	6.213	3.900
	72	16.410	1.360	6.279	5.000
	96	16.395	1.270	6.349	6.180
	120	16.398	1.290	6.419	7.350
	144	16.400	1.300	6.479	8.360
	168	16.397	1.280	6.499	8.690
	192	16.395	1.270	6.509	8.860
	216	16.393	1.270	6.509	8.860

Table 4.8: Swelling rate parameter of cenosphere filled hybrid jute-glass (GJJG) epoxy composite at different environmental conditions

Environment	% of Filler	T_0 (mm)	T_∞ (mm)	TS (%)	Swelling rate parameter ($K_{SR} \times 10^{-3}$ (h^{-1}))
Distilled water	5	7.17	7.63	6.4	25.46
	10	6.27	6.64	5.91	30.35
	15	5.61	5.91	5.50	29.54
	20	7.11	7.35	3.49	34.81
Saline water	5	5.98	6.50	8.86	30.29
	10	6.52	6.94	6.52	38.78
	15	6.44	6.68	3.83	27.64
	20	7	7.17	2.53	34.73

Where T_0 - Initial Thickness of composite sample

T_∞ - Final Thickness of composite sample

TS - Thickness swelling

K_{SR} - Thickness swelling rate parameter

Table 4.9: Diffusion case selection parameter for cenosphere filled hybrid jute-glass (GJJG) Epoxy composite

Environment	Percentage of Cenosphere	n	k	$k(h)^2$
Distilled water	5	0.434	0.116	6.770
	10	0.469	0.095	4.223
	15	0.468	0.096	3.372
	20	0.530	0.069	3.741
Saline water	5	0.433	0.112	4.766
	10	0.418	0.120	5.812
	15	0.374	0.145	0.972
	20	0.477	0.088	4.532

Table 4.10: Diffusivity of cenosphere filled hybrid jute-glass (GJJG) epoxy composite

Environment	Percentage of cenosphere Filler	EMC (%)	Diffusivity ($D_x \times 10^{-6}$ (mm ² /sec)
Distilled water	5	3.26	1.6224
	10	2.14	3.1579
	15	2.61	2.4813
	20	1.82	3.8899
Saline water	5	2.118	2.4621
	10	2.091	2.0346
	15	1.880	2.7091
	20	1.680	2.8846

Chapter 5

Solid particle erosion performance of hybrid jute-glass fiber reinforced epoxy composites

5.1 Introduction

Wear occurs as a natural consequence when two surfaces with a relative motion interact with each other. Wear may be defined as the progressive loss of material from contacting surfaces in relative motion. Scientists have developed various wear theories in which the Physico-Mechanical characteristics of the materials and the physical conditions (e.g. the resistance of the rubbing body and the stress state at the contact area) are taken in to consideration. In 1938 Holm [193] starting from the atomic mechanism of wear, calculated the volume of substance worn over unit sliding path.

Barwell and Strang [194] in 1952, Archard [195] in 1953 and Archard and Hirst [196] in 1956 developed the adhesion theory of wear and proposed a theoretical equation identical in structure with Holm's equation. In 1957, Kragelski [197] developed the fatigue theory of wear. This theory of wear has been widely accepted by scientists in different countries. Because of the Asperities in real bodies, their interactions in sliding is discrete, and contact occurs at individual locations, which, taken together, form the real contact area. Under normal force the asperities penetrate into each other or are flattened out and in the region of real contact points corresponding stress and strain rise. In sliding, affixed volume of material is subjected to the many times repeated action, which weakens the material and leads finally to rupture. In 1973, Fleischer [198] formulated his energy theory of wear. The main concept of this theory is that the separation of wear particles requires that a certain volume of material accumulates a specific, critical store of internal energy. It is known that a large part of the work done in sliding is dissipated as heat, and that small proportion of it accumulates in the

material as internal potential energy. When the energy attains a critical value, plastic flow of the material occurs in this volume or a crack is formed. Further theories of wear are found in [199]. Though all the theories are based on different mechanisms of wear, the basic consideration is the frictional work.

5.2 Types of wear

Wear is a process of removal of material from one or both of two solid surfaces in solid state contact, occurring when two solid surfaces are in sliding or rolling motion together. The rate of removal is generally slow, but steady and continuous. In most basic wear studies where the problems of wear have been a primary concern, the so-called dry friction has been investigated to avoid the influences of fluid lubricants. Dry friction is defined as friction under not intentionally lubricated conditions but it is well known that it is friction under lubrication by atmospheric gases, especially by oxygen [200].

A fundamental scheme to classify wear was first outlined by Burwell and Strang [201]. Later Burwell [202] modified the classification to include five distinct types of wear, namely (1) Abrasive (2) Adhesive (3) Erosive (4) Surface fatigue (5) Corrosive. Figure 5.1 shows the five main categories of wear and the specific wear mechanisms that occur in each category. Each specific mode of wear looks different to the next, and may be distinguished relatively easily.

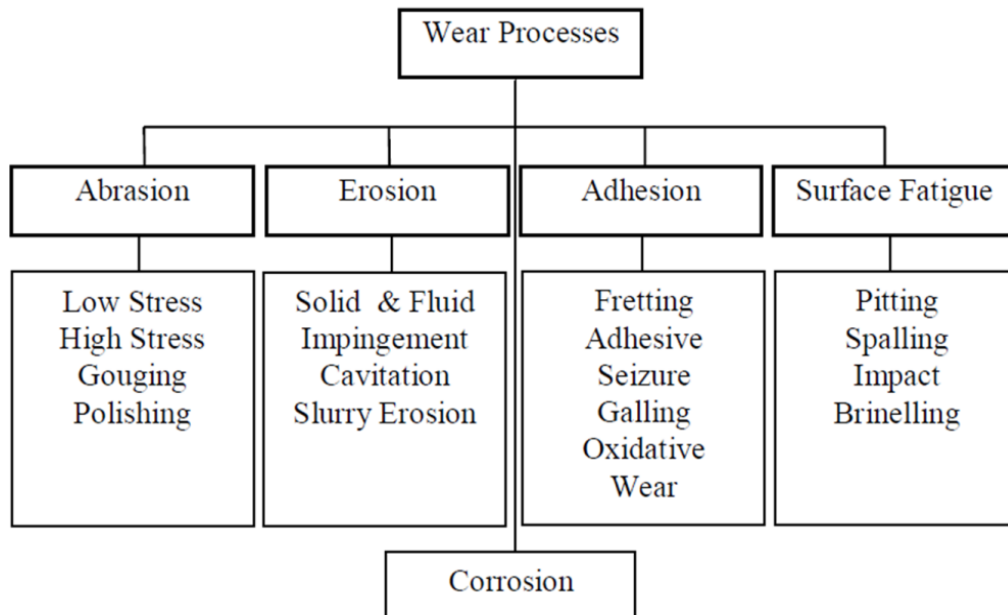


Figure 5.1: Flow chart of various wear mechanisms

5.2.1 Abrasive wear

Abrasive wear occurs when material is removed from one surface by another harder material, leaving hard particles of debris between the two surfaces. It can account for most failures in practice. It can also be called scratching or gouging depending on the severity of wear. Hard particles or asperities that cut or groove one of the rubbing surfaces produce abrasive wear. This hard material may be originated from one of the two rubbing surfaces. In sliding mechanism, abrasion can arise from the existing asperities on one surface (if it is harder than the other), from the generation of wear fragments which are repeatedly deformed and hence get work hardened for oxidized until they became harder than either or both of the sliding surfaces, or from the adventitious entry of hard particles, such as dirt from outside the system. Abrasive wear occurs under two conditions:

1. Two body abrasion; In this condition, one surface is harder than the other rubbing surface as shown in figure 5.2(a). Examples in mechanical operations are grinding, cutting and machining.
2. Three body abrasion; In this case a third body, generally a small particle of grit or abrasive, lodges between the two softer rubbing surfaces, abrades one or both of these surfaces, as shown in figure 5.2(b).

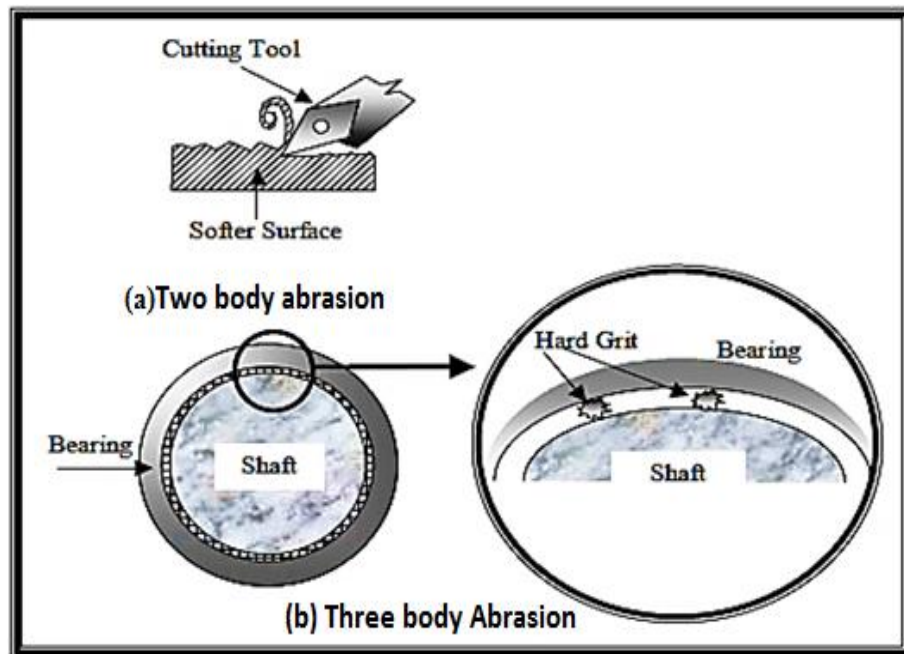


Figure 5.2(a) and (b): Schematic representations of the abrasion wear phenomena[202]

In the microscale, the abrasive wear process is where asperities of the harder surface press into the softer surface, with plastic flow of the softer surface occurring around the harder asperities, as shown in figure 5.2(c). This often leads to what is known as micro ploughing, micro cutting, and micro cracking, when a tangential motion is imposed. Abrasive wear may be reduced by the introduction of hydrodynamic or elasto hydrodynamic lubricants at various film thickness to separate the surfaces and to wash out any contaminant particles. According to the recent tribological survey, abrasive wear is responsible for the largest amount of material loss in industrial practice [199].

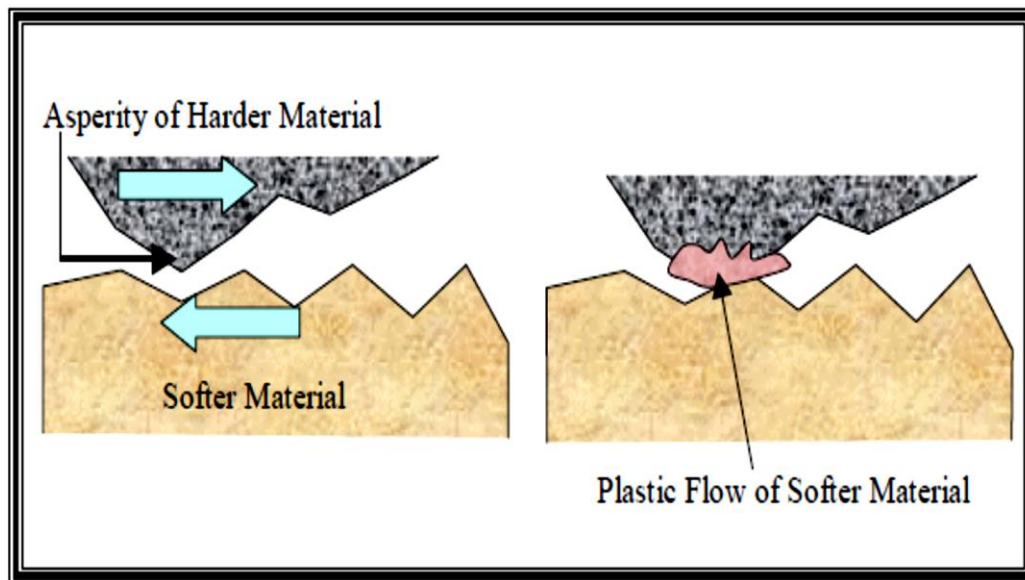


Figure 5.2(c): Abrasion in the microscale [202]

5.2.2 Erosive wear

The impingement of solid particles, or small drops of liquid or gas often cause what is known as erosion of materials and components. Solid particle impact erosion has been receiving increasing attention especially in the aerospace industry. Examples include the ingestion of sand and erosion of jet engines and of helicopter blades. As shown in figure 5.3 the erosion mechanism is simple. Solid particle erosion is a result of the impact of a solid particle A, with the solid surface B, resulting in part of the surface B has been removed. The impinging particles may vary in composition as well as in form. The response of engineering materials to the impingement of solid particles or liquid drops varies greatly depending on the class of material, materials properties (dependant on thermal history, exposure to previous stresses or surface tensions), and the environmental parameters associated with the erosion

process, such as impact velocity, impact angle, and particle size/type. Movement of the particle stream relative to the surface and angle of impingement both have a significant effect on the rate of material removal. When the angle of impingement is normal to the surface, material is displaced by plastic flow or is dislodged by brittle failure. The erosive effect on materials at high temperature is important for the selection of turbine engine materials in the aerospace industry.

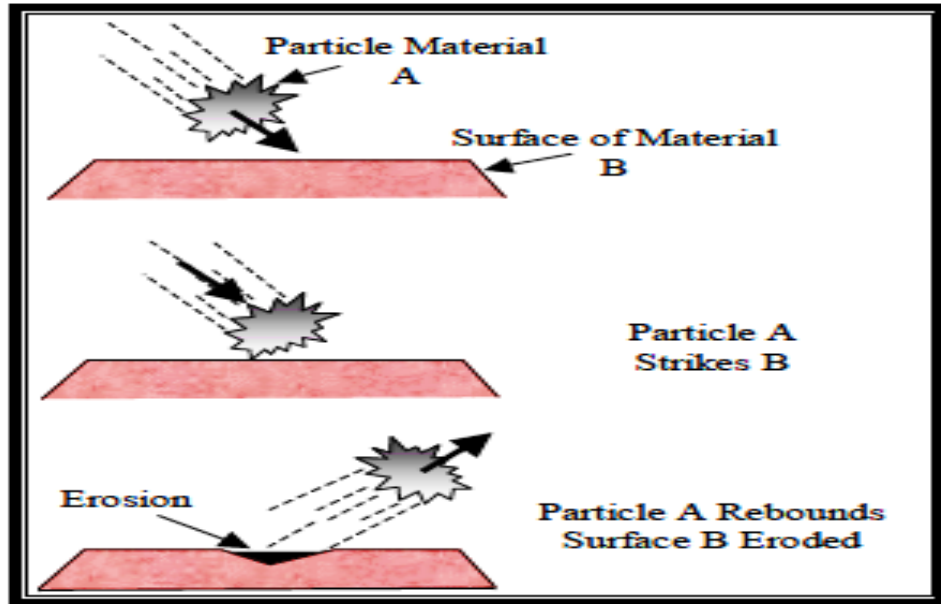


Figure 5.3: Schematic representations of the erosive wear mechanism[202]

5.2.3 Adhesive Wear

Adhesive wear can be defined as the wear due to localized bonding between contacting solid surfaces leading to material transfer between the two surfaces or the loss from either surface. It is often called galling or scuffing, where interfacial adhesive junctions lock together as two surfaces slide across each other under pressure. As normal pressure is applied, local pressure at the asperities become extremely high. Often the yield stress is exceeded, and the asperities deform plastically until the real area of contact has increased sufficiently to support the applied load, as shown in figure 5.4. In the absence of lubricants, asperities cold-weld together or else junctions shear and form new junctions. This wear mechanism not only destroys the sliding surfaces, but the generation of wear particles which cause cavitation and can lead to the failure of the component. An adequate supply of

lubricating films and oxide films resolve the adhesive wear problem occurring between two sliding surfaces.

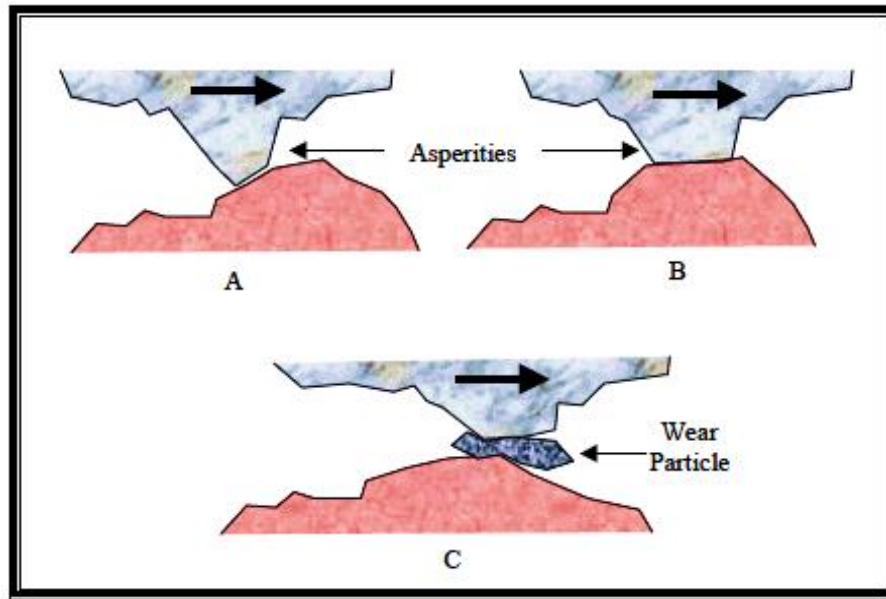


Figure 5.4: Schematic of generation of a wear particle as a result of adhesive wear process[202]

5.2.4 Surface Fatigue

Wear of a solid surface is caused by fracture arising from material fatigue is called surface fatigue. The term ‘fatigue’ is broadly applied to the failure phenomenon where a solid is subjected to cyclic loading involving tension and compression above a certain critical stress. When mechanical machinery move in periodical motion, stresses to the metal surfaces occur, often leading to the fatigue of a material. All repeating stresses in a rolling or sliding contact can give rise to fatigue failure. These effects are mainly based on the action of stresses in or below the surfaces, without the need of direct physical contact of the surfaces under consideration. When two surfaces slide across each other, the maximum shear stress lies some distance below the surface, causing micro cracks, which lead to failure of the component. These cracks initiate from the point where the shear stress is maximum and propagate to the surface as shown in figure 5.5. Materials are rarely perfect, hence the exact position of ultimate failure is influenced by inclusions, porosity, micro cracks and other factors. Fatigue failure requires a given number of stress cycles and often predominates after a component has been in service for a long period of time. The number of stress cycles

required to cause such failure decreases as the corresponding magnitude of stress increases. Vibration is a common cause of fatigue wear.

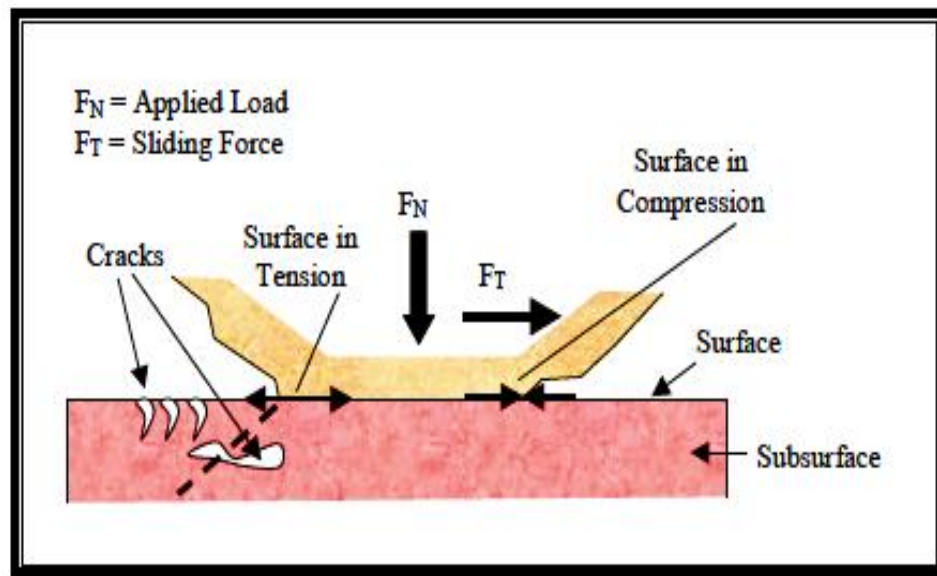


Figure 5.5: Schematic representations of the surface fatigue wear mechanism[202]

5.2.5 Corrosive Wear

Most metals are thermodynamically unstable in air and react with oxygen to form an oxide, which usually develop layer or scales on the surface of metal or alloys when their interfacial bonds are poor. Corrosion wear is the gradual eating away or deterioration of unprotected metal surfaces by the effects of the atmosphere, acids, gases, alkalis, etc. as shown in figure 5.6.

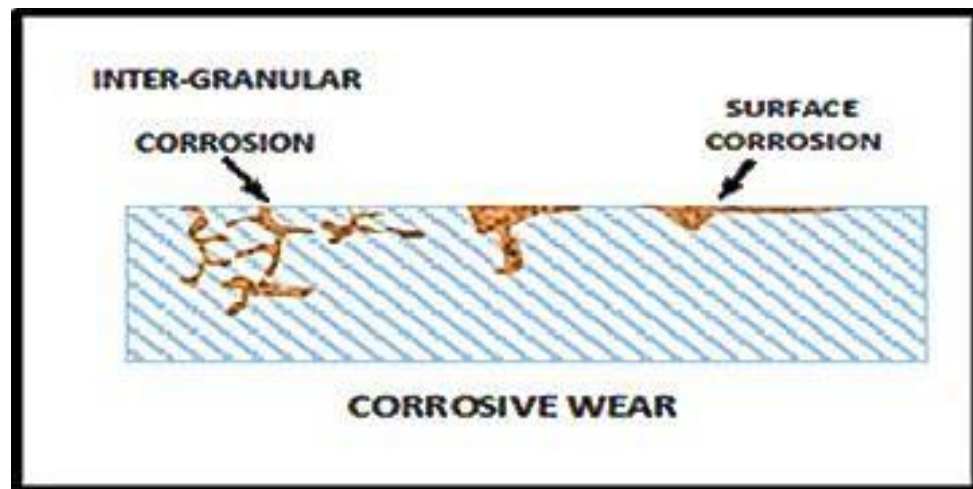


Figure 5.6: Schematic representations of the corrosive wear mechanism

This type of wear creates pits and perforations and may eventually dissolve metal parts. In corrosive wear, the dynamic interaction between the environment and mating material surfaces play a significant role, whereas the wear due to abrasion, adhesion and fatigue can be explained in terms of stress interactions and deformation properties of the mating surfaces. In corrosive wear firstly the connecting surfaces react with the environment and reaction products are formed on the surface asperities. Attrition of the reaction products then occurs as a result of crack formation, and/or abrasion, in the contact interactions of the materials. This process results in increased reactivity of the asperities due to increased temperature and changes in the asperity mechanical properties. Thermally sprayed coatings applied to various material surfaces, such as those depositing using the HVOF (High velocity oxygen fuel coating) process, have proved an effective tool in the prevention of corrosion.

5.3 Symptoms of wear

Wear is not an intrinsic material property but characteristics of the engineering system which depend on load, speed, temperature, hardness, presence of foreign material and the environmental condition [203].

As solid particle erosion occurs whenever hard particles along with gas or liquid medium impinged on a surface at any significant velocity which results in progressive loss of material from a solid surface due to mechanical interaction between that surface and the erodent particles. The structural components like gas turbine blade, helicopter rotor blades and wings of an aircraft are exposed to rainy and dusty environment at high speed encounter the problem of erosion. The process of erosion causes thinning of components, surface roughening, surface degradation, macroscopic scooping appearance and reduction in functional life of the structure.

A summary of the appearance and symptoms of different wear mechanism is indicated in table 5.1 and the same is a systematic approach to diagnose the wear mechanisms.

Table 5.1: Symptoms and appearance of different types of wear [204]

Types of wear	Symptoms	Appearance of the worn out surface
Abrasive	Presence of clean furrows cut out by abrasive particles	Grooves
Adhesive	Metal transfer is the prime symptoms	Seizure, catering rough and torn-out surfaces
Erosion	Presence of abrasives in the fast moving fluid and short abrasion furrows	Waves and troughs
Corrosion	Presence of metal corrosion products	Rough pits or depressions
Fatigue	Presence of surface or subsurface cracks accompanied by pits and spalls.	Sharp and angular edges around pits
Impacts	Surface fatigue, small sub-micron particles or formation of spalls	Fragmentation, peeling and pitting
Fretting	Production of voluminous amount of loose debris	Roughening, seizure and development of oxide ridges
Electric attack	Presence of micro craters or a track with evidence of smooth molten metal	Smooth holes

Hence, solid particle erosion has been considered as a serious problem as it is responsible for many failures in engineering applications. Hence several attempts to understand the basic mechanisms of the erosion were started in the last half of the 20th century and have been continued to the present. In the year of 1995 an article on the past and the future of erosion was presented by Finnie [205]. In this article, the influencing parameters and dominating mechanisms during solid particle erosion were reviewed on the erosion response of metals and ceramic materials. In the same year another article was published by

Meng *et al.*[206] to provide information about the existing wear models and prediction equations.

According to Bitter [207], erosion is a material damage caused by the attack of particles entrained in a fluid system impacting the surface at high speed. Hutchings [208] defines it as an abrasive wear process in which the repeated impact of small particles entrained in a moving fluid against a surface result in the removal of material from the surface. Erosion due to the impact of solid particles can either be constructive (material removal desirable) or destructive (material removal undesirable), and therefore, it can be desirable to either minimize or maximize erosion, depending on the application. The constructive applications include sand blasting, high-speed water-jet cutting, blast stripping of paint from aircraft and automobiles, blasting to remove the adhesive flash from bonded parts, erosive drilling of hard materials. Whereas the solid particle erosion is destructive in industrial applications such as erosion of machine parts, surface degradation of steam turbine blades, erosion of pipelines carrying slurries and particle erosion in fluidized bed combustion systems. In most erosion processes, target material removal typically occurs as the result of a large number of impacts of irregular angular particles, usually carried in pressurized fluid streams.

It is generally recognized that erosive wear is a characteristic of a system and is influenced by many parameters. Laboratory scale investigation if designed properly allows careful control of the tribo system whereby the effects of different variables on wear behaviour of polymer matrix composites scan be isolated and determined. The data generated through such investigation under controlled conditions may help in correct interpretation of the results.

5.4 Solid particle erosion of hybrid polymer matrix composites

Polymer composites are finding an ever increasing application as structural materials in various components and engineering systems. Interest in this area is commensurate with the increasing utilization of polymer based composites in aerospace, transportation and processes industries, where they can be subjected to multiple solid or liquid particle impact. Examples of such applications are pipe line carrying sand slurries in petroleum refining, helicopter rotor blades, pump impeller blades, high speed vehicles and aircraft operating in desert environments, radomes, surfing boats where the components encounter impact of lot of

abrasives like dust, sand, splinters of materials, slurry of solid particle and consequently the material undergoes erosive wear[209-211].

The most important factors influencing the erosion rate of the composite materials can be summarized under four categories.

- i. The properties of the target materials (matrix material properties and morphology, reinforcement type, amount and orientation, interface properties between the matrices and reinforcements etc.)
- ii. Environment and testing conditions (temperature, chemical interaction of erodent with the target)
- iii. Operating parameters (angle of impingement, impact velocity, particle flux mass per unit time etc.) and
- iv. The properties of the erodent (size, shape, type, hardness etc.) [212-214].

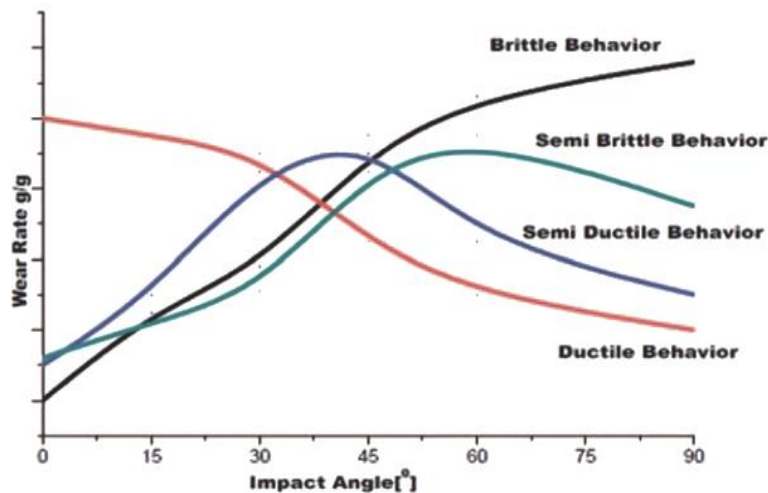


Figure 5.7: Schematic diagram of brittle, semi-brittle, semi-ductile and ductile-type erosive wear

Thus it seems that the erosion resistance of the material can be evaluated after investigating the combination of above parameters. In general, erosion behaviour of materials can be grouped into ductile and brittle when erosion rate is evaluated as a function of impingement angle. The schematic diagram of brittle, semi-brittle, semi-ductile, and ductile type erosive wear is shown in figure 5.7. From the figure the ductile behaviour is characterized by maximum erosion at low impact angle in the range of (15°-30°). On the other hand, if maximum erosion occurs at 90°, then the behaviour can be termed as brittle.

Reinforced composites have also been found to exhibit an intermediate behaviour known as semi-ductile with maximum erosion occurring at an angle in the range of (45°-60°) [215]. However, the above classification is not absolute as the erosion behaviour of a material has a strong dependence on erosion conditions such as impact angle, impact velocity and erodent properties such as shape, hardness, size, the composition of target material, fiber orientation, operating parameters, properties of the erodent, environment, testing conditions and so on. In the literature [211], the erosion behaviour of polymers and its composites has also been characterized by the value of the velocity exponent, ' n ' ($E_r \propto v^n$).

Many researchers have evaluated the resistance of various types of polymers like nylon, epoxy, polypropylene, bismaleimide, etc. and their composites to solid particle erosion. Harsha *et al.* [215] has summarized the work carried out by some of the investigators on solid particle erosion of polymer composites. Roy *et al.* while working on erosive wear of polymer composite revealed that the composite materials present a rather poor erosion resistance as compared to metallic materials [216].

Bajpai [217] have developed a laminated composite using three plant fibers (nettle, grew optiva and sisal) in to polylactic acid polymer and studied the wear and frictional characteristics of developed composites under dry condition at different operating parameters. The results indicate that incorporation of natural fiber mats into polylactic acid matrix significantly improves the wear behaviour of neat polymer.

Mishra and Acharya [218], Deo and Acharya [219] and Gupta *et al.* [220] have reported the tribo potential of sugarcane, lantana camara and bamboo fiber reinforcement in thermoset polymers for enhancing erosive wear resistance. They have the opinion that fiber volume fraction has a significant influence on the erosion rate. Recently Mohanty *et al.* [221] and Ojha *et al.* [222] studied the erosive wear behaviours of date palm leaf fiber reinforced polyvinyl alcohol composites and wood apple shell fibers reinforced epoxy composites. It is reported that [223] if natural fiber is hybridized with a synthetic fiber in the same matrix the properties of natural fiber could be improved by taking the advantage of both the fibers. In this regards various attempt has been made by different researchers to combine varieties of

natural fiber with synthetic fiber. Jose Almeida *et al.* [224] evaluated the enhancement in the properties of curaua polyester composites by incorporating chopped glass fibers with chopped caraus fibre. Patel *et al.* [225] reported that the erosive wear resistance of jute/epoxy composite can be improved significantly by hybridizing with synthetic fiber glass.

Barkoula and Karger-ocsis [226] used glass fiber as reinforcement in thermoplastic polypropylene (PP) composite. They used modified sandblasting apparatus for erosion testing. The experimental parameters used are impact angle(30°,60° and 90°), relative fibre orientation(both parallel and perpendicular),fiber length (discontinuous, continuous) and fiber content (40-60 wt.%). They concluded that the fiber length did not affect the erosive wear behaviour especially at high impact angles, but showed a strong dependence on the relative fibre-orientation at low impact angles (30°).The inclusion of brittle glass fiber led to higher erosive wear rate of the GF/PP composites. As the fibre content increases, the erosion wear rate was found to be higher experimentally.

G. Drensky *et.al* [227] investigated solid particle erosion of a composite material consisting of polyetheretherketone (PEEK) matrix and unidirectional (AS4) carbon fiber. Erosion tests were conducted with 10µm Arizona road dust and 100µm sieved runway sand particles in especially designed erosion tunnel at temperature up to 260°C and impact velocities up to 152.4 m/s. Experimental results were presented for the measured erosion rates of the unidirectional (UD) composite material at two perpendicular fiber alignment settings relative to the impacting particle stream. The results indicated a quasi-ductile behavior with peek erosion rate at 45° impact angle. Overall the erosion rate was found to increase with impact velocity. The fiber alignment orientation relative to the impacting particle stream influenced the erosion rate of the unidirectional composite material. Higher erosion rates were measured at 90° fiber orientation than at 0° at ambient test temperatures.

As new developments are still under way to explore innovative fields for tribo-application of natural fiber based materials, in this chapter an attempt has been made to study the potential of using jute(45°-45°) and glass(0-90°) fiber with different stacking sequences incorporating cenosphere filler to the optimum sequence in epoxy base for tribological

applications. As an initial investigation in the present work the influence of impact velocity, impingement angle and particulate loading on erosive wear has been carried out and results of these observations are presented in the subsequent sections.

5.5 Experiment

5.5.1 Preparation of the test specimens

The preparation of the composite samples of different stacking sequences of hybrid jute-glass reinforced epoxy composites is same procedure as explained in chapter 3 article 3.2.2. Specimens of dimension (25× 25×3) mm were cut from the composite slabs for erosion test by diamond cutter.

5.5.2 Micro-Hardness

Micro-hardness measurement is done using a Lecco Vickers Hardness (LV 700) tester. A diamond indenter, in the form of a right pyramid with a square base and an angle 136° between opposite faces, is forced into the material under a load F . The two diagonals X and Y of the indentation left on the surface of the material after removal of the load are measured and their arithmetic mean L is calculated. In the present study, the load (F) of 10 N is considered and Vickers hardness number is calculated using the following equation

$$H_v = \frac{0.1889F}{L^2} \text{ and } L = \frac{X + Y}{2} \quad (5.1)$$

Where F is the applied load (N), L is the diagonal of square impression (mm), X is the horizontal length (mm) and Y is the vertical length (mm). As shown in figure 5.8, the composite micro-hardness is different for different stacking sequences of hybrid jute-glass epoxy composites. It is found that the sequence S4 (GJJG) had the maximum hardness value 245.17MPa and it is minimum for sequence S1 (JJJJ) of 206 MPa with only jute fiber. Hence it can be concluded here that when two layers of jute fiber are put along with glass fibers, the strength of jute fiber could be increased.

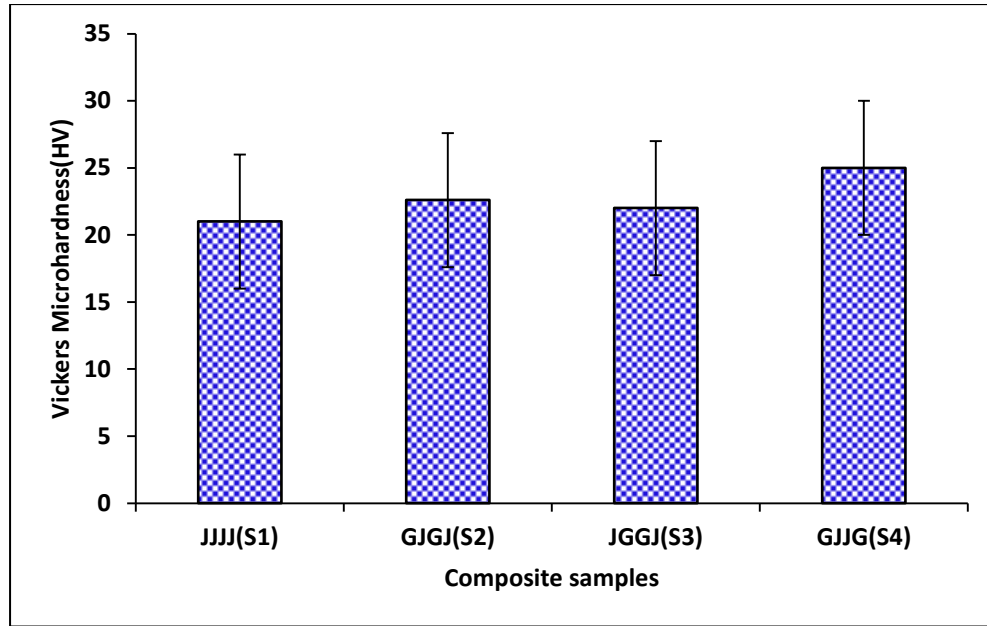


Figure 5.8: Effect of hardness on stacking sequences of hybrid jute-glass epoxy composites

5.5.3 Measurement of impact velocity of erodent particles: Double disc

Method

The most commonly used method for measuring impact velocity of the erodent particle is the double disc method. It consists of a pair of metal disc mounted on a common shaft and the stream of erodent particles is arranged to strike the upper disc, which has a thin radial slit cut in it. The exit particles from nozzle impinge on the upper disc with some of the particles passing through the slit, which eventually erode a mark on lower disc. Two erosion exposures are made, one with stationary disc and other with rotating disc at known rpm. These exposures give rise to erosion marks A and B on the lower disc as shown in figure 5.9. Measurement of the angular displacement between these marks gives a measure of the flight time of the particles as they cross the space between the discs. The particle velocity can be found by using following equation.

$$v = \frac{L}{t} = \frac{Lv360^\circ}{\theta} \quad (5.2)$$

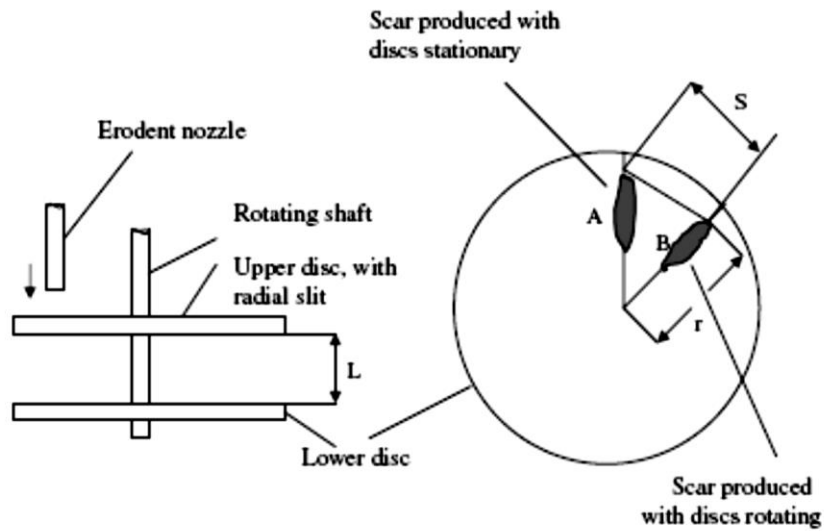


Figure 5.9: Schematic diagram of methodology used for velocity calibration

Where L is the separation of two discs, t is time in second, v is rotation speed of disc per second and θ is angular displacement between the marks. The above equation can also be expressed as follows.

$$v = \frac{2\pi r v L}{S} \quad (5.3)$$

Where r is radius from the disc centre and S is linear separation of two marks. The details of impact velocity calibration at various pressures are given in table 5.2.

Table 5.2: Impact velocity calibration at various pressures

Pressure (bar)	Speed of rotating disc(rpm)	Angle θ (°)	Velocity(m/s)	Avg. impact velocity(m/s)
1 bar	2000	7.0	42.85	47.25
		6.5	46.15	
		6.0	50.00	
		6.0	50.00	
2 bar	2000	4.0	75.00	69.16
		4.5	66.67	
		4.0	75.00	
		5.0	60.00	
3 bar	2000	4.5	66.67	81.84
		4.0	75.00	
		3.5	85.71	
		3.0	100.00	

5.6 Test apparatus and experiment

The schematic diagramme of the erosion test apparatus used for the present investigation designed as per ASTM-G76 standard is shown in figure 5.10(a). The test rig figure 5.10(b) consists of an air compressor, a particle feeder, an air particle mixing and accelerating chamber. The compressed dry air is mixed with the erodent particles, which are fed at a constant rate from a conveyor belt-type feeder into the mixing chamber and then accelerated by passing the mixture through a tungsten carbide converging nozzle of 4 mm diameter. These accelerated particles impact the specimen, and the specimen could be held at various angles with respect to the impinging particles using an adjustable sample holder. The test apparatus has also been fitted with a rotating double disc to measure the velocity of the erodent particle. The impact velocities of the erodent particles has been evaluated experimentally using this rotating double disc method developed and as explained by Ives and Ruff [228].

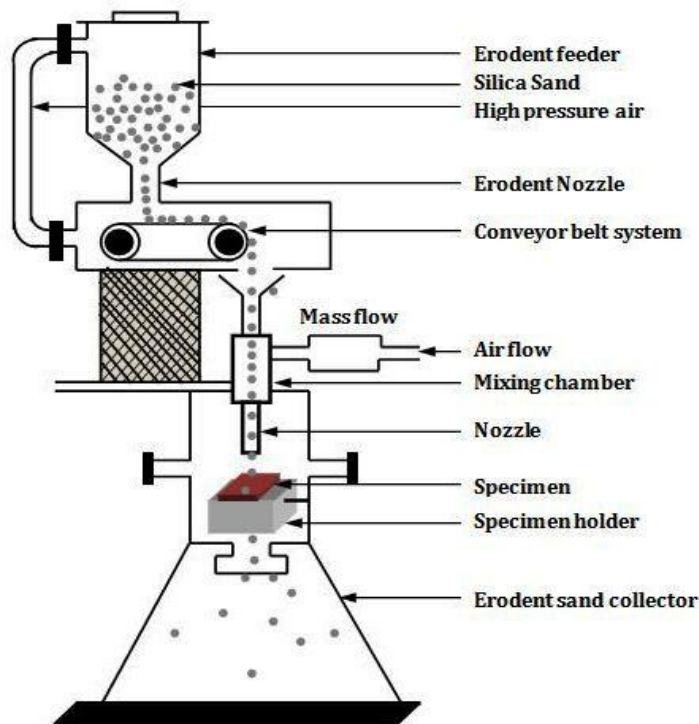


Figure 5.10 (a): Schematic diagram of erosion test rig



- 1 Sand hopper
- 2 Conveyor belt system for sand flow
- 3 Pressure transducer
- 4 Particle-air mixing chamber
- 5 Nozzle
- 6 X-Y and h axes assembly.
- 7 Sample holder

Figure 5.10 (b): Parts of Solid Particle Erosion Test Set up

The conditions under which the erosion test has been carried out are given in table 5.3. A standard test procedure is employed for each erosion test. Wear was measured by mass loss method. The samples were cleaned with a fine brush to remove any sand particles attached to the surface and then wiped with a cotton plug dipped in acetone to avoid any entrapment of wear debris. Then they were dried and weighed to accuracy of 1×10^{-3} g using an electronic balance prior to and after each tests.

The test samples after loading in the test rig were eroded for 3 min at a given impingement angle and then weighed again to determine weight loss (Δw). The erosion rate (E_r) is then calculated by using the following equation.

$$E_r = \frac{\Delta w}{w_e} \quad (5.4)$$

Where Δw is the mass loss of test sample in gm and w_e is the mass of eroding particles (i.e. testing time \times particle feed rate). This procedure has been repeated until the erosion rate attains a constant steady-state value. In the present study the same procedure was repeated for five times (i.e. exposure time was 15min).

The parameter erosion efficiency (η) is defined simply as the fraction of the volume that is actually removed as erosion debris out of the material which is displaced. It is also an important parameter to characterize the nature and mechanism of erosion. The following equation was proposed by Sundararajan *et al.* [229] for calculation of the erosion efficiency (η) for the process.

$$\eta = \frac{2E_r H}{\rho v^2} \quad (5.5)$$

Where ' E_r ' is erosion rate (g/g), ' H ' is hardness of eroding material (BHN), ' ρ ' is density of eroding material (g/cc), and ' V ' is velocity of impact (m/s). The above parameter can be used for identifying the brittle and ductile response of various materials to solid particle erosion. For example, ideal micro ploughing involving just the displacement of the material from the crater without any fracture (and hence no erosion) will have zero erosion efficiency. In contrast, if the material removal is by ideal micro cutting, η will be unity or 100%. If erosion occurs by lip or platelet formation and their subsequent fracture by repeated impacts, as usually in the case of ductile materials, the magnitude of η will be very low, i.e. $\eta \ll 100\%$ and in the range of (0-1). In the case of brittle materials, erosion takes place by spalling and removal of large chunks of material resulting from the interlinking of lateral or radial cracks and thus η can be expected to be even greater than 100%.

Experimental results of the erosion test for different volume fraction of jute-glass fiber reinforced epoxy composites for different stacking sequences with various impingement angle and velocities are tabulated and presented in tables 5.4-5.7. Based on the tabulated results various graphs were plotted and presented in figures 5.11-5.19 for hybrid jute-glass epoxy composites under various test conditions.

5.7 Results and discussion

Figures 5.11-5.13 show the influence of impingement angle (α) on the erosion rate of hybrid jute-glass epoxy composites under different impact velocities (48, 70 and 82 m/s). It is evident from the plot that the erosion rate attains the peak value at an impingement angle of 45° or 60° for all stacking sequences. The minimum erosion rate is observed for the composite (GJJG) of stacking sequence (S4) for all the impact velocities under consideration. The glass fiber being brittle in nature shows higher erosion rate under higher impact angle (90°) as in figure 5.11. It is due to the presence of glass fiber at the outer layer of composites which is harder and stiffer than jute fiber. It is known that impingement angle is one of the most important parameters for the erosion behaviour of materials. In the literatures [230-237] materials as classified as ductile or brittle based on the dependence of their erosion rate with impingement angle. The ductile behaviour is characterized by maximum erosion rate at low impingement angle typically ($15^\circ < \alpha < 30^\circ$). On the other hand, if the maximum erosion rate occurs at normal impact ($\alpha = 90^\circ$), the behaviour of the material is brittle. However reinforced composites have been found to exhibit semi-ductile behaviour with maximum erosion rate at intermediate impingement angles of ($45^\circ < \alpha < 60^\circ$). From the experimental results it is clear that the developed composites respond to solid particle impact neither behaves in a purely ductile nor in a brittle manners. Since the maximum erosion occurs between (45° - 60°) impact angles for all velocities under consideration. Therefore, this behaviour of the composites can be termed as semi-ductile in nature. The same type of behaviour was also reported by Biswas *et al.*[232] while studying the erosive behaviour of red mud filled bamboo-epoxy composites.

The variation of steady-state erosion rate of all composite samples with impact velocities at different impingement angles are shown in figures 5.14 to 5.17 in the form of histograms. It can be observed from these histograms that erosion rate of all composite samples increases with increase in the impact velocity. However, jute-epoxy (JJJJ) composite shows highest variation in the erosion rate with increase in the impact velocities at all impact angles. Also, it is clear from the plot that the best erosion resistance under all impact conditions is achieved for the composite made of jute-glass (GJJG) of stacking sequence (S4).

Irrespective of impingement angle and impact velocity, there is a steady increase in erosion rate with different layered composites of jute-glass has also been observed. At higher velocities it is found that the erosion resistance of composites is dominated by the hybrid composite. Similar type of observation was reported by Miyazaki *et al.* [233], while worked with glass and carbon fiber reinforced polyetheretherketon composites. In the solid particle impact experiment the impact velocity of the erosive particles has a very strong effect on erosion rate. For any material, once the steady state condition has been reached, the erosion rate ' E_r ' can be expressed as a simple power function of impact velocity [234].

$$E_r = kv^n \quad (5.6)$$

Where k is the constant of proportionality includes the effect of all the other variables. The value of ' n ' and ' k ' are found by least-square fitting of the data points in plots which represents the erosion rate dependence on impact velocity by using the power law. The value of ' n ' the velocity exponent is typically between (2-3), although much higher exponent is seen under some circumstances [235]. According to Pool *et al.* [236], for polymeric materials behaving in ductile manner, the velocity exponent ' n ' varies in the range (2-3) while for polymer composites behaving in brittle fashion the value of ' n ' should be in the range of (3-5). For the present investigation the least-squares fits to the data points were obtained by using the power law and the values of ' n ' and ' k ', are summarized in Table 5.8. The velocity exponents found for 30°, 45°, 60° and 90° impingement angles are in the range of (2.26-3.38), (2.44-2.88), (2.61-3.06) and (1.41-1.76) respectively. These velocity exponents at various impingement angles are in conformity with Harsha *et al.* [237] showing semi-ductile material response.

It has also been reported by Sundararajan *et al.* [238] that the erosion efficiency (η), can be used to characterize the nature and mechanism of erosion. They showed that the ductile material possesses very low erosion efficiency i.e. $\eta \lll 100\%$, whereas the brittle material exhibits an erosion efficiency even greater than 100%. The values of erosion efficiencies of composites under this study are calculated using equation 5.5 and are listed in Table 5.9 along with their hardness values and operating conditions. Since the steady-state

erosion rate (E_r) of jute-glass hybrid epoxy composites increases with increase in impact velocity ' v ', which is proportional to ' v^2 ', hence erosion efficiency is expected to increase with increasing ' v '.

Figures 5.18-5.19 shows the variation of erosion efficiency with different impact velocities studied at 45° and 60° impact angle. The lower erosion efficiency of sample was observed in GJJG composite of stacking sequence(S4) indicating better erosion resistance as compared to other stacking sequences(S1,S2 and S3) of jute-glass hybrid epoxy composites at different impact velocities under consideration. The erosion efficiencies of jute E-glass hybrid epoxy composites vary from 2.75 to 12.64% for different impact velocities studied at angle 60° and it varies from 3.68 to 11.21% for 45° impact angle. The dependence of erosion rates of the jute-glass epoxy composites of varying stacking sequences with impact velocity is very strong at different impingement angles, as indicated by the velocity exponents (n) were in the range of (1.41-3.38). Thus, by observing erosion efficiency and velocity exponents (n) of jute-glass fiber reinforced composites erosion behaviour can be broadly classified as semi-ductile. This also confirms to the results plotted in Figures 5.11 to 5.13.

5.8 Surface Morphology of Eroded Surfaces

SEM analysis has been carried out for the developed composite samples where optimum results have been obtained to know the morphological behaviour with the experimental parameters.

Figure 5.20(a) shows the crater formed and the damage caused to the composite. It shows extensive damage of fibres. Figure 5.20(b) also shows the damage of fibers but still fibers are not pull-out from the matrix. This might have happened due to lower impact velocity. No cracks are also observed on the matrix.

Figure 5.20(c) shows the chipping out of jute fibers but there is no damage found to the glass layers. The removal of the jute fibre by particle impact on the surface is clearly visible. After removal of the outer layer the particles enters to the glass fibre layer. It is found that breaking of glass fibres took place but chipping of the fibres from the matrix is prevented by increasing no of layers of glass fiber.

It can be justified from this fact that erosion resistance of the natural fiber jute can be improved significantly by hybridising with synthetic fiber glass. It can also be concluded

from the surface of the samples that material removal is mainly due to micro-cutting and micro-ploughing.

5.9 Conclusion

Experiments were conducted to characterize the effect of erosion rate on hybrid jute-glass epoxy composites with specific fibre orientation of different stacking sequences with silica sand as erodent. Based on the results the following conclusions were drawn. Layering sequences (JJJJ, JGJG, GJGJ, GJJG) and the velocity of impact has a significant influence on the erosion rate of the hybrid composites.

1. The influence of impingement angle on erosive wear of all composites under consideration exhibit semi ductile behaviour with maximum wear rate at 45° impingement angle.
2. The erosive wear rate of hybrid composite GJJG of stacking sequence (S4) with two jute layers in between glass layers at extreme ends gives the lowest value.
3. In the composites, erosion rate(E_r) displays power law behaviour with particle velocity(v) as $E_r \propto v^n$. The velocity exponents are in the range of (1.41-3.38) for various materials studied for different impingement angles(30° - 90°) and impact velocities (48-72 m/s).
4. It is clear from this study that erosive strength of natural fiber (Jute) can be increased by hybridization with synthetic fiber glass.
5. SEM studies of worn surfaces support the involved mechanism and reveal the good interfacial bonding between woven jute-glass and epoxy matrix and confirmed material removal is mainly due to micro-cutting and micro-ploughing.

6. Possible use of these composites in components such as pipes carrying coal dust, desert structure, low cost housing, boats/sporting equipments, partition boards, doors and window panels is recommended.

Table 5.3: Test parameters of erosion test

Erodent	Silica sand
Erodent size(μm)	(200 \pm 50)
Impingement angle(α°)	30,45,60,90
Impact velocity(m/s)	48,70,82
Erodent feed rate(g/min)	(2.06 \pm 0.50)
Test temperature	Room temperature
Nozzle to sample distance(mm)	10
Nozzle diameter	5
Time of impact	15min

Table 5.4: Weight loss and Erosion rate of JJJJ (S1) epoxy composites with respect to impingement angle due to erosion for a period of 15min

Velocity(m/s)	Impact Angle($^\circ$)	Weight loss ' Δw '(g)	Erosion Rate $\times 10^{-4}$ (g/g)
48	30 $^\circ$	0.005	2.14
	45 $^\circ$	0.012	5.13
	60 $^\circ$	0.007	4
	90 $^\circ$	0.006	2.99
70	30 $^\circ$	0.014	5.120
	45 $^\circ$	0.018	10.92
	60 $^\circ$	0.022	8.0
	90 $^\circ$	0.007	5.0
82	30 $^\circ$	0.019	9.980
	45 $^\circ$	0.045	21.23
	60 $^\circ$	0.030	23.94
	90 $^\circ$	0.064	18.35

Table 5.5: Weight loss and Erosion rate of hybrid epoxy composite JGGJ (S2) with respect to impingement angle due to erosion for a period of 15min

Velocity(m/s)	Impact Angle(°)	Weight loss 'Δw'(g)	Erosion Rate × 10 ⁻⁴ (g/g)
48	30°	0.008	2.14
	45°	0.009	3.13
	60°	0.007	2.14
	90°	0.006	2.14
70	30°	0.02	4.06
	45°	0.035	9.02
	60°	0.021	7.03
	90°	0.02	3.21
82	30°	0.019	8.69
	45°	0.034	17.93
	60°	0.034	17.92
	90°	0.025	14.24

Table 5.6: Weight loss and Erosion rate of hybrid epoxy composite GJGJ (S3) with respect to impingement angle due to erosion for a period of 15min

Velocity(m/s)	Impact Angle(°)	Weight loss 'Δw'(g)	Erosion Rate × 10 ⁻⁴ (g/g)
48	30°	0.008	2.14
	45°	0.011	4.27
	60°	0.008	3.42
	90°	0.008	2.14
70	30°	0.016	1.29
	45°	0.025	7.26
	60°	0.028	4.83
	90°	0.02	2.85
82	30°	0.022	8.55
	45°	0.034	14.8
	60°	0.033	14.25
	90°	0.019	10.24

Table 5.7: Weight loss and Erosion rate of hybrid epoxy composite GJJG(S4) with respect to impingement angle due to erosion for a period of 15min

Velocity(m/s)	Impact Angle(°)	Weight loss 'Δw'(g)	Erosion Rate × 10 ⁻⁴ (g/g)
48	30°	0.006	2.14
	45°	0.007	2.14
	60°	0.006	2.56
	90°	0.004	2.99
70	30°	0.009	1.11
	45°	0.015	4.66
	60°	0.023	3.4
	90°	0.018	1.05
82	30°	0.020	4.7
	45°	0.027	11.51
	60°	0.025	10.25
	90°	0.022	6.09

Table 5.8: Parameters characterizing the velocity dependence of erosion rate of hybrid jute-glass epoxy composites

Type of composite	Impact Angle(°)	k	n	R ²
JJJJ	30	2×10^{-10}	3.3869	1
	45	3×10^{-9}	2.8826	0.8735
	60	8×10^{-9}	2.6161	0.7999
	90	2×10^{-7}	1.7685	0.8367
JGGJ	30	1×10^{-8}	2.5724	0.994
	45	1×10^{-8}	2.6589	0.8705
	60	3×10^{-9}	2.9286	0.8616
	90	1×10^{-6}	1.5501	0.8708
GJGJ	30	3×10^{-9}	2.8792	0.9852
	45	3×10^{-8}	2.4478	0.8617
	60	5×10^{-9}	2.8775	0.9088
	90	2×10^{-6}	1.4122	0.7261
GJJG	30	5×10^{-8}	2.2658	0.9481
	45	4×10^{-8}	2.4417	0.8825
	60	3×10^{-9}	3.0675	0.8751
	90	2×10^{-6}	1.51	0.6593

Table 5.9: Erosion Efficiency of hybrid jute-glass epoxy composites

Impingement Angle	Velocity (m/s)	Erosion Efficiency(η)			
		S1(JJJJ) H=21(BHN)	S2(JGGJ) H=21.5(BHN)	S3(GJGJ) H=22(BHN)	S4(GJJG) H=24(BHN)
30°	48	3.2980	3.2400	3.3073	3.6855
	70	3.7095	2.8938	0.94115	0.94481
	82	5.2702	3.5993	4.5346	2.7778
45°	48	7.9030	4.7359	6.6146	3.6855
	70	7.9132	6.4217	5.2811	3.7778
	82	11.2111	9.3019	7.8494	6.8027
60°	48	6.1646	3.2400	5.2916	4.4227
	70	5.7972	5.0033	3.5145	2.7589
	82	12.6422	9.2967	7.5577	6.0580
90°	48	4.6102	3.2400	5.2916	4.4227
	70	3.6232	2.2884	2.0714	0.84846
	82	9.6902	7.3875	5.4309	3.5993

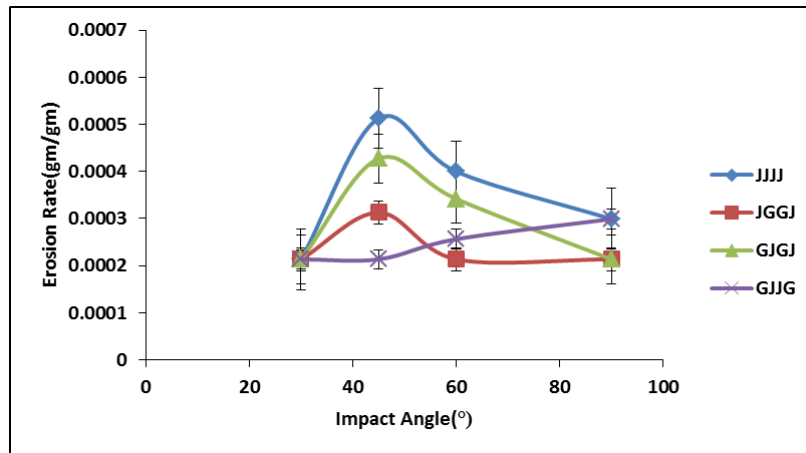


Figure 5.11: Variation of erosion rate of hybrid jute-glass composite with different impingement angles at velocity 48m/s

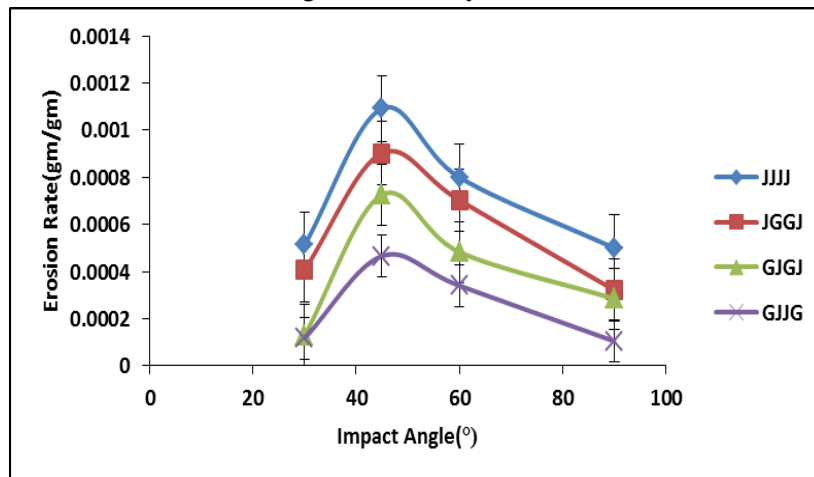


Figure 5.12: Variation of erosion rate of hybrid jute-glass composite with different impingement angles at velocity 70m/s

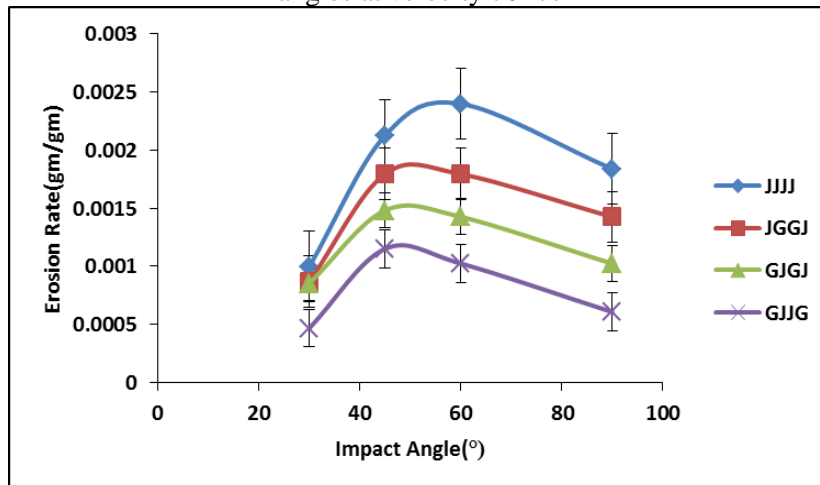


Figure 5.13: Variation of erosion rate of hybrid jute-glass composite with different impingement angles at velocity 82m/s

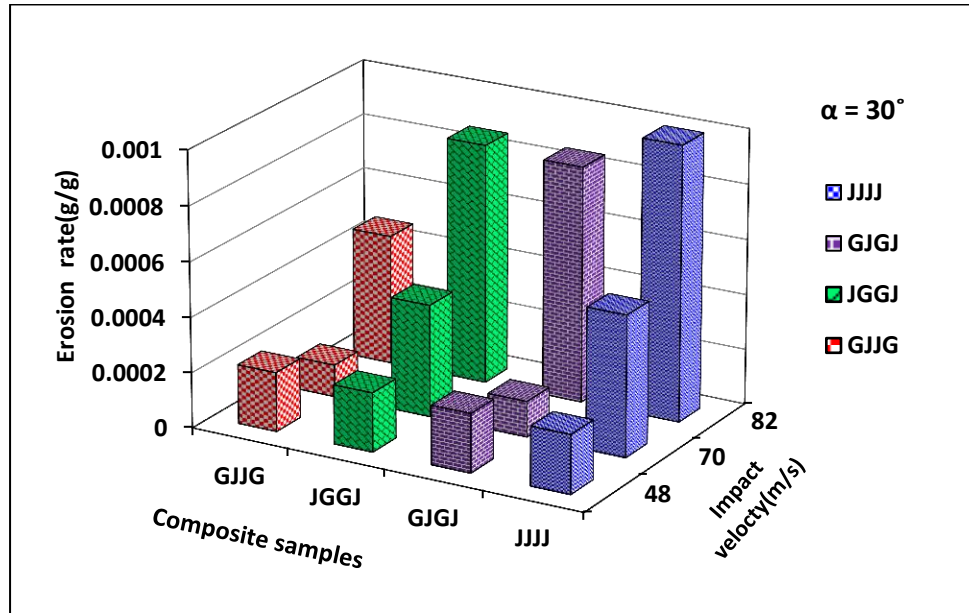


Figure 5.14: Histogram showing the steady state erosive wear rates of hybrid composites at different impact velocities (48, 70 and 82 m/s) for 30° impact angle

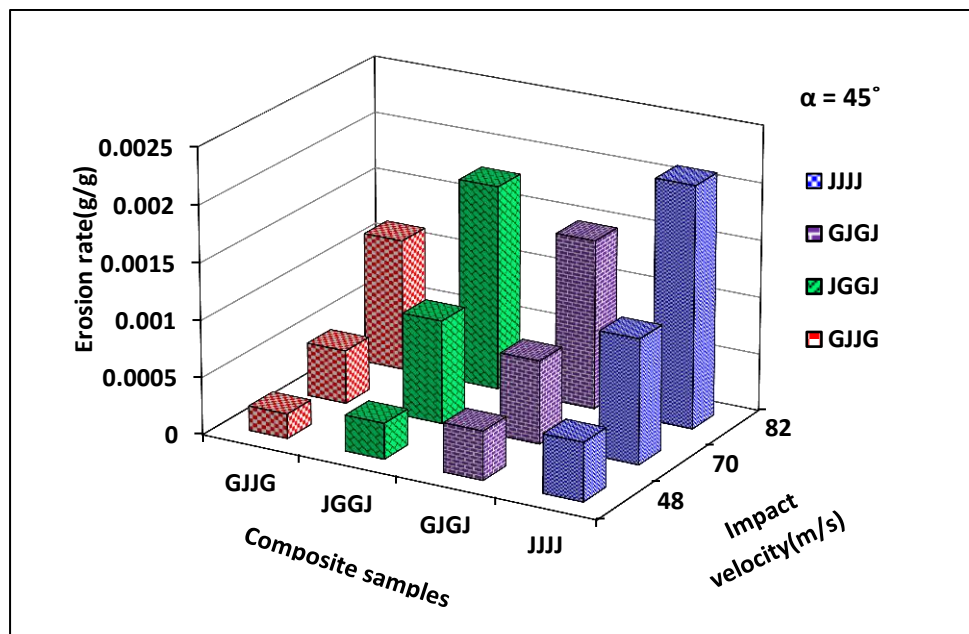


Figure 5.15: Histogram showing the steady state erosive wear rates of hybrid composites at different impact velocities (48, 70 and 82 m/s) for 45° impact angle

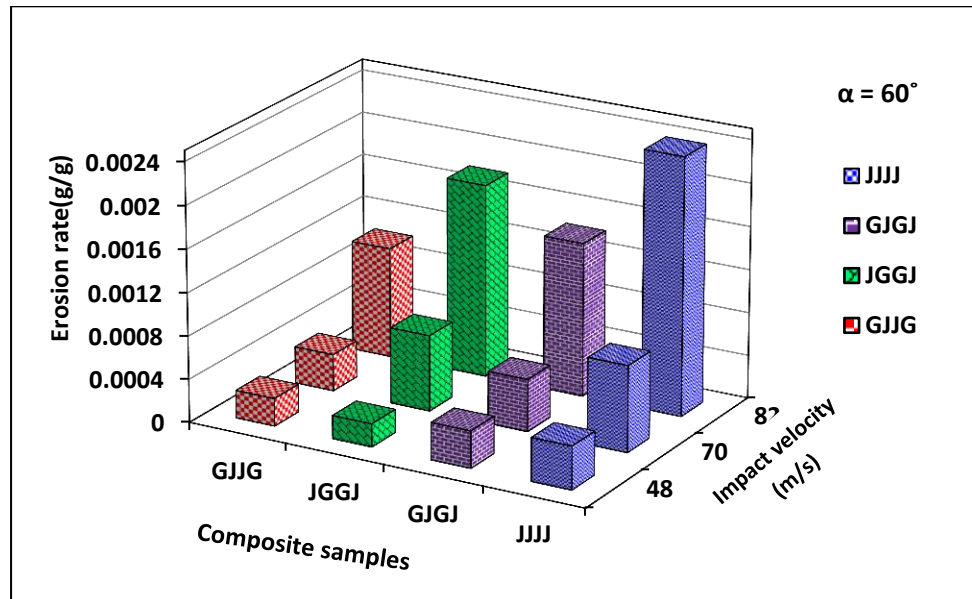


Figure 5.16: Histogram showing the steady state erosive wear rates of hybrid composites at different impact velocities (48,70 and 82 m/s) for 60° impact angle

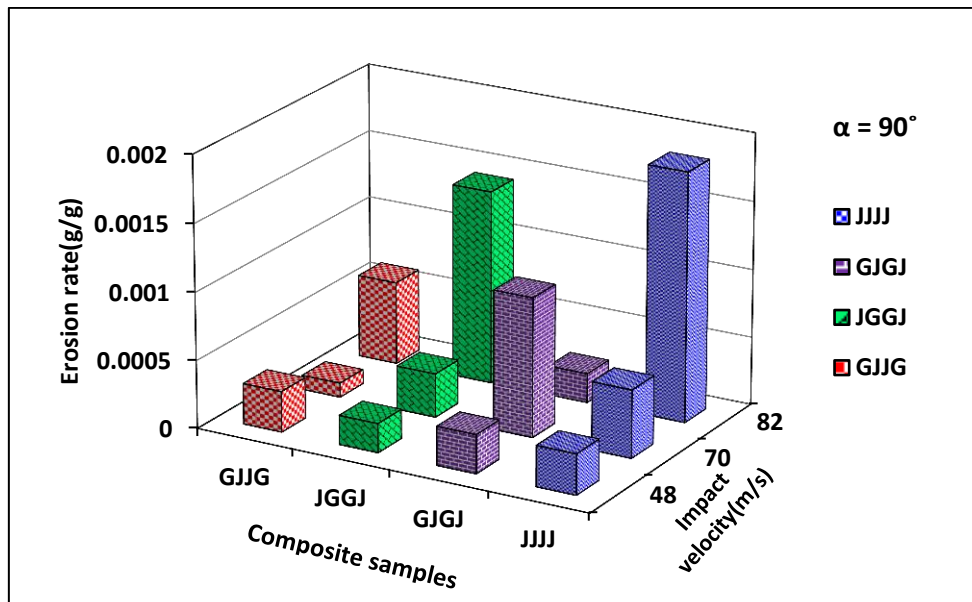


Figure 5.17: Histogram showing the steady state erosive wear rates of hybrid composites at different impact velocities (48,70 and 82 m/s) for 90° impact angle

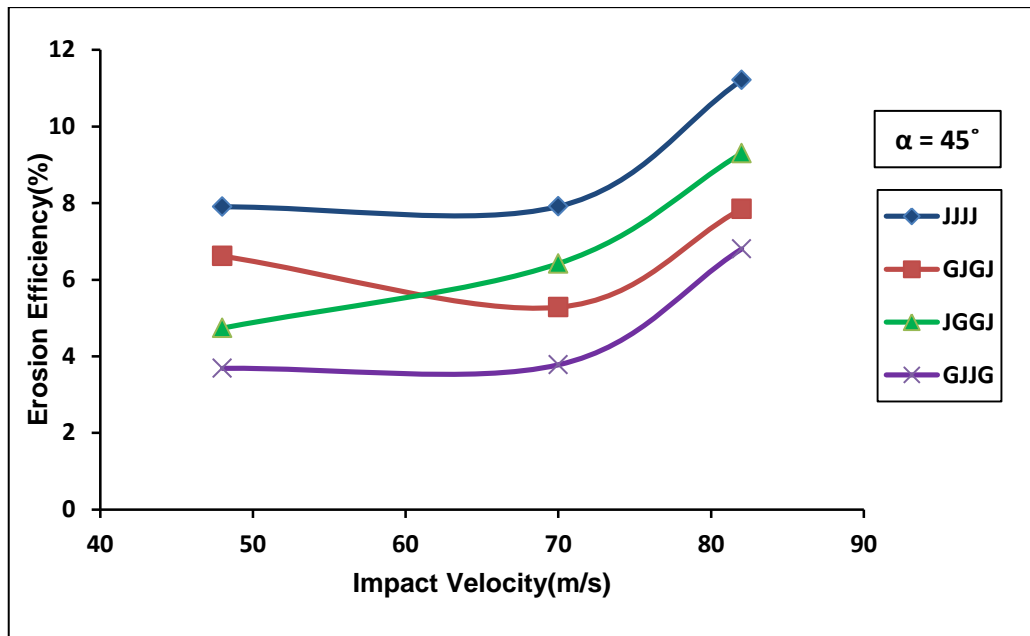


Figure 5.18: Variation of erosion efficiency of hybrid composites with particle velocity at impingement angle 45°

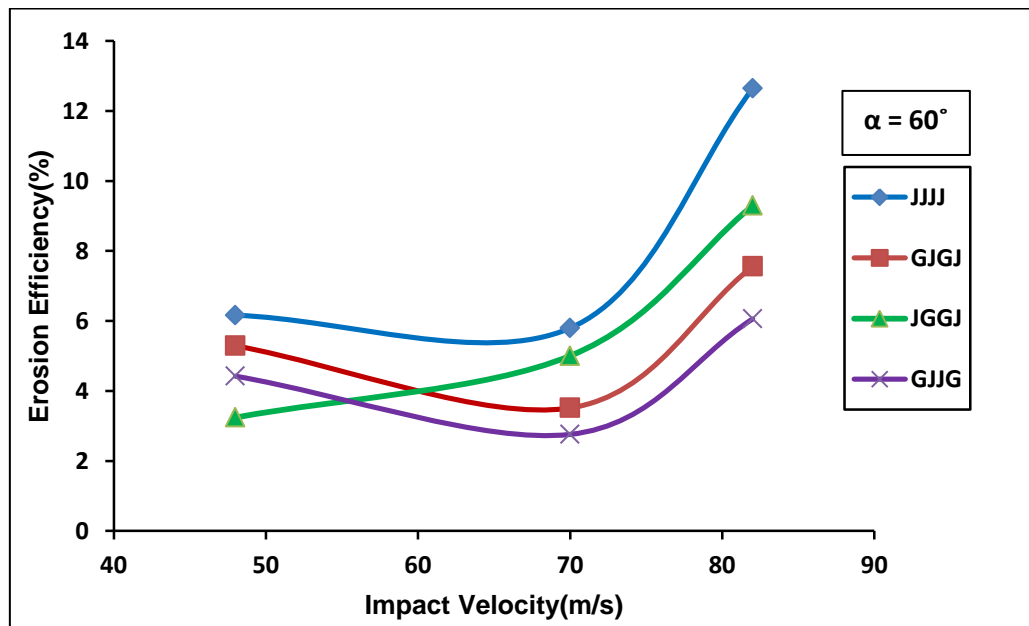


Figure 5.19: Variation of erosion efficiency of hybrid composites with particle velocity at impingement angle 60°

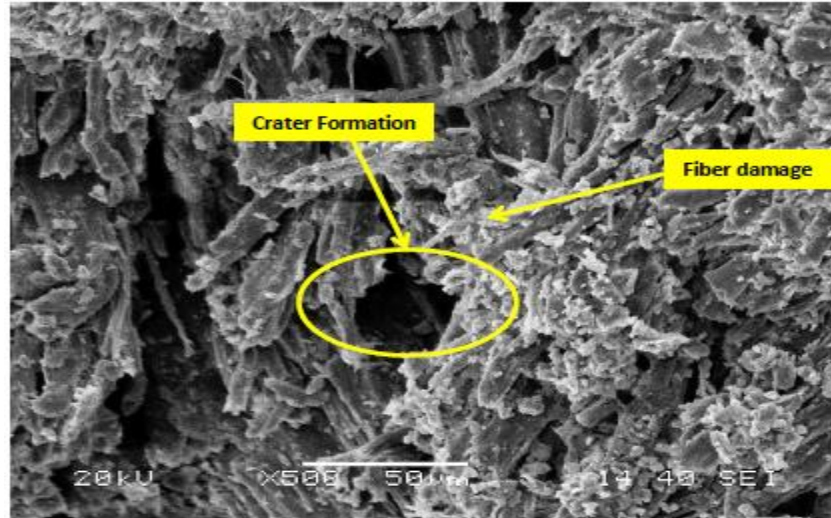


Figure 5.20 (a): GJJG composite at (45°)

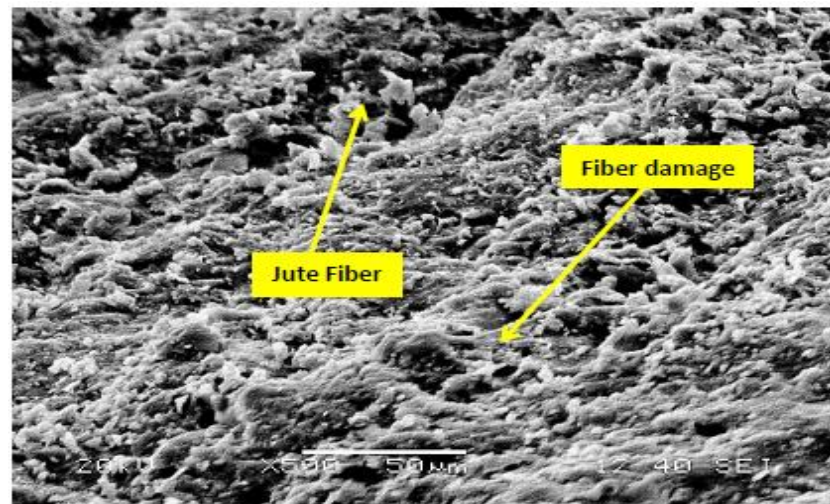


Figure 5.20 (b): GJJG composite at (45°)

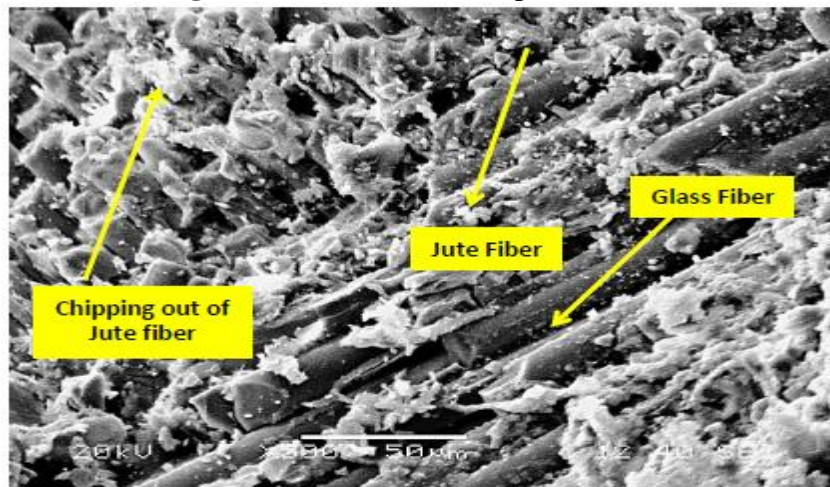


Figure 5.20 (c): JGGJ composite at (60°)

Chapter 6

Solid particle erosion studies of cenosphere filled hybrid jute-glass epoxy composites

6.1 Introduction

Now-a-days the environmental awareness attracted researchers to develop new hybrid composites with addition of more than one reinforcement from natural resources, such as natural fiber/natural fiber or natural fiber/nano/particulate filler from organic sources as an alternative to synthetic one. The term filler is very broad and encompasses a very wide range of materials that plays an important role for the improvement in performance of polymers and their composites. In the fiber reinforced plastics composites fillers may be added to the polymeric matrix for one or more of the following reasons (1) Reduction of material cost, (2) Increase of modulus, (3) Increases properties like abrasion resistance, hardness and reduces shrinkages (4) Fine dispersion, homogeneity, inertness and production of a smoother surface (5) Low water absorption and chemical stability and (6) Improve mechanical properties to some extent and in some cases to improve process ability.

Although in fiber reinforced plastic (FRP), a judicious selection of matrix and the reinforcing phase can lead to a composite with a combination of strength and modulus comparable to or even better than those of conventional metallic materials, their physical and mechanical properties can further be modified by addition of a solid filler phase to the matrix body during the composite preparation. In addition the fracture surface energies of epoxy and polyester resin and their resistance to crack propagation are relatively low. If particulate filler is added to these brittle resins, the particles inhibit crack growth. As the weight fraction of filler is varied, the fracture energy increases up to a critical weight fraction and then decreases again. Fillers affect the tensile properties according to their packing characteristics, size and interfacial bonding. The maximum volumetric packing fraction of filler reflects the

Chapter 6 Solid particle erosion studies of cenosphere filled jute-glass epoxy composites

size distribution and shapes of the particles. The particles like silica (SiO_2), titanium dioxide (TiO_2), calcium carbonate (CaCO_3), or polyhedral oligomeric silsesquioxane (POSS), *etc.*, are inorganic filler. However, the fillers, such as coir nanofiller, fly ash, red mud, cenosphere, carbon black, cellulosic nano filler were used judiciously as reinforcement to make hybrid composites combining both natural and synthetic fibers[239-243].

Solid particle erosion is a dynamic process that causes material removal from the target surface from the impact zone due to repeated impacts of fast moving solid particles by a micromechanical deformation/fracture process. This causes thinning of components, surface roughening, surface degradation, macroscopic scooping appearance, and consequently, reduces the functional life of the structure. Aktas Alaattin[244] reported that solid particle erosion of glass fiber-reinforced composite could be strengthened with metal powder at various parameter settings like impact velocity, impingement angle and different percentages of the metal powder embedded to the matrix. The results show that the erosion rate of the composites with and without powder is the highest when the particles impact angle is between 15° and 30° . Mohammed Ismail *et al.* [245] studied the solid particle erosion characteristics of the CSP (cenosphere) filled carbon-epoxy(C-E) composites and the experimental results were compared with those of unfilled C-E composites. The comparative study made by the authors indicated that the cenosphere filled C-E composites exhibit better erosive wear performance than that of the unfilled C-E composites. It is also reported that the cenosphere filled and unfilled C-E composites showed ductile erosion behaviour, with maximum erosion at 30° impingement angle.

Chand *et al.* [246] found the wear resistance of HDPE (High density polyethylene) cenosphere composite greatly increased with silane treatment of cenospheres. They have the opinion that wear rate of HDPE composite increases with increasing weight concentration of cenospheres probably due to increase in filler-filler interaction. As reported [247-249] mechanical and tribological performance of the date palm fiber/epoxy composites get enhanced by addition of graphite filler but high content of the graphite deteriorates the mechanical properties. Natural fiber/particulate filler based hybrid composites can be utilized in building and construction sector, transportation (automobiles, railway coaches, aerospace),

packaging, consumer products and also could be possible to produce acoustic insulator and extremely thermally stable materials.

In this work, experiments were carried out to study the effect of cenosphere filler, impingement angle and particle impact velocity on the solid particle erosion wear response of Jute-glass fiber reinforced hybrid epoxy composites.

6.2 Materials and method

6.2.1 Raw Materials Used

Raw materials used in this experimental work are listed below.

1. Jute fiber
2. E-glass fiber
3. Cenosphere filler
4. Epoxy resin and Hardener

6.2.2 Jute fiber

The details of the jute fiber, its chemical constituents used for the present investigation are explained in chapter 3 article 3.2.1.1.

6.2.3 E glass fiber

The details of the glass fiber used for the present investigation are explained in chapter 3 article 3.2.1.2.

6.2.4 Epoxy resin and Hardener

The details of the epoxy resin and hardener used in preparation of sample for the erosion test are same as explained in chapter 3 article 3.2.1.3.

6.2.5 Cenosphere filler

The details of the cenosphere filler, its chemical constituents used for the present investigation are explained in chapter 3 art. 3.5.1.4.

6.3 Methods

6.3.1 Preparation of Composites

It is clear from the earlier experiments of solid particle erosion test for different sequences of jute-glass fiber reinforced epoxy composites that the hybrid laminate, (GJJG) with two extreme glass piles on either side is the optimum combination with good balance

Chapter 6 Solid particle erosion studies of cenosphere filled jute-glass epoxy composites

between the properties, Hence for the present investigation, we have introduced particulate filler cenosphere into the optimum combination(i.e.)GJJG.Four groups of laminate composite samples were prepared with varying weight percentage of cenosphere (5%,10%,15% and 20%). The layout of glass fiber was kept at (0-90°) and for the jute it was changed to (45°-45°) orientation. The preparation of the test samples were carried out as per the procedure explained in chapter 3 article 3.2.2. From the composite slab specimens of dimension (25×25×3) mm were cut for the erosion test.

6.3.2 Test apparatus and Experiment

The erosion test apparatus for the present case is one which is used earlier. The details of the test apparatus, procedure and the conditions under which the test has been carried out is same for this investigation and has been explained in details in chapter 5 article 5.6.

6.4 Results and discussions

The experimental results of the erosion test of jute-glass (GJJG) hybrid epoxy composite for different doses of cenosphere particulate with different angle of impingement and with different impact velocities are tabulated and presented in tables 6.1 to 6.4.

Figures (6.1-6.3) show the erosion rate of hybrid composite (GJJG) with different impact velocities (48, 70 and 82 m/sec) of various weight percentage (5, 10, 15 and 20 wt. %) of cenosphere filler. It is clear from the plot that the erosion rate of hybrid composite increases with increase in impact velocities. It is observed from the plot that at higher velocity (82m/s) the filled composite shows peak erosion (E_{max}) at 60° impact angle. Whereas for lower velocities (48 and 70m/s) the peak erosion is at 45° impact angle. As explained earlier in chapter 5 the ductile and brittle behaviour of the material can be characterised by the maximum impact angle. For the hybrid composite of GJJG without cenosphere filler at different impact velocities, the peak erosion rate was found to be at 45° impact angle and the minimum erosion at 30° impact angle showing semi ductile in nature. However by the incorporation of cenosphere particulate the response was changed to purely

Chapter 6 Solid particle erosion studies of cenosphere filled jute-glass epoxy composites

semi-ductile. The reduction in material loss in these particulate filled composites can be attributed to two reasons. One is the improvement in the bulk hardness of the composite with addition of these ceramic rich particles. Secondly, during the erosion process, the filler particles absorb a good part of the kinetic energy results in less amount of energy being available to be absorbed by the matrix body and the reinforcing phases i.e. glass and jute fiber. These two factors together lead to enhancement of erosion wear resistance of the hybrid composites. Similar types of observation in their work are also reported by Biswas S. *et al.* [242], Srivastava V. K. *et al.* [250] and Rout A. K. *et al.* [251] with addition of red mud, fly ash and rice-husk filler to the hybrid composites respectively.

The variation of the steady state erosion rate of cenosphere filled glass-jute developed composites with different impact velocities at an impingement angle of (30°-90°) is shown in figures 6.4-6.7 in the form of histograms. It is clear from the plot that the erosion rate of all composite samples increases with increase in the impact velocities. It is also observed from the graphs that the composite with 20 wt. percentage of cenosphere filler shows lowest erosion rate as compared to other percentages of cenosphere filled GJJG composites with all impact velocities under consideration. For any material, once the steady state condition has been reached, the erosion rate ' E_r ' can be expressed as a simple power function of impact velocity as described in equation 5.6. For the present investigation the least-squares fits to the data points were obtained by using the power law and the values of ' n ' and ' k ', are summarized in table 6.5. The velocity exponents found for 30°, 45°, 60° and 90° impingement angles are in the range of (1.22-3.12), (2.4-3.5), (1.79-3.0) and (1.84-3.2) respectively.

The semi-ductile response of cenosphere filled GJJG composites is also confirmed from the values of ' n ' and ' k ' as explained in previous chapter 5. The loss of ductility may be due to the presence of particulate filler (cenosphere) and largely to the stacking sequences for the hybrid composites. This can further be explained as follows. The erosion of fibers is mainly caused by damage mechanisms as micro-cracking or plastic deformation due to the impact of silica sand. Such damage is supposed to increase with the increase of kinetic energy loss. According to Hutchings *et al.* [208], the kinetic energy loss is maximum at

Chapter 6 Solid particle erosion studies of cenosphere filled jute-glass epoxy composites

normal impact (90°), where erosion rates are maximum for semi-ductile materials. Hence, although the polymer matrix itself is brittle, the developed composites show semi-ductile response.

As discussed earlier the erosion efficiency (η) plays an important role to characterize the nature and mechanism of erosion. Here also for the cenosphere filled hybrid developed composites, the erosion efficiency has been calculated as per equation 5.5 and are listed in table 6.6 along with their hardness values and operating conditions. The erosion efficiency along with different impact velocities for various weight percent of cenosphere filled GJJG composites are shown in figures 6.8-6.9. The erosion efficiencies of cenosphere filled jute-glass hybrid composites of different weight percentages vary in range from 1.77 to 12.14% for different impact velocities studied at angle 60° and also vary from 1.53 to 10.77% for 45° impact angle and confirmed the semi-ductile nature of the material which in good agreement with the steady-state erosion rate. From literatures[235,238] it is found that the ductile material possesses very low erosion efficiency ($\eta \ll 100\%$), whereas the brittle material exhibits an erosion efficiency even greater than 100%. It is observed that high erosion efficiency indicates decrease in erosion resistance of the hybrid composites. In the present case with addition of low percentage (5wt.%) of particulate filler the efficiency values found to be 12.14%. As cenosphere amount increases to 20wt.%, the erosion efficiency decreases to 5.72% indicating better erosion resistance of developed composites for suitable industrial and tribological applications.

Similar observations are also reported by Srivastava *et al.*[250] while they worked with glass fiber reinforced fly-ash filled epoxy composite. Basing on their work, they have identified the brittle and ductile response of various materials considering the erosion mechanism as explained in chapter 5. Thus it can be concluded that erosion efficiency is not exclusively a material property, but also depends on other operational variables such as impact velocity and impingement angle. Thus lower erosion efficiency of cenosphere filled jute-glass epoxy composite indicates better erosion resistance of developed GJJG composites.

6.4.1 Surface morphology of eroded surfaces

Figures 6.10 and 6.11 show the SEM micrographs of cenosphere filled GJJG hybrid composite eroded at 45° and 60° impingement for a velocity of 82m/sec for lower and higher efficiency samples. Figure 6.10 (a) shows the micrographs of 5wt.% of cenosphere filled developed composites. It shows clearly the local removal of matrix material from the surface due to impact of erodent particle. Fiber breakages at the impacted surfaces are also visible. Small cavities are being formed on the surface of the composite. This might have happened due to compressive stresses developed on the surface of the composite due to indentation of sand particles. Breaking of fibers also took place due to this impact. The fibres after breaking are dislodged from the surface giving rise to formation of cavities. Figure 6.10 (b) shows the same micrograph with high magnification showing clearly the grooves formed and the broken fibres.

Figure 6.11 (a) shows the micrograph for 20 wt.% of cenosphere filled GJJG hybrid epoxy composite. Here also the local removal of matrix took place but the formations of cavities are less. Fiber breakage and removal from the matrix are also less. This might have happened due to higher weight percentage cenosphere particles which restricted the impact velocity to erode the surface. This in turn increases the resistance of the composite. Figure 6.11 (b) is the same micrograph with higher magnification which shows the formation of smaller and less number of grooves in comparison to figure 6.10 (b).

6.5 Conclusions

Experiments were carried out to study the effect of cenosphere as particulate filler with varying weight percentages on the solid particle erosion wear behaviour of glass-jute reinforced epoxy composite with silica sand as erodent. Based on the above studies the following conclusions are made.

1. Successful fabrication of new class of epoxy based hybrid composites with cenosphere filler has been achieved.

Chapter 6 Solid particle erosion studies of cenosphere filled jute-glass epoxy composites

2. Different weight percentage of cenosphere particles influenced the erosion wear behaviour of the hybrid GJJG epoxy composite significantly.
3. The erosion rate increases with the increase of impact velocities from 48m/s to 82m/s.
4. The results indicate that cenosphere filled glass-jute composites have more wear resistance than hybrid composite of specific fibre orientation and 20% by weight of cenosphere filled sample gives improved erosion properties compared to 10 and 15% by weight of cenosphere filled developed composites.
5. The influence of impingement angle on the erosive wear performance of cenosphere filled composite exhibited semi-ductile nature. The erosion efficiency for the composite also confirms the semi-ductile response of the hybrid composites.
6. From SEM analysis it is observed that overall erosion damage of composites consists of matrix removal, fiber breakage and formation of cavities due to impact velocity. However presence of cenosphere filler restricts not only the erosion wear also resists the breaking of fibers and formation of cavities, which in turns improves the resistance of the developed composite.
7. The potential use of these composites in components such as pipes carrying coal dust, helicopter fan blades, desert roof structures, industrial fans and low cost housing is recommended.

Table 6.1: Weight loss and Erosion rate of 5% Cenosphere filled hybrid GJJG epoxy composites with respect to impingement angle due to erosion for a period of 15min

Velocity (m/s)	Impact Angle(°)	Weight loss ' Δw '(g)	Erosion Rate $\times 10^{-4}$ (g/g)
48	30°	0.004	1.04
	45°	0.004	1.04
	60°	0.004	1.2
	90°	0.003	0.9
70	30°	0.007	1.823
	45°	0.011	2.864
	60°	0.013	3.385
	90°	0.025	6.51
82	30°	0.024	6.25
	45°	0.028	7.291
	60°	0.026	6.77
	90°	0.02	5.208

Table 6.2: Weight loss and Erosion rate of 10% Cenosphere filled hybrid GJJG epoxy composites with respect to impingement angle due to erosion for a period of 15min

Velocity (m/s)	Impact Angle(°)	Weight loss ' Δw '(g)	Erosion Rate $\times 10^{-4}$ (g/g)
48	30°	0.008	2.08
	45°	0.011	2.86
	60°	0.008	2.08
	90°	0.008	2.08
70	30°	0.016	4.166
	45°	0.025	6.510
	60°	0.028	7.291
	90°	0.02	5.208
82	30°	0.022	5.729
	45°	0.034	8.854
	60°	0.033	8.593
	90°	0.019	4.947

Table 6.3: Weight loss and Erosion rate of 15% Cenosphere filled hybrid GJJG epoxy composites with respect to impingement angle due to erosion for a period of 15min

Velocity (m/s)	Impact Angle(°)	Weight loss ' Δw '(g)	Erosion Rate $\times 10^{-4}$ (g/g)
48	30°	0.008	2.08
	45°	0.009	2.39
	60°	0.007	1.83
	90°	0.006	1.70
70	30°	0.02	5.208
	45°	0.035	9.114
	60°	0.021	5.468
	90°	0.02	5.208
82	30°	0.019	4.947
	45°	0.034	8.854
	60°	0.034	8.854
	90°	0.025	6.51

Table 6.4: Weight loss and Erosion rate of 20% Cenosphere filled hybrid GJJG epoxy composites with respect to impingement angle due to erosion for a period of 15min

Velocity (m/s)	Impact Angle(°)	Weight loss ' Δw '(g)	Erosion Rate $\times 10^{-4}$ (g/g)
48	30°	0.006	1.62
	45°	0.007	2.06
	60°	0.006	1.57
	90°	0.004	1.3
70	30°	0.009	2.343
	45°	0.015	3.906
	60°	0.023	5.989
	90°	0.018	4.687
82	30°	0.020	5.208
	45°	0.027	7.031
	60°	0.025	6.510
	90°	0.022	5.729

Table 6.5: Parameters characterizing the velocity dependence of erosion rate of cenosphere filled hybrid glass-jute (GJJG) epoxy composites

Cenosphere filler content (%)	Impact Angle(°)	k	n	R²
5	30	8×10^{-12}	4.2199	1
	45	2×10^{-14}	5.7384	0.9936
	60	7×10^{-14}	5.4873	0.9938
	90	6×10^{-14}	5.4326	0.9769
10	30	5×10^{-9}	2.7155	0.9032
	45	6×10^{-10}	3.3548	0.9923
	60	6×10^{-11}	3.8737	0.9756
	90	9×10^{-10}	3.1452	0.7368
15	30	9×10^{-8}	1.9268	0.2913
	45	6×10^{-10}	3.3168	0.9886
	60	1×10^{-10}	3.6032	0.9322
	90	1×10^{-9}	2.9915	0.7924
20	30	5×10^{-7}	1.4642	0.3056
	45	2×10^{-9}	3.0233	0.9332
	60	5×10^{-10}	3.2389	0.8931
	90	2×10^{-8}	2.2477	0.4152

Table 6.6: Erosion efficiency (η) of cenosphere filled hybrid glass-jute (GJJG) epoxy composites

Impact Angle(°)	Velocity (m/s)	Erosion Efficiency (η)			
		5%CSGJJG H=20.8(BHN)	10%CSGJJG H=22(BHN)	15%CSGJJG H=24(BHN)	20%CSGJJG H=23(BHN)
30°	48	1.5397	3.3584	3.7466	2.6400
	70	3.5503	3.1128	1.1010	0.9195
	82	5.0629	4.8079	5.2771	2.6245
45°	48	1.5397	4.6179	4.3050	3.3571
	70	7.5880	6.8329	6.1828	3.5708
	82	10.7701	9.9201	9.1347	6.4273
60°	48	1.7766	3.3584	3.2963	2.5585
	70	5.5692	5.3145	4.0654	2.6053
	82	12.1449	9.9145	8.7953	5.7237
90°	48	1.3324	3.3584	3.0621	2.1185
	70	3.4807	2.4295	2.3715	0.80459
	82	9.3090	7.8785	6.3202	3.4007

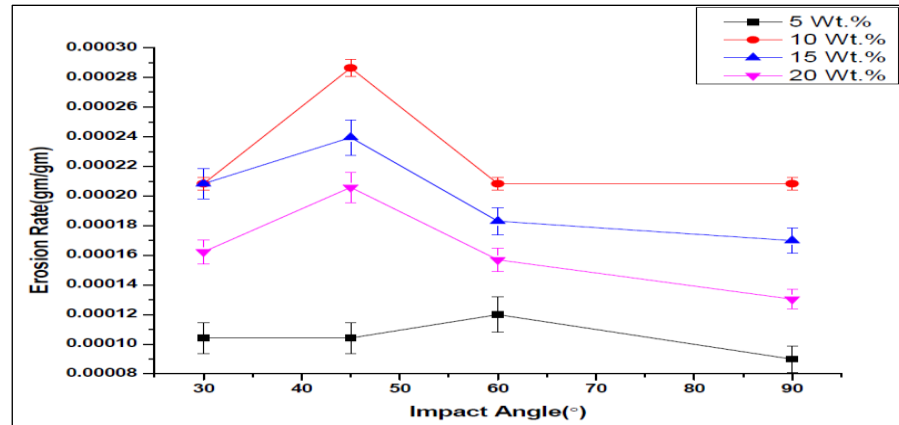


Figure 6.1: Variation of erosion rate of cenosphere filled jute-glass (GJJG) composites with different impingement angles at velocity 48m/s

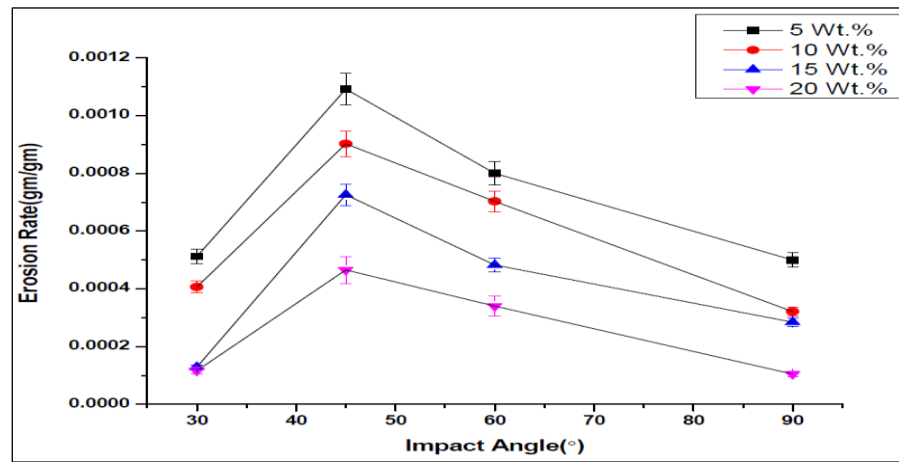


Figure 6.2: Variation of erosion rate of cenosphere filled jute-glass (GJJG) composites with different impingement angles at velocity 70 m/s

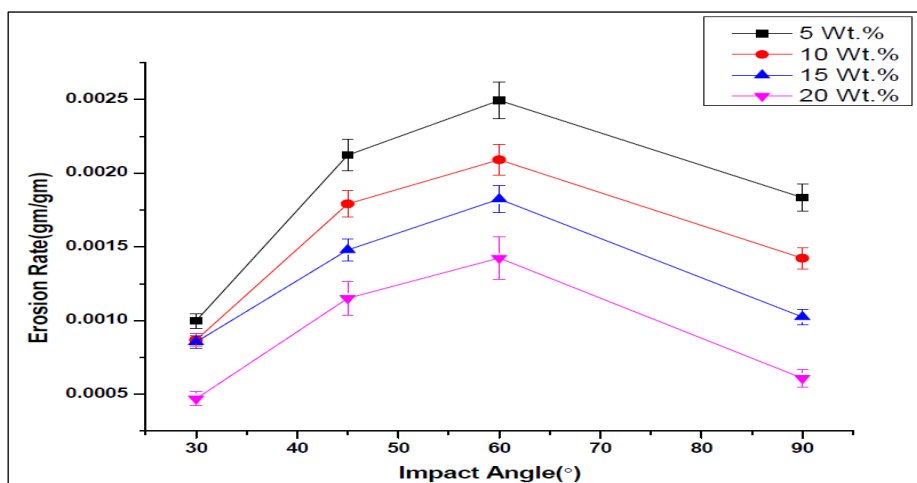


Figure 6.3: Variation of erosion rate of cenosphere filled jute-glass (GJJG) composites with different impingement angles at velocity 82 m/s

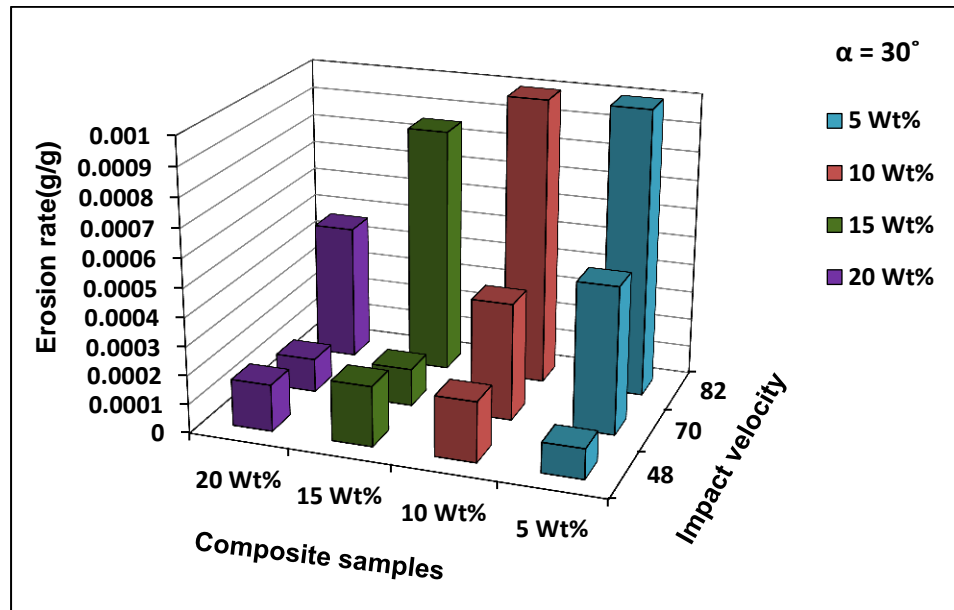


Figure 6.4: Histogram showing the steady state erosion wear rates of cenosphere filled hybrid GJJG composites at three impact velocities (48,70,82m/s) for 30° impact angle

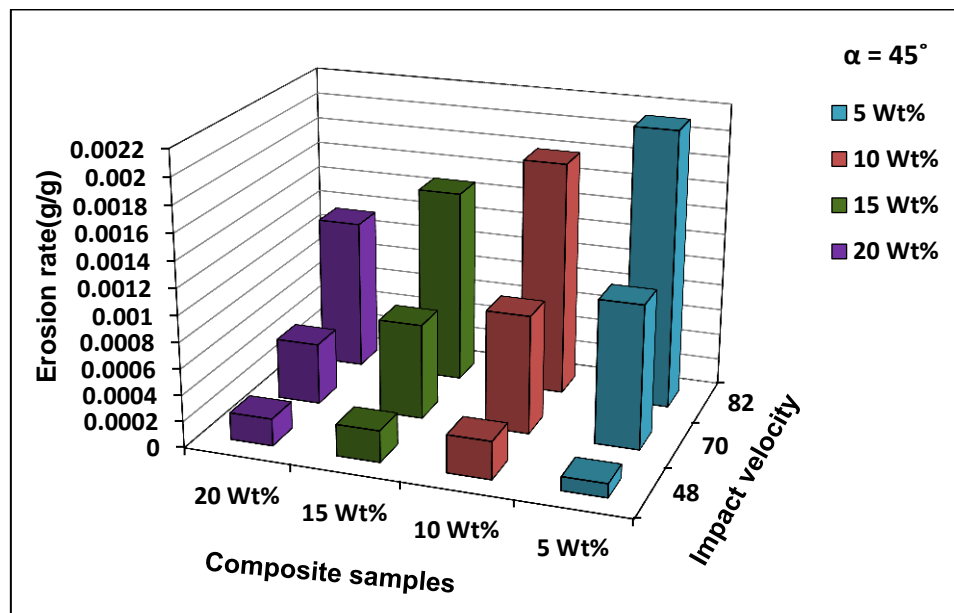


Figure 6.5: Histogram showing the steady state erosion wear rates of cenosphere filled hybrid GJJG composites at three impact velocities (48,70,82m/s) for 45° impact angle

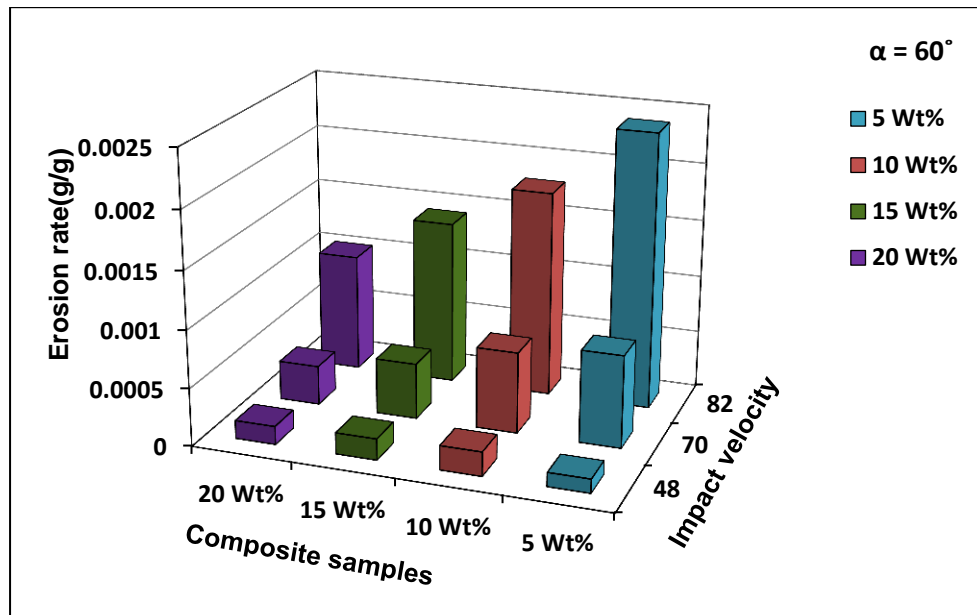


Figure 6.6: Histogram showing the steady state erosion wear rates of cenosphere filled hybrid GJJG composites at three impact velocities (48,70,82m/s) for 60° impact angle

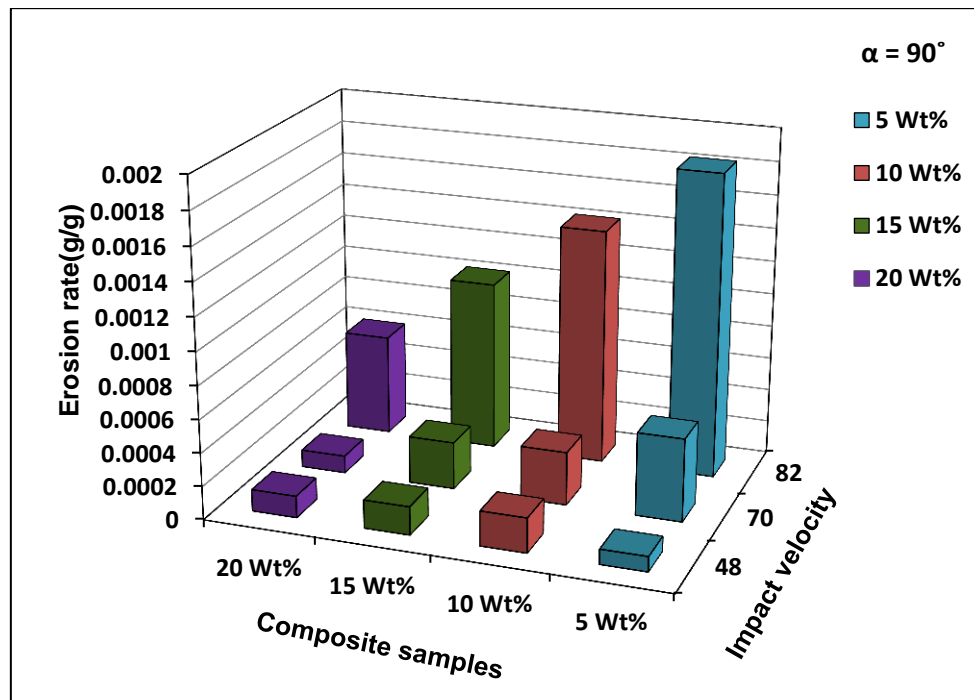


Figure 6.7: Histogram showing the steady state erosion wear rates of cenosphere filled hybrid GJJG composites at three impact velocities (48,70,82m/s) for 90° impact angle

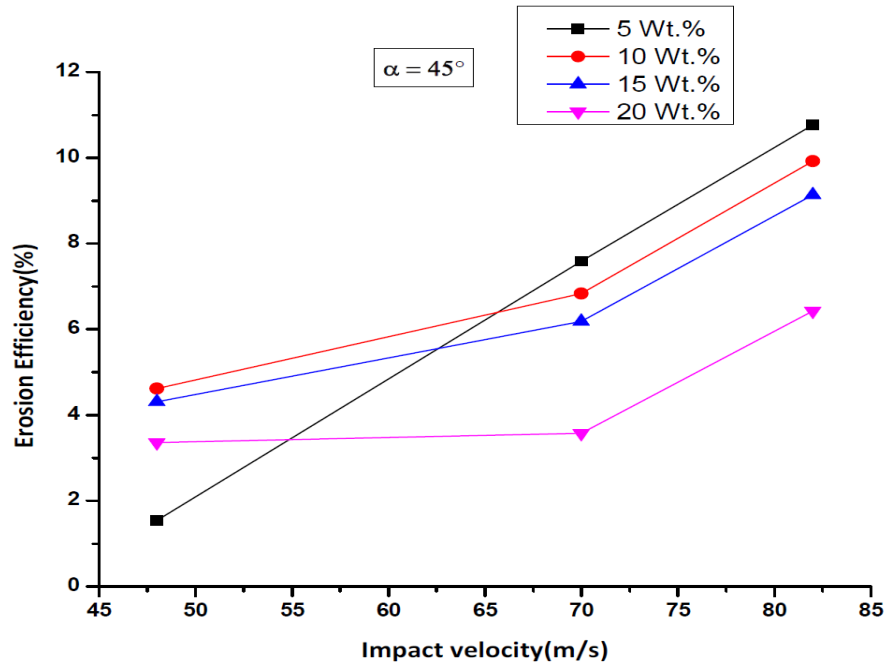


Figure 6.8: Erosion efficiency as a function of impact velocity for cenosphere filled hybrid glass-jute (GJJG) epoxy composites at angle 45°

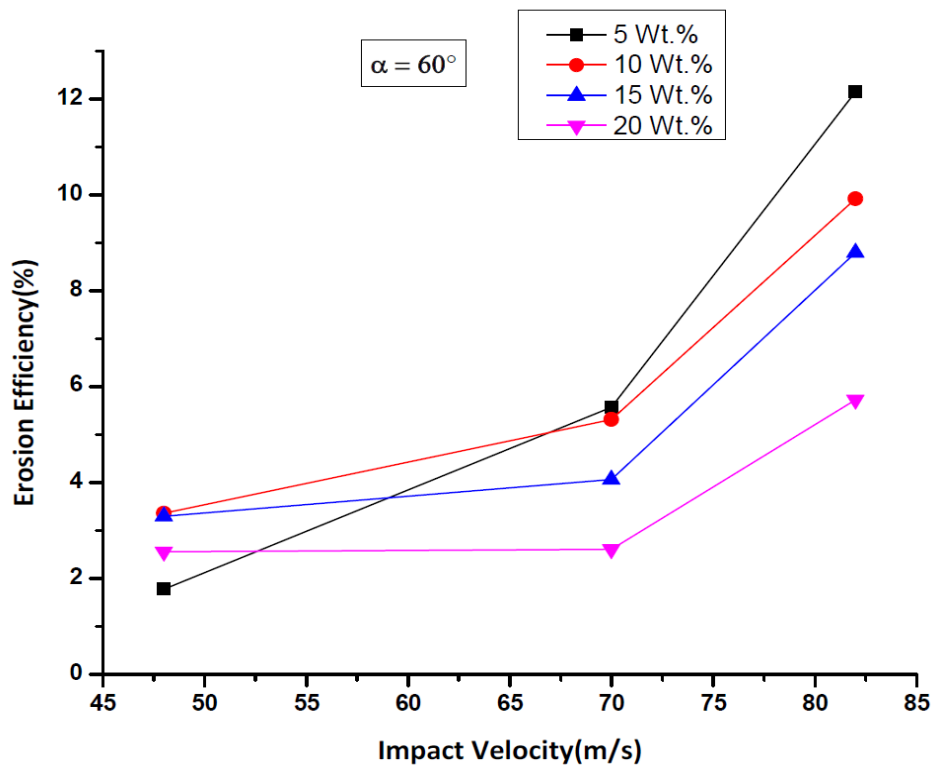


Figure 6.9: Erosion efficiency as a function of impact velocity for cenosphere filled hybrid glass-jute (GJJG) epoxy composites at angle 60°

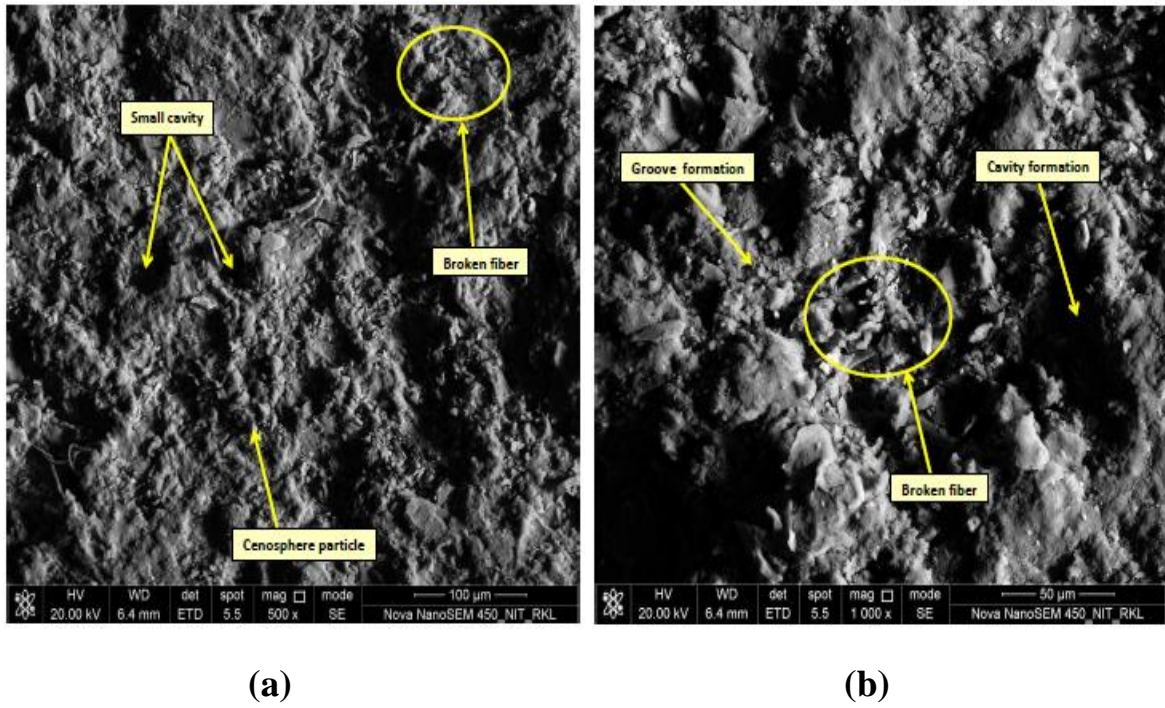


Figure 6.10 (a) and (b): Micrographs of eroded surface of 5 wt. % of cenosphere filled glass-jute (GJJG) composite at lower (500x) and higher (1000x) magnification at angle 45°

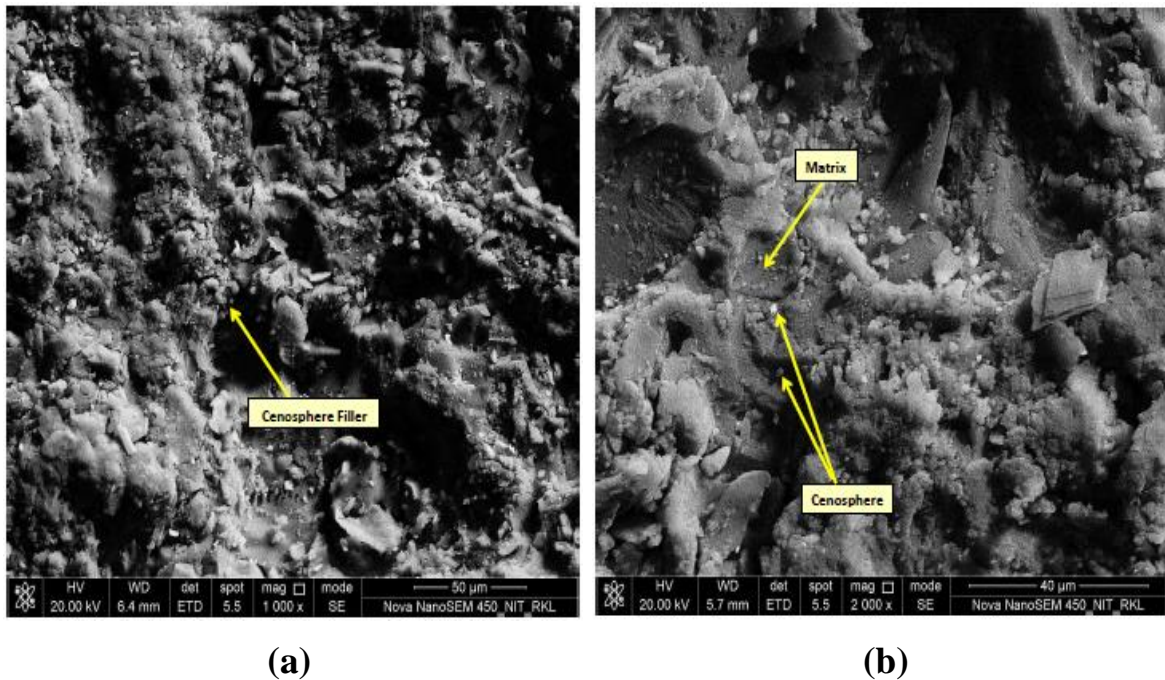


Figure 6.11 (a) and (b): Micrographs of eroded surface of 20 wt. % of cenosphere filled glass-jute (GJJG) composite at lower (1000x) and higher (2000x) magnification at angle 60°

Chapter 7

Three-body abrasive wear studies of cenosphere filled hybrid glass-jute epoxy composites

7.1 Introduction

Wear is a progressive loss of material from the solid surface due to the relative motion between the contacting surface and substance. There are a wide range of applications for fiber reinforced polymer composites in wear related situations such as bearings, gears, sprockets, sleeves, valve guides, seals, brakes etc. [252-253]. The attraction of these applications lies in their excellent strength to weight ratio, light weight, resistance to corrosion, self-lubricating properties, low coefficient of friction, favorable wear characteristics, ease of processing and economic feasibility. A number of material processing strategies have been used to improve the wear performance of polymers. These include the incorporation of organic and inorganic fillers as well as glass, carbon, and aramid fibers. Abrasive wear can be defined as the wear that occurs when a hard surface slides against and cuts groove from a softer surface. It is one of the major types of wear which contributes almost 63% of the combined cost for wear in the industry. Abrasive wear can occur in two ways, i.e. two-body abrasion and three-body abrasion. In two-body abrasion, a rough surface or abrasive particle slides over the surface and removes material, whereas in three-body abrasion, the material of the surface is removed by the sliding and rolling action of the particles. Three-body abrasive wear problem occurs in most of the engineering and agriculture mechanical components, whereas two-body abrasion arises largely in material removal operations. In the past few years, several studies on polymer composites subjected to abrasive wear are available [254-259]. The wear process of these composites is fairly complex. The interaction of the matrix and fiber/filler materials and in some cases the coupling agents as well complicates the fracture process which results in the formation of wear debris. The incorporation of fiber has showed both positive and negative results on the abrasive wear behavior of a polymer. The reason to incorporate fillers into a polymer is to

improve the tribological, mechanical, and thermal properties and to reduce the cost of the final product. In the past two decades, due to technological importance of composite materials, various filler and fiber-reinforced polymer composites have emerged as a subject of extensive research on three body abrasive wear behaviour[260-262].

In general, the mechanical and tribological properties of particulate-filled polymer composites depend strongly on size, shape, and distribution of filler particles in the polymer matrix as well as good adhesion at the interface surface. Suresha and Chandramohan[263] showed that silicon carbide filled glass fabric vinyl ester composite gives better abrasive wear performance compared to graphite filled ones. Biswas and Satpathy [264] evaluated the tribological response of red mud filled glass-epoxy (G-E) composites using Taguchi design of experiments. They concluded that the utilization of red mud filled composites gives better wear performance compared to unfilled ones.

Satapathy *et al.*[265] studied the particulate filled polymer composites and reported that these composites are considerable interest not only from an economic view point, but also as modifiers especially the physical properties of the polymers. Their work showed the successful fabrication of a multi component hybrid composite (using epoxy as matrix, random glass fiber as reinforcement and alumina, SiC and pine bark dust as filler) by simple hand lay-up technique. An environmental waste like pine bark can also be beneficial for composite making purposes. Incorporation of these fillers modify the tensile, flexural, and impact strengths of the composites. A steady decline in the tensile strength was noticed in the filled composites whereas the presence of these particulate matters has caused improvement in impact and flexural strengths of the composites. Abrasive wear rate decreased with increase in abrading distance for all the samples. However, the pine bark-filled composite showed better abrasive wear resistance. It was also found that the abrasive wear rate was higher in SiC filled glass fiber reinforced epoxy composites.

During the past decade fly ash cenospheres have been dispersed in different matrices, such as cement, polyester and epoxy for producing composites in the bulk for variety of industrial applications[266-268]. Chand *et al.*[269] investigated on the correlation of mechanical and tribological properties of organosilane modified cenosphere filled high density polyethylene (HDPE) composites. The silane treatment cenosphere resulted in considerable improvement in the impact strength and density of the composites which

ultimately translated into better wear performance of composites even in severe abrasive conditions. Wear rate of high density polyethylene composite increases with increasing the weight concentration of cenosphere probably due to increased filler-filler interaction. It was also observed that less than or equal to 10 wt. percentage of cenosphere appears to be an optimum concentration for achieving better mechanical and tribological performance in the composites. No work is till done on three body abrasive wear performance of cenosphere filled hybrid glass-jute(GJJG) epoxy composites for specific fiber orientation.

In the present work, experiments were carried out to study the effect of cenosphere filler on the three-body abrasive wear response of hybrid glass-jute(GJJG) epoxy composites. Wear mechanisms involved in the material removal process were studied with the aid of advanced optical microscopy.

7.2 Materials and Method

7.2.1 Raw Materials Used

Raw materials used in this experimental work are listed below.

1. Jute fiber
2. E-glass fiber
3. Epoxy resin and Hardener
4. Cenosphere filler

7.2.1.1 Jute fiber

The details of the jute fiber, its chemical constituents used for the present investigation are explained in chapter 3 art. 3.2.1.1.

7.2.1.2 E glass fiber

The details of the glass fiber used for the present investigation are explained in chapter 3 art. 3.2.1.2.

7.2.1.3 Epoxy resin and Hardener

The details of the epoxy resin and hardener used for the preparation of abrasion test specimens are same as explained in chapter 3 art. 3.2.1.3.

7.2.1.4 Cenosphere filler

The details of the cenosphere filler, its chemical constituents used for the present investigation are explained in chapter 3 art. 3.5.1.4.

7.3 Methods

7.3.1 Fabrication of the test specimens

Hybrid laminates of woven jute and glass mat for composite GJJG were prepared by hand lay-up technique. Four groups of laminate composite samples were made with varying weight percentage of cenosphere (5%,10%,15% and 20%). The layout of fiber for glass was kept at (0-90°) and for jute it was changed to (45°-45°) orientation. A wooden mold of dimension (150×60×5) mm was used for manufacturing the composite slab. For easy removal of the composite teflon sheet and silicon spray are used which prevents adhesion between mold wall and composite sample. The epoxy (LY 556) and hardener (HY 951) were mixed in a ratio of 10:1 to which cenosphere were added and mixed properly by gentle stirring. Pre-impregnated jute and glass fiber were kept in the mold with the proper sequence. The load was applied from the top surface of composites and the molds were allowed to cure for 72h at room temperature. After 72h the samples were taken out of the mold and cut to required shape and size. The abrasion test samples of size (75mm×25mm×5mm) were prepared from the laminates using a diamond cutter.

7.3.2 Three-Body Abrasion Test and Experimental Set up

The three-body abrasion wear test was performed on dry sand rubber/wheel abrasion tester as per ASTM G 65 test standards. The schematic diagram of the abrasive wear test rig and its setup is shown in figures 7.1 (a) and (b), respectively. The setup for the test is capable of creating a three-body abrasive wear environment for analyzing the wear properties of the prepared composites. The apparatus consists of sample holder, nozzle, abrasive hopper, rubber wheel, particle collecting bag, steel disk, and an arrangement for the application of load. Dry angular silica sand of size (150-250) μm with sharp edges was used as abrasive for the present study. The abrasive particles of particular size were stored in abrasive hopper. The samples were cleaned with acetone in ultrasonic cleaner and then dried. The initial weight was measured using an electronic balance having a least count of (1×10^{-3}) g. The samples were then mounted on the specimen holder and pressed against the chlorobutyl

rubber wheel using a lever arm with a specified force while controlled flow of abrasive particles abraded the surface. The chlorobutyl rubber wheel used is of thickness 12.7 mm rimmed on a 228 mm diameter wheel. The wheel was rotated at a speed ranging from 200 to 1000 rpm at an approximate sliding velocity of 0.83 to 4.16 m/s. Static force of 5, 10, 15 and 20 N were applied on the specimen using dead load on the load arm. The pivot axis of the lever arm lies in plane, tangential to the rubber wheel surface and normal to the horizontal diameter along which the load was applied and moisture free silica abrasive particles were passed between the specimen and the rubber wheel. The specimen holder was designed to ensure that wear scar location remains the same, even after removal and replacement of samples. The abrasive feeding system consists of a hopper that allows silica sand to fall under gravity through the nozzle onto a rubber wheel. The rubber wheel was rotated by a motor through timer belt and the speed of the motor determined the discharge rate of silica sand. The contacting surface of the rubber wheel was in the direction of the flow of sand. The experimental conditions are presented in table 7.1. All tests were performed in a dry environment at laboratory room temperature. Each abrasion test lasted for 5 minutes. After completion of each test the specimen was removed from the holder, cleaned with acetone and weight loss measurements were recorded. This procedure was repeated until the abrasive wear rate attains a steady-state value. Wear volume were computed from the weight loss measurements. The same test procedure and conditions were maintained and new samples were taken for every set of applied load, sliding speeds and abrasive particle sizes.

Figure 7.2 shows the schematic representation of different zones on the wear scar under three-body abrasive wear test condition[270]. The wear scar has three different zones: an entrance zone where abrasive first comes into contact with specimen, central zone in which particle may roll as well as slide and an exit area where abrasive particles leave the specimen. The entrance and exit areas subjected to multiple indentations by angular abrasive particles, whereas in central zone the angular particles have a rolling component to their motion across the specimen surface and it creates repeated contact on the loading surface. These may lead to localized fatigue damage and removal of the material surface. Figures 7.3 (a) and (b) show the abraded samples of hybrid woven jute-glass epoxy composites and the cenosphere filled developed composites respectively.

7.3.3 Calculation for Abrasive Wear

The volumetric and specific wear rate values were determined by considering factors like abrasive particle size, sliding velocity, sliding distance, normal load and fiber loading as per the following equations.

$$\Delta V = \frac{\Delta m}{\rho} (mm^3) \quad (7.1)$$

$$w_r = \frac{\Delta V}{M_a} \left(\frac{m^3}{g} \right) \quad (7.2)$$

$$K_0 = \frac{\Delta V}{Ld} \left(\frac{m^3}{Nm} \right) \quad (7.3)$$

Where Δm is the mass loss (g), ρ the density of the test material (g/cc), M_a the mass of the abrasive (g), ΔV the volume loss (mm^3), L is the load applied on the sample (N), d the sliding distance (m), W_r is the wear rate and K_0 is the specific wear rate.

7.4 Results and discussions

7.4.1 Effect of cenosphere on abrasive wear behaviour of glass-jute epoxy composites

The experimental results of the three-body abrasion wear test for different weight percentage of cenosphere filled hybrid glass-jute(GJJG) epoxy composite at various loads and sliding distances are tabulated and presented in tables 7.2 to 7.3.

The variation of abrasive wear volume, wear rate and specific wear rate of cenosphere filled hybrid glass-jute (GJJG) epoxy composites at different applied loads (5-20N varied in steps of 5 N at contact pressures of 1.89,3.78,5.68 and 7.6 N/cm² respectively) for various developed abrasive specimens are shown in figures 7.4-7.6. It is observed from the graphs that for all the hybrid composites used in this study there is a near linear wear volume loss with respect to applied load. The highest wear rate is found to be for hybrid glass-jute(GJJG) composite without cenosphere particle with a value of 0.77mm³/g at 20N and the lowest for

20wt.% of cenosphere filled GJJG composite of value $0.21\text{mm}^3/\text{g}$ at the same load. It is also observed that the wear rate of 5wt.% cenosphere filled hybrid composite is more than that of 20wt. percentage filled hybrid composites. This is due to the higher matrix-filler interaction and better adhesion between the fiber, matrix and filler in the developed composites [271].

Figures 7.7-7.9 show the variation of abrasive wear volume, wear rate and specific wear rate of cenosphere filled hybrid glass-jute (GJJG) epoxy composites as a function of sliding distances for different composites. For all the composites tested, it is observed that the specific wear rate decreases with increase in filler content. At all loading conditions, the highest specific wear rate is for 5wt.% of cenosphere filled glass-jute(GJJG) composite with a value of $3.853 \times 10^{-11} \text{m}^3/(\text{N m})$ and the lowest value of $2.22 \times 10^{-11} \text{m}^3/(\text{N m})$ for 20wt.% of cenosphere filled composites for abrading distance of 2292m. The specific wear rate strongly depends on the applied load and abrading distance for all the developed composites. The phenomenon of decrease in specific wear rate is due to the fabric nature and the presence of glass fiber at outer surface of composites. This is also attributed to the fact that at lower abrading distance low modulus matrix was exposed and at higher abrading distance high modulus fiber was exposed to abrasion [272].

This can further be explained by the fact that when the abrasive particles get entrapped between the rubber wheel and the composite samples, due to high stress of the hard abrasive particles, ploughing action takes place on the sample surface leading to removal of more matrix material. The lowest wear rate is due to the presence of higher cenosphere wt. percentage on the surface of the developed composite that act as an effective barrier to prevent the large-scale deformation of the epoxy matrix. The higher filler loading into hybrid glass-jute composites is thought to create a hard surface and this results in reduced wear loss in developed composites. Severe damage to the fiber and epoxy matrix is the primary reason for the higher wear rate using silica as abrasive in most of abrasion wear. This is because abrasive particles can be embedded on the softer surface and groove the harder one. More debris and micro cracks in the matrix were obvious due to deformation of the softened matrix under high contact pressure.

Chand N. and Naik A.M. *et al.* [273] observed that glass fibres provide better resistance against abrasive wear, which is reflected from the present study and high weight fraction of glass fibres in the composites show less wear loss as compared to composites containing less glass fibres. In the present work also, similar observations were found which are in agreement with the findings reported in the literatures [262,273].

7.4.2 Worn surface morphology of abraded surfaces

In order to understand the details of abrasion wear mechanisms of cenosphere filled hybrid glass-jute(GJJG) epoxy composites of specific fibre orientations, advanced optical micrographs of worn surfaces at various loads are shown in figures 7.10-7.11.

Figures 7.10(a) and (b) shows the micrographic study of abraded hybrid glass-jute (GJJG) epoxy composite. Damage is caused to the specimen surface by sliding the abrasive particles. It is also observed that cracks are developed along the matrix surface due to application of loads. Small grooves are also found on surface.

From figure 7.11(a) it is observed that at higher load (20N) and low cenosphere content (5wt.%) the fibres are exposed from glass-jute composites while abraded along the surface. From figure 7.11(b) it is found that when cenosphere amount increases to 20wt.% at the same load, there is less damage to the composite and matrix surface indicating improved resistance against abrasion. Matrix debonding and expose of fiber at the interface is not visible. This might have happened due to higher weight percent (20 wt.%) cenosphere particles which are distributed evenly on the specimen surface. Hard cenosphere particles abrading time is more than the glass fiber, hence are not exposed so easily.

7.5 Conclusions

From abrasive wear studies of cenosphere filled woven hybrid glass-jute (GJJG) epoxy composites, the following conclusions are drawn.

1. Abrasion resistance of unfilled and filled glass-jute epoxy composites strongly depends on the experimental test parameters such as applied load, sliding speed and abrasive particle size.

Chapter 7 Three body abrasive wear of cenosphere filled glass-jute epoxy composites

2. Cenosphere filled hybrid glass-jute (GJJG) epoxy composites showed high abrasion resistance than unfilled composites.
3. The abrasive wear volume increases with increase in filler content. Inclusion of cenosphere in developed composites is found to be beneficial for resisting abrasion wear of glass fiber.
4. Microscopic studies of worn surfaces support the involved mechanisms and indicate that distribution of cenosphere particles on the composite surface increases the abrading resistance of the developed composites.

Table 7.1: Test conditions of three-body abrasive wear test

Test variables	Test parameters
Load	5 N, 10 N, 15 N, 20N
Rotational speed of rubber wheel	(200±5) rev/min (V = 2.4 m/s)
Diameter of rubber wheel	228.6mm
Abrasive particles	Silica sand, Angular
Abrasive size	(150-250) µm
Sand Flow rate	(250±50) g/min
Size of the specimen	(75×25×5)mm ³

Table 7.2: Abrasive Wear rate, wear volume and specific wear rate of cenosphere filled hybrid glass-jute (GJJG) epoxy composites at different Loads

Load(N)	Composite Types	Wear Volume (mm ³)	Wear Rate (mm ³ /g)	Specific wear rate (×10 ⁻¹¹) (m ³ /Nm)
5	GJJG	101.922	0.10	4.019
	5%CSGJJG	149.038	0.14	2.411
	10%CSGJJG	139.038	0.13	2.158
	15%CSGJJG	119.038	0.11	1.561
	20%CSGJJG	109.038	0.10	1.377
10	GJJG	288.713	0.28	4.029
	5%CSGJJG	229.785	0.22	2.811
	10%CSGJJG	202.873	0.20	2.501
	15%CSGJJG	179.8109	0.17	1.806
	20%CSGJJG	159.038	0.15	1.562
15	GJJG	442.633	0.44	4.40
	5%CSGJJG	299.567	0.29	3.070
	10%CSGJJG	266.984	0.26	2.888
	15%CSGJJG	215.821	0.21	2.307
	20%CSGJJG	172.197	0.17	2.105
20	GJJG	770.258	0.77	4.705
	5%CSGJJG	338.911	0.33	3.853
	10%CSGJJG	309.315	0.30	3.528
	15%CSGJJG	252.958	0.25	2.509
	20%CSGJJG	211.676	0.21	2.219
CSGJJG: Cenosphere filled hybrid glass-jute(GJJG) epoxy composite				

Table 7.3: Abrasive Wear rate, wear volume and specific wear rate of cenosphere filled hybrid glass-jute (GJJG) epoxy composites at different sliding distances

Sliding distance (m)	Composite Types	Wear Volume (mm ³)	Wear Rate (mm ³ /g)	Specific wear rate (×10 ⁻¹¹) (m ³ /Nm)
143	GJJG	102	0.10	4.020
	5%CSGJJG	149	0.14	2.411
	10%CSGJJG	139	0.13	2.158
	15%CSGJJG	119	0.11	1.561
	20%CSGJJG	109	0.10	1.377
573	GJJG	289	0.28	4.030
	5%CSGJJG	230	0.22	2.811
	10%CSGJJG	203	0.20	2.501
	15%CSGJJG	180	0.17	1.806
	20%CSGJJG	159	0.15	1.562
1289	GJJG	443	0.44	4.400
	5%CSGJJG	300	0.29	3.070
	10%CSGJJG	268	0.26	2.888
	15%CSGJJG	216	0.21	2.307
	20%CSGJJG	172.2	0.17	2.105
2292	GJJG	770	0.77	4.710
	5%CSGJJG	339	0.33	3.853
	10%CSGJJG	309	0.30	3.528
	15%CSGJJG	253	0.25	2.509
	20%CSGJJG	212	0.21	2.220
CSGJJG: Cenosphere filled hybrid glass-jute(GJJG) epoxy composite				

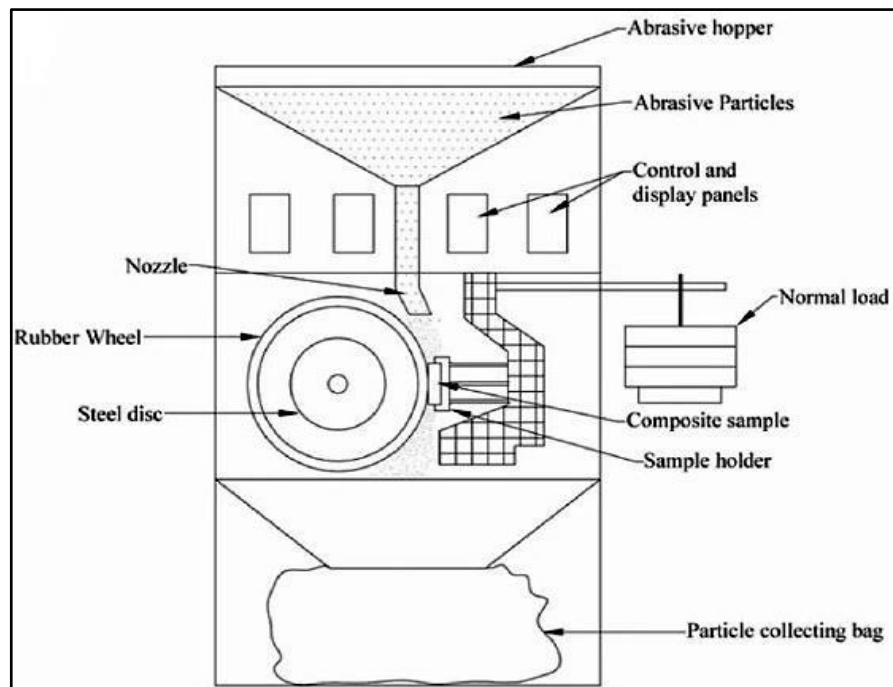


Figure 7.1(a): Schematic diagram of abrasive wear test rig

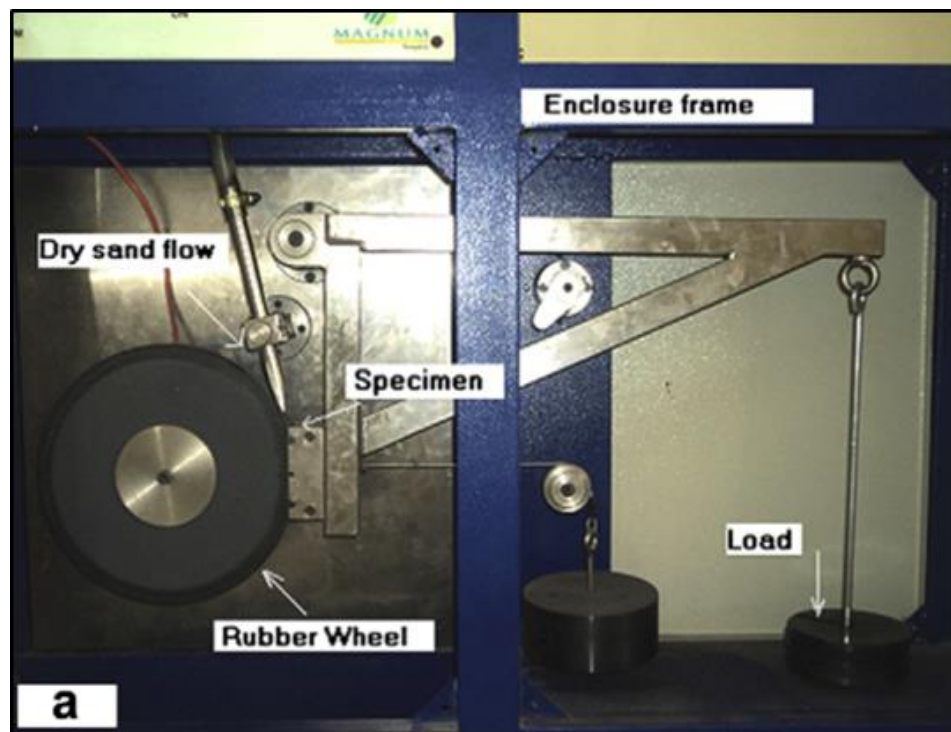


Figure 7.1(b): Dry sand rubber/wheel abrasion test setup

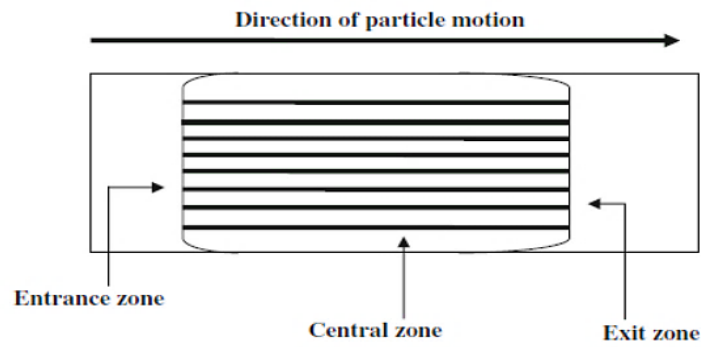


Figure 7.2: Schematic representation of different zones on the wear scar

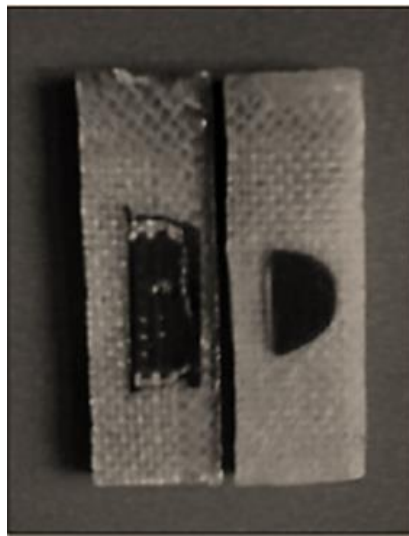


Figure 7.3 (a): Photographic image of the abraded hybrid glass-jute (GJJG) epoxy composite

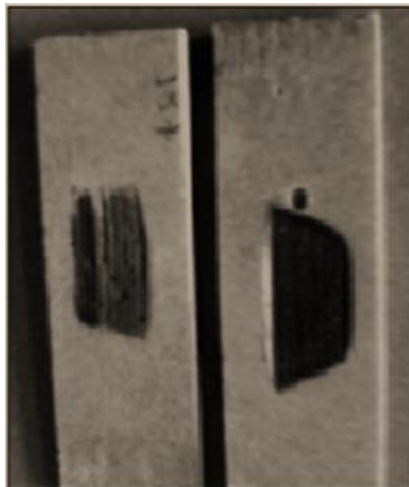


Figure 7.3(b): Photographic image of the abraded cenosphere filled glass-jute (GJJG) epoxy composite

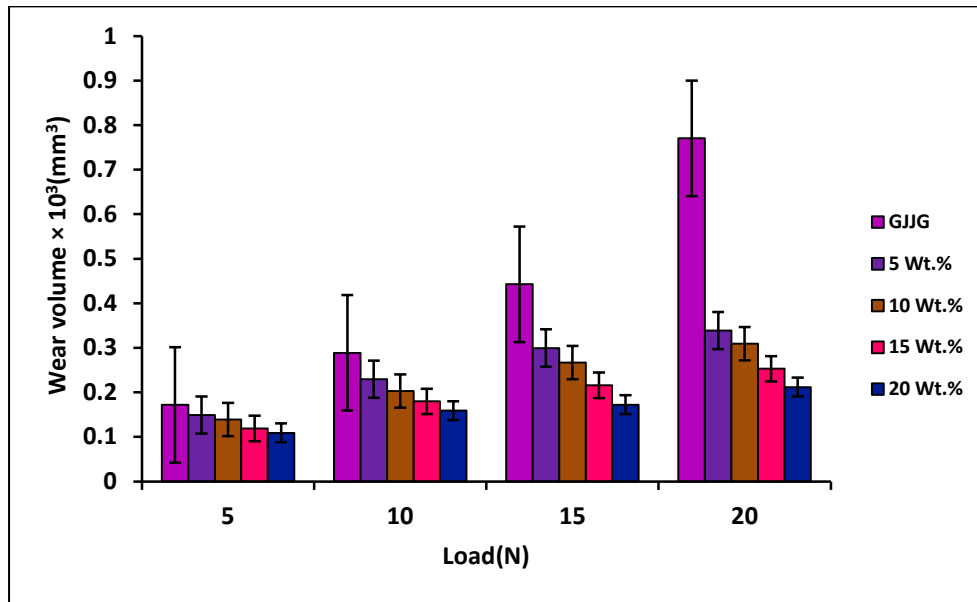


Figure 7.4: Variation of wear volume with respect to loads (N) for different cenosphere weight percentage of abraded hybrid glass-jute (GJJG) epoxy composites

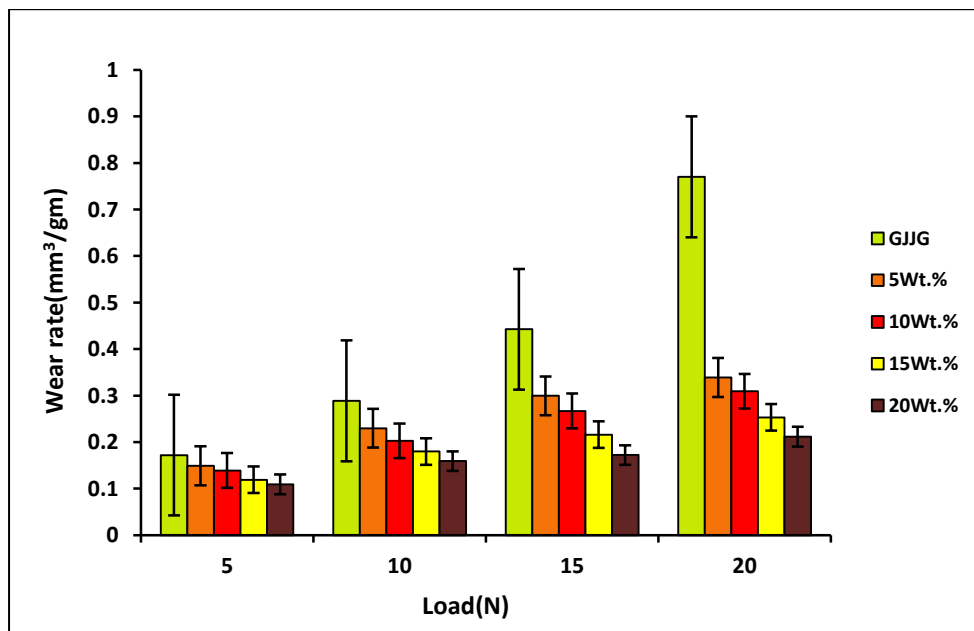


Figure 7.5: Variation of wear rate with respect to loads (N) for different cenosphere wt. percentage of abraded hybrid glass-jute (GJJG) epoxy composites

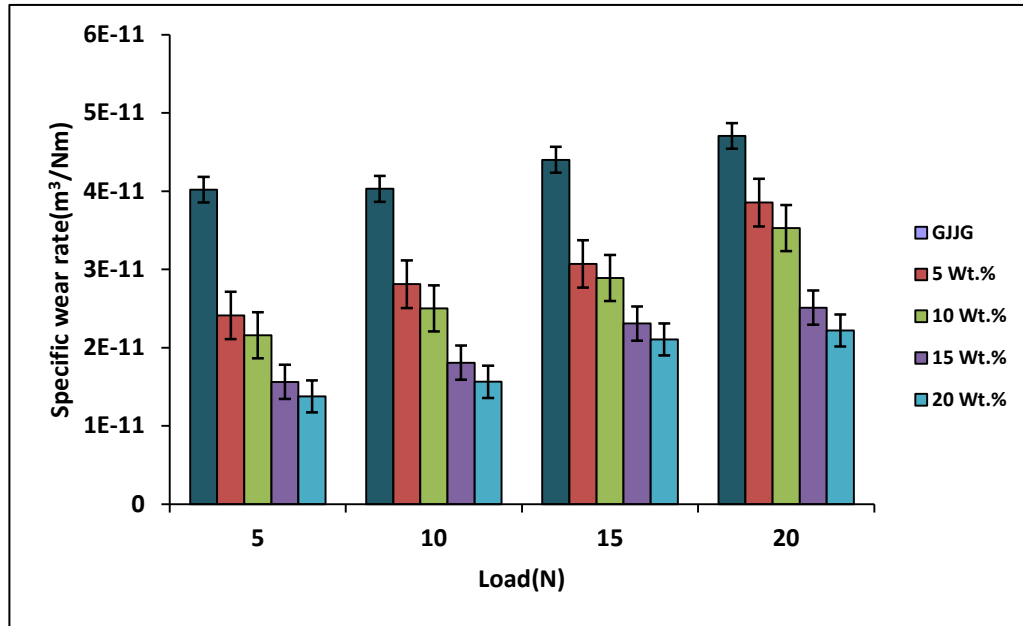


Figure 7.6: Variation of specific wear rate with respect to loads (N) for different cenosphere weight percentage of abraded hybrid glass-jute (GJJG) epoxy composites

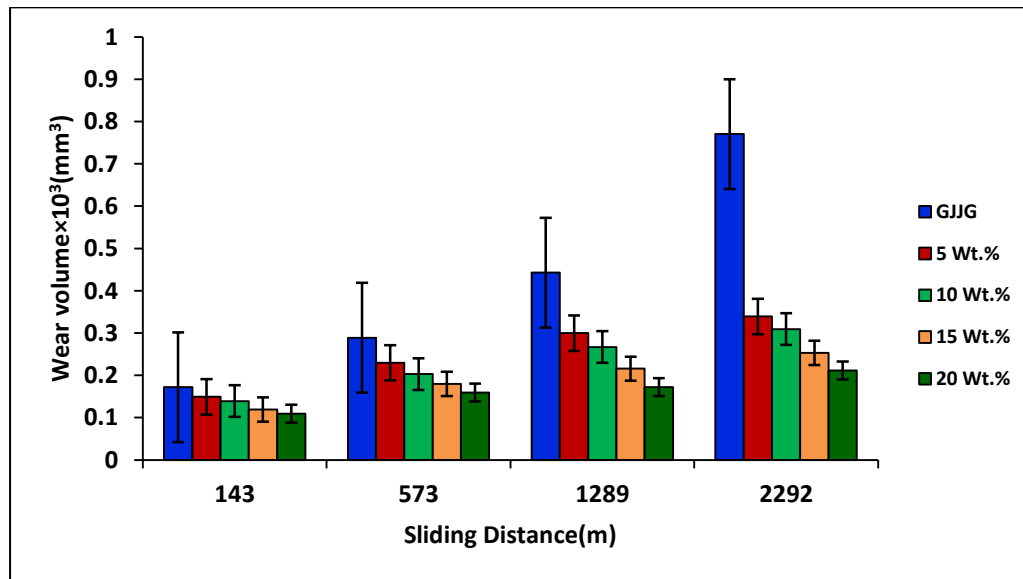


Figure 7.7: Variation of wear volume with respect to sliding distances (m) for different cenosphere wt. percentage of abraded hybrid glass-jute (GJJG) epoxy composites

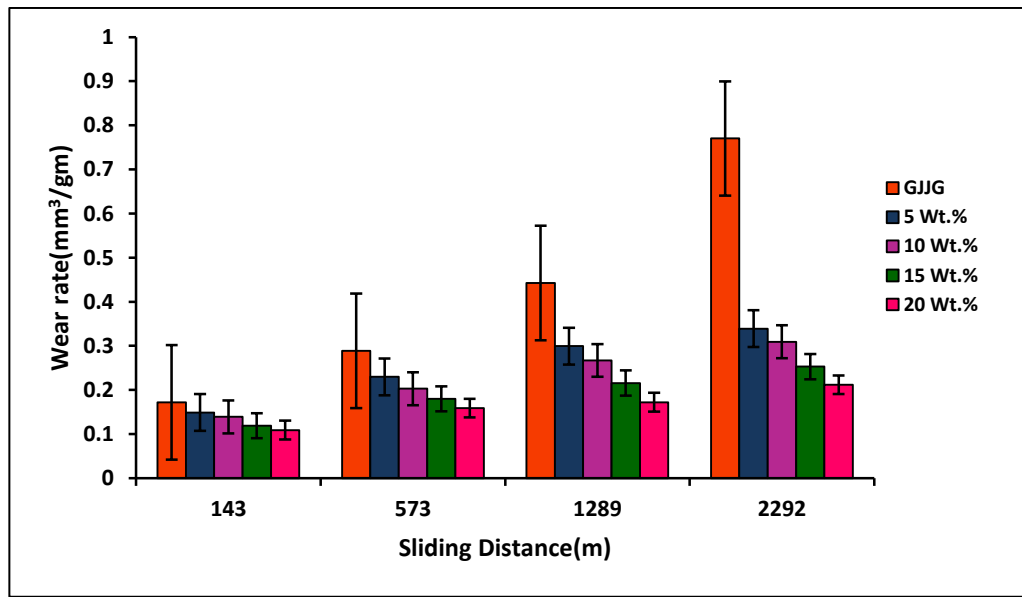


Figure 7.8: Variation of wear rate with respect to sliding distances (m) for different cenosphere wt. percentage of abraded hybrid glass-jute (GJJG) epoxy composites

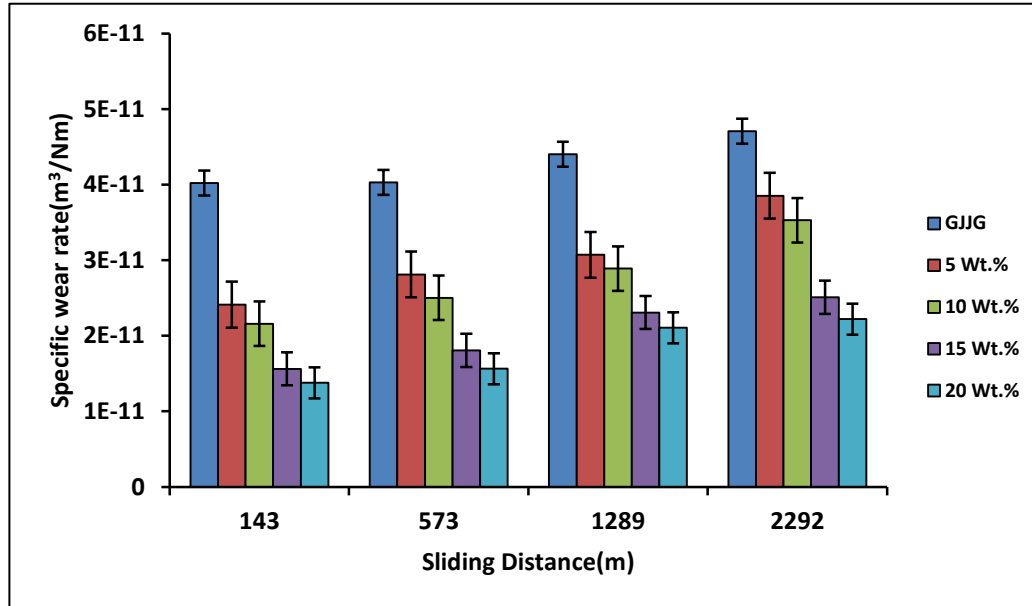


Figure 7.9: Variation of specific wear rate with respect to sliding distances (m) for different cenosphere wt. percentage of abraded hybrid glass-jute (GJJG) epoxy composites

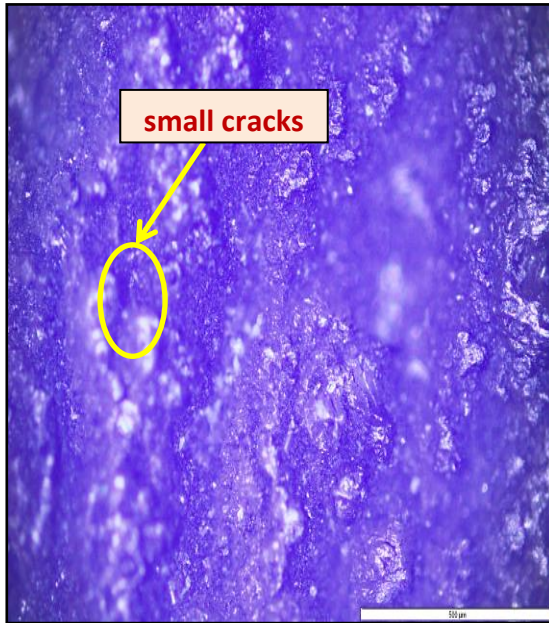


Fig. 7.10(a) Micrograph of hybrid GJJG composite at load 10N

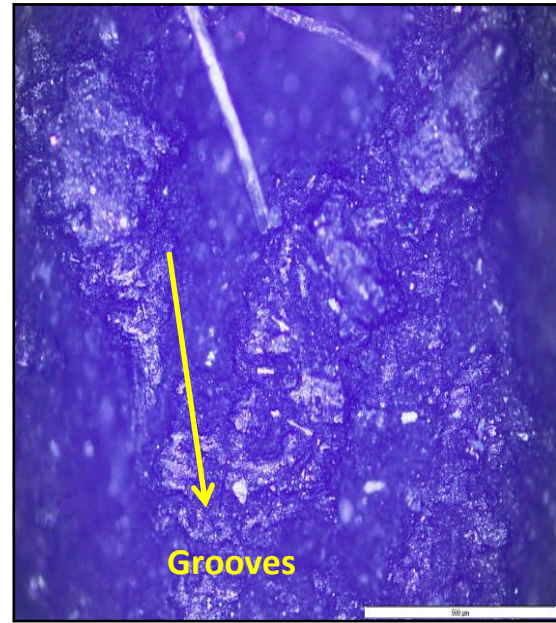


Fig. 7.10(b) Micrograph of hybrid glass-jute (GJJG) composite at load 20N

Figure 7.10: Microscopic pictures of hybrid glass-jute(GJJG) epoxy composites at various loads

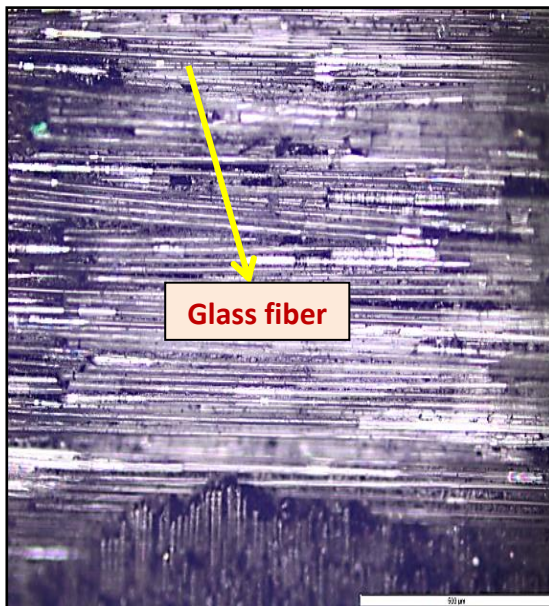


Fig. 7.11(a) Micrograph of 5wt.% cenosphere filled GJJG composite at load 20N

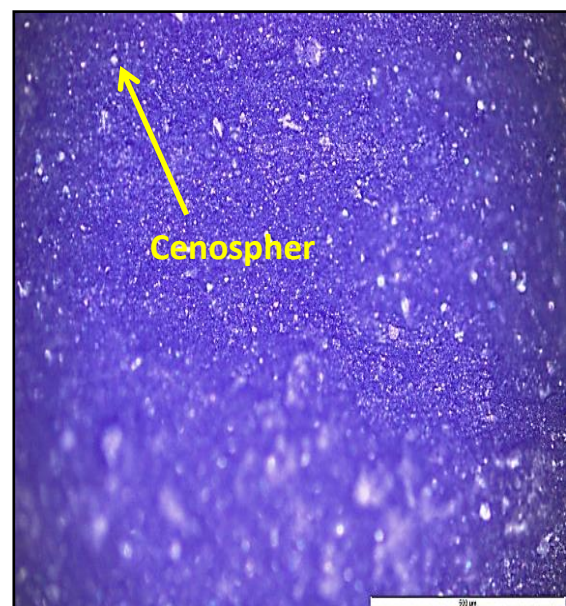


Fig. 7.11 (b) Micrograph of 20wt.% cenosphere filled GJJG composite at load 20N

Figure 7.11: Microscopic pictures of cenosphere filled abraded hybrid glass-jute(GJJG) epoxy composites

Chapter 8

Conclusions and Scope for Future Work

8.1 Conclusions

The conclusions drawn from the present investigation are as follows:

1. Jute (45° - 45°) and glass (0 - 90°) fiber of bidirectional orientation can successfully be fabricated to produce hybrid composites by suitable bonding with resin for the development of value added products.
2. Effect of stacking sequence on tensile, flexural and interlaminar shear strength results of hybrid jute and glass fabric reinforced epoxy composite indicates that the properties of jute composites can be considerably improved by incorporation of glass fiber at extreme ends.
3. There is a good dispersibility of cenosphere (ceramic rich industrial waste) filler in the matrix, which improves the strength and work fracture of the composites.
4. Inclusion of cenosphere to the hybrid composite GJJG indicates that the filler addition enhanced the mechanical properties with their modulus. Fifteen weight percent of cenosphere reinforcement gives the best combination among the tested composites.
5. Both layered and cenosphere filled hybrid jute-glass composites shows semi-ductile response to solid particle erosion. It is also found that the erosive wear of the developed composite with 20wt. percentage of cenosphere filler is the lowest. From the experimental results the erosion efficiency (η) is found in the range 1.77% to 12.64%.
6. The fracture surface study with addition of cenosphere filler indicates the breaking of glass fiber without their detachment from the matrix, which in turn improves the erosion resistance of the developed composites.
7. Fickian's diffusion process can be used to describe the moisture absorption behaviour of both hybrid and cenosphere filled jute-glass epoxy composite.
8. The abrasive wear rate of the cenosphere filled hybrid fiber reinforced composite is influenced by several parameters e.g. sliding velocity, sliding distance and normal

load. The wear rate of the composite is found to be more sensitive to normal load in comparison to sliding velocity.

8.2 Recommendation for further research

1. In the present investigation we have used jute and glass fabric to prepare a hybrid epoxy composite. However there exists other natural fibers like bamboo, sisal, hemp, bagasses etc. along with different matrices which could be tried and a final conclusion can be drawn their after.
2. In the present investigation hand-lay-up technique is used to fabricate the composite. However there exists other manufacturing process for polymer matrix composites. They could be tried and analyzed, so that a final conclusion can be drawn from there. However the results provided in this thesis can act as a base for the utilization of this composite.
3. From this work it is found that fly ash cenosphere fillers significantly improve the mechanical and tribological performance of the composite. Other ceramic or metal micro/nano fillers could be tried and the results can be compared between micro and nano filler addition.
4. In the erosion and abrasion test sand particles of size (200 ± 50) microns only have been used. This work can be further extended to other particle size and particles like glass beads etc. to study the effect of particle size and type of particles on the wear behaviour of the composites.

REFERENCES

1. Lubin, Hand book of composites, Van Nostarnd, New York, 1982.
2. Encyclopedia of Polymer Science Engineering, H.F. Mark Edition, John Wiley and Sons, New York, 1985
3. Agarwal, B.D. and Broutman, L.J. Analysis and performance of fiber composites, John Wiley & Sons, New York, pp.3-12, 1980.
4. Richardson T., Composites-A design guide, Industrial Press Inc., 200 Madison Avenue, New York, 1987.
5. Warner S.B., Fibre Science., Prentice Hall, Engle wood Cliffs, New Jersey, 1995.
6. Mallick P.K., Fibre reinforced composite materials, manufacturing and design, Marcel Dekker, Inc., New York, Chapter 1, p.18, 1988.
7. Idicula M., Neelakandan N.R., Thomas S., Oommen S., Joseph K. A Study of the Mechanical properties of randomly oriented short banana and sisal hybrid fiber reinforced Polyester composites. *Journal of Applied Polymer Science*, 96, 1699-1709, 2005.
8. Idicula M., Malhotra S.K., Thomas S. Dynamic mechanical analysis of randomly oriented intimately mixed short banana/sisal hybrid fibre reinforced polyester composites. *Composites Science and Technology*, 65, 1077-1087, 2005.
9. Chand, Navin and Pradeep K. Rohatgi. *Natural fibres and their composites*. Periodical Experts Book Agency, 1994.
10. Chand N., Dwivedi U.K. Effect of coupling agent on high stress abrasive wear of chopped fibre-reinforced polypropylene composites, *Wear*, 261, 1057-1063, 2006.
11. Tong J., Ren L., Li J. and Chen B. Abrasive wear behaviour of bamboo, *Tribology International*, 28(5), pp. 323-327, 1995.
12. Jain S., Kumar R. and Jindal U.C. Mechanical behaviour of bamboo and bamboo composites. *Journal of Material Science*, 27, pp. 4598-4604, 1992.
13. Hinrichsen, G., A. K. Mohanty, and M. Khan. Influence of chemical surface modification on the properties of biodegradable jute fabrics-polyester amide composites. *Composites Part A: Applied Science and Manufacturing (UK)*, 31(2), 143-150, 2000.
14. Joseph PV, Joseph K, Thomas S. Effect of processing variables on the mechanical properties of sisal-fiber-reinforced polypropylene composites. *Composites science and Technology*. 59(11), 1625-40, August 1999.
15. Mukherjee, P. S. and Satyanarayana, K. G. Structure and properties of some vegetable fibers-II. Pineapple leaf fiber, *Journal of Material Science*, 21, pp. 51-56, 1986.

16. Hirao, K., Inagaki, H., Nakamae, K., Kotera, M. and Nishino, T. K. Kenaf Reinforced Biodegradable Composite, *Composites Science and Technology*, 63, pp.1281-1286, 2003.
17. Vazquez, A., Dominguez V. A., Kenny J. M. Bagasse Fiber-Polypropylene Based Composites, *Journal of Thermoplastic Composite Materials*. 12(6), pp. 477-497, 1999.
18. International Jute Study Group, *Ministry Of Textiles*, Govt. of India, Source: Zimbio, 2012.
19. Carus, M., Eder, A., Dammer, L., Korte, H., Scholz, L., Essel, R. and Breitmayer, E. Wood plastic composites and natural fibre composites (NFC): European and global markets and future trends. *Nova-Institute GmbH*, 2012.
20. Bledzki, A. K., and Gassan, J. Composites reinforced with cellulose based fibres. *Progress in polymer science*, 24(2), 221-274, 1999.
21. Kizil'shtein LY, Dubov IV, Shpitsgluz AL, Parada SG. Components of ashes and slags of heat power plants. *Energoatomizdat*, Moscow.1995.
22. Rothon, R. N. *Particulate fillers for polymers*. Rapra Technology Limited, 12(9), 2001
23. Vernon J. Hurst Fly ash beneficiation process October 1978, US Patent 4121945.
24. Ahmaruzzaman, M. A review on the utilization of fly ash. *Progress in Energy and Combustion Science*, 36(3), 327-363, 2010.
25. Dhingra, A.K. Metal replacement by composite. *Journal of Minerals, Metals and Materials Society*, 38(3), pp 17-17, 1986.
26. Mehrabian, R., Riek, R. G. and Flemings, M.C. Preparation and casting of Metal particulate non-metal composites. *Metallurgical Transactions*, 5(8), 1899-1905, 1974.
27. Eliasson, J. and Sandström, R. Applications of aluminium matrix composites. *Key Engineering Materials*, 104-107, pp. 3-36, 1995.
28. Robson, D., Hague, J., Newman, G., Jeronomidis, G. and Ansell, M., *Survey of natural materials for use in structural composites as reinforcement and matrices*. Biocomposites Centre, University of Wales, 1993.
29. Joseph, K., Varghese, S., Kalaprasad, G., Thomas, S., Prasannakumari, L., Koshy, P. and Pavithran, C. Influence of interfacial adhesion on the mechanical properties and fracture behavior of short sisal fiber reinforced polymer composites. *European Polymer Journal*, 32(10), 1243-1250, 1996.
30. Patel, R., Patel, R. and Patel, V. Investigation of kinetics of curing of triglycidyl-p-aminophenol with aromatic diamines by differential scanning calorimetry. *Journal of Thermal Analysis and Calorimetry*, 34(5-6), pp.1283-1293, 1988.
31. Yu, L., Dean, K., and Li, L. Polymer blends and composites from renewable resources, *Progress in polymer science*, 31(6), 576-602, 2006.

32. Bax, B., and Mussig, J. Impact and tensile properties of PLA/Cordenka and PLA/flax composites. *Composites Science and Technology*, 68(7), 1601-1607, 2008.
33. Oksman, K., Skrifvars, M., and Selin, J. F. Natural fibers as reinforcement in polylactic acid (PLA) composites. *Composites science and technology*, 63(9), 1317-1324, 2003.
34. Meinander, K., Niemi, M., Hakola, J.S., and Selin, J.F. Polylactides-degradable polymers for fibres and films. *In Macromolecular Symposia*, 123(1), 147-153, 1997.
35. Jiang, L., and Hinrichsen, G. Flax and cotton fiber reinforced biodegradable polyester amide composites, Characterization of biodegradation. *Die Angewandte Makromolekulare Chemie*, 268(1), 18-21, 1999.
36. Riedel, U., and Nickel, J. Natural fiber-reinforced biopolymers as construction Materials new discoveries. *Die Angewandte Makromolekulare Chemie*, 272, 34-40, 1999.
37. Keller, A., Bruggmann, D., Neff, A., Müller, B. and Wintermantel, E. Degradation kinetics of biodegradable fiber composites, *Journal of Polymers and the Environment*, 8(2), pp.91-96, 2000.
38. Leaversuch, Robert D. Wood-fiber composites build promising role in extrusion. *Modern Plastics(USA)*, 77(12), 56-58, 2000.
39. Holbery, J. and Houston. Natural-fiber-reinforced polymer composites in automotive applications. *Journal of The Minerals, Metals and Materials Society (TMS)*, 58(11), 80-86, 2006.
40. Burgueno, R., Quagliata, M. J., Mehta, G. M., Mohanty, A. K., Misra, M., and Drzal, L. T. Sustainable cellular biocomposites from natural fibers and unsaturated polyester resin for housing panel applications. *Journal of Polymers and the Environment*, 13(2), 139-149, 2005.
41. Rials, T. G., Wolcott, M. P. and Nassar, J. M. Interfacial contributions in lignocellulosic fiber reinforced polyurethane composites. *Journal of applied polymer science*, 80(4), 546-555, 2001.
42. Mueller, D. H., and Krobjilowski, A. New discovery in the properties of composites reinforced with natural fibers. *Journal of Industrial Textiles*, 33(2), 111-130, 2003.
43. Eichhorn, S. J., Baillie, C. A., Zafeiropoulos, N., Mwaikambo, L. Y., Ansell, M. P., Dufresne, A. and Wild, P. M. Review: current international research into cellulosic fibers and composites. *Journal of materials Science*, 36(9), 2107-2131, 2001.
44. Brouwer, W.D. Natural fibre composites in structural components, alternative for sisal. *In On the Occasion of the Joint FAO, CFC Seminar, Rome, Italy*, 2000.

45. Bodros, E., Pillin, I., Montrelay, N. and Baley, C. Could biopolymers reinforced by randomly scattered flax fibre be used in structural applications? *Composites Science and Technology*, 67(3), pp.462-470, 2007.
46. Pal, P. K. Jute reinforced plastics: a low cost composite material. *Plastics and Rubber Processing and Applications*, 4(3), 215-219, 1984.
47. Mohanty, A. K., Misra, M. and Drzal, L. T. Sustainable bio-composites from renewable resources: opportunities and challenges in the green materials world. *Journal of Polymers and the Environment*, 10(1-2), pp.19-26, 2002.
48. Joseph, S., Sreekala, M. S., Oommen, Z., Koshy, P., and Thomas, S. A comparison of the mechanical properties of phenol formaldehyde composites reinforced with banana fibres and glass fibres. *Composites Science and Technology*, 62(14), 1857-1868, 2002.
49. Roe, P. J. and Ansell, M. P. Jute-reinforced polyester composites. *Journal of Materials Science*, 20(11), 4015-4020, 1985.
50. Lu, X., Zhang, M. Q., Rong, M. Z., Shi, G. and Yang, G.C. Self-reinforced melt processable composites of sisal. *Composites science and technology*, 63(2), 177-186, 2003.
51. Baiardo, M., Zini, E. and Scandola, M. Flax fibre-polyester composites. *Composites Part A: Applied Science and Manufacturing*, 35(6), 703-710, 2004.
52. George, J., Sreekala, M. S. and Thomas, S. A review on interface modification and characterization of natural fiber reinforced plastic composites. *Polymer Engineering and Science*, 41(9), 1471-1485, 2001.
53. Valadez-Gonzalez, A., Cervantes-Uc, J.M., Olayo, R. and Herrera-Franco, P.J. Effect of fiber surface treatment on the fiber-matrix bond strength of natural fiber reinforced composites. *Composites Part B: Engineering*, 30(3), pp.309-320, 1999.
54. Rana, A.K., Mitra, B.C. and Banerjee, A.N. Short jute fibre reinforced polypropylene composites: dynamic mechanical study. *Journal of Applied Polymer Science*, 71, 531-539, 1999.
55. Nair, K.C., Diwan, S. M. and Thomas, S. Tensile properties of short sisal fiber reinforced polystyrene composites. *Journal of Applied Polymer Science*, 60(9), 1483-1497, 1996.
56. Mariatti, M., Jannah, M., Bakar, A. A. and Khalil, H. A. Properties of banana and pandanus woven fabric reinforced unsaturated polyester composites. *Journal of composite materials*, 42(9), 931-941, 2008.
57. El-Tayeb, N.S.M. Development and characterization of low-cost polymeric composite materials. *Materials and Design*, 30(4), 1151-1160, 2009.

58. Jacob, M., Thomas, S. and Varughese, K. T. Mechanical properties of sisal/oil Palm hybrid fiber reinforced natural rubber composites. *Composites Science and Technology*, 64(7), 955-965, 2004.
59. Pothan, L. A., Oommen, Z. and Thomas, S. Dynamic mechanical analysis of banana fiber reinforced polyester composites. *Composites Science and Technology*, 63(2), 283-293, 2003.
60. Yousif, B. F., and El-Tayeb, N. S. M. Mechanical and tribological characteristics of OPRP and CGRP composites. *The Proceedings ICOMAST, GKH Press, Melaka, Malaysia*, 384-387, 2006.
61. Tong, J., Arnell, R. D., and Ren, L. Q. Dry sliding wear behaviour of bamboo. *Wear*, 221(1), 37-46, 1998.
62. Tong, J., Ma, Y., Chen, D., Sun, J. and Ren, L. Effects of vascular fiber content on abrasive wear of bamboo. *Wear*, 259(1), 78-83, 2005.
63. Hornsby, P. R., Hinrichsen, E., and Tarverdi, K. Preparation and properties of polypropylene composites reinforced with wheat and flax straw fibres: part I fibre characterization. *Journal of Materials Science*, 32(2), 443-449, 1997.
64. Pothan, L. A., Thomas, S. and Neelakantan, N. R. Short banana fiber reinforced polyester composites: mechanical, failure and aging characteristics. *Journal of Reinforced Plastics and Composites*, 16(8), 744-765, 1997.
65. Gassan, J. A study of fibre and interface parameters affecting the fatigue behaviour of natural fibre composites. *Composites Part A: Applied Science and Manufacturing*, 33(3), 369-374, 2002.
66. Hepworth, D. G., Hobson, R. N., Bruce, D. M. and Farrent, J. W. The use of unretted hemp fibre in composite manufacture. *Composites Part A: Applied Science and Manufacturing*, 31(11), 1279-1283, 2000.
67. Joseph, P. V., Joseph, K. and Thomas, S. Short sisal fiber reinforced polypropylene composites: the role of interface modification on ultimate properties. *Composite interfaces*, 9(2), 171-205, 2002.
68. El-Sayed, A. A., El-Sherbiny, M. G., Abo-El-Ezz, A. S., and Aggag, G. A. Friction and wear properties of polymeric composite materials for bearing applications. *Wear*, 184(1), 45-53, 1995.
69. Ranganathan, S.R. and Pal, P.K. Jute plastics composites for the building industry *popular plastic*, 31, 22-24, 1986.
70. Ranganathan, N., Oksman, K., Nayak, S.K. and Sain, M. Regenerated cellulose fibers as impact modifier in long jute fiber reinforced polypropylene composites: Effect on mechanical properties, morphology and fiber breakage. *Journal of Applied Polymer Science*, 132(3), 2015.

71. Shah, A. N., and Lakkad, S. C. Mechanical properties of jute-reinforced plastics. *Fibre Science and Technology*, 15(1), 41-46, 1981.
72. Karmakar, A.C. and HinrichSen, G. *Polymer Plastic Technology Engineering*, 30, 609, 1991.
73. Rana, A.K. and Jayachandran, K. Jute fiber for reinforced composites and its prospects. *Molecular Crystals and Liquid Crystals*, 353(1), 35-45, 2000.
74. Ray, D., Sarkar, B. K., Rana, A. K., and Bose, N. R. The mechanical properties of vinyl ester resin matrix composites reinforced with alkali-treated jute fibres. *CompositesPart A: applied science and manufacturing*, 32(1), 119-127, 2001.
75. Dash, B.N., Rana, A.K., Mishra, H.K., Nayak, S.K., Mishra, S.C. and Tripathy, S.S. Novel, low-cost jute-polyester composites. Part 1: Processing, mechanical properties, and SEM analysis. *Polymer Composites*, 20(1), pp.62-71, 1999.
76. Giridhar and Rao. Moisture absorption characteristics of natural fiber composites. *Journal of Reinforced plastics composites*. 5(2), 141-150, 1986.
77. Ray, D., Sarkar, B. K., & Rana, A. K. Fracture behaviour of vinyl ester resin matrix composites reinforced with alkali-treated jute fibers. *Journal of applied polymer science*, 85(12), 2588-2593, 2002.
78. Mitra, B. C., Basak, R. K., & Sarkar, M. Studies on jute-reinforced composites, its limitations and some solutions through chemical modifications of fibers. *Journal of Applied Polymer Science*, 67(6), 1093-1100, 1998.
79. Rahman, M. R., Huque, M. M., Islam, M. N., & Hasan, M. Improvement of physico-mechanical properties of jute fiber reinforced polypropylene composites by post-treatment. *Composites Part A: Applied Science and Manufacturing*, 39(11), 1739-1747, 2008.
80. Ahmed, K. S., and Vijayarangan, S. Tensile, flexural and interlaminar shear properties of woven jute and jute-glass fabric reinforced polyester composites. *Journal of materials processing technology*, 207(1), 330-335, 2008.
81. Santulli, C., and Caruso, A. P. A comparative study on falling weight impact properties of jute/epoxy and hemp/epoxy laminates. *Malaysian Polymer Journal*, 4(1), 19-29, 2009.
82. Kanakasabai, P., Deshpande, A. P., and Malhotra, S. K. Effect of fabric treatment and Filler content on jute polyester composites. Composite Technology Center, IIT Madras Chennai.
83. Acharya, S. K., Mishra, P. and Mishra, S. C. Effect of environment on the Mechanical properties of fly ash-jute-polymer composite. *Indian Journal Engineering Material Science*, 15,483-488, 2008.

84. Ramesh M. and Palanikumar K. Comparative evaluation on properties of hybrid glass fiber-sisal/jute reinforced epoxy composites. *Procedia Engineering*, 51,745-750, 2013.
85. Doan, T. T. L., Brodowsky, H., and Mader, E. Jute fibre/epoxy composites: surface properties and interfacial adhesion. *Composites Science and Technology*, 72(10), 1160-1166, 2012.
86. Davey, S.W. A Foundational Investigation of Vinyl Ester / Cenosphere Composite Materials for Civil and Structural Engineering. PhD Dissertation, University of Southern Queensland, Australia, 2005.
87. Suresha, B., Chandramohan, G. and Jayaraju, T., Influence of cenosphere filler additions on the three-body abrasive wear behavior of glass fiber reinforced epoxy composites. *Polymer Composites*, 29(3), pp.307-312, 2008.
88. Gu, Jian, Gaohui Wu, and Xiao Zhao. Effect of surface-modification on the dynamic behaviors of fly ash cenospheres filled epoxy composites. *Polymer composites*, 30(2), 232-238,2009.
89. Deepthi, M. V., Sharma, M., Sailaja, R. R. N., Anantha, P., Sampathkumaran, P., and Seetharamu, S. Mechanical and thermal characteristics of high density polyethylene-fly ash Cenospheres composites. *Materials and Design*, 31(4), 2051-2060, 2010.
90. Chand, N., Sharma, P. and Fahim, M. Correlation of mechanical and tribological properties of organosilane modified cenosphere filled high density polyethylene. *Materials Science and Engineering: A*, 527(21), pp.5873-5878, 2010.
91. Das, A. and Satapathy, B.K. Structural, thermal, mechanical and dynamic mechanical properties of cenosphere filled polypropylene composites. *Materials & Design*, 32(3), pp.1477-1484, 2011.
92. Altaheel, M., Abdullah, M.A., Ranganathaiah, C., Kothandaraman, B., Raj, J.M. and Chandrashekara, M.N. Characterization of ACS modified epoxy resin composites with fly ash and cenospheres as fillers: mechanical and microstructural properties. *Polymer composites*, 32(1), pp.139-146, 2011.
93. Wasekar, P.A., Kadam, P.G. and Mhaske, S.T. Effect of cenosphere concentration on the mechanical, thermal, rheological and morphological properties of nylon 6. *Journal of Minerals and Materials Characterization and Engineering*, 11(08), pp.807-812. 2012.
94. Ismail M, Bheemappa S, Rajendra N. Investigations on Mechanical and erosive wear behaviour of cenosphere filled carbon-epoxy composites. *In International Conference on Mechanical, Automotive and Materials Engineering (ICMAME'2012)* Jan. 7 pp.7-8,2012.

95. Arivalagan, P., Suresha, B., Chandramohan, G., Krishnaraj, V. and Palaniappan, N. Mechanical and abrasive wear behavior of carbon fabric reinforced epoxy composite with and without fly ash cenospheres. *Journal of Composite Materials*, 47(23), 2925-2935, 2012.
96. Sharma, J., Chand, N. and Bapat, M.N. Effect of cenosphere on dielectric properties of low density polyethylene. *Results in Physics*, 2, pp.26-33, 2012.
97. Jena, H., Pandit, M.K. and Pradhan, A.K. Effect of cenosphere on mechanical properties of bamboo-epoxy composites. *Journal of Reinforced Plastics and Composites*, 32(11), pp.794-801, 2013.
98. Chauhan, S.R. and Thakur, S. Effects of particle size, particle loading and sliding distance on the friction and wear properties of cenosphere particulate filled vinylester composites. *Materials & Design*, 51, pp.398-408, 2013.
99. Kulkarni, M.B., Bambole, V.A. and Mahanwar, P.A. Effect of particle size of fly ash cenospheres on the properties of acrylonitrile butadiene styrene filled composites. *Journal of Thermoplastic Composite Materials*, 27(2), pp.251-267, 2014.
100. Thakur S. and Chauhan S. Effect of micron and submicron size cenosphere particulate on mechanical and tribological characteristics of vinylester composites. *Proceedings of the Institution of Mechanical Engineers, Part J: Journal of Engineering Tribology*, 228(4), 415-423, 2014.
101. Thakur, S. and Chauhan, S.R. Friction and sliding wear characteristics study of submicron size cenosphere particles filled vinylester composites using taguchi design of experimental technique. *Journal of Composite Materials*, 48(23), pp.2831-2842, 2014.
102. Roy, A.S., Saravanan, S., Ramamurthy, P.C. and Madras, G. Dielectric impedance studies of poly (vinylbutyral)-cenosphere composite films. *Polymer Composites*, 35(8), pp.1636-1643, 2014.
103. Khoshnoud, Parisa and Abu-Zahra, Nidal. Effect of Cenosphere Fly Ash on the Thermal, Mechanical, and Morphological Properties of Rigid PVC Foam Composites. *Journal of Research Updates in Polymer Science*, 4(1), pp.1-14, 2015.
104. Bheemappa, S., Chandrashekar, A. and Srinivas, S. Mechanical and Three-Body abrasive wear behaviour of cenosphere filled epoxy composites. *International Journal of Material Science*, 5(1), pp.7-15, 2015.
105. Satapathy, S. and Kothapalli, R.V. Influence of fly ash cenospheres on performance of coir fiber-reinforced recycled high-density polyethylene biocomposites. *Journal of Applied Polymer Science*, 132(28), 2015.

106. Allan, G.G., Carroll, P., Negri, A.R., Raghuraman, M., Ritzenthaler, P. and Yabiaoui, A. The micro porosity of pulp; the precipitation of inorganic fillers within the micropores of the cell wall. *Tappi Journal*, 75(1), 175-178,1992.
107. Lee, S.Y. Trans crystallization behaviour and interfacial strength of a semi crystalline polymer combined with thermo mechanical pulp (TMP) fiber. M.S.Thesis.University of Idaho, Maiscow, ID. 72 p. 2002.
108. Ma, C.G., Rong, M. Z., Zhang, M.Q. and Friedrich, K.Irradiation-induced surface graft polymerization onto calcium carbonate nanoparticles and its toughening effects on polypropylene composites. *Polymer Engineering and Science* 45(4),529-538,2005.
109. Lee, S.Y., Shupe, T.F., Groom, L.R., and Hse, C.Y. Heterogeneous nucleation of a semicrystalline polymer on fiber surfaces In: Recent Developments in wood composites.91-97, 2006.
110. Mullin, J.W. Crystallization, 4th Ed. Butterworth-heinemann Ltd. Oxford, England.527, ISBN 0 7506 4833 3, 2001.
111. Gasser, U., Weeks, E.R., Schofield, A., Pusey, P.N. and Weitz1, D.A. Real-space imaging of nucleation and growth in colloidal crystallization. *Science*. 292(5515), 258-262, 2001.
112. Sawyer, W. G., Freudenberg, K. D., Bhimaraj, P., and Schadler, L. S. A study on the friction and wear behavior of PTFE filled with alumina nanoparticles. *Wear*, 254(5), 573-580,2003.
113. Kim, J. I., Kang, P. H., and Nho, Y. C. Positive temperature coefficient behaviour of polymer composites having a high melting temperature. *Journal of Applied Polymer Science*, 92(1), 394-401,2004.
114. Nikkeshi, S., Kudo, M. and Masuko, T. Dynamic viscoelastic properties and thermal properties of Ni powder-epoxy resin composites. *Journal of Applied Polymer Science*, 69(13), 2593-2598, 1998.
115. Zhu, K. and Schmauder, S.Prediction of the failure properties of short fiber reinforced composites with metal and polymer matrix. *Computational Materials Science*, 28(3), 743-748, 2003.
116. Rusu, M., Sofian, N., and Rusu, D. Mechanical and thermal properties of zinc powder filled high density polyethylene composites. *Polymer Testing*, 20(4), 409-417, 2001.
117. Tavman, I.H., Thermal and mechanical properties of copper powder filled polyethylene composites. *Powder Technology*, 91(1), 63-67, 1997.
118. Rothon, R.N. Mineral fillers in thermoplastics: filler manufacture. *Journal of Adhesion*, 64(1), 87-109, 1997.

119. Rothon, R.N. Effects of particulate fillers on flame retardant properties of composites. *Advances in polymer science*, 139, 67-107, 1999.
120. Nielsen, L.E., Landel, R.F. Mechanical properties of polymers and composites. 2nd ed. New York: Marcel Dekker, 377-459, 1993.
121. Peters S.T. Handbook of composites. 2nd ed. London: Chapman and Hall, 242- 243, 1998.
122. Young, R. J. and Beaumont, P. W. R. Failure of brittle polymers by slow crack growth. *Journal of Materials Science*, 12(4), 684-692, 1977.
123. Kinloch, A. J., Maxwell, D. L. and Young, R. J. The fracture of hybrid-particulate composites. *Journal of materials science*, 20(11), 4169-4184, 1985.
124. Young, R. J., Maxwell, D. L., and Kinloch, A. J. The deformation of hybrid-particulate composites. *Journal of materials science*, 21(2), 380-388, 1986.
125. Koh, S. W., Kim, J. K., and Mai, Y. W. Fracture toughness and failure mechanisms in silica-filled epoxy resin composites: effects of temperature and loading rate. *Polymer*, 34(16), 3446-3455, 1993.
126. Cantwell, W. J. and Roulin-Maloney, A. C. Fractography and failure mechanisms of polymers and composites, *Elsevier Applied Science*, London, pp. 233-289, 1989.
127. Imanaka, M., Takeuchi, Y., Nakamura, Y., Nishimura, A. and Iida, T. Fracture toughness of spherical silica-filled epoxy adhesives. *International journal of adhesion and adhesives*, 21(5), 389-396, 2001.
128. Wang, H., Bai, Y., Liu, S., Wu, J., and Wong, C. P. Combined effects of silica filler and its interface in epoxy resin. *Acta Materialia*, 50(17), 4369-4377, 2002.
129. Yamamoto I, Higashihara T, Kobayashi T. Effect of Silica-Particle Characteristics on Impact/Usual Fatigue Properties and Evaluation of Mechanical Characteristics of Silica-Particle Epoxy Resins. *JSME International Journal Series A Solid Mechanics and Material Engineering*. 46(2), 145-53, 2003.
130. Nakamura, Y., Yamaguchi, M., Kitayama, A., Okubo, M., and Matsumoto, T. Effect of particle size on fracture toughness of epoxy resin filled with angular-shaped silica. *Polymer*, 32(12), 2221-2229, 1991.
131. Nakamura, Y., Yamaguchi, M., Okubo, M., and Matsumoto, T. Effect of particle size on impact properties of epoxy resin filled with angular shaped silica particles. *Polymer*, 32(16), 2976-2979, 1991.
132. Nakamura, Y., Yamaguchi, M., Okubo, M., and Matsumoto, T. Effects of particle size on mechanical and impact properties of epoxy resin filled with spherical silica. *Journal of applied polymer science*, 45(7), 1281-1289, 1992.

133. Satyanarayana, K.G., Sukumaran, K., Mukherjee, P.S., Pavithran, C., and Pillai, S.G.K. Natural Fiber Polymer Composites, *Journal of Cement and Concrete Composites*, 12(2), 117-136, 1990.
134. Satyanarayana, K.G., Sukumaran, K., Kulkarni, A.G., Pillai, S.G.K., and Rohatgi, P.K. Fabrication and properties of natural fiber-reinforced polyester composites, *Composites*, 17(4), 329-333, 1986.
135. Schneider J.P., Karmaker A.C. Mechanical performance of short jute fibre reinforced polypropylene. *Journal of Material Science Letters*. 15 (3), 201-202, 1996.
136. Mansur, M. A. and Aziz, M. A. Study of bamboo-mesh reinforced cement composites. *International Journal of Cement composites and lightweight concrete*, 5(3), 165-171, 1983.
137. Hu, Ruihua and Lim Jae-Kyoo. Fabrication and mechanical properties of completely biodegradable hemp fiber reinforced polylactic acid composites. *Journal of Composite Materials*, 41(13), 1655-1669, 2007.
138. Ochi, Shinji. Mechanical properties of kenaf fibers and kenaf/PLA composites. *Mechanics of Materials*, 40(4-5), 446-452, 2008.
139. Arbelaiz, A. Fernandez, B., Cantero G., Llano-Ponte R., Valea A., Mondragon I. Mechanical properties of flax fibre/polypropylene composites. Influence of fibre/matrix modification and glass fibre hybridization. *Composites: Part A* 36, 1637-1644, 2005.
140. Ahmed K. Sabeel, Vijayarangan S., Rajput Chhaya. Mechanical Behavior of Isothalic Polyester-based Untreated Woven Jute and Glass Fabric Hybrid Composites. *Journal of Reinforced Plastics and Composites*, 25(15), 2006.
141. Zaini, M. J., Fuad, M. A., Ismail, Z., Mansor, M. S., and Mustafah, J. The effect of filler content and size on the mechanical properties of polypropylene/oil palm wood flour composites. *Polymer International*, 40(1), 51-55, 1996.
142. Pavithran, C., Mukherjee, P. S., and Brahmakumar, M. Coir-glass intermingled fibre hybrid composites. *Journal of Reinforced Plastics and Composites*, 10(1), 91-101, 1991.
143. Mohan, R., Shridhar, M. K., and Rao, R. M. V. G. K. Compressive strength of jute-glass hybrid fibre composites. *Journal of Materials Science Letters*, 2(3), 99-102, 1983.
144. Pavithran, C., Mukherjee, P.S., Brahmakumar, M. and Damodaran, A.D. Impact properties of sisal-glass hybrid laminates. *Journal of materials science*, 26(2), 455-459, 1991.
145. Mishra, S., Mohanty, A.K., Drzal, L.T., Misra, M., Parija, S., Nayak, S.K. and

- Tripathy, S.S. Studies on mechanical performance of biofiber/glass reinforced polyester hybrid composites. *Composite Science Technology*. 63, 1377-1385, 2003.
146. John, K., and Venkata Naidu, S. Sisal fibre/glass fibre hybrid composites: impact and compressive properties. *Journal of Reinforced Plastic Composite*. 23 (12), 1253-1258, 2004.
147. John, K., and Venkata Naidu, S. Effect of fibre content and fibre treatment of flexural properties of sisal fibre/glass fibre hybrid composites. *Journal of Reinforced Plastic Composite*. 23(15), 1601-1605, 2004.
148. John, K. and Venkata Naidu, S. Tensile properties of unsaturated polyester based sisal fibre-glass fibre hybrid composites. *Journal of Reinforced Plastic Composite*. 23 (17), 1815-1819, 2004.
149. Agarwal, Bhagwan D., Lawrence J. Broutman, and K. Chandrashekhara. Analysis and performance of fiber composites. John Wiley & Sons, 2006.
150. Wambua, P., Ivens, J. and Verpoest, I. Natural fibres: can they replace glass in fibre reinforced plastics? *Composites science and technology*, 63(9), 1259-1264, 2003.
151. Friedrich, Klaus. Stoyko Fakirov, and Zhong Zhang, eds. Polymer composites: From nano to macro scale. *Springer Science and Business Media*, New York, 2005.
152. Sudheer, M., Subbaya K. M., Jawali Dayananda and Bhat Thirumaleshwara. Mechanical properties of potassium titanate whisker reinforced epoxy resin composites. *Journal of Minerals and Materials Characterization and Engineering* 11(2), 193-210, 2012.
153. Ramnath, B. V., Manickavasagam, V. M., Elanchezhian, C., Krishna, C. V., Karthik, S. and Saravanan, K. Determination of mechanical properties of intra-layer abaca-jute-glass fiber reinforced composite. *Materials and Design*, 60, 643-652, 2014.
154. Satapathy A., Jha A.K., Mantry S. and Singh S.K. Processing and characterization of Jute-epoxy Composites Reinforced with SiC derived from rice husk. *Journal of Reinforced Plastics and Composites*. 29(18), 2869-78, 2010.
155. Jawaid M, Abdul Khalil HPS and Abu Bakar A. Mechanical performance of oil palm empty fruit bunches/jute fibers reinforced epoxy hybrid composites. *Materials Science and Engineering A*. 527(29-30), 7944-7949, 2010.
156. Ahmed S.K., Mallinatha V. and Amith S.J. Effect of ceramic fillers on mechanical properties of woven jute fabric reinforced epoxy composites. *Journal of Reinforced Plastic composite*. 30(15), 1315-1326, 2011.
157. Rowell, R.M. Chemical modification of agro-resources for property enhancement, paper and composites from agro-based resources. CRC Press. pp. 351-375, 1997.
158. Espert, A., Vilaplana, F. and Karlsson, S. Comparison of water absorption in natural cellulosic fibres from wood and one-year crops in polypropylene composites and its

- influence on their mechanical properties. *Composites Part A: Applied science and manufacturing*, 35(11), pp.1267-1276, 2004.
159. Sanadi, A.R., Caulfield, D.F. and Jacobson, R.E. Agro-Fibre thermoplastic composites, paper and composites from agro-based resources, Boca Raton: CRC Press: Lewis Publishers. Chapter 12, pp.377-401, 1997.
160. Maya Jacob John and Anandjiwala Rajesh D. Recent Developments in Chemical Modification and Characterization of Natural Fiber-Reinforced Composites. *Polymer composites*, 29(2), pp.187-207, 2008.
161. Joseph, P.V., Joseph, K. and Thomas, S. Effect of processing variables on the mechanical properties of sisal-fiber-reinforced polypropylene composites *Composite Science Technology*, 59(11), pp.1625-40, 1999.
162. Rahman, M.R., Huque, M.M., Islam, M.N. and Hasan, M. Improvement of physico-mechanical properties of jute fiber reinforced polypropylene composites by post-treatment. *Composites Part A: Applied Science and Manufacturing*, 39(11), pp.1739-1747, 2008.
163. Patel B.C. and Acharya S.K. Environmental effect of water absorption and flexural strength of red mud filled jute fiber/polymer composite. *International Journal of Engineering, Science and Technology*, 4(4), pp.49-59, 2012.
164. George J., Bhagawan, S.S. and Thomas, S. Effects of environment on the properties of low-density polyethylene composites reinforced with pineapple-leaf fiber. *Composite Science Technology*, 58(9), pp.1471-85, 1998.
165. Joseph, P.V. et al. Environmental effects on the degradation behaviour of sisal fibre reinforced polypropylene composites. *Composites Science and Technology*, 62(10-11), pp.1357-1372, 2002.
166. Stark, N. Influence of moisture absorption on mechanical properties of wood flour-polypropylene composites. *Journal of Thermoplastic Composite Material*, 14, pp.421-32, 2001.
167. Thomas, Selvin P., Sreekumar, P.A., Saiter, J.M., Joseph K., Unnikrishnan, G. and Thomas, S. Effect of fiber surface modification on the mechanical and water absorption characteristics of sisal/polyester composites fabricated by resin transfer molding. *Composite Part A* 40, pp.1777-1784, 2009.
168. Masoodi R. and Pillai KM. A study on moisture absorption and swelling in bio-based jute-epoxy composites. *Journal of Reinforced Plastic Composites*, 31, 285-294, 2012.
169. Osman Ekhlas A., Sbarski Igor et al. Kenaf/recycled jute natural fibers unsaturated polyester composites: water absorption/dimensional stability and mechanical properties, *International Journal of Computational Materials Science and Engineering*, 1(1), 1250010-17, 2012.

170. Zamri, Mohd. Hafiz, Hazizan Md. Akil, Azhar Abu Bakar, Zainal Arifin Mohd. Ishak, and Leong Wei Cheng. Effect of water absorption on pultruded jute/glass fibre reinforced unsaturated polyester hybrid composite. *Journal of Composite Material*, 46, 51-61, 2011.
171. Jena, H., Pradhan, A.K. and Pandit, M.K. Studies on water absorption behaviour of bamboo-epoxy composite filled with cenosphere. *Journal of Reinforced Plastics and Composites*, 33(11), 1059-1068, 2014.
172. Gu, J., Wu, G. and Zhao, X. Effect of surface modification on the dynamic behaviour of fly ash cenosphere filled epoxy composite. *Polymer composite*, 30(2), 232-238, 2009.
173. Roncero N.B., Torres A.L., Colom J.F. and Vidal T. The effect of xylanase on lignocellulosic components during the bleaching of wood pulps. *Bio resource Technology*, 96(1), pp. 21-30, 2005.
174. Deo, C.R. and Acharya, S.K. Preparation and characterization of polymer matrix composite using natural fiber Lantna-Camara. pp. 39-40, 2010.
175. Samal, S.K., Mohanty, S. and Nayak, S.K. Polypropylene-Bamboo/Glass Fiber Hybrid Composites: Fabrication and Analysis of Mechanical, Morphological, Thermal, and Dynamic Mechanical Behavior. *Journal of reinforced plastics and composites*, 28(22), 2729-2747, 2009.
176. Zhang, X.J., Yi, X.S. and Xu, Y.Z. Cure-induced phase separation of epoxy/DDS/PEEK-Carbon composites and its temperature dependency. *Journal of Applied Polymer Science*, 109(4), 2195-2206, 2008.
177. Zhang, Jin, Qipeng Guo, and Bronwyn L. Fox. Study on thermoplastic-modified multifunctional epoxies: Influence of heating rate on cure behaviour and phase separation. *Composites Science and Technology*, 69(7), 1172-1179, 2009.
178. Zeriouh A. and Belbirl L. Thermal decomposition of a Moroccan wood under a nitrogen atmosphere. *Thermochimica Acta* 258, 243-248, 1995.
179. Idrus, M.M., Hamdan, S., Rahman, M.R. and Islam, M.S. Treated Tropical wood sawdust-polypropylene polymer composite: Mechanical and Morphological Study. *Journal of Biomaterials and Nan biotechnology*, 2, 435-444, 2011.
180. Davies, P., Mazeas, F. and Casari, P. Sea water aging of Glass reinforced composites: Shear Behaviour and Damage Modelling. *Journal of Composite Materials*, 35(15), pp. 1343-1372, 2001.
181. Shi, S.Q. and Gardner, D.J. Effect of density and polymer content on the hygroscopic thickness swelling rate of compression molded wood fiber/polymer composites, *Wood and Fiber Science*, 38(3), pp. 520-526, 2006.

182. Matuana, L.M., Balatinecz, J.J., Sodhi, R.S. and Park, C.B. Surface characterization of esterified cellulosic fibres by XPS and FTIR spectroscopy. *Wood Science and Technology*, 35(3), pp.191-201, 2001.
183. Marom, Gad. The role of water transport in composite materials. In *Polymer permeability*, Springer Netherlands, pp. 341-374, 1985.
184. Marcovich, N.E., Reboredo, M.M. and Aranguren, M.I. Moisture diffusion in polyester wood flour composites. *Polymer* 40(26), pp.7313-7320, 1999.
185. Wang, W., Sain, M. and Cooper, P.A. Study of moisture absorption in natural fibre plastic composites. *Composites Science and Technology*, 66(3), pp.379-386, 2006.
186. Crank. Mathematics of Diffusion, Oxford University Press, Oxford, pp.347, 1975.
187. Shen C. and Springer G. Moisture absorption and desorption of composite materials. *Journal of composite Material*.10 (1), 2-20, 1976.
188. Tajvidi, M., Najafi, S.K. and Moteei, N. Long-term water uptake behaviour of natural fiber/polypropylene composites. *Journal of Applied Polymer Science*, 99(5), pp.2199-2203, 2006.
189. Fujita H. *Advances in Polymer Science*.196, 3(1), 1961.
190. Barrie J.A. Water in Polymers: Diffusion in Polymers. J.Crank and G.S.Park, editors, Academic Press, New York, 259, 1968.
191. Dhakal, H.N., Zhang, Z.Y. and Richardson, M.O.W. Effect of water absorption on the mechanical properties of hemp fibre reinforced unsaturated polyester composites. *Composite Science and Technology*, 67(7), 1674-1683, 2007.
192. Holm, R. The friction force over the real area of contact. *Wiss. Veroff. Siemens-Werk*, 17(4), 38-42, 1938.
193. Barwell, F. T. and Strang, C. D. Metallic Wear, *Proceeding Royal Society London, A*, 212 (III): pp. 470-477, 1952.
194. Archard, J. Contact and rubbing of flat surfaces. *Journal of applied physics*, 24(8), 981-988, 1953.
195. Archard, J. F. and Hirst, W. The wear of metals under unlubricated conditions. *Proceedings of the Royal Society of London. Series A. Mathematical and Physical Sciences*, 236(1206), 397-410, 1956.
196. Kragelsky, I.V., Dobychin, M.N., Komalov, V.S. Friction and Wear calculation Methods. Pergamon Press, USSR, ISBN 0-08-025461-6, 1982.
197. Fleischer, G. Energetische Methode der Bestimmung des Verschleisses. In: *Schmierungstechnik*, 4(9), 269-274, 1973.
198. Zum Gahr, K. H. *Microstructure and wear of materials*. Elsevier (10), 1987.

199. Soda, N., Kimura, Y. and Tanaka, A. Wear of some face centered cubic metals during unlubricated sliding part I. Effects of load, velocity and atmospheric pressure on wear. *Wear*, 33(1), 1-16, 1975.
200. Burwell, J. T., and Strang, C. D. Metallic wear. *Proceedings of the Royal Society of London. Series A, Mathematical and Physical Sciences*, 470-477, 1952.
201. Burwell Jr, J. T. Survey of possible wear mechanisms. *Wear*, 1(2), 119-141, 1957.
202. Stokes, J. Theory and application of the high velocity oxy-fuel (HVOF), Thermal spray process. Dublin City University. ISBN 1-87232-753-2, ISSN 1649-8232, 2008.
203. Ashby, M. F., and Lim, S. C. Wear-mechanism maps. *Scripta Metallurgica et Materialia*, 24(5), 805-810, 1990.
204. Ko, P. L. Metallic wear-A review with special references to vibration-induced wear in power plant components. *Tribology International*, 20(2), 66-78, 1987.
205. Finnie, I. Some reflections on the past and future of erosion. *Wear*, 186, 1-10, 1995.
206. Meng, H. C. and Ludema, K. C. Wear models and predictive equations: their form and content, *Wear*, 181-183, pp.443-457, 1995.
207. Bitter, J. G. A. A study of erosion phenomena: Part II. *Wear*, 6(3), 169-190, 1963.
208. Hutchings, I. M., Winter, R. E., and Field, J. E. Solid Particle Erosion of Metals: The Removal of Surface Material by Spherical Projectiles. *Proceedings of the Royal Society of London. Series A, Mathematical and Physical Sciences*, 348(1654), 379-392, 1976.
209. Pool, K.V., Dharan, C.K. H. and Finnie, I. Erosive wear of composite materials. *Wear*, 107(1), 1-12, 1986.
210. Kulkarni, S. M. Influence of matrix modification on the solid particle erosion of Glass/epoxy composites. *Polymers and polymer composites*, 9(1), 25-30, 2001.
211. Rajesh, J. J., Bijwe, J., Tewari, U. S., and Venkataraman, B. Erosive wear behaviour of various polyamides. *Wear*, 249(8), 702-714, 2001.
212. Barkoula, N. M., and Karger-Kocsis, J. Solid particle erosion of unidirectional glass fiber reinforced epoxy composites with different fiber/matrix adhesion. *Journal of reinforced plastics and composites*, 21(15), 1377-1388, 2002.
213. Tewari, U. S., Harsha, A. P., Häger, A. M., and Friedrich, K. Solid particle erosion of carbon fibre and glass fibre-epoxy composites. *Wear*, 63, 549-557, 2003.
214. Bhushan, B. *Principles and applications of tribology*. John Wiley and Sons, 2013.
215. Harsha A.P., Arjula Suresh, Ghosh M.K. Solid particle erosion of unidirectional fibre reinforced thermoplastic composites, *Wear*, 267, 1516-1524, 2009.
216. Roy, M., Vishwanathan, B. and Sundararajan, G. The solid particle erosion of polymer matrix composites. *Wear*, 171(1), 149-161, 1994.

217. Bajpai, P. K., Singh, I., and Madaan, J. Tribological behavior of natural fiber reinforced PLA composites. *Wear*, 297(1), 829-840, 2013.
218. Mishra, P., and Acharya, S. K. Anisotropy abrasive wear behavior of bagasse fiber reinforced polymer composite. *International Journal of Engineering, Science and Technology*, 2(11), 104-112, 2010.
219. Deo, C. and Acharya, S. K. Solid particle erosion of lantana camara fiber-reinforced polymer matrix composite. *Polymer-Plastics Technology and Engineering*, 48(10), 1084-1087, 2009.
220. Gupta, A., Kumar, A., Patnaik, A., and Biswas, S. Effect of different parameters on mechanical and erosion wear behavior of bamboo fiber reinforced epoxy composites. *International Journal of Polymer Science*, doi:10.1155/2011/592906, 2011.
221. Mohanty, J. R., Das, S. N., Das, H. C., Mahanta, T. K. and Ghadei, S. B. Solid particle erosion of date palm leaf fiber reinforced polyvinyl alcohol composites. *Advances in Tribology*, 2014.
222. Ojha Shakuntala, Gujjala Raghavendra and Acharya S.K. Effect of filler loading on mechanical and tribological properties of wood apple shell reinforced epoxy composite. *Advances in Materials Science and Engineering*, pp.1-9, 2014, Doi.org/10.1155/2014/538651.
223. Jawaid, M. H. P. S., and Abdul Khalil, H. P. S. Cellulosic/synthetic fibre reinforced polymer hybrid composites: A review. *Carbohydrate Polymers*, 86(1), 1-18, 2011.
224. Almeida Jr, J. H. S., Amico, S. C., Botelho, E. C., and Amado, F. D. R. Hybridization effect on the mechanical properties of curaua/glass fiber composites. *Composites Part B: Engineering*, 55, 492-497, 2013.
225. Patel, B. C., Acharya, S. K., and Mishra, D. Effect of stacking sequence on the erosive wear behaviour of jute and jute-glass fabric reinforced epoxy composite. *International Journal of Engineering, Science and Technology*, 3(1), 2011.
226. Barkoula, N. M., and Karger-Kocsis, J. Effects of fibre content and relative fibre orientation on the solid particle erosion of GF/PP composites. *Wear*, 252(1), 80-87, 2002.
227. Drensky, G., Hamed, A., Tabakoff, W. and Abot, J., Experimental investigation of polymer matrix reinforced composite erosion characteristics. *Wear*, 270(3), pp.146-151, 2011.
228. Ruff, A. W., and Ives, L. K. Measurement of solid particle velocity in erosive wear. *Wear*, 35(1), 195-199, 1975.
229. Sundararajan, G., Roy, M. and Venkataraman, Erosion efficiency-a new parameter to characterize the dominant erosion micromechanism. *Wear*, 140(2), 369-381, 1990.

230. Arjula, S., and Harsha, A. A. Study of erosion efficiency of polymers and polymer composites. *Polymer testing*, 25(2), 188-196, 2006.
231. Barkoula, N.M. and Karger-Kocsis, J. Review processes and influencing parameters of the solid particle erosion of polymers and their composites. *Journal of materials science*, 37(18), 3807-3820, 2002.
232. Biswas, S., and Satapathy, A. A comparative study on erosion characteristics of red mud filled bamboo-epoxy and glass-epoxy composites. *Materials & Design*, 31(4), 1752-1767, 2010.
233. Miyazaki, N. and Hamao, T. Solid particle erosion of thermoplastic resins reinforced by short fibers. *Journal of composite materials*, 28(9), 871-883, 1994.
234. Moore, D. F. Principles and applications of tribology (Vol.1). Oxford: Pergamon Press, 1975.
235. Roy, M., Vishwanathan, B., and Sundararajan, G. The solid particle erosion of polymer matrix composites. *Wear*, 171(1), 149-161, 1994.
236. Pool, K. V., Dharan, C. K. H., and Finnie, I. Erosive wear of composite materials. *Wear*, 107(1), 1-12, 1986.
237. Harsha, A. P., Tewari, U. S. and Venkatraman, B. Solid particle erosion behaviour of various polyaryletherketone composites. *Wear*, 254(7), 693-712, 2003.
238. Sundararajan, G., Roy, M., and Venkataraman, B. Erosion efficiency-a new parameter to characterize the dominant erosion micromechanism. *Wear*, 140(2), 369-381, 1990.
239. Srivastava V.K. and Shembekar P.S. Tensile and fracture properties of epoxy resin filled with fly ash particles, *Journal of material science* 25, 3512-3516, 1990.
240. Raghavendra, G., Ojha, S., Acharya, S.K. and Pal, S.K. A comparative analysis of woven jute/glass hybrid polymer composite with and without reinforcing of fly ash particles. *Polymer Composites*, 37(3), 658-665, 2016.
241. Patnaik, A., Satapathy, A., Chand, N., Barkoula, N.M. and Biswas, S. Solid particle erosion wear characteristics of fiber and particulate filled polymer composites: A review. *Wear*, 268(1), pp.249-263, 2010.
242. Biswas, S., Patnaik, A. and Kaundal, R. Effect of red mud and copper slag particles on physical and mechanical properties of bamboo fiber reinforced epoxy composites. *Advances in Mechanical Engineering*, 4, pp.141248-54, 2012.
243. Satapathy A., Patnaik A. and Pradhan M.K. A study on processing, characterization and erosion behavior of fish (Labeo-rohita) scale filled epoxy matrix composites. *Materials and Design*, 30, 2359-2371, 2009.
244. Aktas Alaattin. Solid particle erosion of glass epoxy composite strengthened by metal powder. *Journal of Thermoplastic Composite Materials*, 25(8), 949-963, 2012.

245. Ismail, M., Bheemappa, S. and Rajendra, N. Investigation on mechanical and erosive wear behaviour of cenosphere filled carbon epoxy composites, *International conference on mechanical, Automotive and Materials Engineering*, pp.7-8, 2012.
246. Chand Navin, Sharma Pratibha and Fahim. Correlation of mechanical and tribological properties of organosilane modified cenosphere filled high density polyethylene. *Materials Science and Engineering A* 527, 5873-5878, ISSN 0921-5093, 2010.
247. Shalwan, A. and Yousif, B. F. Influence of date palm fibre and graphite filler on mechanical and wear characteristics of epoxy composites. *Materials and Design*, 59, 264-273, 2014.
248. Sunil Thakur and Santram Chauhan. Effect of micron and submicron size cenosphere particulate on mechanical and tribological characteristics of vinylester composites. *Journal of Engineering Tribology*, 228(4), 415-423, 2014.
249. S.R. Chauhan *et al.* Effects of particle size, particle loading and sliding distance on the friction and wear properties of cenosphere particulate filled vinylester composites. *Materials and Design*, 51, 398-408, 2013.
250. Srivastava V. K., Pawar A. G. Solid particle erosion of glass fiber reinforced fly-ash filled epoxy resin composites. *Composites Science and Technology*, 66(15), 3021-3028, 2006.
251. Rout A. K. and Satapathy A. Study on mechanical and tribo-performance of rice-husk filled Glass-epoxy hybrid composites. *Materials and Design*, 41, 131-141, 2012.
252. Friction, Lubrication and Wear Technology, ASM International Materials Park, OH, USA, 1992.
253. Hutchings, I.M. Tribology: Friction and Wear of Engineering Materials. Edward Arnold, London. pp.156-162, 1992.
254. Chand N. and Dwivedi U.K. Effect of coupling agent on abrasive wear behaviour of chopped jute fibre reinforced polypropylene composites. *Wear*, 261, 1057-1063, 2006.
255. Tong J., Ren L., Li Jianqiao, and Chen B. Abrasive wear behaviour of bamboo. *Tribology International*, 28(5), 323-327, 1995.
256. Tripathy, Bhawani S., and Michael J. Furey. Tribological behaviour of unidirectional graphite epoxy and carbon PEEK composite. *Wear*, 162, 385-396, 1993.
257. Pihitili H. and Tosun N. Effect of load and speed on the wear behaviour of woven glass fabrics and aramid fibre reinforced composites. *Wear*, 252, 979-984, 2002.
258. El-Tayeb N.S.M. and Yousif B.F. Evaluation of glass fibre reinforced polymer composites for multi-pass abrasive wear applications. *Wear*, 262(9-10), 1140-1151, 2007.

259. Harsha A.P. and Tewari U.S. Two-Body and Three-Body abrasive wear behaviour of polyaryletherketone composites, *Polymer Testing*, 22(4), 403-418, 2003.
260. Suresha B., Chandramohan G., Siddaramaiah KNS, *et al.* Mechanical and three-body abrasive wear behaviour of three dimensional glass-fabric reinforced vinyl ester composite. *Material Science and Engineering A*, 480(1), 573-579, 2008.
261. Mohan N., Natarajan S. and Kumaresha Babu S. P. The Role of synthetic and natural fillers on three-body abrasive wear behaviour of Glass fabric epoxy hybrid composites. *Journal of Applied Polymer Science*, 124, 484-494, 2012.
262. Suresha B., Ramesh B.N., Subbaya K.M., *et al.* Mechanical and three body abrasive wear behaviour of carbon epoxy composite with and without graphite filler. *Journal of Composite Material*, 44, 2509-2519, 2010.
263. Suresha B. and Chandramohan G. Three-body abrasive wear behaviour of particulate filled glass vinyl ester composites. *Journal of material processing Technology*, 200(1), 306-311, 2008.
264. Biswas S. and Satpathy A. Tribo performance analysis of red mud filled glass epoxy composites using taguchi experimental design. *Material Design*, 30(8), 2841-2853, 2009.
265. Satapathy A., Patnaik A. and Biswas S. Investigations on three-body abrasive wear and mechanical properties of particulate filled glass epoxy composites. *Malaysian Polymer Journal*, 5(2), 37-48, 2010.
266. Devi, M.S., Murugesan, V., Rengaraj, K. and Anand, P. Utilization of fly ash as filler for unsaturated polyester resin. *Journal of Applied Polymer Science*, 69(7), 1385-1391, 1998.
267. Maher M.H. and Balaguru P.N. Properties of flowable high volume fly ash-cement composite. *Journals of Materials in Civil Engineering*, 5(2), 212-225, 1993.
268. Suresha B., Chandramohan G., Siddaramaiah *et al.* Influence of cenosphere filler additions on three body abrasive wear behaviour of glass fiber-reinforced epoxy composites. *Polymer Science*, 29(3), 307-312, 2008.
269. Chand N., Sharma P. and Fahim M. Correlation of mechanical and tribological properties of organosilane modified cenosphere filled high density polyethylene. *Materials Science and Engineering A*. 527, 5873-5878, 2010.
270. Kumar Saurabh, Harsha A.P., Goyal H.S. *et al.* Three-body abrasive wear behaviour of aluminium alloys. *Journal of Engineering Tribology*, 227(4), 328-338, 2012.
271. Suresha B., Chandrashekar A. and Srinivas S. Mechanical and Three-body abrasive wear behaviour of cenosphere filled epoxy composites. *International Journal of Material Science*, 5(1), 7-15, 2015.
272. Suresha B., Chandramohan G., Siddaramaiah *et al.* Three-body abrasive wear

- behaviour of carbon and glass fiber reinforced epoxy composites. *Materials Science and Engineering A*, 443, 285-291, 2007.
273. Chand N., Naik A. and Neogi S. Three-body abrasive wear of short glass fiber polyester composite. *Wear*, 242(1), 38-46, 2000.

Dissemination

Internationally indexed journals

1. Soma Dalbehera and S.K. Acharya. **“Study on mechanical properties of natural fiber reinforced woven jute-glass hybrid epoxy composites”**, Advances in Polymer Science and Technology: An International Journal, 2014, ISSN 2277-7164, Vol. 4(1), pp.1-6.
2. Soma Dalbehera and S.K. Acharya. **“Effect of cenosphere addition on the mechanical properties of jute-glass fiber hybrid epoxy composites”**, Journal of Industrial Textiles, 46(1), 177-188, 2016.
3. Soma Dalbehera and S.K. Acharya. **“Impact of cenosphere on the erosion wear response of woven hybrid Jute-Glass epoxy composites”**, Advances in Polymer Technology, 2016, 21662,10.1002/adv.21662,Wiley Periodicals.
4. Soma Dalbehera and S.K. Acharya. **“Impact of stacking sequence on tribological wear performance of woven jute-glass hybrid epoxy composites”**, Tribology-Materials, Surfaces & Interfaces, 2015, ISSN: 1751-5831, Vol. 9(4), pp.196-201.
5. Soma Dalbehera and S.K. Acharya. **“Effect of cenosphere addition on erosive wear behaviour of jute-glass reinforced composite using taguchi experimental design”**,Materials Today: Proceedings 2 (2015) 2389-2398, Elsevier.
6. Soma Dalbehera and S.K. Acharya. **“Effect of cenosphere on moisture absorption performance of woven hybrid jute-glass epoxy composites”**, Polymer Composites. (under review).

Conferences

1. Soma Dalbehera and S.K. Acharya. “**Effect of cenosphere on mechanical properties of Jute-E-Glass fiber hybrid composites**”, Presented for 6th International Congress of Environmental Research (ICER), December 19-21, 2013, Aurangabad, Maharashtra, India.
2. Soma Dalbehera and S.K. Acharya. “**Study on mechanical Properties evaluation of natural fiber reinforced woven jute-glass hybrid epoxy composites**”, Presented for International Conference on Metallurgical and Materials processes, Products and Applications (ICMMPPA), January 8-10, 2014, OP Jindal Institute of Technology (OPJIT), Raigarh, India.
3. Soma Dalbehera and S.K. Acharya. “**Study on effect of stacking sequence on the tribological property of woven jute-glass fiber reinforced epoxy composite**”, Presented for ASIATTRIB-2014, International Conference, February 17-20, Jaypee Palace Hotel and Convention Centre, Agra, India.
4. Soma Dalbehera and S.K. Acharya. “**Effect of cenosphere addition on erosive wear behaviour of jute-glass reinforced composites using taguchi Experimental Design**”, Presented for 4th International Conference on Materials Processing and Characterization (ICMPC), March 14-15, 2015, GRIET, Hyderabad, India.
5. Soma Dalbehera and S.K. Acharya. “**Effect of cenosphere on erosive wear behaviour of woven jute-glass hybrid epoxy composites**”, Presented for 17th ISME Conference on Advances in Mechanical Engineering, October 3-4, 2015, IIT Delhi, New Delhi, India.
6. Soma Dalbehera and S.K. Acharya. “**Effect of cenosphere addition on erosive wear behaviour of woven jute-glass reinforced epoxy composites**”, Presented on All India Seminar on Recent Trends in Mechanical Engineering (RTME), February 21-22, 2015, The Institution of Engineers, Odisha State Centre, Bhubaneswar, Odisha.



Ms. Soma Dalbehera is a faculty member in the Department of Mechanical Engineering, Government Polytechnic Nayagarh, Odisha. She has three and half years of research and three years of teaching experience in her field. This dissertation is being submitted for the fulfillment of the Ph.D. degree. The contact address is below.

Address:-

Government polytechnic Nayagarh

AT:-Ghasadeipur

PO:-Nandighar

Odagaon

DIST-Nayagarh

PIN-752081

Odisha

E mail: somacutm@gmail.com

Phone: 9937994512 (M)

Residence:-

Plot No: N3/345

PO: I.R.C.VILLAGE

DIST: Khurda

Bhubaneswar

PIN-751015

Phone : (0674)2553345

Odisha

India